Attachment

Sediment Mobilization Assessment

Draft
Geomorphology, Sediment Transport, and Vegetation Assessment Appendix

Draft
April 2011

Sediment Mobilization Assessment

Report Prepared by:

Jianchun Huang, P.E., Ph.D., Hydraulic Engineer
Sedimentation and River Hydraulics Group, Technical Service Center

Signature:_____

Blair P. Greimann, P.E., Ph.D., Hydraulic Engineer
Sedimentation and River Hydraulics Group, Technical Service Center

Signature:_____

Peer Reviewed by:

David Varyu, M.S., Hydraulic Engineer
Sedimentation and River Hydraulics Group, Technical Service Center

Signature:_____

Table of Contents

Exhibits

Tables

Figures

This page left blank intentionally.

List of Abbreviations and Acronyms

1D	one-dimensional
cfs	cubic feet per second
MEI	Mussetter Engineering, Inc.
mm	millimeter
PEIS	Programmatic Environmental Impact Statement
Reclamation	U.S. Department of the Interior, Bureau of Reclamation
RP	River Post
SJRRP	San Joaquin River Restoration Program
TSC	Technical Service Center
yr	year

1.0 Introduction

The Denver Technical Service Center (TSC) of the U.S. Department of the Interior, Bureau of Reclamation (Reclamation), was requested to perform an analysis of the sediment mobilization and reach-averaged sediment transport of the San Joaquin River between Friant Dam and Mendota Pool. This assessment is in support of the San Joaquin River Restoration Program (SJRRP) Programmatic Environmental Impact Statement (PEIS) and is part of a more comprehensive analysis that focuses on the sediment transport and geomorphic characteristics of the San Joaquin River. Additional reports will analyze the effect of the SJRRP to bed elevation and grain size in this reach. The main goal of this analysis is to determine the effects of the SJRRP relative to Baseline Conditions. Previous analysis of the sediment transport characteristics have been performed by McBain and Trush (2002) and Mussetter Engineering, Inc. (MEI) (2002a). The purpose of this study is to verify those previous analyses and compare the conditions under the SJRRP to Baseline Conditions. Baseline Conditions and conditions under the SJRRP are defined in Appendix H, Modeling, of the PEIS. Conditions under the SJRRP are termed Project Conditions in this report.

The current study reach covers Project Reach 1 from Friant Dam to Gravelly Ford, which, in terms of river post distances (RP), extends from RP 267.5 to RP 229.0, and Project Reach 2, which extends from Gravelly Ford to Mendota Dam (RP 229.0 to RP 204.8) (Figure 1-1).

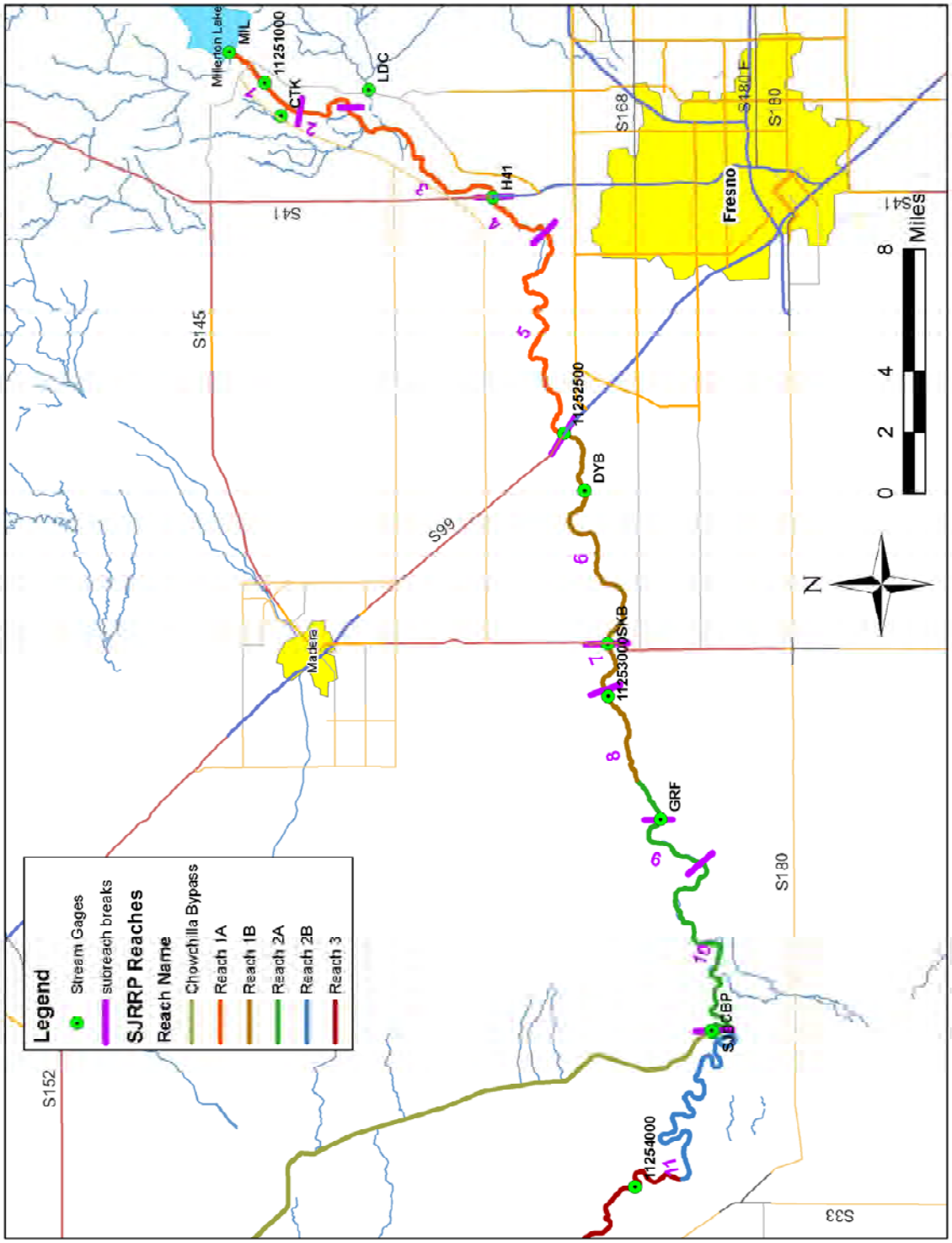

Figure 1-1.
Overview Map of Study Area (SJRRP Reaches 1 and 2)

2.0 Input Data

2.1 Hydrology

Three different hydrologic sets were analyzed in this report: Baseline Conditions, Project Conditions, and Historical Gage data.

The Baseline Conditions refer to the simulated flows in the San Joaquin River if current water operations were followed. CalSim II was used to develop the Baseline Conditions, assuming that current water operations were followed and the Historical hydrologic conditions occur again. The monthly average flows from CalSim II were then downscaled to daily flows. These daily flows are also used in HEC5Q simulations of the river temperature. The details of the hydrologic modeling of the Baseline Conditions are given in Appendix H of the PEIS.

The Project Conditions are also referred to as Alternative A in this report. These are the simulated flows in the San Joaquin River under the SJRRP and if the historic hydrology were to occur again. Details of the Baseline and Project scenarios are found in Appendix H of the PEIS. Two sets of Baseline and Project scenarios were developed: Future and Existing. For the purposes of this report, however, the Future and Existing scenarios are considered identical. This is based upon an analysis of the flow-duration curves that found no significant difference between the two scenarios. The Project conditions assume that the maximum flow in Reach 4b1 will be 475 cubic feet per second (cfs).

The Historical Gage data were taken from U.S. Geological Survey stream gages shown in Figure 1-1. Of the gages shown in the figure, four gage stations provided Historical hydrology; these are listed in Table 2-1. The records for the other gages were not complete. Flow-duration curves were computed for each of these gages. The endpoint of the reaches used in the analysis did not always correspond to the gage locations. For these reaches, flow-duration curves were linearly interpolated from the gage values based upon the distance of the downstream end of the reach, relative to the gage locations.

Table 2-1.
Stream Gages Used to Derive Flow-Duration Curves

Description	Stream Gage ID	River post (miles)	HEC-RAS XC	Agency
San Joaquin River below Friant Dam	MIL	267.5	XS596	Reclamation
San Joaquin River near Gravelly Ford	GRF	227.5	XSA213	Reclamation
Chowchilla Bypass downstream from Chowchilla Bifurcation Structure	CBP	-	-	California Department of Water Resources
San Joaquin River downstream from Chowchilla Bifurcation Structure	SJB	216	XSA97	Reclamation

Key:
ID = Irrigation District

The flow-duration curves using the Historical Gage data, Baseline Conditions, and Alternative A are given in Figures 2-1 through 2-3 for Friant Dam, Gravelly Ford, and San Joaquin below Chowchilla stream gages, respectively. A common period from January 1, 1980, to May 31, 1997, was used to develop the flow-duration curves. This period of flow records was available for the gages shown in these figures. For the Friant Dam and Gravelly Ford stream gages, the Alternative A flows have a higher frequency of flows above 100 cfs and below 2,300 cfs, compared to Baseline Conditions. Alternative A flows also show a slightly lower frequency of flows above 2,300 cfs. There is a significant increase in flows in the San Joaquin River below the Chowchilla Control Structure because the maximum release to the San Joaquin River was increased to 4,500 cfs where, under Baseline Conditions, it is approximately 1,500 cfs, except when there are uncontrolled spills at Friant.

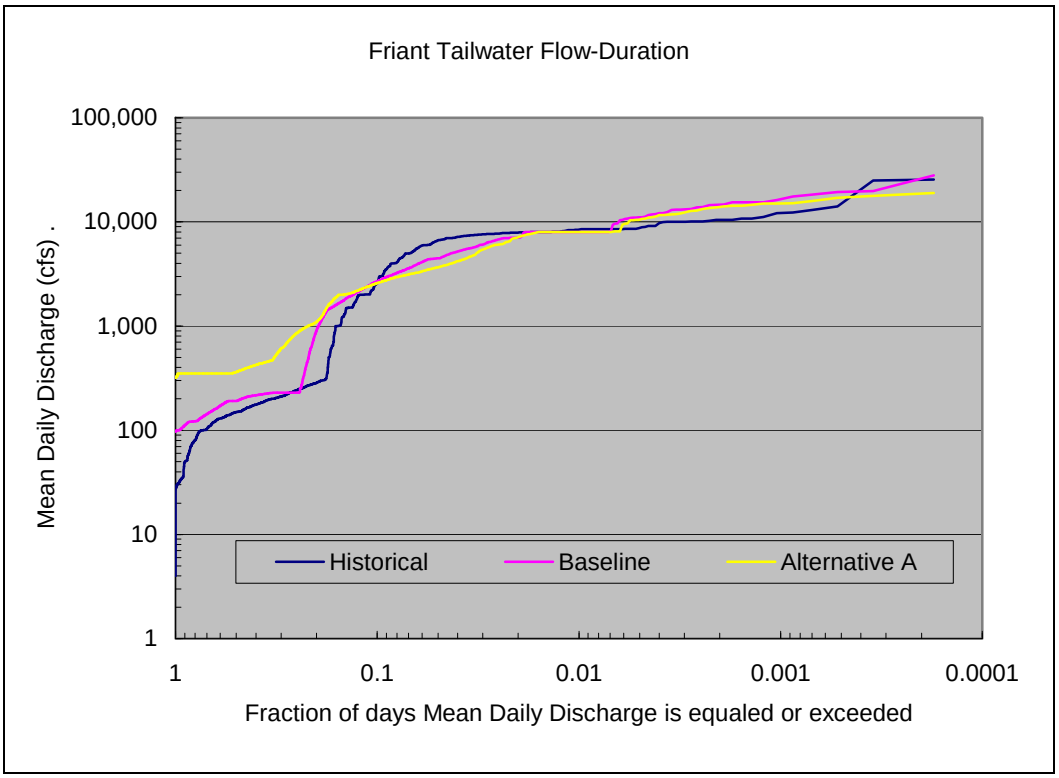

Note: The flow-duration curves are based upon daily average flow records from January 1, 1980, to May 31, 1997.

Figure 2-1.
Flow-Duration Curves at Friant Dam

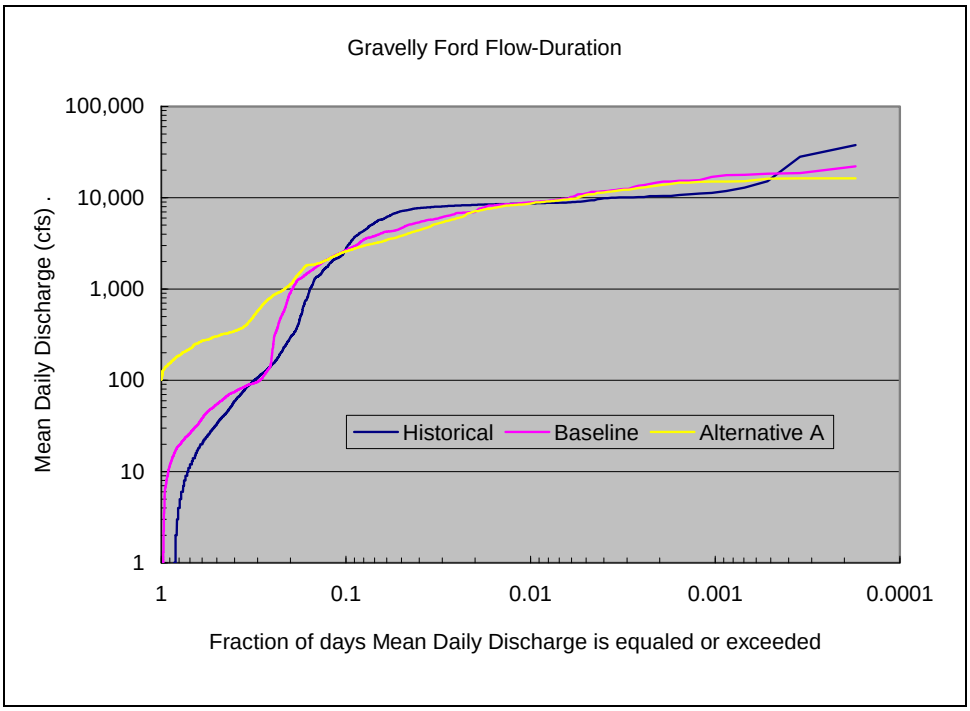

Note: The historical flow-duration curve is based upon daily average flow records from January 1, 1980, to May 31, 1997.

Figure 2-2.
Flow-Duration Curves at Gravelly Ford

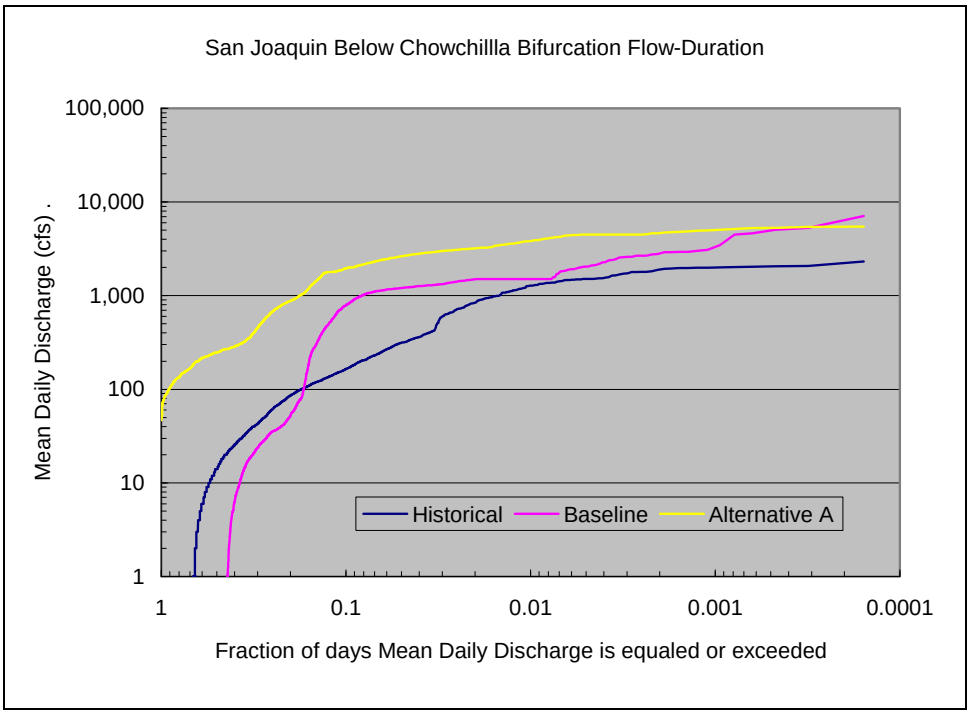

Figure 2-3.
Flow-Duration Curves on San Joaquin River Downstream from Chowchilla Bifurcation Structure from January 1, 1980, to May 31, 1997

2.2 Hydraulic Model

A HEC-RAS model was used to simulate flow hydraulics from Friant Dam to the Mendota Dam. MEI (2002a) created a one-dimensional (1D) hydraulic analysis of the project reach using 1998 geometry and the U.S. Army Corps of Engineers HEC-2 step-backwater computer program (MEI 2002). MEI has transferred it into HEC-RAS format. The results reported in this study refer to the HEC-RAS model provided to Reclamation in April 2008.

To calculate sediment transport capacity and incipient motion, a uniform discharge simulation was performed. The discharge ranges from 100 cfs to 15,000 cfs, which covers the typical discharge range of interest.

The downstream boundary is set at the Mendota Dam (XSA2, RP 204.6). During flows less than 1,500 cfs, the water surface elevation is set as the pool elevation of 152.7 feet at Mendota Dam. For higher elevations, the pool elevation was estimated using a weir equation.

$$H = H_0 + \left(\frac{Q}{CB}\right)^{2/3} \qquad (2.2.1.1.1.1)$$

where: H = pool elevation at the dam
H0 = dam crest elevation =153.1 feet
Q = discharge
B = dam width (382 feet)
C = weir coefficient (=3.0)

The moving average velocity is calculated to indicate the location of significant hydraulic changes. As an example, Figure 2-4 shows the moving average velocity for discharge of 5,000 cfs upstream from the Chowchilla Bifurcation Structure and 1,000 cfs downstream from the structure.

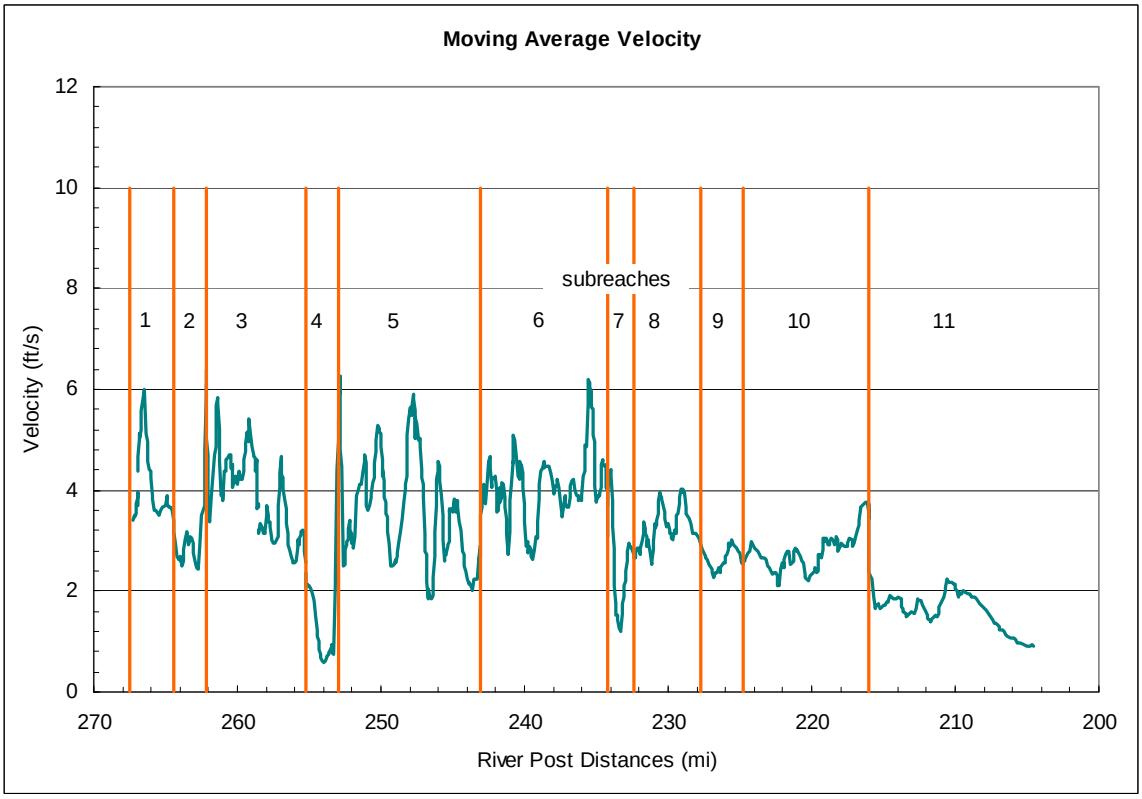

Note: Velocities are the cross-sectional averaged velocity from the HEC-RAS model.

Figure 2-4.
A Moving Average of the Cross-Sectional Velocity for a Flow of 5,000 cfs Used to Identify Reach Breaks Upstream from Chowchilla Bypass Structure

The original six subreaches from MEI (2002a) are kept and additional subreaches were added. Subreach 2 from RP 264.4 to Ledger Island Bridge was added for the 2.2-mile reach that has relative low velocity due to the backwater effects from the Ledger Island Bridge. Subreach 4 from Highway 41 Bridge to Lower Gravel Pit Crossing was added for the 2.3-mile reach that has relative low velocity due to the backwater effect from Lower Gravel Pit Crossing. Subreach 7 from Highway 145 Bridge to RP 232.5 was added due to the low velocity in a gravel pit at that location. Finally, a separation just downstream from Gravelly Ford was added due to bed transition from gravel bed to sand-bed.

The 1D model was used to compute the total velocity, top width, hydraulic radius, and friction slope for each cross section, then reach-averaged for the 11 subreaches defined in Table 2-2. Channel slopes were calculated from the thalweg elevation difference between the upstream cross section and downstream cross section, divided by the channel length. These results are used for the sediment transport capacity and incipient motion analyses.

Table 2-2.
Subreach Boundaries Used in the Sediment Capacity and Incipient Motion Study

Subreach	Project Reach	Sub-reach	Upstream Limit		Downstream Limit		Length
			Cross Section	River Post	Cross Section	River Post	(miles)
Friant Dam to River Post 264.4	1a	1	XS596	267.5	XS556	264.4	3.1
River Post 264.3 to Ledger Island Bridge	1a	2	XS555	264.4	XS527	262.2	2.2
Ledger Island Bridge to Highway 41 Bridge	1a	3	XS526	262.2	XS422.5	255.2	7.1
Highway 41 Bridge to Lower Gravel Pit Crossing	1a	4	XS422	255.2	XS387	252.9	2.2
Lower Gravel Pit Crossing to Highway 99 Bridge	1a	5	XS384	252.9	XS227	243.1	9.8
Highway 99 Bridge to Highway 145 Bridge	1b	6	XS226	243.1	XS92	234.2	8.9
Highway 145 Bridge to River Post 232.5	1b	7	XS91	234.2	XS59	232.3	1.9
River Post 232.5 to Gravelly Ford	1b	8	XS58	232.3	XSA213	227.6	4.8
Gravelly Ford to end Left Bank levee	2a	9	XSA212	227.6	XSA187	224.7	2.9
End Left Bank levee to Bifurcation Structure	2a	10	XSA186	224.7	XSA97	216.0	8.7
Bifurcation Structure to Mendota Dam	2b	11	XSA94	216.0	XSA2	204.6	11.4

2.3 Sediment Data and Parameters

2.3.1 Surface Bed Material

Surface bed material data was used in the sediment mobilization analysis and in the sediment transport analysis. The bed material data were taken from the 29 surface samples collected in February 2008 (Reclamation 2008a). To supplement the data for the sediment mobilization study in Reach 1a, Stillwater Sciences' pebble count data (Stillwater Sciences 2003) were also used. Figure 2-5 shows the measured D_{50} in each subreach using Stillwater Sciences' (2003) and Reclamation's (2008a) data. The D_{50}, the median sediment size, decreases from almost 90 millimeter (mm) in Subreach 1 to 0.56 mm in Subreach 11, as shown in Figure 2-5.

The sediment load computation requires the fraction of material by weight in each size class present in the bed. Stillwater Sciences' data were not used to compute the sediment transport loads. The fraction in each size class is given in Table 2-3.

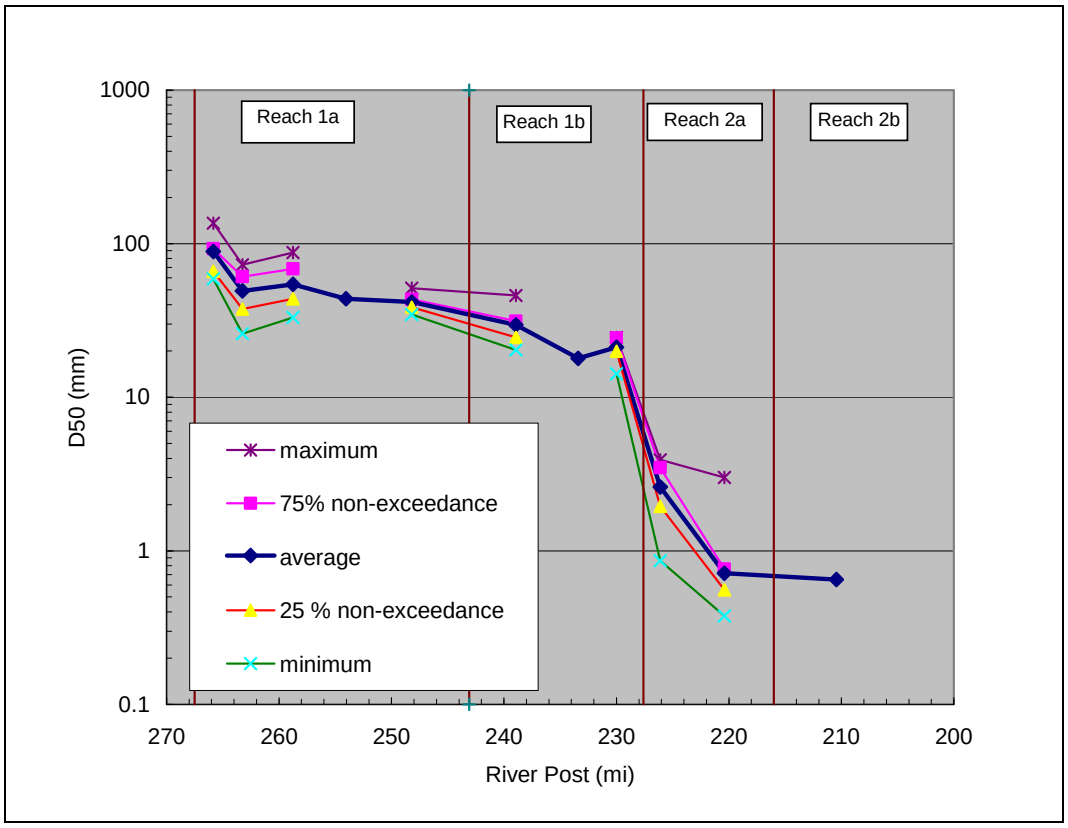

Figure 2-5.
Mean Bed Surface Sediment Size for Each Subreach Used in the Sediment Transport Capacity and Incipient Motion Study

Table 2-3.
Reach-Averaged Cumulative Grain Size Distribution for Each Subreach Used in the Sediment Transport Capacity and Incipient Motion Study

Subreach		0.063 mm	0.125 mm	.025 mm	0.5 mm	1 mm	2 mm	4 mm	8 mm
1	XS596-XS556	0.0001	0.0002	0.0004	0.0007	0.0012	0.0018	0.0027	0.0044
2	XS555-XS527	0.0001	0.0001	0.0002	0.0004	0.0008	0.0013	0.0018	0.0028
3	XS526-XS422.5	0.0008	0.0014	0.0047	0.0094	0.0127	0.0167	0.0203	0.0257
4	XS422-XS387	0.0015	0.0023	0.0069	0.0216	0.0538	0.0833	0.0983	0.1265
5	XS384-XS227	0.0019	0.0029	0.0078	0.0242	0.0604	0.0929	0.111	0.1457
6	XS226-XS92	0.0013	0.0020	0.0040	0.0127	0.0355	0.0568	0.0749	0.1141
7	XS91-XS59	0.0062	0.0075	0.0156	0.0402	0.0488	0.0571	0.0689	0.0982
8	XS58-XSA213	0.0099	0.0134	0.0331	0.0882	0.1528	0.2003	0.2265	0.2719
9	XSA212-XSA187	0.0203	0.0285	0.0592	0.2019	0.4564	0.6358	0.7082	0.7628
10	XSA186-XSA97	0.0313	0.0460	0.0959	0.3546	0.7022	0.8524	0.8921	0.9270
11	XSA94-XSA2	0.0153	0.0241	0.0781	0.4354	0.8539	0.9865	1.0000	1.0000

Subreach		16 mm	32 mm	64 mm	128 mm	256 mm	D16	D50	D84
1	XS596-XS556	0.0113	0.0465	0.2086	0.9048	1.0000	52.00	85.54	120.00
2	XS555-XS527	0.0085	0.0503	0.2991	0.8883	1.0000	43.44	81.06	120.93
3	XS526-XS422.5	0.0385	0.1140	0.4717	0.9346	1.0000	34.98	66.77	111.10
4	XS422-XS387	0.1765	0.2819	0.6840	1.0000	1.0000	12.73	46.61	90.11
5	XS384-XS227	0.2346	0.5017	0.9248	1.0000	1.0000	8.95	31.86	55.70
6	XS226-XS92	0.2590	0.6356	0.9949	1.0000	1.0000	9.96	24.93	47.47
7	XS91-XS59	0.2381	0.6276	1.0000	1.0000	1.0000	10.87	25.50	47.51
8	XS58-XSA213	0.4060	0.7607	1.0000	1.0000	1.0000	1.11	19.23	40.26
9	XSA212-XSA187	0.8931	0.9977	1.0000	1.0000	1.0000	0.41	1.18	12.06
10	XSA186-XSA97	0.9828	0.9993	1.0000	1.0000	1.0000	0.30	0.67	1.89
11	XSA94-XSA2	1.0000	1.0000	1.0000	1.0000	1.0000	0.29	0.56	0.98

Key:
mm = millimeter

2.3.2 Reference Sediment Transport

A specific amount of sediment transport is termed a reference sediment transport. The term reference sediment transport is used instead of incipient sediment motion, because the latter does not have a unique definition; therefore, the conditions under which incipient motion occurs are difficult to define (Buffington and Montgomery 1997). We define three specific stages of sediment transport. These stages of sediment transport are primarily dependent upon the Shield's number, θ:

$$\theta = \frac{\tau_g}{\gamma(s-1)D_{50}} \qquad (2.3.2.1.1.1)$$

where: θ = dimensionless Shield's number
τ_g = grain shear stress
γ = specific weight of water
s = relative specific density of sediment
D_{50} = mean sediment size

Table 2-4 contains the definition of the three stages of sediment transport. The Shield's numbers associated with these different stages are approximates and subject to field verification. We choose these values as best estimate of the conditions on the San Joaquin River based upon personnel communication with MEI and values in the literature. A typical value for the reference Shield's stress is 0.04 (Parker 1990; Buffington and Montgomery 1997; Andrews 2000). However, there is significant variation, and Mueller et al. (2005) found it to vary between 0.01 and 0.1. Mueller et al (2005) found that the reference Shield's number was proportional to the river slope and suggested that the reference shear stress be approximated by:

$$\theta_r = 2.18S + 0.021$$

which for a slope of 0.0007 in the San Joaquin River, is $\theta_r = 0.023$.

Wilcock and Crowe (2003) use $\theta_r = 0.021$ if the fraction of sand in the surface layer is above 0.2, and $\theta_r = 0.03$ if the surface is devoid of sand. Exhibit A contains detailed information on the analytical methods used to compute the Shield's number for the entire reach at a variety of flows.

Table 2-4.
Suggested Stages of Sediment Transport Based Upon Shield's Number

Shield's Number	Description
0.03	**Slight Mobilization**: There will be a small, but measurable, sediment transport rate.
0.045	**Significant Mobilization:** Many particles are moving and there is a significant sediment transport rate. Some sand is mobilized in the interstitial spaces of the bed.
0.06	**Full Mobilization:** Practically all the bed material is in motion and there is significant reworking of river bed sediment and mobilization of sand within interstitial spaces.

This page left blank intentionally.

3.0 Results

3.1 Reach-Averaged Sediment Mobilization

The reach-averaged hydraulics were used to compute the flow at which there is different degrees of mobilization on a reach-averaged scale. If there is reach-averaged full mobilization, the majority of cross sections are experiencing a Shield's number of 0.06. If there is reach-averaged significant mobilization, the majority of cross sections are experiencing a Shield's number of 0.045. If there is reach-averaged slight mobilization, the majority of cross sections are experiencing a Shield's number of 0.03. The reach-averaged hydraulic data are given in Exhibit B. The discharge associated with each different stage of sediment transport is given in Figure 3-1. A maximum of 40,000 cfs was simulated in this analysis and therefore in some instances the flow must be larger than 40,000 cfs to attain the given reference shear stress.

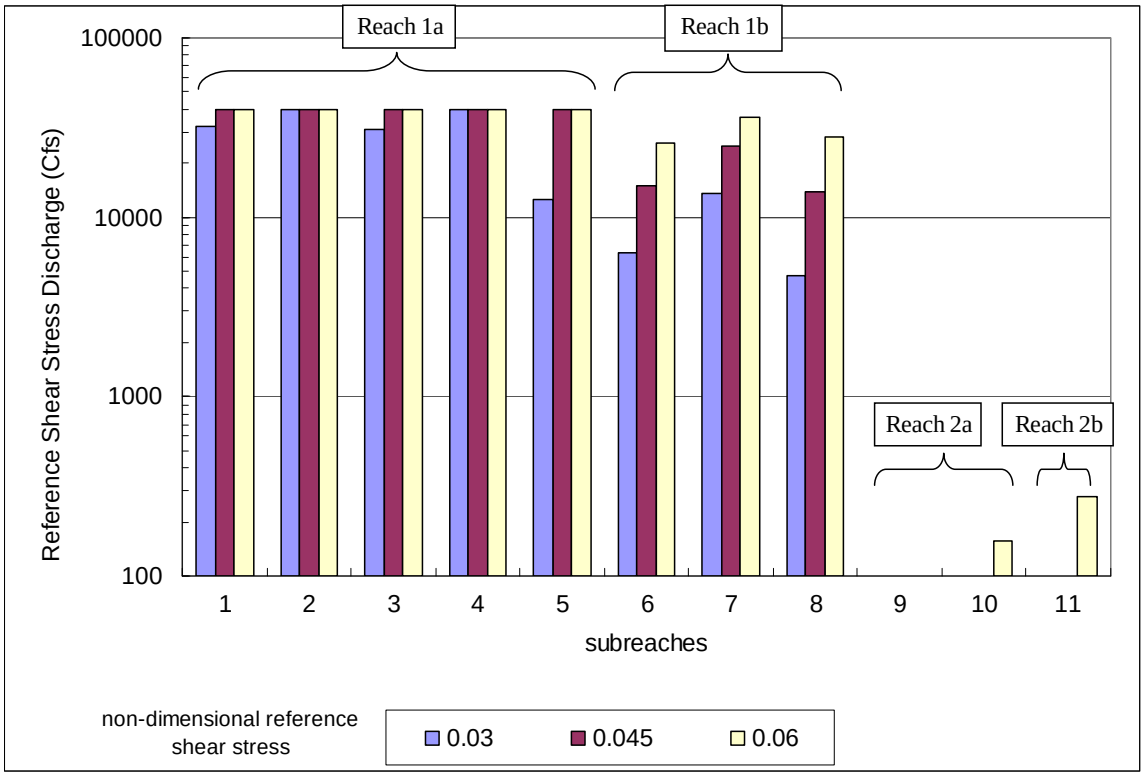

Figure 3-1.
Discharge at Various Reference Sediment Transport Conditions

Based upon the simulated hydraulics and sediment transport characteristics, Reach 1a experiences no reach-averaged slight mobilization for flows less than 10,000 cfs. We also predict that Reach 1b is not mobilized for flows less than 4,000 cfs. While Reach 1b does have reach-averaged slight mobilization for flows more than 4,000 cfs, it does not experience significant mobilization until the flow exceeds 10,000 cfs. The sand-bedded subreaches downstream from Gravelly Ford are somewhat movable, even for the hydraulic calculations associated with the smallest discharge simulated of 100 cfs.

3.2 Local Sediment Mobilization

Because little reach-averaged mobilization is predicted to occur in Reach 1, the mobilization of sediment in localized areas is analyzed. This analysis is necessarily limited by the fact that only 1D hydraulic results are used. If two-dimensional hydraulic results are available, more detailed analysis of sediment mobilization can be performed. Such analysis may be necessary if gravel augmentation is performed.

To show the ability of the maximum release under the SJRRP to transport sediment, an 8,000-cfs flow was simulated with HEC-RAS from Friant Dam to the Chowchilla Bifurcation Structure. The flow downstream from Chowchilla Bifurcation Structure on the San Joaquin River was limited to 4,500 cfs. The hydraulic results were analyzed at each cross section to determine the particle size that would experience a Shield's number of 0.03, 0.045, and 0.06. The bed material samples collected by Reclamation in February 2008, and the pebble count samples from Stillwater in 2002 and MEI in 1998, were matched to the cross section located closest to that sample. The results are shown in Figures 3-2 through 3-4. If the sampled D_{50} is above the line for a given flow rate, the Shield's number is not reached and "non-mobility" is predicted.

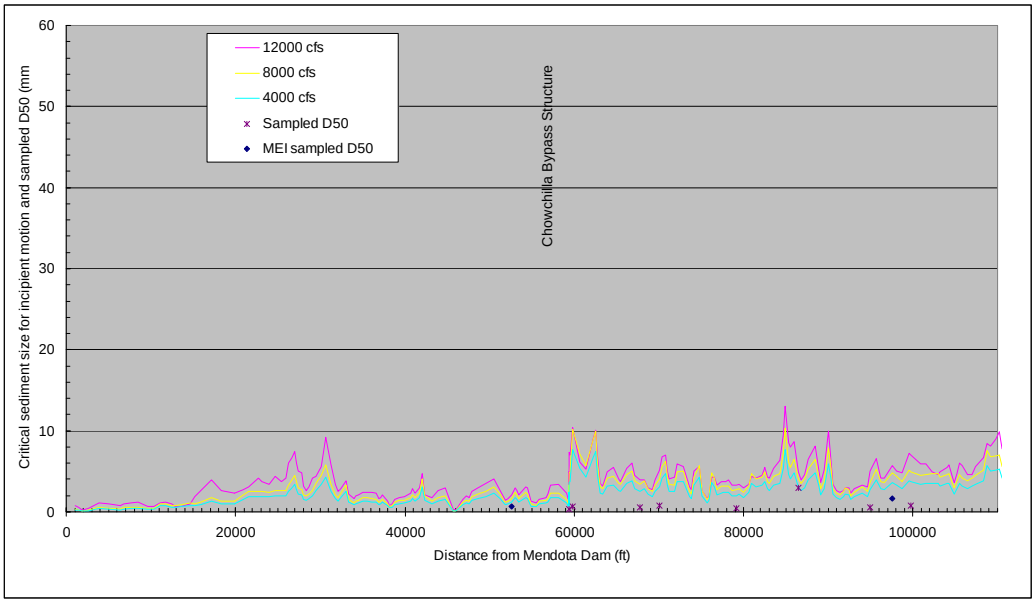

Figure 3-2.
Diameter at Which the Shield's Number Equals 0.045 at a Variety of Flows (Lower Reach 1b)

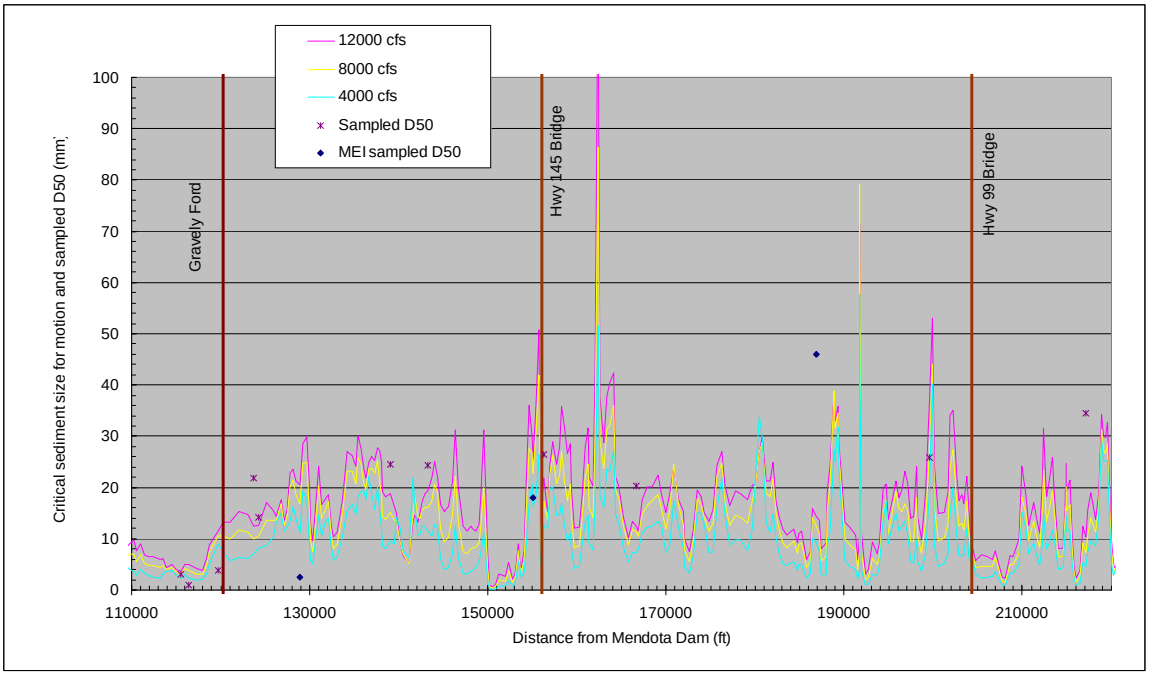

Figure 3-3.
Diameter at Which the Shield's Number Equals 0.045 at a Variety of Flows
(Lower Reach 1a and Upper Reach 1b)

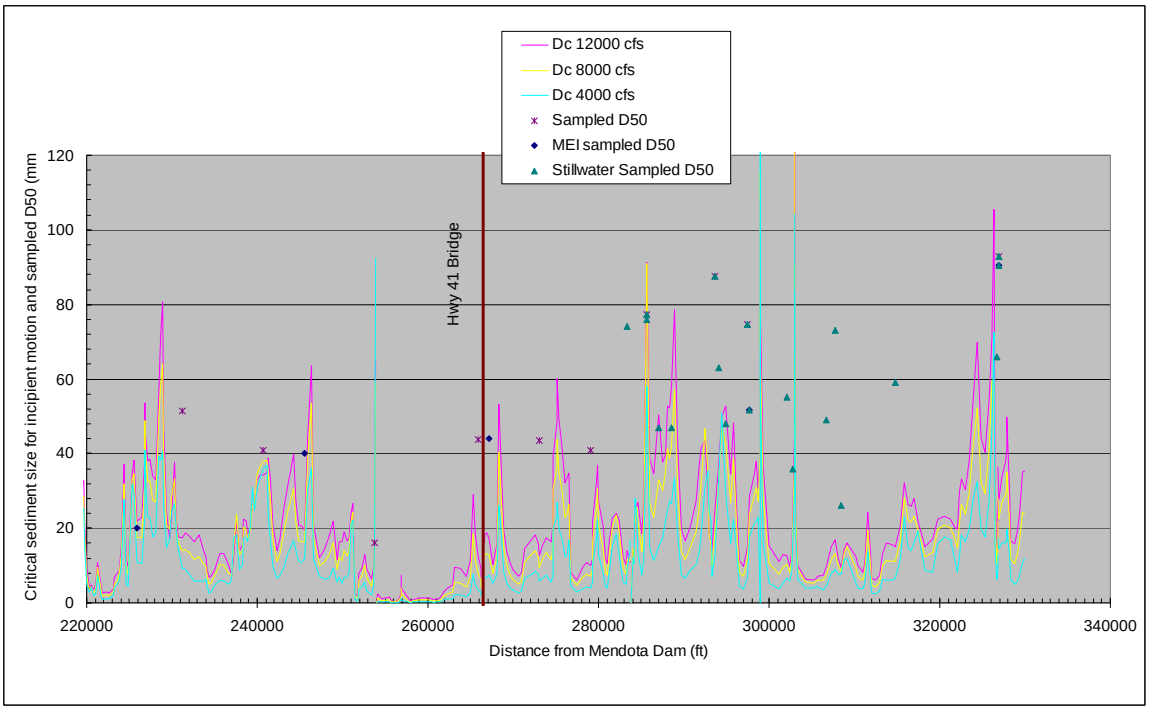

Figure 3-4.
Diameter at Which the Shield's Number Equals 0.045 at a Variety of Flows
(Reach 1a)

Downstream from Gravelly Ford, the model predicts that sediment moves at all cross sections at the given discharges. Upstream from Gravelly Ford, most of the samples had a D_{50} greater than that mobilized at a reference Shield's number of 0.045. Because of the scatter of data and the difficulty in using this graph, a more detailed analysis of the fraction of samples mobilized is performed.

The fraction of samples that experience various Shield's number over the full range of project flows was computed for Reaches 1a and 1b. The bed material samples collected by Reclamation in February 2008, and the pebble count samples from Stillwater in 2002 and MEI in 1998, were matched to the cross section located closest to that sample. There is considerable uncertainty in computing a local shear stress with a 1D model. However, the main purpose of this analysis is to compare the relative mobilization under Baseline and Project conditions, it is not to compute the absolute mobilization occurring. Mobilization of sediment at a local scale is difficult to predict because it requires a detailed hydraulic model that can accurately resolve the near-bed shear stresses. It also requires detailed topographic and bathymetric information. Lastly, it requires a detailed map of the bed material. The limitations of the assumptions made in this report are acknowledged, but the comparison between Baseline and Project conditions will remain valid, even if the absolute values of the degree of mobilization are uncertain.

The fraction of samples experiencing a given Shield's number was computed for a range of flows. The results are shown in Figures 3-5 through 3-7. Also shown in the figures are empirically fit functions that were used to represent the fraction of bed samples at which a specific Shield's number is exceeded. The function only represents current conditions and does not reflect future bed material changes induced by altered flows and/or channel and sediment management actions. Various functional forms were tried and the function with the best fit to the data was determined to be:

$$F = \frac{a}{\theta}\left[Q + b\theta^2\right]^{0.5} \qquad (3.2.1.1.1.1)$$

where: F is the fraction of sediment samples experiencing a Shield's number of θ or greater at a flow rate of Q in cfs

Parameters a and b were fit to each project reach. This analysis is intended to be a first approximation of mobilization that needs to be verified by field measurements. It is only to be used for the current channel hydraulic conditions. The parameter values used for Project Reaches 1a and 1b are given in Table 3-1. Graphs of the equations for Project Reaches 1a and 1b are given in Figure 3-8 and Figure 3-9.

In Reach 1a, we estimate that about 17 percent of the gravel sample sites will be slightly mobilized (Shield's number = 0.03) and 6 percent will be significantly mobilized (Shield's number = 0.045) at a flow of 8,000 cfs. In Reach 1b, approximately 43 percent of the gravel sample sites will be slightly mobilized and about 28 percent of the sites will be significantly mobilized at a flow of 8,000 cfs. These conclusions are subject to field verification of sediment mobilization. Several field studies to verify mobilization are recommended in the conclusions section.

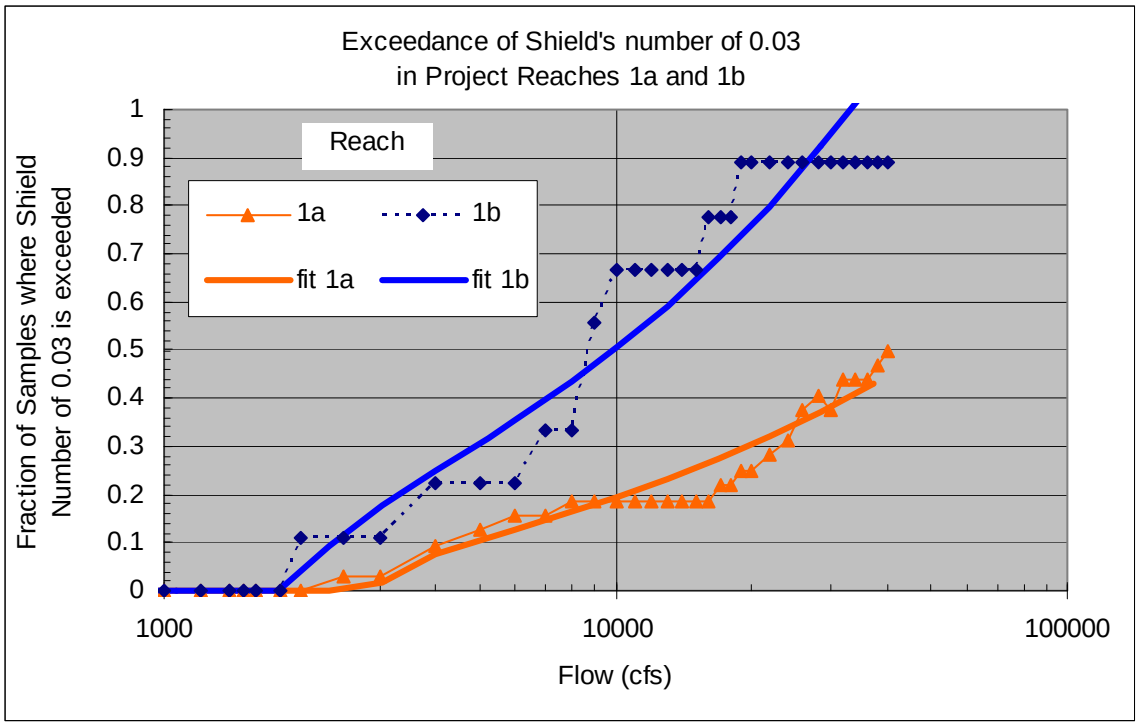

Note: Lines with symbols are a computed fraction of sample sites mobilized and solid lines are empirical fit functions.

Figure 3-5.
Fraction of Samples Experiencing a Shield's Number of 0.03 or Higher in Project Reaches 1a and 1b

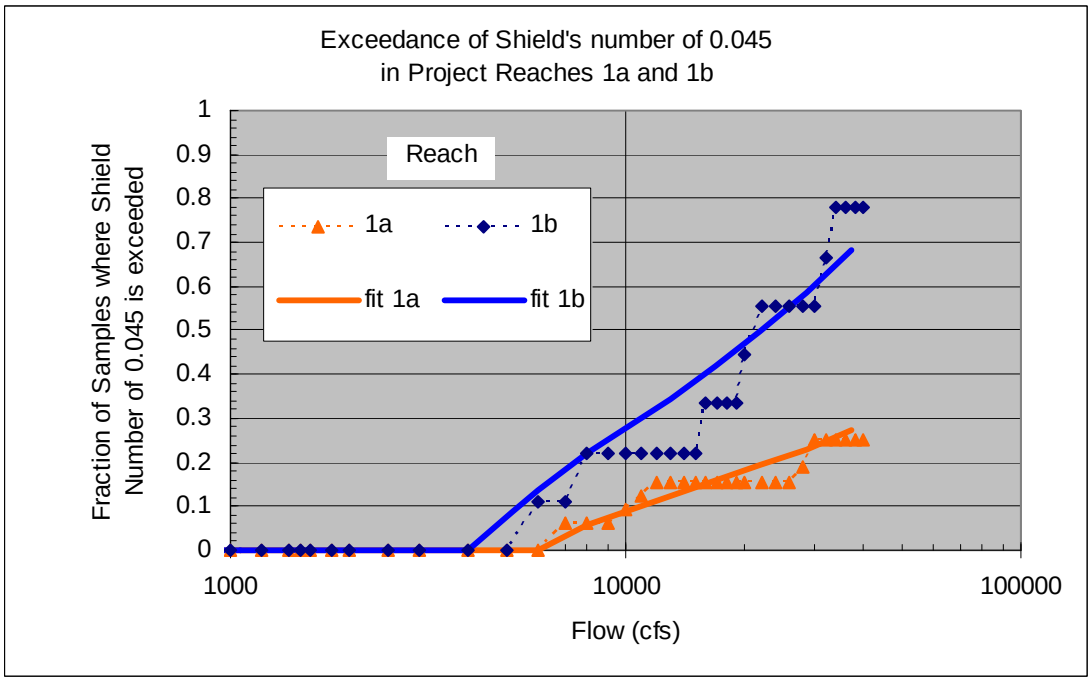

Note: Lines with symbols are a computed fraction of sample sites mobilized and solid lines are empirical fit functions.

Figure 3-6.
Fraction of Samples Experiencing a Shield's Number of 0.045 or Higher in Project Reaches 1a and 1b

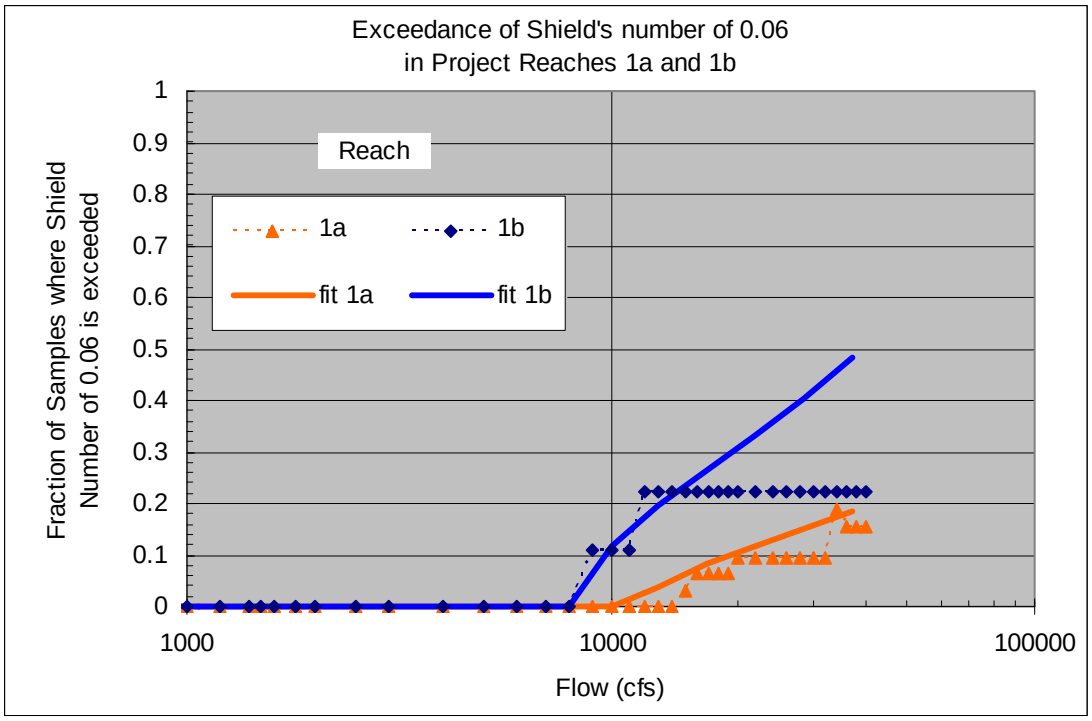

Note: Lines with symbols are a computed fraction of sample sites mobilized and solid lines are empirical fit functions.

Figure 3-7.
Fraction of Samples Experiencing a Shield's Number of 0.06 or Higher in Project Reaches 1a and 1b

Table 3-1.
Values for Bed Material Mobilization (Equation 3.1) in Project Reaches 1a and 1b for Existing Bed Material

Reach	*a*	*b*
1a	7.0E-5	-3.3E+6
1b	1.7E-4	-2.3E+5

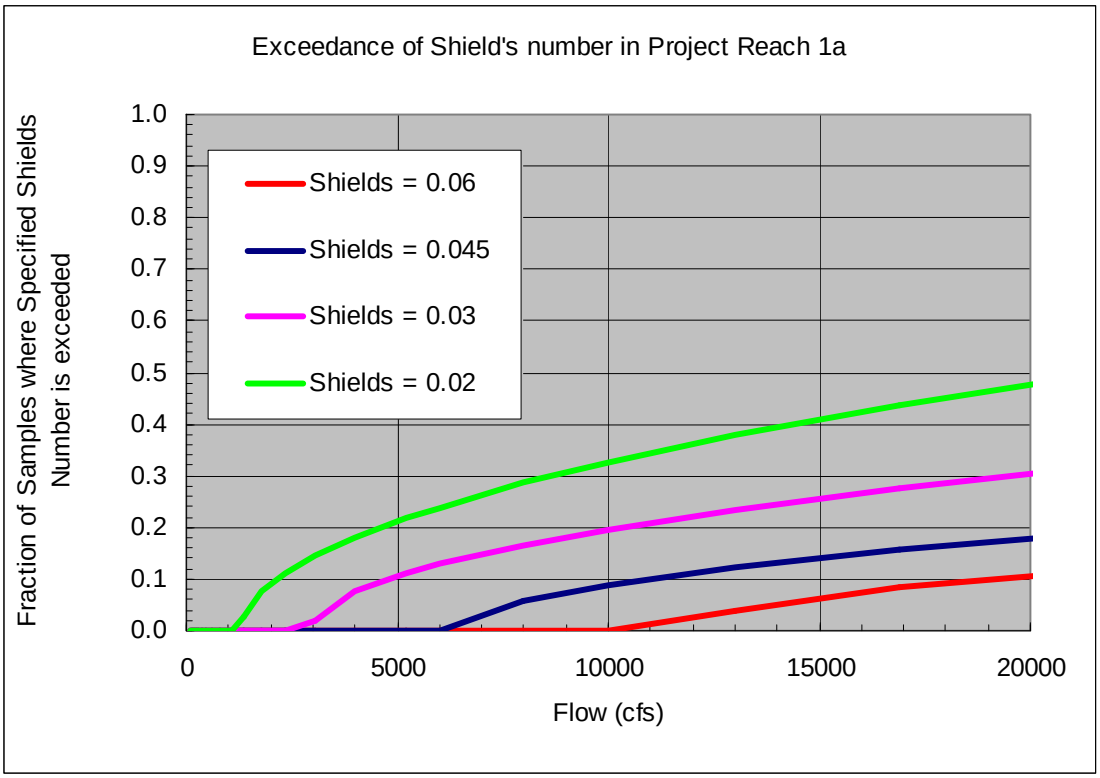

Figure 3-8.
Fraction of Samples Experiencing a Shield's Number in Project Reach 1a

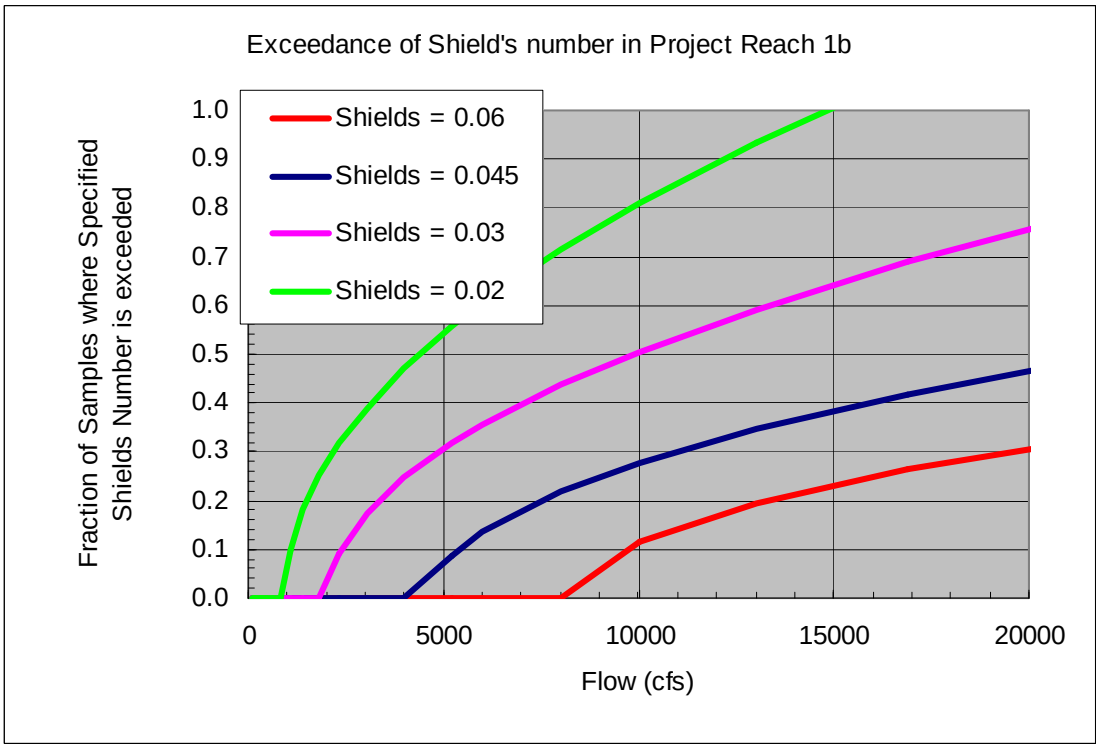

Figure 3-9.
Fraction of Samples Experiencing a Shield's Number in Project Reach 1b

If the flow is increased to 10,000 cfs, the number of sites slightly mobilized in Project Reach 1a will be increased from 17 percent to 20 percent. The number of sites slightly mobilized in Project Reach 1b will be increased from 44 percent to 50 percent. Therefore, there will be an increase in mobilization if the flow is increased from 8,000 to 10,000 cfs, but the increase is relatively small. We estimate that the flow would have to be increased to more than 20,000 cfs to slightly mobilize half of the sites in Reach 1a.

3.2.1 Mobilization under Historic, Baseline, and Project Conditions

An index of bed mobilization can be computed from summing the fraction of sites experiencing a given reference shear:

$$M = \sum_{i=1}^{nf} F_i$$

where: F = fraction of sites experiencing a given reference shear at flow i
nf = number of daily average flows
M = Mobilization index

The mobilization index, M, is an index of the total mobilization within a given reach. We believe it could be a useful metric to compare the mobilization of gravel under various conditions and compared to Historical Conditions. The mobilization index was computed for years 1980 to 2003 for Reaches 1a and 1b. It was computed for the Historical Gage daily average flow data, Baseline Conditions flow data, and Alternative A daily flow data. The stream flows were taken from Friant Dam for Reach 1a and from Gravelly Ford for Reach 1b. The index was also computed for reference shear stresses of 0.02, 0.03, 0.045, and 0.06. The results are shown in Figures 3-10 through 3-17.

Figure 3-12 shows the mobilization index for a reference Shield's number of 0.03 in Reach 1a. Alternative A has the smallest amount of mobilization, except for Year 1993. However, this year had an almost insignificant amount of mobilization. For all years other than 1993, the Historical Gage data show more mobilization than the Baseline Conditions. The flow modeling methodology may underestimate the peak releases from Friant Dam because it is based upon daily average flow data and during peak releases there may be significant variation within 1 day. Therefore, the Baseline Conditions show less mobilization than Historical Gage data. Alternative A shows less mobilization than the Baseline Conditions because there is an increase in flows under 2,300 cfs and a decrease in the frequency of flows more than 2,300 cfs under Alternative A. Because very little mobilization occurs at flows below 8,000 cfs, there is less gravel mobilization under Alternative A in Reach 1a.

Figure 3-13 shows the mobilization index for a reference Shield's number of 0.03 in Reach 1b. Overall, there is significantly more mobilization in Reach 1b because the bed material in this reach is significantly finer than in Reach 1a. The difference between the scenarios is different from Reach 1a, too. Alternative A generally shows similar to more mobilization than Baseline Conditions for most years. Also, Alternative A shows at least

some mobilization in all years, where Baseline Conditions shows little or no mobilization in Reach 1b for many years.

The mobilization index for a reference Shield's number of 0.045 in Reach 1a is shown in Figure 3-14. Alternative A shows the least mobilization at a reference Shield's number of 0.045 for all years except 1983. In Reach 1b, Alternative A has relatively more mobilization than Baseline Conditions for most years and some degree of mobilization for all years (Figure 3-15). The mobilization index for a reference Shield's number of 0.06 is small for all scenarios in Reach 1a (Figure 3-16). This means that there are very few sites where a reference Shield's number of 0.06 is exceeded in Reach 1a and very few sites that become fully mobilized under any condition. In Reach 1b, more sites exceed a reference Shield's number of 0.06, but Alternative A shows less mobilization than Baseline Conditions (Figure 3-17).

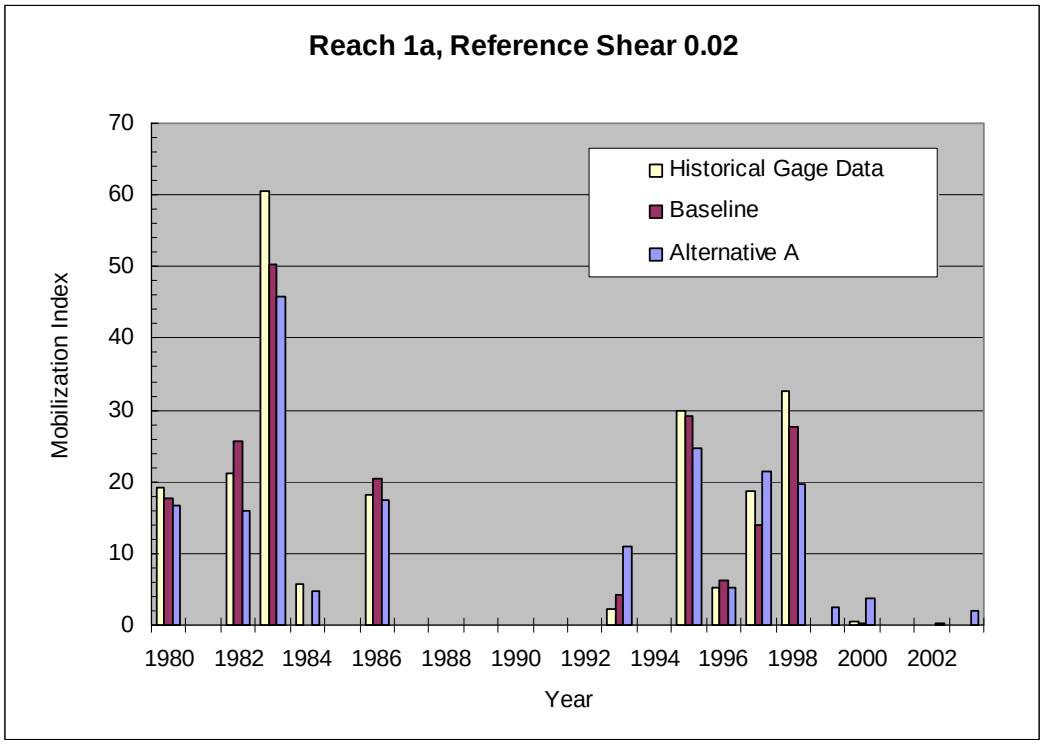

Figure 3-10.
Mobilization Index of the Historical Gage Data, Baseline Conditions, and Alternative A for Reach 1a for a Reference Shield's Number of 0.02

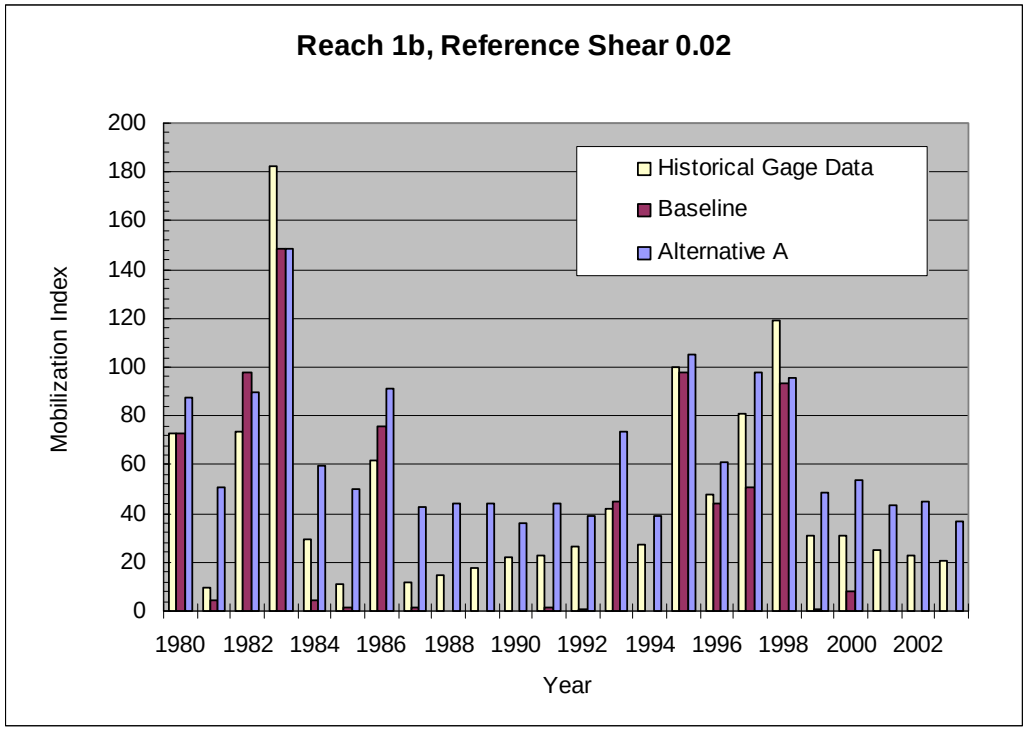

Figure 3-11.
Mobilization Index of the Historical Gage Data, Baseline Conditions, and Alternative A for Reach 1b for a Reference Shield's Number of 0.02

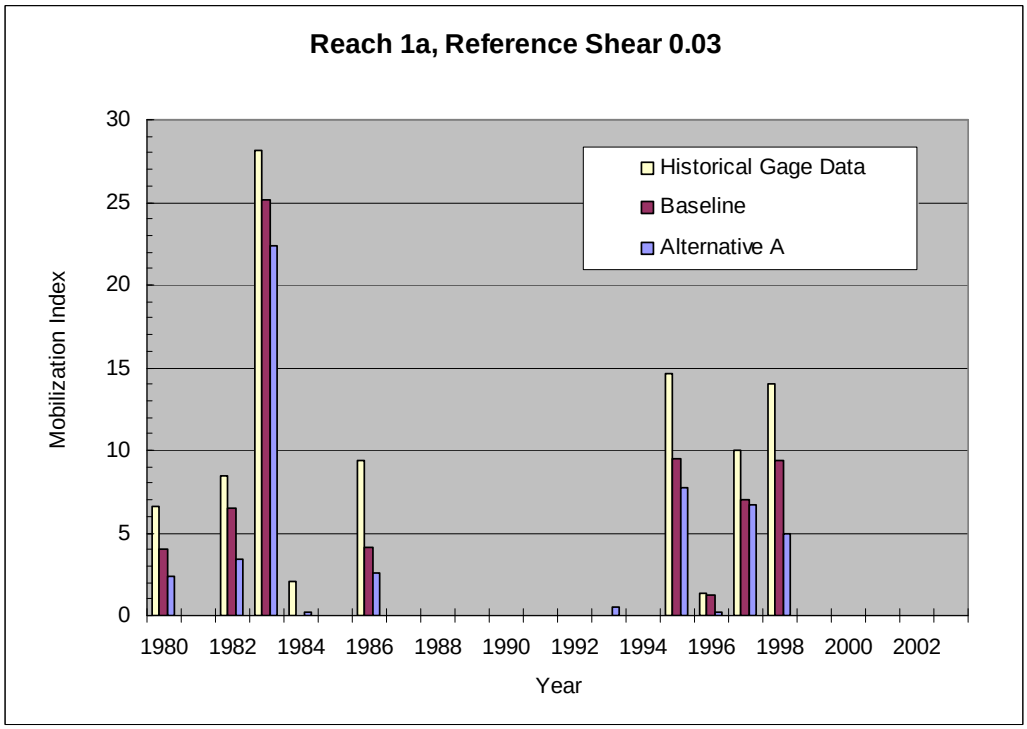

Figure 3-12.
Mobilization Index of the Historical Gage Data, Baseline Conditions, and Alternative A for Reach 1a for a Reference Shield's Number of 0.03

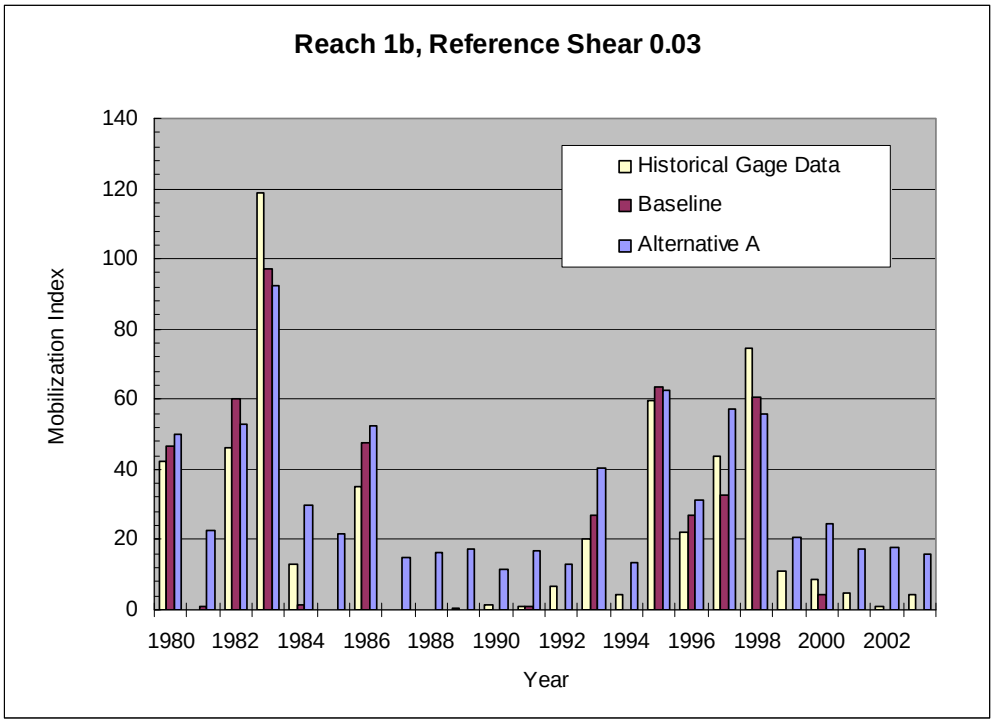

Figure 3-13.
Mobilization Index of the Historical Gage Data, Baseline Conditions, and Alternative A for Reach 1b for a Reference Shield's Number of 0.03

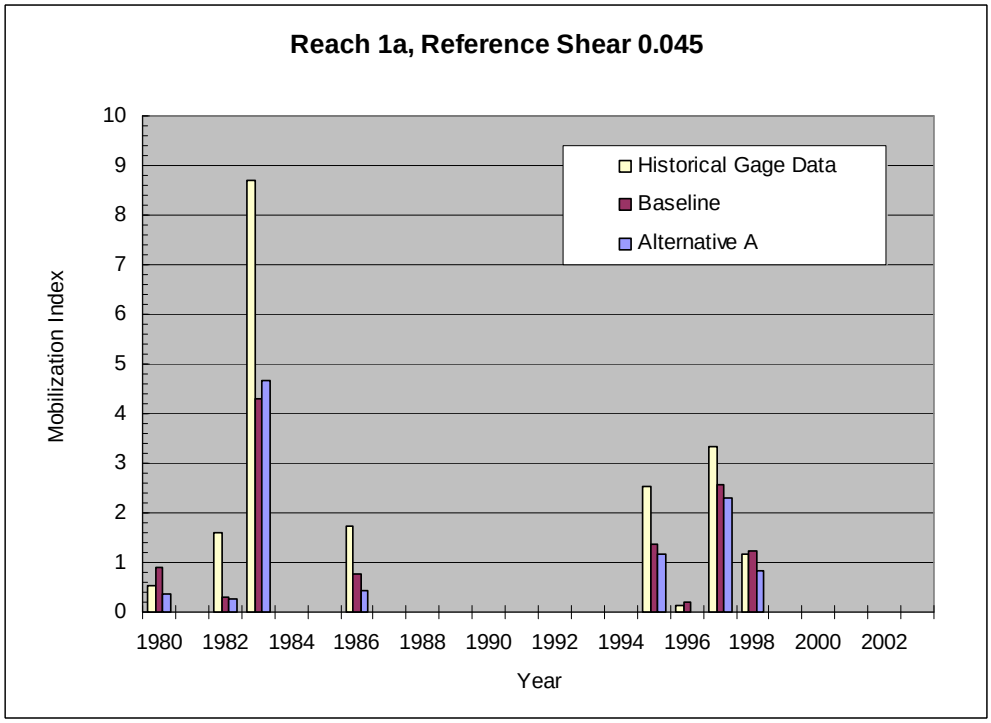

Figure 3-14.
Mobilization Index of the Historical Gage Data, Baseline Conditions, and Alternative A for Reach 1a for a Reference Shield's Number of 0.045

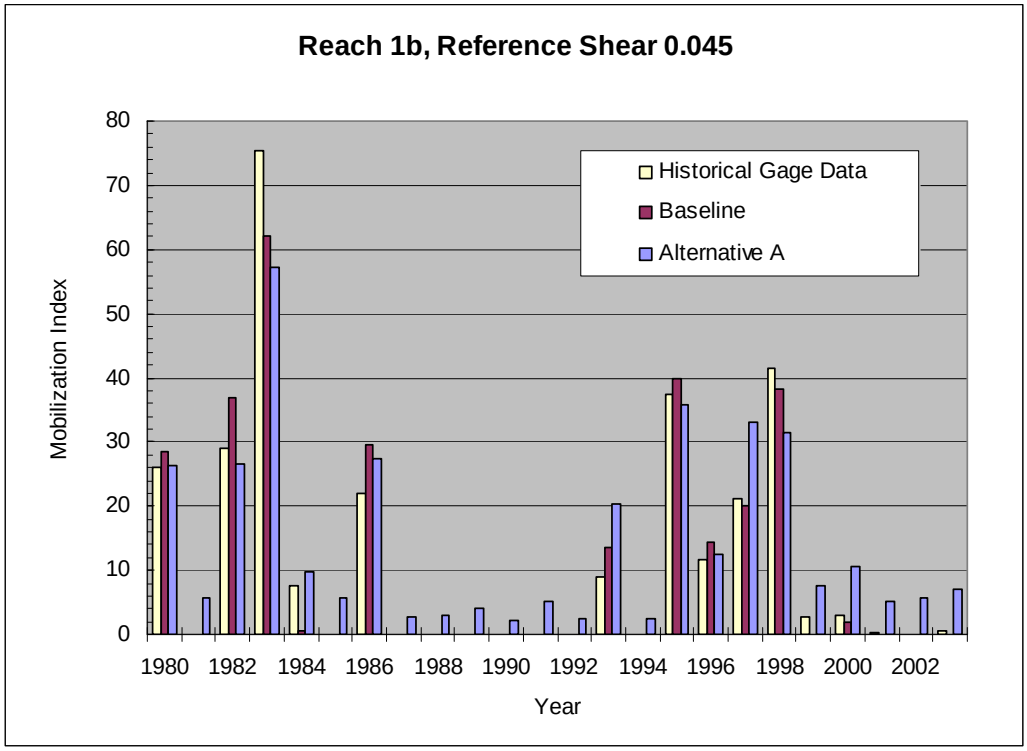

Figure 3-15.
Mobilization Index of the Historical Gage Data, Baseline Conditions, and Alternative A for Reach 1b for a Reference Shield's Number of 0.045

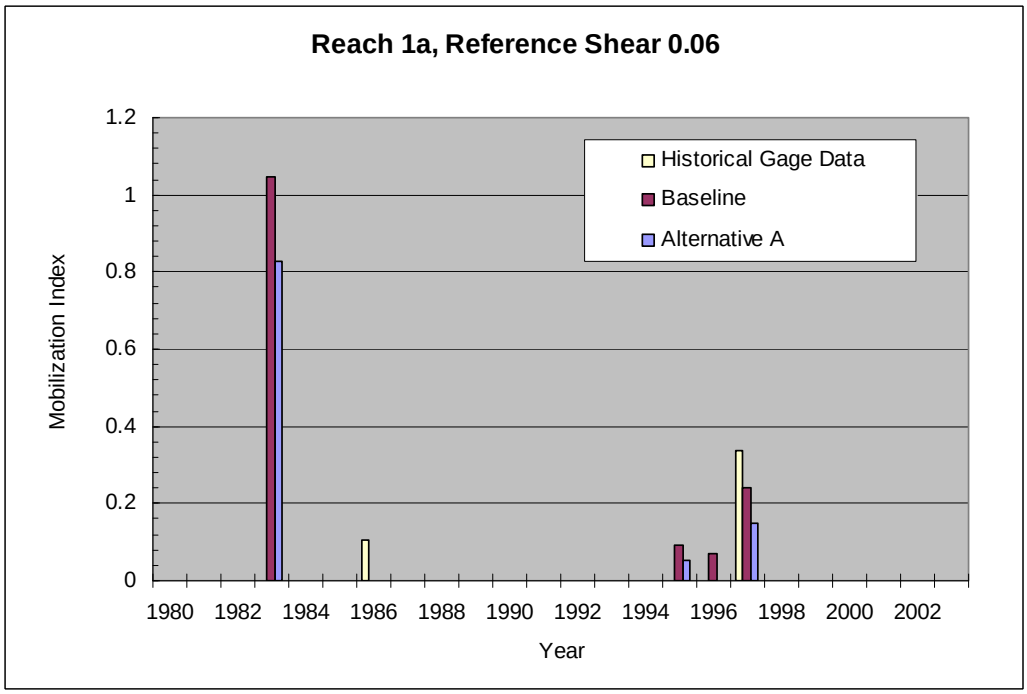

Figure 3-16.
Mobilization Index of the Historical Gage Data, Baseline Conditions, and Alternative A for Reach 1a for a Reference Shield's Number of 0.06

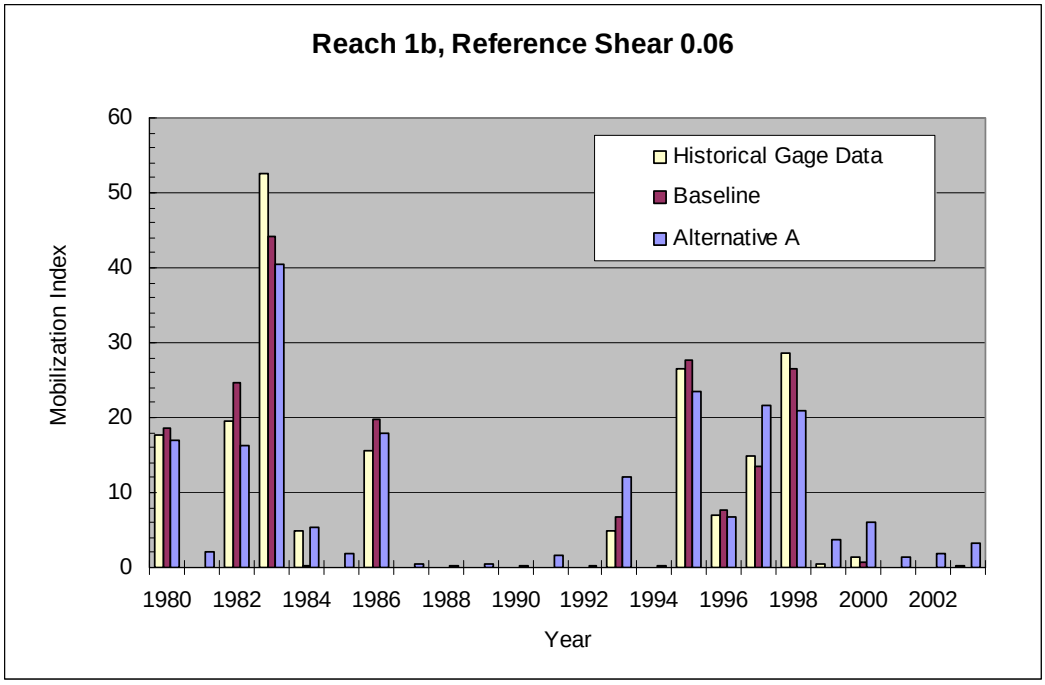

Figure 3-17.
Mobilization Index of the Historical Gage Data, Baseline Conditions, and Alternative A for Reach 1b for a Reference Shield's Number of 0.06

3.3 Mobilization of Augmented Gravel

To simulate a theoretical gravel augmentation effort in Reaches 1a and 1b, we assumed that the entire Reach 1 was composed of a single D_{50} and then we computed the fraction of sample sites mobilized under these conditions. We used D_{50}s of 20 mm, 30 mm, and 40 mm, and computed the parameter values a and b (see Equation 3.1) for Reaches 1a and 1b (see Table 3-2). The results are shown in Figures 3-18 through 3-20. A comparison between the mobilization of the augmented gravel versus the mobilization of the existing bed material is shown in Figures 3-21 and 3-22.

The fraction of sites mobilized in Reach 1a at a reference Shield's number of 0.045 for several different flows is given in Table 3-3. The current median bed material size in Reach 1a is approximately 40 mm and therefore the mobilization of the bed with a D_{50} is similar to Existing Conditions. Reducing the D_{50} from the existing to 30 mm will increase the fraction of significantly mobilized sites from 0.06 at a flow of 8,000 to 0.15. Reducing the median bed material size to 20 mm will increase the fraction of significantly mobilized sites at a flow of 8,000 cfs to 0.24, a factor of 4 increase.

The current median bed material size in Reach 1b is about 20 mm and therefore augmented with gravels larger than this will decrease bed mobility in this reach (Figure 3-22).

Table 3-2.
Values for Bed Material Mobilization in Project Reaches 1a and 1b for Existing Bed Material and Augmented Gravel

Reach and Bed Material	a	b
Existing Bed Material		
1a	7.0E-5	-3.3E+6
1b	1.7E-4	-2.3E+5
D_{50} = 20 mm		
1a	1.7E-4	-2.0E+6
1b	1.9E-4	-2.5E+6
D_{50} = 30 mm		
1a	1.1E-4	-2.0E+6
1b	1.4E-4	-4.0E+6
D_{50} = 40 mm		
1a	6.5E-5	-2.5E+6
1b	1.0E-4	-6.0E+6

Key:
mm = millimeter

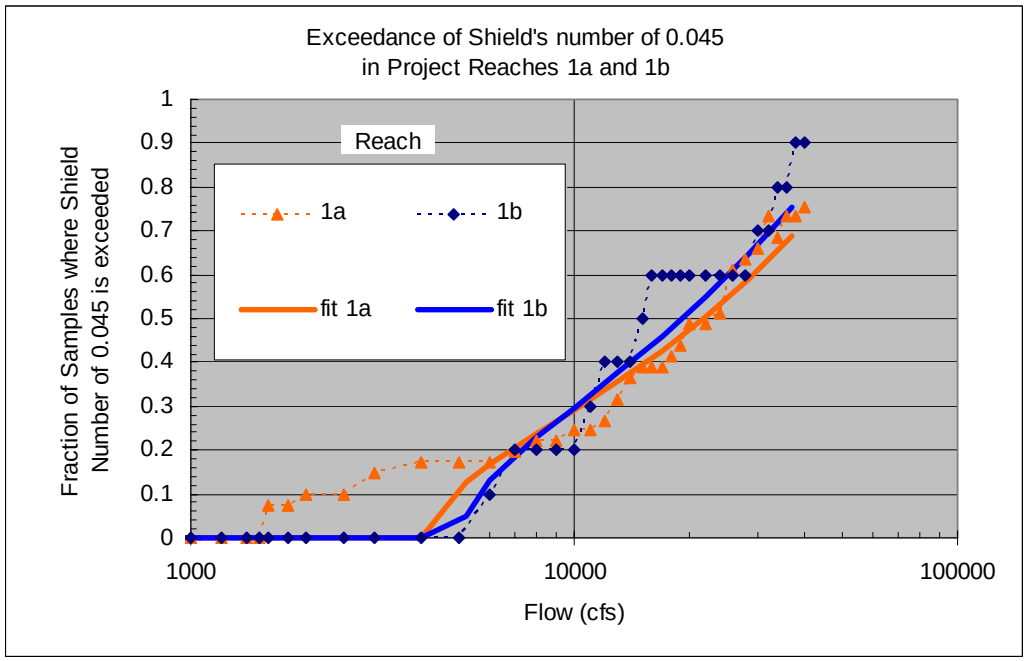

Figure 3-18.
Fraction of Sample Sites Where Shield's Number of 0.045 is Exceeded in Project Reaches 1a and 1b Assuming Augmented Gravel Size D_{50} of 20 mm

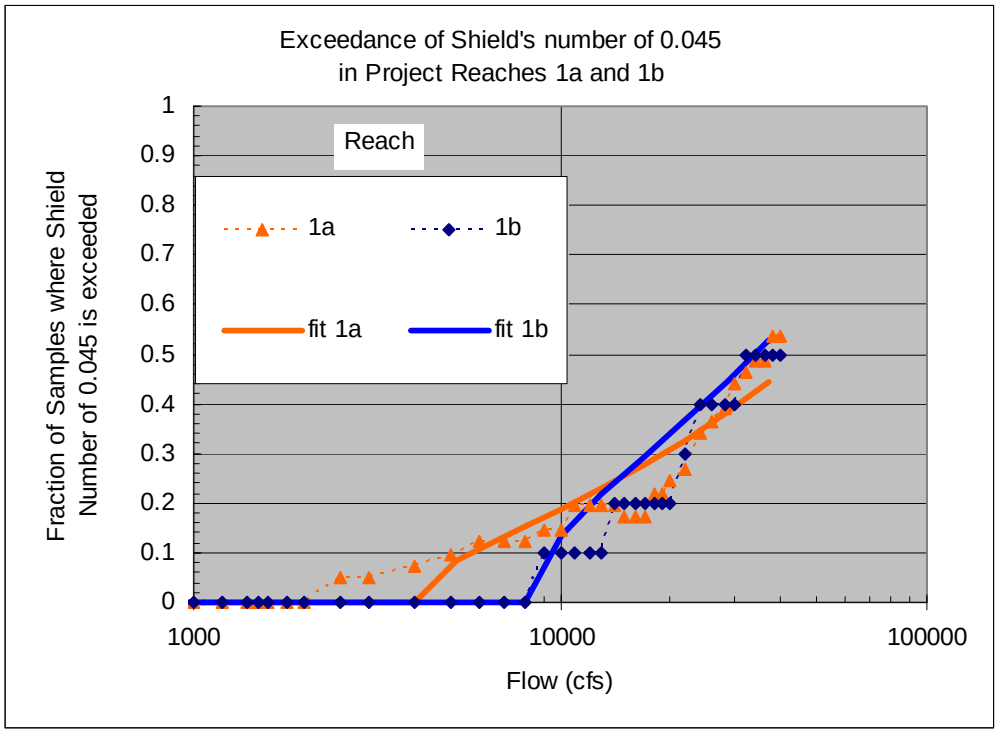

Figure 3-19.
Fraction of Sites Experiencing a Shield's Number of 0.045 or Higher in Project Reaches 1a and 1b Assuming Augmented Gravel Size of 30 mm

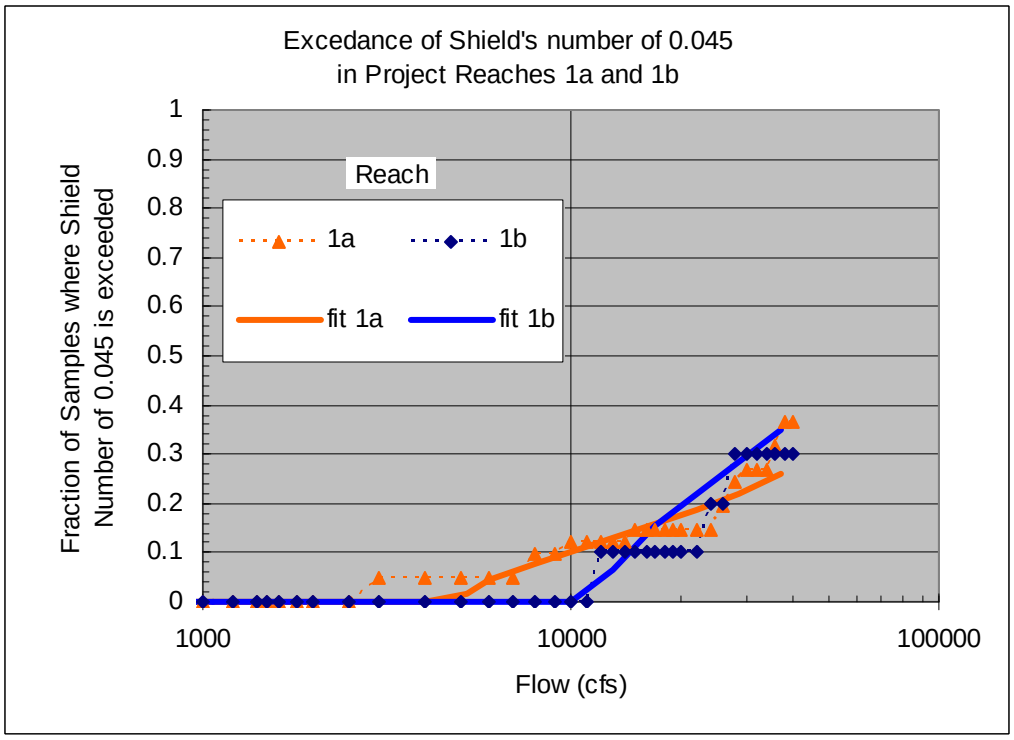

Figure 3-20.
Fraction of Sites Experiencing a Shield's Number of 0.045 or Higher in Project Reaches 1a and 1b Assuming Augmented Gravel Size of 40 mm

Table 3-3.
Fraction of Sample Sites Mobilized at a Shield's Number of 0.045 for Reach 1a for Various Bed Material D_{50s}

Bed Material D_{50}	Fraction mobilized at a Shield's number = 0.045			
	4,000 cfs	6,000 cfs	8,000 cfs	10,000 cfs
Existing	0	0	0.06	0.09
40 mm	0	0	0.08	0.10
30 mm	0	0.11	0.15	0.19
20 mm	0	0.17	0.24	0.29

Key:
cfs = cubic feet per second
mm = millimeter

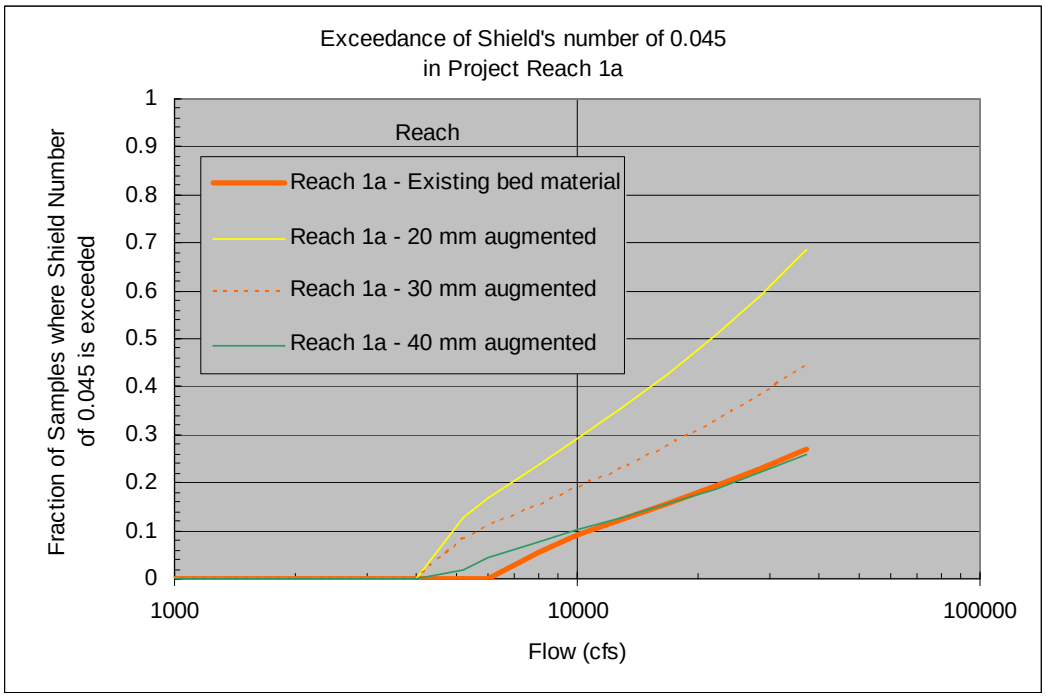

Figure 3-21.
Comparison of Mobilization for Existing and Augmented Gravel in Reach 1a

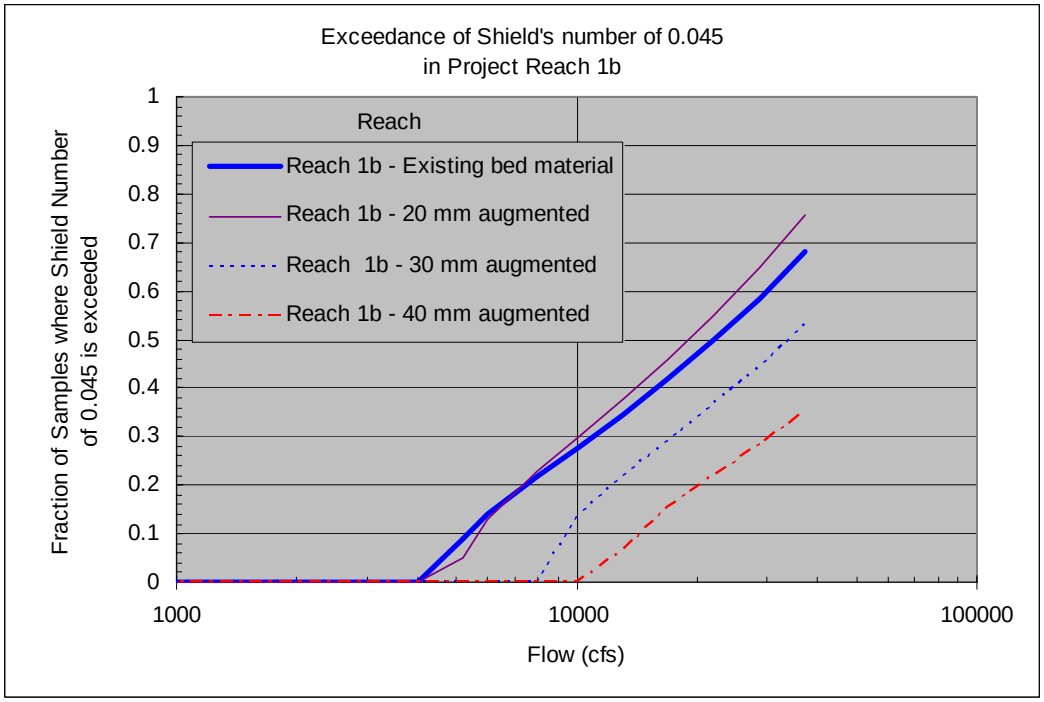

Figure 3-22.
Comparison of Mobilization for Existing and Augmented Gravel in Reach 1b

3.4 Sediment Mobilization after Channel Management

Various channel management strategies were analyzed to determine if sediment mobilization could be increased by reducing the main channel width and/or main channel depth as defined by the bank stationing. A separate FORTRAN program was written that reads bank locations and cross-section data from a HEC-RAS geometry file and calculates and outputs the new cross-section geometry by reducing the width and depth within the main channel. Figure 3-23 shows examples of the modified channel cross sections after reducing the width by 25 percent and 50 percent, compared with the original channel. Figure 3-24 shows examples of the modified channel cross sections after reducing both the width and depth by 25 percent and 50 percent, compared with the original channel. Channel management was only designed in Reaches 1a and 1b. The sediment is easily mobilized in Reaches 2a and 2b at low discharges and no channel management is necessary.

Results show that reducing the main channel width and depth does not improve the sediment mobilization. Figure 3-25 shows the incipient motion discharge in each subreach at various channel management options. For all channel management options, the flow required to mobilize sediment is increased. Sediment incipient motion usually occurs at high flow when the water is spilling into the floodplain. Reducing the main channel geometry reduces the flow in the main channel and the energy that can be used to transport sediment at high flow.

Figure 3-26 shows the fraction of sample sites mobilized for the various channel maintenance strategies. The results are similar to the reach-averaged results. Reducing the width and/or depth will decrease the mobilization of gravel in the San Joaquin River.

These results are assuming the entire width and/or depth is modified throughout Reach 1. It may be possible to locally increase mobilization of sediment by selective modification of river geometry. However, the sites must be relatively confined so that larger flows are not forced out of bank. In addition, locally reducing the width or depth may cause backwater conditions upstream from the site and decrease mobilization upstream from the channel modification.

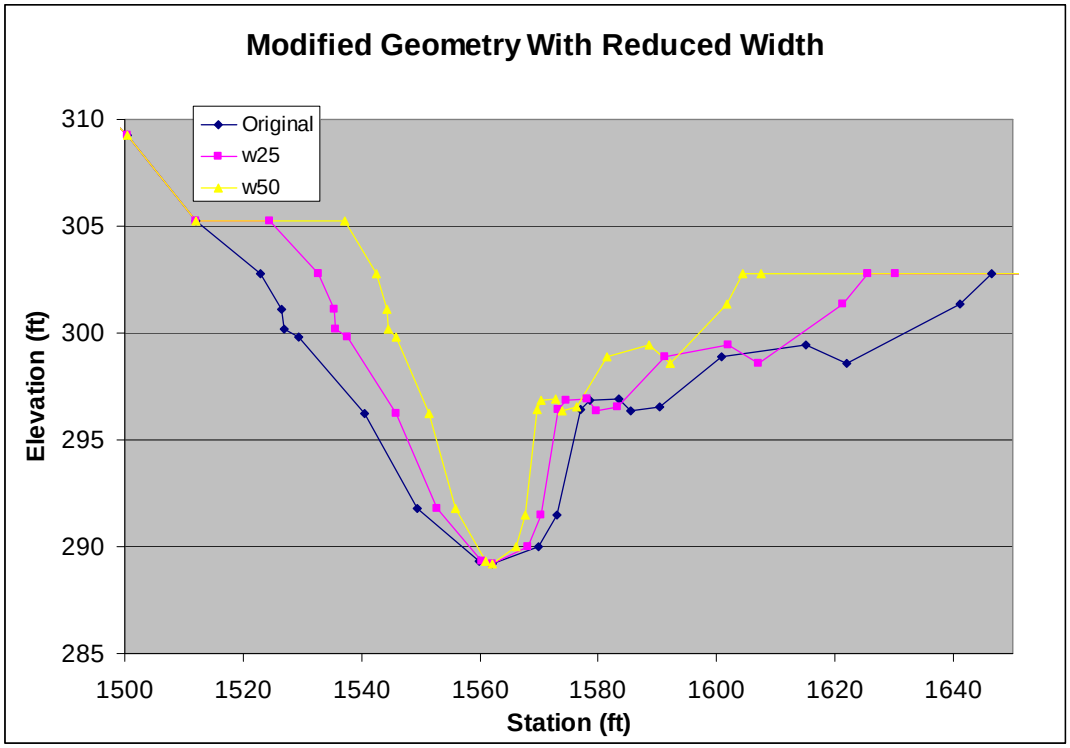

Figure 3-23.
Example of Modified Channel Cross Sections After Reducing the Main Channel Width by 25 Percent and 50 Percent

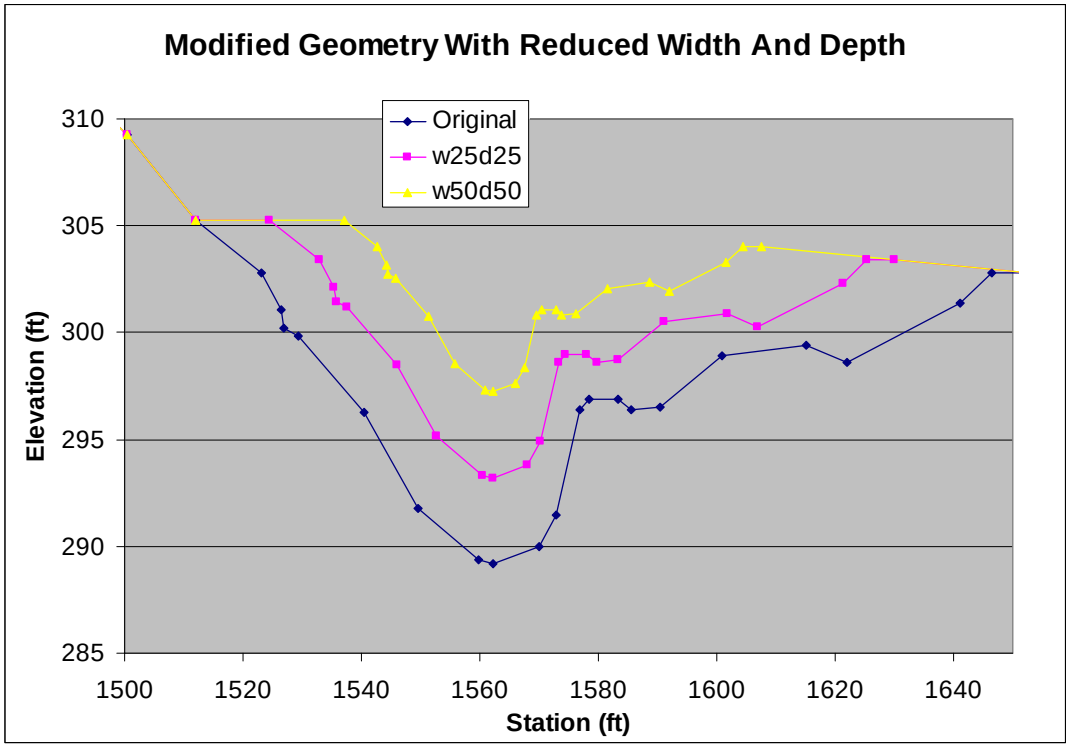

Figure 3-24.
Example of Modified Channel Cross Sections After Reducing the Main Channel Width and Depth by 25 Percent and 50 Percent

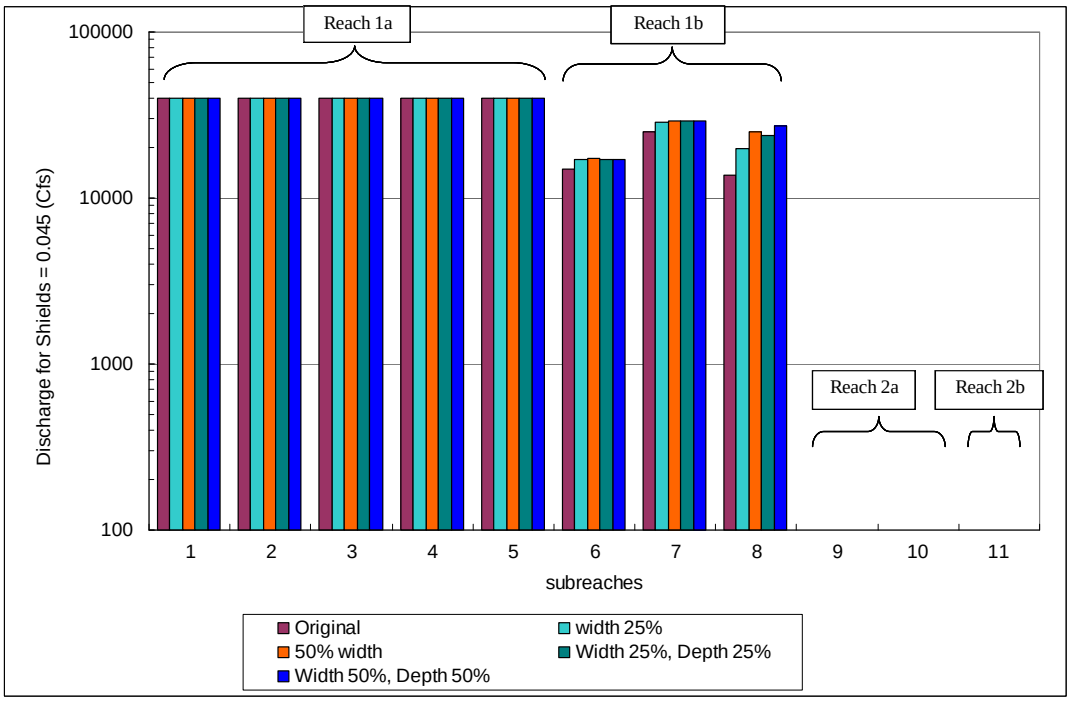

Figure 3-25.
Discharge Required to Achieve Reference Shield's Number of 0.045 and Mobilize Subreach D_{50} for Various Channel Management Options

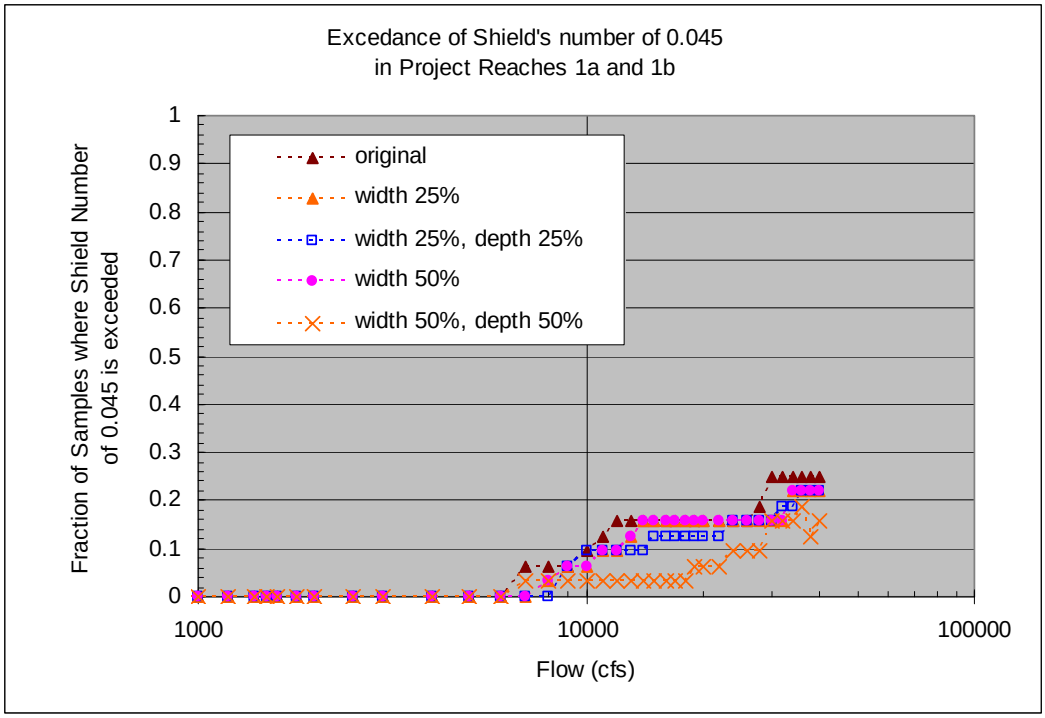

Figure 3-26.
Fraction of Samples Where a Shield's Number of 0.045 is Achieved in Project Reaches 1a for Various Channel Management Strategies

3.5 Sediment Transport Capacity

The reach-averaged sediment transport capacity was calculated with the averaged hydraulic properties and averaged bed material size fractions. Three methods are used:

- Parker (1990): gravel transport equation combined with Engelund and Hansen's (1972) sand transport equation
- Wilcock and Crowe (2003): gravel-sand-mixed transport equation combined with Engelund and Hansen's (1972) sand transport equation
- Wu et al. (2000): non-uniform sediment transport for gravel and sand

Results using the Parker equation are given in Figure 3-27, Wilcock and Crowe's equation in Figure 3-28, and Wu et al.'s formula in Figure 3-29. The shear stress is corrected as specified in each method. In Parker's model, the equivalent roughness height, k_s, is set to 2 D_{90}, and in Wilcock and Crowe's method k_s = 2 D_{65}. Wu et al. has a shear stress correction implicit in the formula.

The reach-averaged hydraulics did not cause significant mobilization of the coarse gravel in Project Reaches 1a and 1b, and therefore there is also little sediment transport predicted in these reaches. Reaches 2a and 2b have much higher transport capacities because these are sand-bed reaches, which are easily mobilized. In the next section, these

sediment transport capacities are combined with the flow-duration curves to predict the annual average transport rates for both the Baseline and Project conditions.

Determining the best predictor of sediment capacity requires sediment load samples; therefore, transport equations and associated parameters within the transport formulae are treated as a sensitivity parameter pending a sampling program. Two parameters, the non-dimensional reference Shield's number, θ_r, and hiding coefficient, α, are used in all three methods. The standard values of these two parameters are listed in Table 3-4. Sensitivity analysis was performed for the Parker's gravel transport equation combined with Engelund and Hansen's sand transport equation and results were given in Exhibit C. These parameters may be calibrated once field measurements of bed load and suspended load are obtained.

Table 3-4.
Standard Parameters Used in Transport Formula

Equation	θ_r	α
Parker (1990)	0.04	0.9
Wilcock and Crowe (2003)	0.021	0.33
Wu et al. (2000)	0.03	0.6

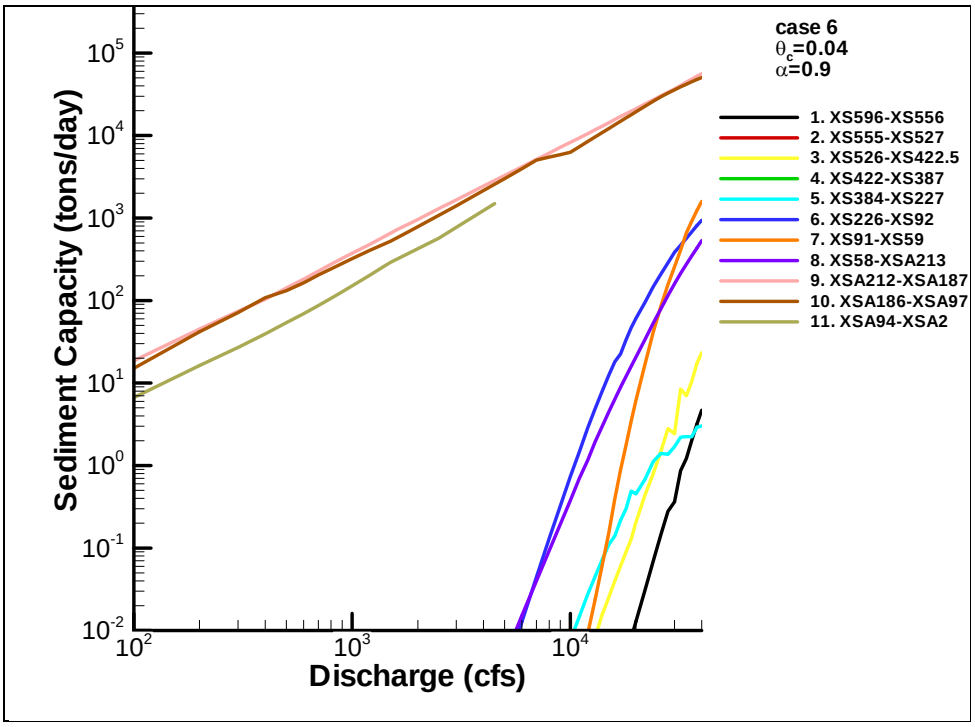

Figure 3-27.
Sediment Transport Capacity with Parker's Gravel-Sand-Mixed Equation Combined with Engelund and Hansen's Sand Equation

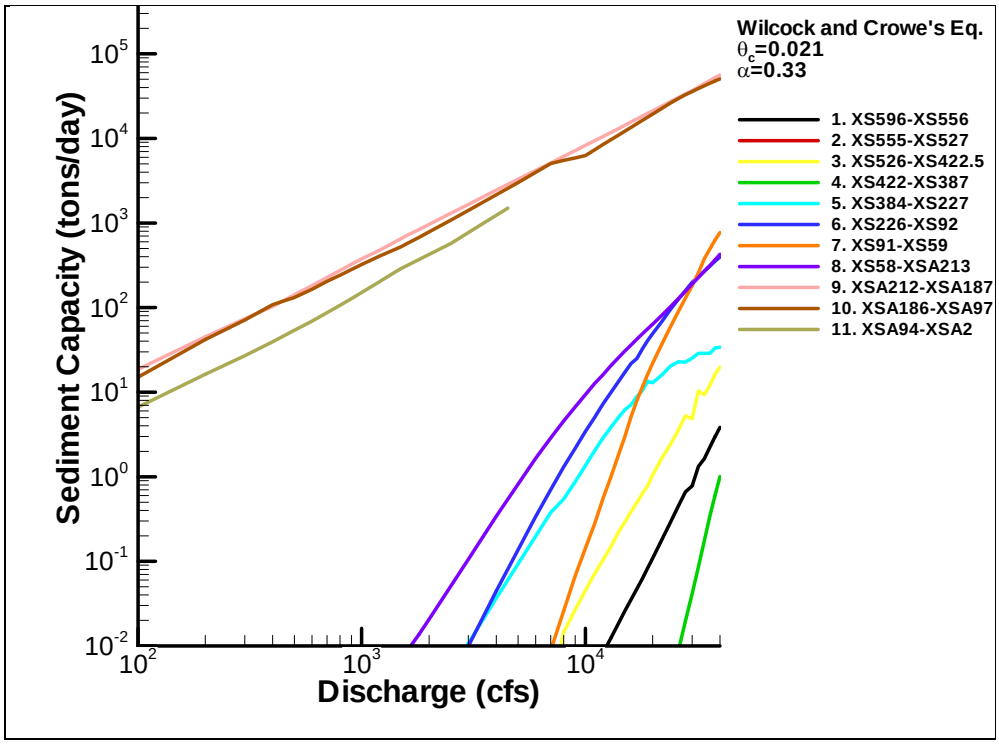

Figure 3-28.
Sediment Capacity with Wilcock and Crowe's Gravel-Sand-Mixed Equation Combined with Engelund and Hansen's Sand Equation

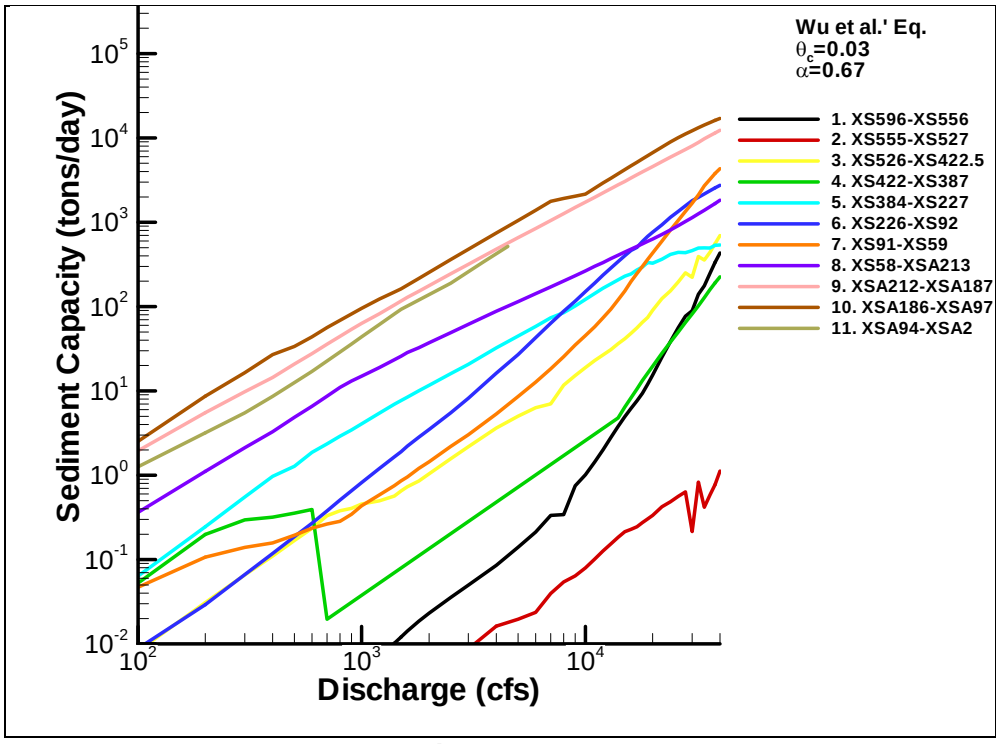

Figure 3-29.
Sediment Capacity with Wu et al.'s Nonuniform Sediment Transport Formula

3.5.1 Annual Sediment Load of Historic Hydrology

The reach-averaged annual sediment load was predicted by the sediment transport capacity and flow-duration curves, based upon the period from January 1, 1980, through May 31, 1997, as described in the hydrology section. The three methods and associated parameters (Table 3-4) discussed in the previous section were used for Reaches 1a and 1b. In Reaches 2a and 2b, where the channel bed was sand dominated, Engelund and Hansen's method, Laursen's modified version formula, Brownlie's method, and Yang's 1973 sand formula were used. The average annual sediment load in each reach using the historic hydrology is given in Figure 3-30. The bar graphs show the average along with the predicted range of sediment transport, as computed using the various formulae. Sensitivity analysis was performed and the results are given in Exhibit D of this report.

The small and large gravel transport was calculated to be less than 10 tons/year (yr) for most of Reach 1a, and generally less than 100 tons/yr for Reach 1b. The sand transport in Reach 1 is limited by the sand supply. The analysis only considers the sand available in the bed material sampled in the point bars and underwater portions of the channel. At high flows, it is likely that more sand supply exists in the over bank areas and in the pools in Reach 1. However, it is difficult to quantify this additional source and it has not been extensively sampled or mapped. The sand loads presented in Reach 1 for all conditions are considered lower bound estimates and the actual transport rates could be much higher.

The largest predicted gravel load is just downstream from Gravelly Ford where some medium gravel exists. Downstream from Gravelly Ford, very fine gravel (2 mm to approximately 4 mm) exists, which also gives high predicted annual gravel loads in this reach. The annual sand transport is largest in Reach 2a with approximately 86,000 tons/yr being transported. Reach 2b transports significantly less sediment, approximately 4,300 tons/yr, because this reach has a lower slope and is downstream from where flood flows are diverted into the bypass system.

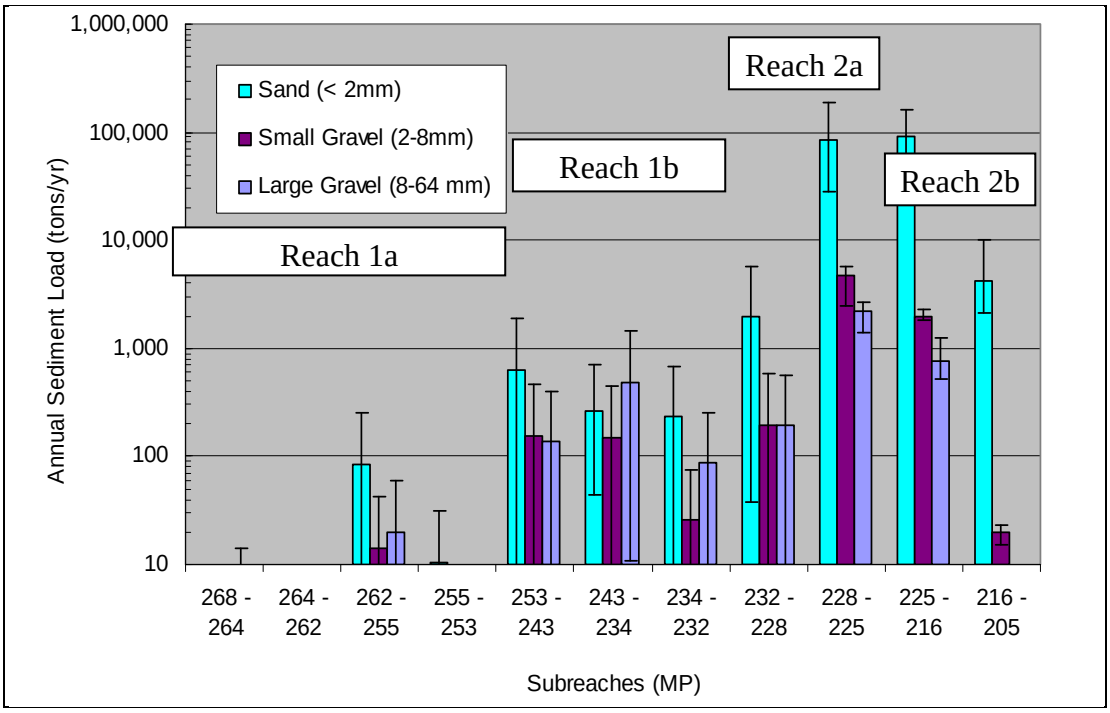

Figure 3-30.
Computed Annual Sediment Load Predicted by Averaging Three Different Methods Using the Historical Hydrology for All Flows Between January 1, 1980, and May 31, 1997

3.5.2 Annual Sediment Load of Baseline Conditions Hydrology

The reach-averaged annual sediment load under Baseline Conditions hydrology was predicted using the sediment transport capacity and flow-duration curves based upon the period from January 1, 1980, through September 30, 2003. A longer period of record was used in this case because the main goal of this analysis was to compare Baseline Conditions against Project Conditions (Alternative A). A longer period of flow record will give a more representative flow-duration curve. The same sediment transport equations were used as the calculations with Historical hydrology.

The small and large gravel transport were each generally calculated to be less than 10 tons/yr for most of Reach 1a, and generally less than 100 tons/yr for Reach 1b (Figure 3-31). The estimates for the sand-sized sediment transport in this reach are considered to be lower estimates because of the uncertainty in the availability of sand in this reach.

The sand transport just upstream from the Chowchilla Bypass (lower part of Reach 2a) is estimated to be 66,000 tons/yr. The small and large gravel transport is 1,400 tons/yr and 520 tons/yr, respectively, in the lower part of Reach 2a. The sand transport between Chowchilla Bypass to Mendota Pool (Reach 2b) is 3,400 tons/yr under Baseline Conditions.

The sand sediment load under Baseline Conditions is decreased in the lower three reaches relative to the Historical Conditions.

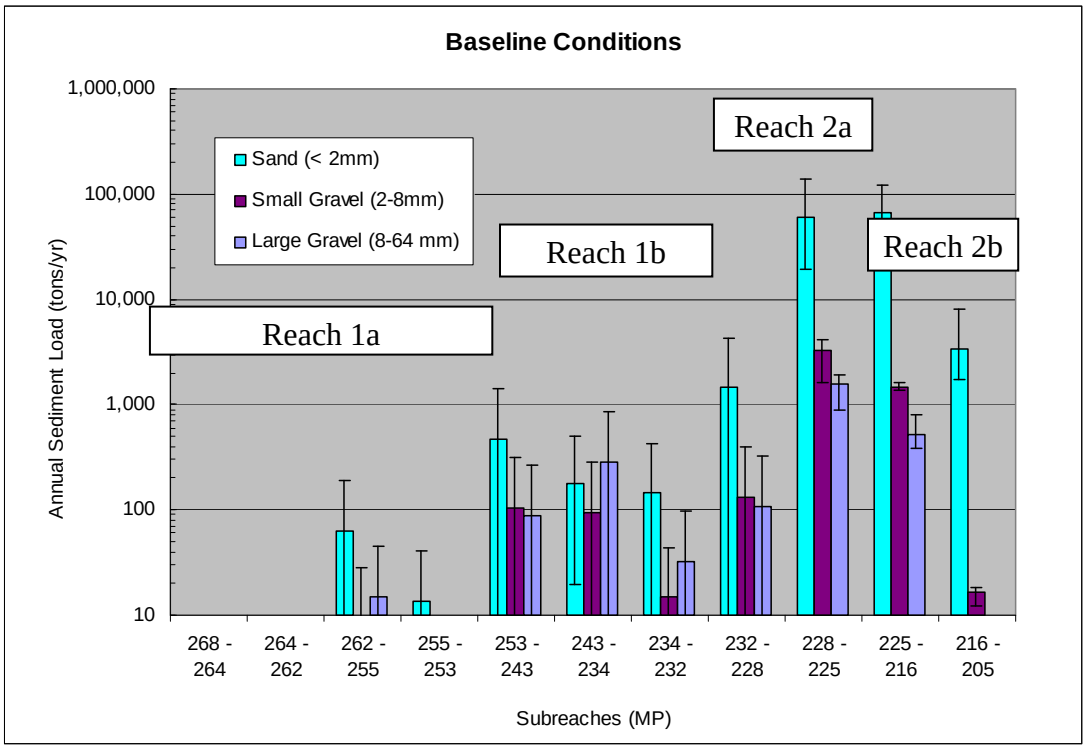

Figure 3-31.
Computed Annual Baseline Conditions Sediment Load Predicted By Averaging Three Different Methods for All Flows Between January 1, 1980, and September 30, 2003

Water Year 1997 was a wet year with the highest peak discharge since the construction of Friant Dam. The probability that such a peak flow occurs in the near future is considered low. Thus, the Baseline hydrology was simulated to compute the annual sediment loads based upon the period from January 1, 1980, through September 30, 2003, without Water Year 1997 (Figure 3-32). The difference between the Baseline hydrology with and without Water Year 1997 is shown in Figures 3-33 and 3-34. Compared with the annual load with Water Year 1997, the annual sand and gravel transports decreases without Water Year 1997 an average of 6 percent to 12 percent in Project Reaches 1a, 1b, and 2a. For example, in the upper part of Reach 2a, the predicted sand transport decreases from 60,000 tons/yr to 55,000 tons/yr, small gravel from 3,300 tons/yr to 3,000 tons/yr, and large gravel from 1,600 tons/yr to 1,400 tons/yr. Without Water Year 1997, sediment transport downstream from the Chowchilla Bifurcation Structure decreases about 4 percent. The sand and small gravel transports decreases from 3,430 tons/yr and 16.4 tons/yr to 3,280 tons/yr and 15.6 tons/yr, respectively.

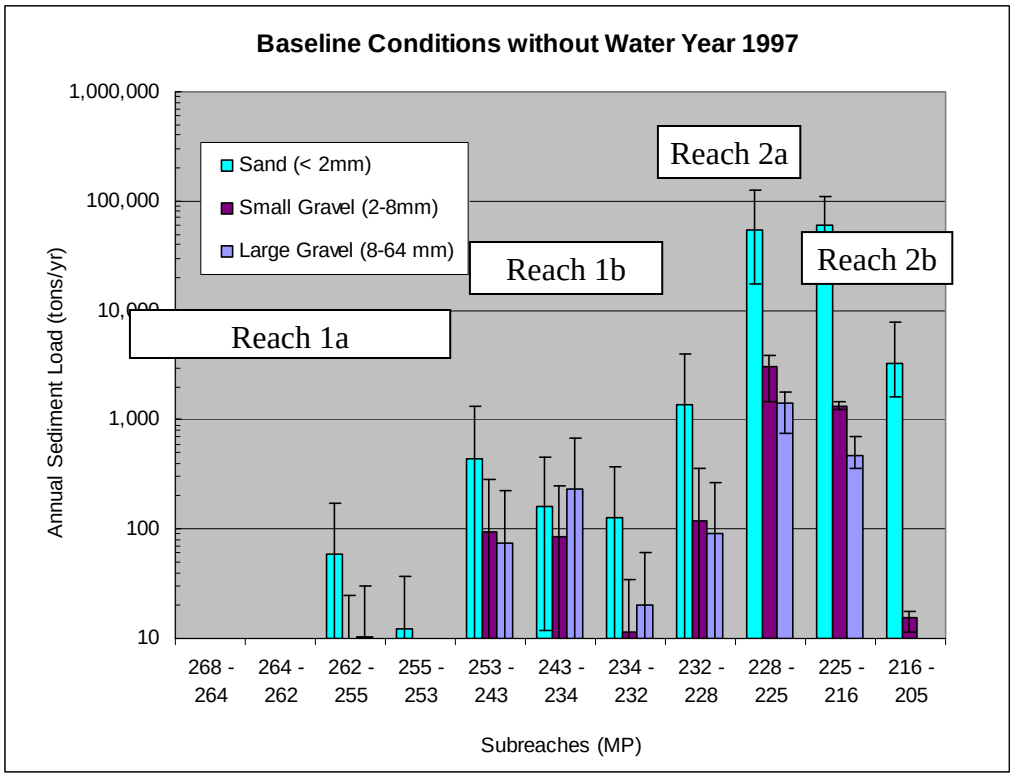

Figure 3-32.
Computed Annual Sediment Load Predicted By Averaging Three Different Methods Using Period from January 1, 1980, and September 30, 2003 Without Water Year 1997

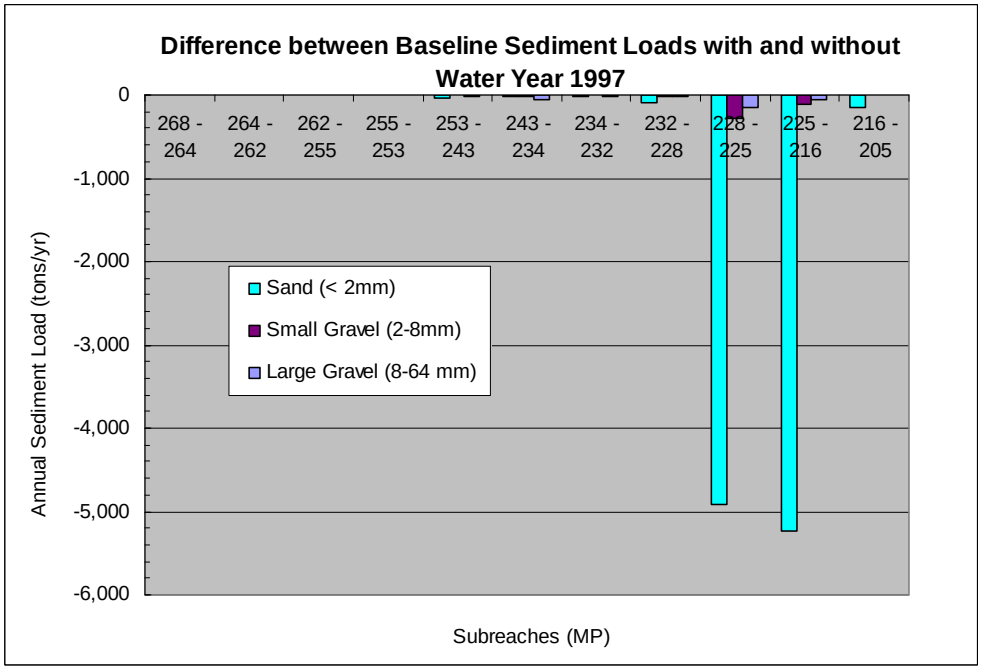

Figure 3-33.
Difference Between Baseline Sediment Loads With and Without Water Year 1997 for Sand and Gravel Size Sediment

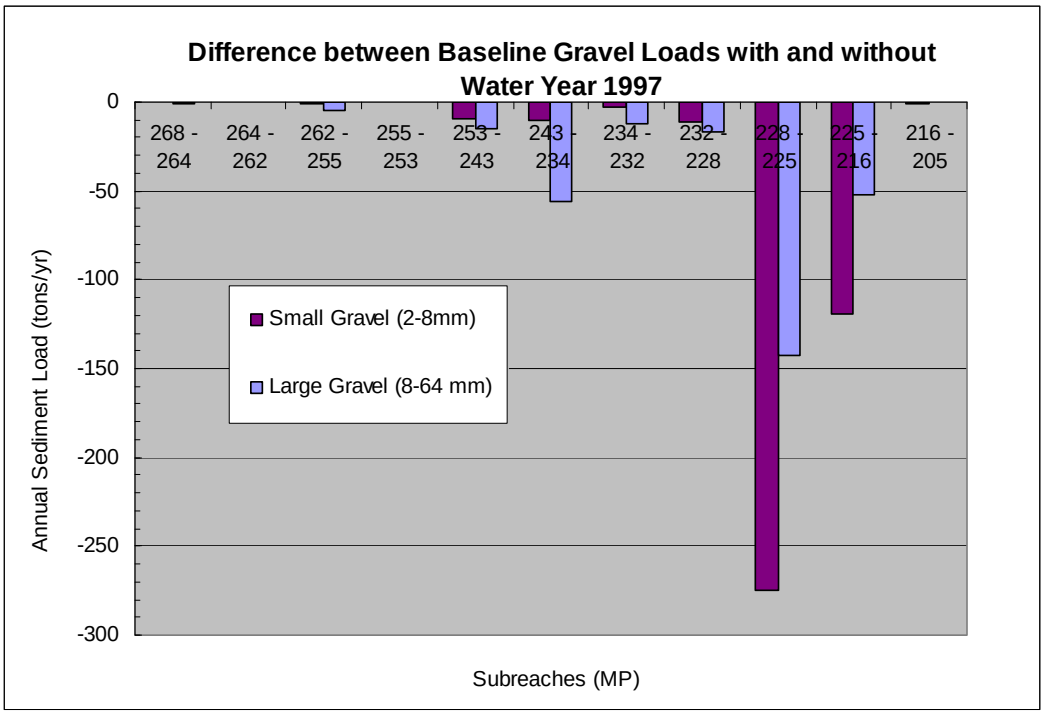

Figure 3-34.
Difference Between Baseline Gravel Loads With and Without Water Year 1997 for Gravel Sized Sediment (> 2 mm)

3.5.3 Annual Sediment Load of Alternative A Hydrology

The annual sediment load under Alternative A (Project) hydrology was predicted and the results are displayed in Figure 3-35 for the same hydrologic period as the Baseline Conditions. The differences between the Baseline and Project conditions sediment load are shown in Figures 3-36 and 3-37.

In reaches upstream from the Chowchilla Bypass Structure, Alternative A hydrology distributes more water to flows under 2,300 cfs and less to flows above 2,300 cfs. Since all gravels are transported at flow higher than 2,300 cfs, Alternative A decreases the gravel transport relative the Baseline Conditions by an average of 9 percent to 20 percent in Reach 1. However, it increases the gravel transport by 3 percent in the upper part of Reach 2a. Sand transport is initiated even during low flows and Alternative A hydrology usually increases the sand transport; however, it decreases the sand transport by 3 percent in the low part of Reach 2a.

Alternative A significantly increases flow distributed into Reach 2b downstream from the Chowchilla Bifurcation Structure for all flow ranges, as compared to Baseline Conditions. The reach shows about a fivefold increase in sand and small gravel transport relative to Baseline Conditions. The sand transport increases from about 3,400 tons/yr to 17,000 tons/yr, and the small gravel increases from about 16 tons/yr to 87 tons/yr. No large gravel exists in Reach 2b.

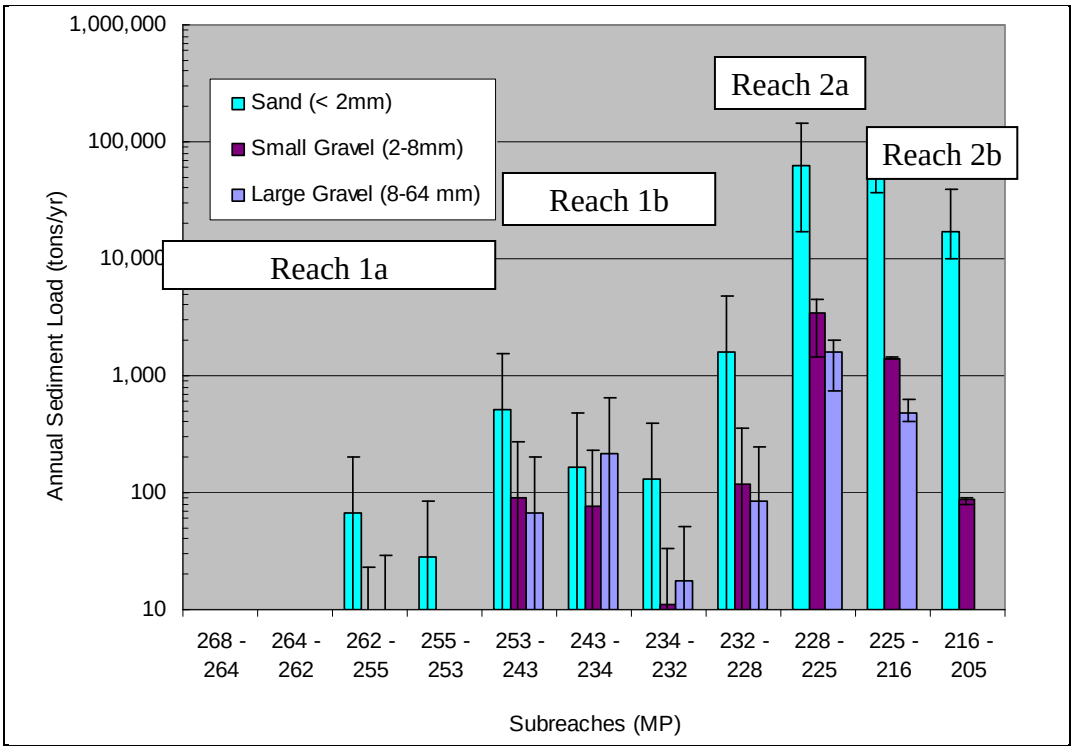

Figure 3-35.
Range of Current Annual Sediment Load Predicted by Three Different Methods Under Alternative A Hydrology

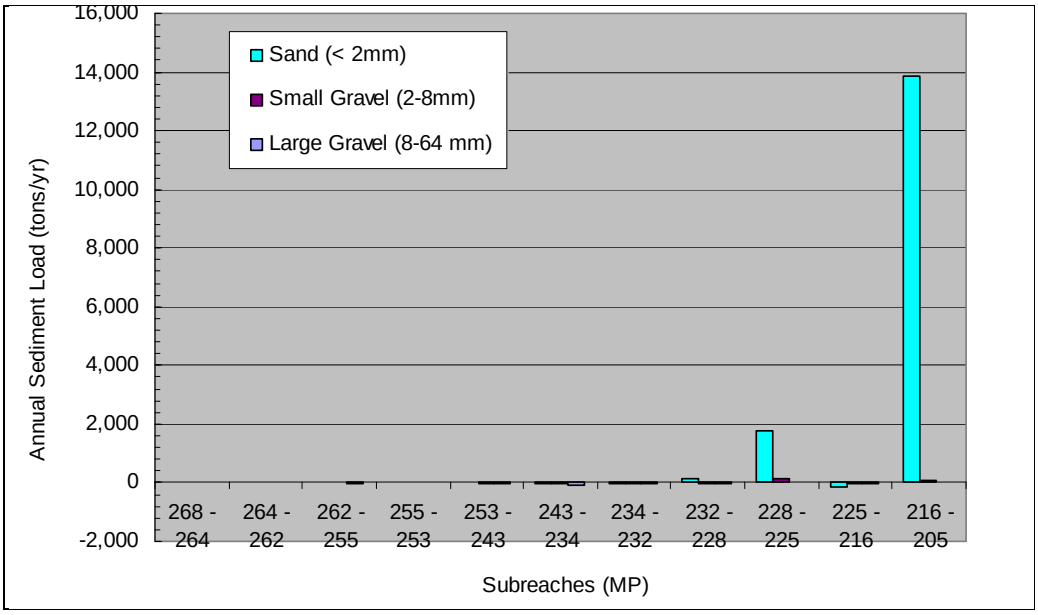

Note: Positive value indicates an increase under Alternative A relative to Baseline Conditions.

Figure 3-36.
Difference Between Alternative A and Baseline Conditions in the Computed Sand and Gravel Sediment Transport

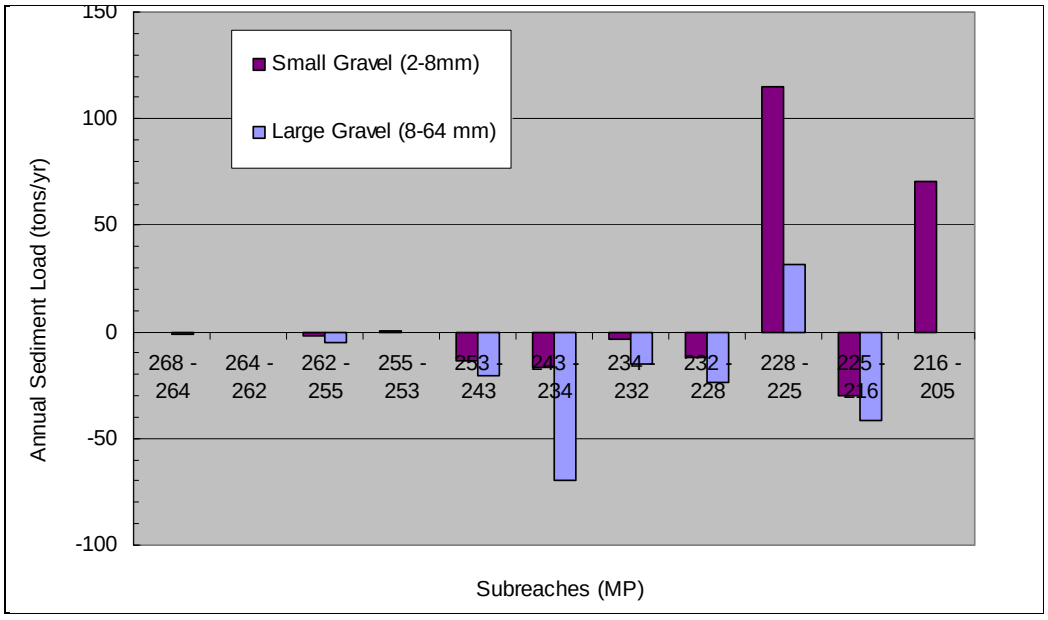

Note: Positive value indicates an increase under Alternative A relative to Baseline Conditions.

Figure 3-37.
Difference Between Alternative A and Baseline Conditions for Gravel Sized Sediment (> 2 mm)

The Alternative A hydrology was simulated to compute the annual sediment loads based upon the period from January 1, 1980, through September 30, 2003, without Water Year 1997 (Figure 3-38). The difference between the Alternative A hydrology with and without Water Year 1997 is shown in Figures 3-39 and 3-40. Compared to with Water Year 1997, the annual sand and gravel transport decreases an average of 8 percent to 12 percent in Reaches 1a, 1b, and 2a. For example, the sand transport in the upper part of Reach 2a decreases from 62,000 tons/yr to 57,000 tons/yr, small gravel from 3,400 tons/yr to 3,200 tons/yr, and large gravel from 1,600 tons/yr to 1,500 tons/yr. Without Water Year 1997, sediment transport downstream from the Chowchilla Bifurcation Structure decreases about 4 percent. The sand and small gravel transport decreases from 17,300 tons/yr to 16,500 tons/yr and from 87 tons/yr to 83 tons/yr, respectively.

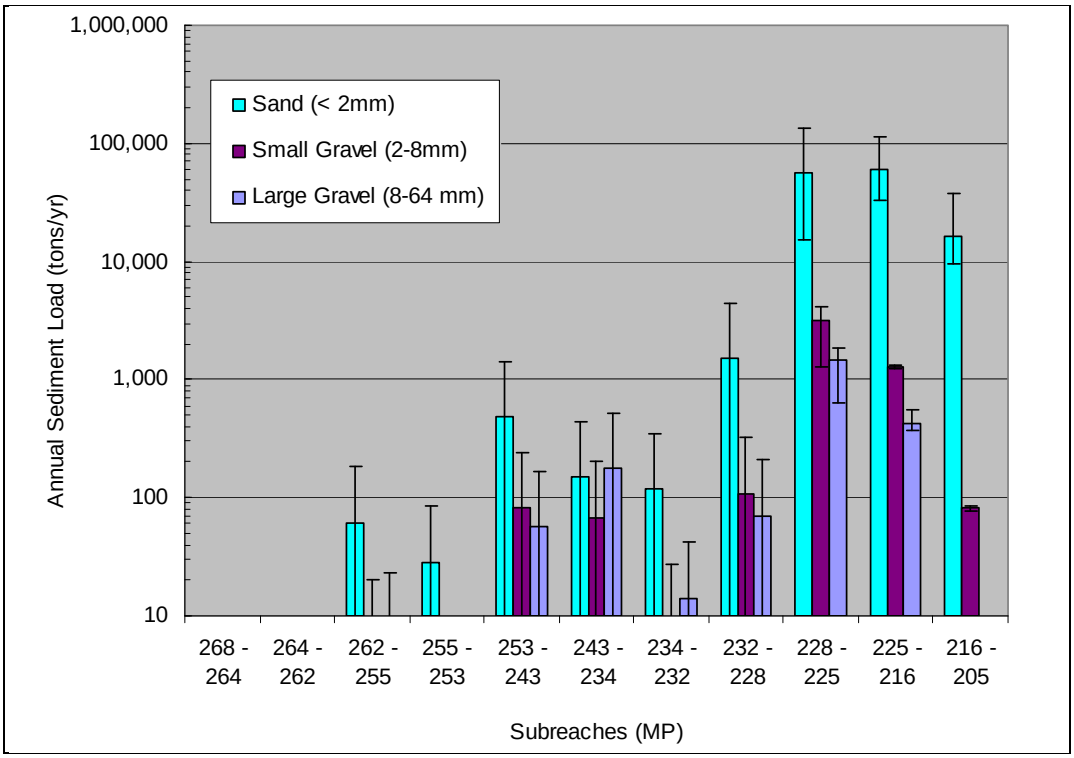

Figure 3-38.
Range of Alternative A Annual Sediment Load Predicted by Three Different Methods Without Water Year 1997

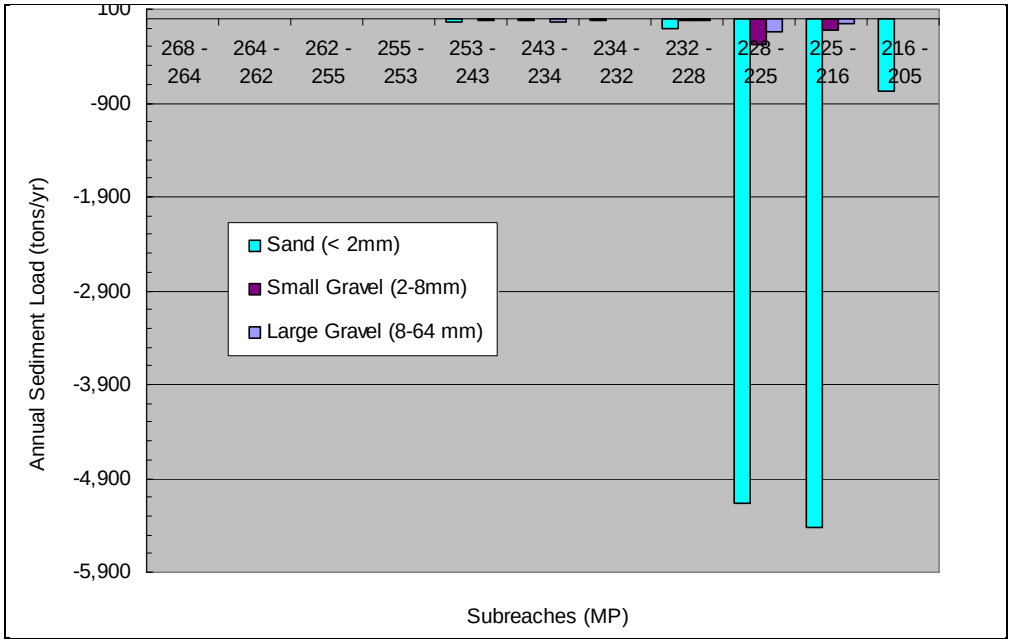

Figure 3-39.
Difference Between Alternative A Sediment Loads With and Without Water Year 1997

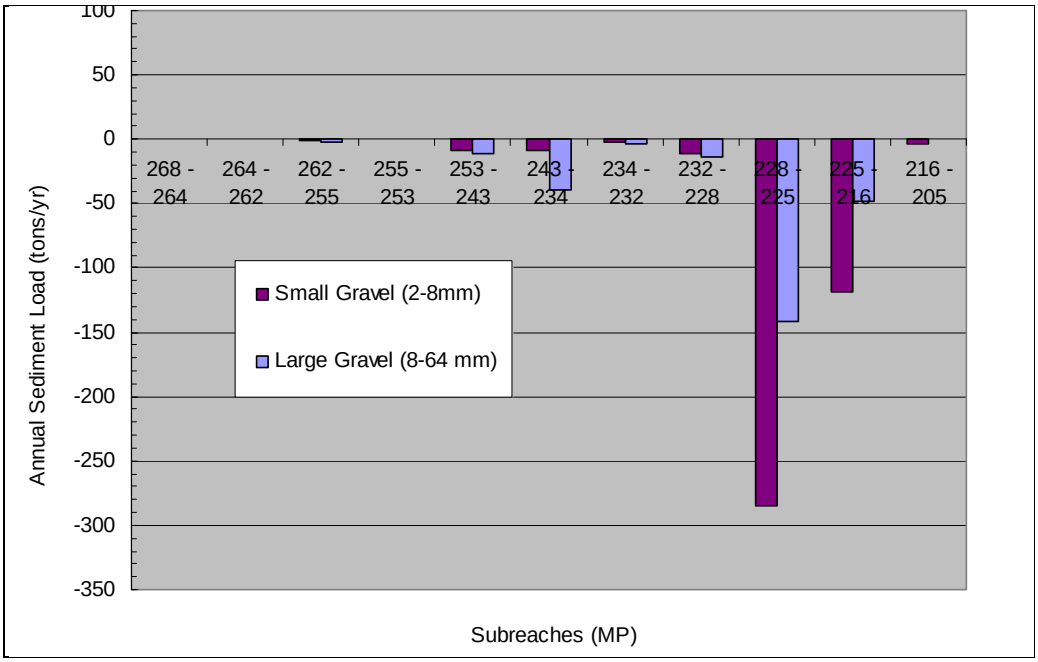

Figure 3-40.
Difference Between Alternative A Gravel Loads With and Without Water Year 1997

This page left blank intentionally.

4.0 Summary

Reference sediment motion computations predict that gravel is not mobilized on a reach scale in Reach 1 under Baseline or Project conditions for flows that are projected to occur under these conditions. However, a small percentage of gravel is predicted to be locally mobilized at flows less than 10,000 cfs in Reaches 1a and 1b. To analyze the local mobilization of sediment, an empirical function was used to estimate the fraction of sediment sample sites that will experience a certain reference Shield's number at given flow events. A mobilization index based upon this empirical function was computed to predict a relative measure of the mobilization of sediment between alternative conditions.

Based upon hydrology modeling of the SJRRP presented in Appendix H, Modeling, of the PEIS, there may be a decrease in the frequency of flows above 2,300 cfs under Project Conditions and a significant increase in the frequency of flows between 100 and 2,300 cfs in Reach 1. The decrease in the frequency of the higher flows is because there are fewer uncontrolled spills at Friant Dam under Project Conditions. These hydrology changes have consequences to the mobilization of sediment. The overall mobilization of gravel will be decreased under Project Conditions as compared to Baseline Conditions because Project Conditions decrease the frequency of the largest flows. However, under Project Conditions there will be more years in which at least some mobilization of gravel occurs as compared to Baseline Conditions.

We also estimated the fraction of mobilization if gravel augmentation strategies change the composition of the existing surface bed material. Reducing the bed material size in Reach 1a from its current median value of about 40 mm to 30 mm will increase the fraction of mobilized sites by a factor of about 2.5 at a flow of 8,000 cfs. Reducing the bed material size from the existing size to a median diameter of 20 mm will increase the faction of mobilized sites by a factor of 4 at a flow of 8,000 cfs.

Reducing the channel width and/or depth throughout Reach 1 does not increase predicted sediment mobility of the bed material in that reach. The mobility will likely decrease if the width or depth is reduced because the channel will have less capacity and more of the flow will be conveyed in the overbank areas, leaving less flow in the main channel. To increase the mobility of the bed sediment, the flow would have to be confined to the main channel.

The predicted annual average gravel transport capacity under Project Conditions hydrology showed a slight decrease relative to Baseline Conditions in Reach 1a and 1b. However, the sand transport is predicted to increase by about 7 percent in the lower part of Project Reach 2a under Project Conditions because of the large increase in flows below 2,300 cfs. The sand transport rate is virtually unaffected in the upper part of Project Reach 2a. The sand transport in Project Reach 2b is substantially increased from 3,400 tons/yr under Baseline Conditions to more than 17,000 tons/yr under Project Conditions due to the large increase in flows in this reach.

This page left blank intentionally.

5.0 References

Andrews, E.D. 2000. "Bed material transport in the Virgin River, Utah," *Water Resources Research,* 36(2), 585-596.

Brownlie, W.R. 1981. Prediction of flow depth and sediment discharge in open channels, Report KH-R-43A, W.M. Keck Laboratory of Hydraulics and Water Resources, Division of Engineering and Applied Science, California Institute of Technology, Pasadena, CA.

Buffington, J.M., and D.R. Montgomery. 1997. "A systematic Analysis of Eight Decades of Incipient Motion Studies, with special Reference to Gravel-Bedded Rivers," Water Resources Research, Vol. 33, No. 8, pp. 1993-2029.

Bunte, K., and S.R. Abt. 2001. Sampling surface and subsurface particle-size distributions in wadeable gravel- and cobble-bed streams for analyses in sediment transport, hydraulics, and streambed monitoring. Gen. Tech. Rep. RMRS-GTR-74. Fort Collins, CO: U.S. Department of Agriculture, Forest Service, Rocky Mountain Research Station. 428 p.

Church, M., D.G. McLean, and J.F. Walcott, 1987. River bed gravels: sampling and analysis. In: Sediment Transport in Gravel-Bed Rivers, C.R. Thorne, J.C. Bathurst and R.D. Hey (eds.), John Wiley and Sons, Chichester, p. 43-88.

Engelund, F., and E. Hansen. 1972. *A monograph on sediment transport in alluvial streams,* Teknish Forlag, Technical Press, Copenhagen, Denmark.

Federal Highways Administration. 1975. *Highways in the River Environment, Hydraulic and Environmental Design Considerations,* US Department of Transportation.

Graham, D.J., S.P. Rice, and I. Reid. 2004. A transferable methods for the automated grain sizing of river gravels, Water Resources Research, Volume 41, W07020.

Huang, J., and B.P. Greimann. 2007. User's Manual for SRH-1D 2.0 (Sedimentation and River Hydraulics – One Dimension Version 2.0), Bureau of Reclamation, Technical Service Center (www.usbr.gov/pmts/sediment).

López, R., and J. Barragán. 2008. "Equivalent Roughness of Gravel-Bed Rivers," *Journal of Hydraulic Engineering,* ASCE, 134(6):847-851.

McBain & Trush, Inc. (eds.). 2002. San Joaquin River Restoration Study Background Report. Prepared for Friant Water Users Authority, Lindsay, CA, and Natural Resources Defense, Council. San Francisco, California.

Mueller, E., J. Pitlick, and J.M. Nelson. 2005. “Variation in the reference Shields stress for bed load transport in gravel-bed streams and rivers,” *Water Resources Research*, Vol. 41, W04006, doi:10.1029/2004WR003692.

Mussetter Engineering, Inc. 2002a. “Hydraulic and Sediment Continuity Modeling of the San Joaquin River from Friant Dam to Mendota Dam, California,” U.S. Bureau of Reclamation, Contract No. 98-CP-20-20060.

———. 2002b. “Hydraulic and Sediment Continuity Modeling of the San Joaquin River from Mendota Dam to the Merced River,” U.S. Bureau of Reclamation, Contract No. 99-CP-20-2080.

Parker, G. 1990. "Surface based bedload transport relationship for gravel rivers," *Journal of Hydraulic Research*, Vol. 28(4), 417–436.

———. 1991. Selective sorting and abrasion of river gravel. II: Applications, *Journal of Hydraulic Engineering*, 117(2): 150-171.

Reclamation. 2008a. San Joaquin Data Collection Report Sediment Sampling February 4-6, 2008. San Joaquin River Restoration Project, Technical Service Center, Bureau of Reclamation. Denver, Colorado.

———. 2008b. Hydrology of the San Joaquin River. San Joaquin River Restoration Project, Draft, Technical Service Center, Bureau of Reclamation. Denver, Colorado.

Stillwater Sciences, Inc. 2003. Restoration Objectives for the San Joaquin River, Prepared for Natural Resources Defense Council and Friant Water Users Authority.

U.S. Department of the Interior, Bureau of Reclamation. *See* Reclamation.

van Rijn, L.C. 1982. “Equivalent Roughness of Alluvial Bed,” Proceedings American Society of Civil Engineers Vol. 108(10):1215-1218.

Wilcock, P.R., and J.C. Crowe. 2003. “Surface-Based Transport Model for Mixed-Size Sediment,” *Journal of Hydraulic Engineering*, ASCE, 129(2):120-128.

Wu, W., S.S.Y. Wang, and Y. Jia. 2000. "Nonuniform sediment transport in alluvial rivers," *Journal of Hydraulic Research*, Vol. 38(6):427-434.

Yang, C.T. 1973. "Incipient motion and sediment transport," Journal of Hydraulic Division, ASCE, Vol. 99(10), 1679-1704.

Exhibit

Reference Sediment Motion

Draft
Sediment Mobilization Assessment Attachment

Draft
April 2011

Reference Sediment Motion

The reference condition that is most commonly used is where the non-dimensional transport rate, W^*, is equal to 0.002 (Parker 1990).

$$W^* = \frac{(s-1)gq_s}{\rho_s(\tau_g/\rho)^{1.5}} = 0.002$$

where: s = relative specific density
g = acceleration of gravity
q_s = sediment transport rate
ρ_s = sediment density
τ_g = grain shear stress
ρ = water density

The transport rate, q_s, is primarily dependent upon the Shield's number, θ:

$$\theta = \frac{\tau_g}{\gamma(s-1)D_{50}} \qquad (1.0)$$

where: θ = dimensionless Shield's number
τ_g = grain shear stress
γ = specific weight of water
s = relative specific density of sediment
D_{50} = mean sediment size

The Shield's number that gives $W^* = 0.002$ is termed the reference Shield's stress. It can be described as the condition when many particles are moving and there is a small, but measureable, sediment transport rate. In our analysis, it corresponds to a Shield's number of 0.03.

The total shear stress can be separated into grain shear stress and form drag. Grain shear stress is commonly understood to be responsible for bedload transport and the shear stress due to form drag is commonly ignored. The channel grain shear stress τ_g is calculated as :

$$\tau_g = \gamma R' S \qquad (2.0)$$

where: R' = channel hydraulic radius due to grain shear stress
S = friction slope

The total shear stress is partitioned into that due to form drag and that due to grain roughness. Manning's equation is valid for the channel hydraulic radius due to grain shear stress:

$$U = \frac{C_m}{n_g} R'^{\frac{2}{3}} S_f^{\frac{1}{2}} \tag{3.0}$$

where: C_m = 1.0 for SI units, and 1.486 for English units
or $C_m = (g/9.81)^{\frac{1}{3}}$, and R' is the hydraulic radius due to grain shear stress

Dividing this equation by the Manning's equation gives:

$$\frac{R'}{R} = \left(\frac{n_g}{n} \right)^{1.5} \tag{4.0}$$

Where: R is the total hydraulic radius and n is the total Manning's roughness coefficient.

The Manning's roughness coefficient for the bed grains, n_g, can be computed from the roughness height. First, the logarithmic velocity distribution is integrated over the depth to yield (López and Barragán, 2008):

$$\frac{U}{u_*'} = \frac{1}{\kappa} \ln \frac{R'}{k_s} + 6.25 \tag{5.0}$$

where: κ is the von Karman constant (0.4), u_* is the shear velocity, and the log-law constant has assumed to be 6. Eq (5.0) can be approximately fit by the power law relation:

$$\frac{U}{u_*'} = 8.1 \left(\frac{R'}{k_s} \right)^{\frac{1}{6}} \tag{6.0}$$

where: k_s is a representative roughness height (see Figure a-1)

Parker (1991) also used Eq (6.0) to approximate the roughness coefficient in gravel bed streams. The fit is best for R/k_s values between 5 and 200, which is the value most all natural rivers will fall into. The error associated in predicting Manning's n values with this approximation is less than 3 percent. The value of R/k_s on the San Joaquin for high flows will be between 20 and 100.

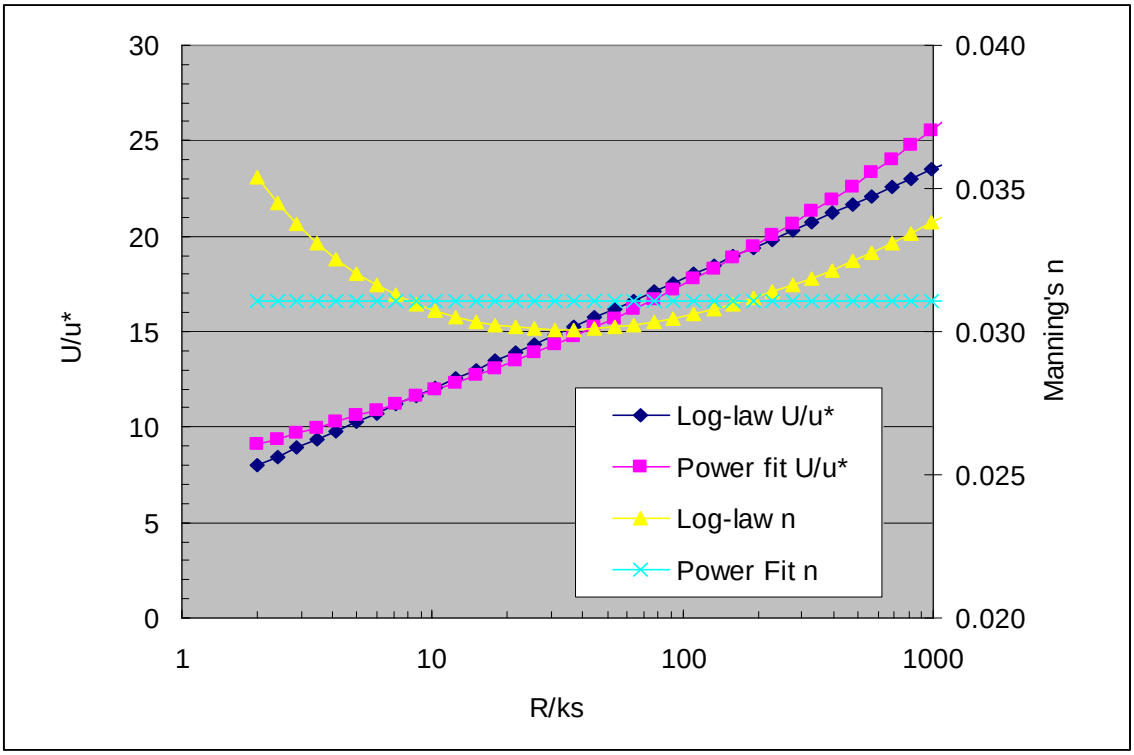

Also shown on the figure is the comparison between assuming k_s = 240 mm

Figure A-1.
Comparison Between Eq. (5.0) and (6.0)

Manning's roughness coefficient (n) due to grain shear, n_g, can then be computed from the roughness height using the following dimensionally consistent formula:

$$n_g = 0.058(k_s/g)^{\frac{1}{6}} \tag{7.0}$$

Several different relations in alluvial rivers have been proposed for k_s ranging from 0.95 D_{50} (Federal Highway Administration 1975) to 3 D_{90} (van Rijn 1982). A more recent publication, López and Barragán (2008), suggests that 2.4D_{90}, 2.8D_{84}, and 6.1D_{50} all give equivalent predictions of Manning's Roughness coefficient for river beds with gravel size or larger sediment, with a nonsinuous alignment and a flow path free of vegetation or obstacles. In their publication, they use the log law approximation (5.0) to compute Manning's n, but as shown above, the error associated with using the power fit approximation (6.0) is less than 3 percent. In the gravel bed reaches of the San Joaquin River, D_{50} varies between approximately 20 to 80 mm. Using k_s = 6.1D_{50}, gives n_g = 0.03 to 0.038 in the gravel bed reaches. For most of the San Joaquin River, the calibrated Manning's roughness coefficient in the main channel was 0.035. The grain roughness is assumed to be less than or equal to the main channel roughness coefficient in all calculations presented in this report.

This page left blank intentionally.

Exhibit

Average Channel Hydraulic Data

Draft
Sediment Mobilization Assessment Attachment

SAN JOAQUIN RIVER
RESTORATION PROGRAM

Draft
April 2011

Table B-1.
Subreach 1 Averaged Channel Hydraulic Data

Subreach 1		XS596-XS556				
Q Total	Q Chan	Vel Chan	Top Width Chan	Hydr Radius Chan	Frctn Slope	slope
(cfs)	(cfs)	(ft/s)	(ft)	(ft)	(Ft/ft)	(Ft/ft)
100	100.00	0.95	97.67	2.68	0.0003390	0.0004105
200	199.99	1.20	108.65	3.00	0.0004228	0.0004105
300	299.96	1.40	115.90	3.24	0.0004828	0.0004105
400	399.90	1.57	120.24	3.45	0.0005278	0.0004105
500	499.82	1.71	123.60	3.63	0.0005636	0.0004105
600	599.69	1.84	126.95	3.79	0.0005911	0.0004105
700	699.56	1.96	130.14	3.93	0.0006131	0.0004105
800	799.42	2.08	132.37	4.05	0.0006302	0.0004105
900	899.24	2.18	134.68	4.16	0.0006441	0.0004105
1000	999.01	2.27	136.78	4.27	0.0006512	0.0004105
1200	1198.39	2.43	144.91	4.36	0.0006716	0.0004105
1400	1397.41	2.58	148.79	4.54	0.0006859	0.0004105
1500	1496.85	2.65	151.14	4.61	0.0006931	0.0004105
1600	1596.25	2.72	152.65	4.70	0.0007002	0.0004105
1800	1794.95	2.85	155.39	4.88	0.0007115	0.0004105
2000	1993.52	2.98	157.72	5.05	0.0007191	0.0004105
2500	2488.46	3.22	163.51	5.46	0.0007284	0.0004105
3000	2982.26	3.43	168.61	5.84	0.0007314	0.0004105
4000	3964.31	3.77	179.44	6.54	0.0007277	0.0004105
5000	4937.03	4.10	185.13	7.18	0.0007374	0.0004105
6000	5903.71	4.39	191.13	7.74	0.0007473	0.0004105
7000	6864.30	4.66	194.30	8.31	0.0007586	0.0004105
8000	7817.19	4.93	196.02	8.87	0.0007076	0.0004105
9000	8761.89	5.16	197.35	9.41	0.0007760	0.0004105
10000	9701.00	5.36	198.44	9.93	0.0007779	0.0004105
11000	10629.07	5.55	199.31	10.43	0.0007790	0.0004105
12000	11551.82	5.73	200.00	10.94	0.0007758	0.0004105
13000	12462.94	5.90	200.47	11.41	0.0007766	0.0004105
14000	13364.72	6.06	200.74	11.87	0.0007768	0.0004105
15000	14258.53	6.22	200.96	12.31	0.0007767	0.0004105
16000	15146.40	6.36	201.15	12.75	0.0007749	0.0004105
17000	16028.31	6.50	201.30	13.18	0.0007737	0.0004105
18000	16901.74	6.63	201.44	13.60	0.0007721	0.0004105
19000	17777.38	6.76	201.56	14.00	0.0007729	0.0004105
20000	18651.89	6.89	201.65	14.39	0.0007728	0.0004105
22000	20378.18	7.14	201.78	15.14	0.0007744	0.0004105
24000	22093.95	7.37	201.90	15.86	0.0007763	0.0004105
26000	23798.44	7.59	202.00	16.56	0.0007798	0.0004105
28000	25489.80	7.80	202.06	17.24	0.0007817	0.0004105
30000	27154.93	7.92	202.06	18.07	0.0007613	0.0004105
32000	28865.55	8.18	202.06	18.56	0.0007842	0.0004105
34000	30506.02	8.33	202.06	19.27	0.0007745	0.0004105
36000	32145.21	8.51	202.06	19.83	0.0007795	0.0004105
38000	33779.19	8.69	202.06	20.40	0.0007830	0.0004105
40000	35389.13	8.85	202.06	20.96	0.0007849	0.0004105

Table B-2.
Subreach 2 Averaged Channel Hydraulic Data

subreach 2		XS596-XS556				
Q Total	Q Chan	Vel Chan	Top Width Chan	Hydr Radius Chan	Frctn Slope	slope
(cfs)	(cfs)	(ft/s)	(ft)	(ft)	(Ft/ft)	(Ft/ft)
100	99.86	0.62	142.71	2.32	0.0001336	0.0004128
200	199.53	0.85	150.42	2.64	0.0002047	0.0004128
300	299.10	1.04	153.87	2.88	0.0002808	0.0004128
400	398.43	1.20	157.06	3.09	0.0003335	0.0004128
500	497.60	1.34	159.92	3.28	0.0003710	0.0004128
600	596.64	1.45	166.22	3.39	0.0004052	0.0004128
700	695.56	1.56	172.25	3.51	0.0004271	0.0004128
800	794.36	1.60	175.51	3.67	0.0004321	0.0004128
900	893.04	1.65	178.93	3.84	0.0004312	0.0004128
1000	991.67	1.71	181.66	4.00	0.0004355	0.0004128
1200	1188.46	1.82	186.99	4.28	0.0004489	0.0004128
1400	1384.57	1.93	190.49	4.57	0.0004587	0.0004128
1500	1482.58	1.98	191.60	4.71	0.0004606	0.0004128
1600	1580.32	2.03	192.60	4.85	0.0004638	0.0004128
1800	1774.75	2.13	194.41	5.11	0.0004741	0.0004128
2000	1967.65	2.22	196.05	5.37	0.0004820	0.0004128
2500	2444.21	2.42	199.50	5.96	0.0004976	0.0004128
3000	2912.80	2.59	202.65	6.49	0.0005081	0.0004128
4000	3811.48	2.85	206.29	7.52	0.0005086	0.0004128
5000	4657.10	3.03	207.79	8.46	0.0004524	0.0004128
6000	5468.07	3.19	208.57	9.31	0.0004168	0.0004128
7000	6287.91	3.42	209.00	9.93	0.0004483	0.0004128
8000	7082.75	3.60	209.20	10.58	0.0004521	0.0004128
9000	7836.88	3.70	209.36	11.28	0.0004412	0.0004128
10000	8576.82	3.82	209.51	11.91	0.0004445	0.0004128
11000	9323.66	3.95	209.63	12.45	0.0004513	0.0004128
12000	10070.35	4.08	209.72	12.97	0.0004561	0.0004128
13000	10791.38	4.20	209.76	13.46	0.0004594	0.0004128
14000	11492.76	4.30	210.20	13.91	0.0004616	0.0004128
15000	12181.19	4.39	210.23	14.37	0.0004570	0.0004128
16000	12853.92	4.45	210.26	14.88	0.0004427	0.0004128
17000	13508.53	4.52	210.27	15.35	0.0004291	0.0004128
18000	14188.81	4.61	210.29	15.78	0.0004184	0.0004128
19000	14823.39	4.69	210.29	16.17	0.0004090	0.0004128
20000	15430.72	4.76	210.29	16.54	0.0004009	0.0004128
22000	16651.23	4.92	210.29	17.23	0.0003945	0.0004128
24000	17840.96	5.05	210.29	17.91	0.0003880	0.0004128
26000	19018.38	5.19	210.29	18.51	0.0003849	0.0004128
28000	20148.38	5.30	210.29	19.16	0.0003800	0.0004128
30000	20737.30	5.04	210.29	20.54	0.0002911	0.0004128
32000	22344.26	5.52	210.29	20.32	0.0003733	0.0004128
34000	23112.44	5.41	210.29	21.22	0.0003166	0.0004128
36000	24313.26	5.60	210.29	21.52	0.0003312	0.0004128
38000	25475.21	5.77	210.29	21.84	0.0003426	0.0004128
40000	26677.94	5.94	210.29	22.19	0.0003532	0.0004128

Table B-1.

subreach 3	Subreach 3 Averaged Channel Hydraulic Data					
Q Total	Q Chan	Vel Chan	Top Width Chan	Hydr Radius Chan	Frctn Slope	slope
(cfs)	(cfs)	(ft/s)	(ft)	(ft)	(Ft/ft)	(Ft/ft)
100	99.76	1.03	109.82	1.93	0.0007670	0.0007533
200	199.16	1.33	120.49	2.27	0.0008563	0.0007533
300	298.29	1.53	129.33	2.52	0.0009106	0.0007533
400	397.18	1.69	135.87	2.72	0.0009422	0.0007533
500	495.91	1.83	141.10	2.91	0.0009635	0.0007533
600	594.26	1.96	145.04	3.07	0.0009777	0.0007533
700	692.21	2.08	148.25	3.23	0.0010231	0.0007533
800	789.76	2.17	151.80	3.37	0.0009789	0.0007533
900	887.02	2.25	155.22	3.51	0.0009097	0.0007533
1000	984.19	2.33	158.17	3.66	0.0008801	0.0007533
1200	1175.93	2.40	165.32	3.98	0.0007936	0.0007533
1400	1365.24	2.47	169.96	4.34	0.0007503	0.0007533
1500	1460.48	2.53	172.97	4.45	0.0007607	0.0007533
1600	1555.56	2.59	174.31	4.57	0.0007623	0.0007533
1800	1743.91	2.69	176.13	4.80	0.0007426	0.0007533
2000	1931.45	2.81	177.37	5.00	0.0007451	0.0007533
2500	2392.77	3.06	180.28	5.51	0.0007515	0.0007533
3000	2848.09	3.28	182.33	5.98	0.0007524	0.0007533
4000	3740.66	3.67	184.46	6.84	0.0007443	0.0007533
5000	4606.52	3.95	185.63	7.70	0.0007132	0.0007533
6000	5446.08	4.13	186.55	8.64	0.0006868	0.0007533
7000	6256.06	4.25	186.79	9.68	0.0006389	0.0007533
8000	7117.09	4.71	187.06	9.66	0.0007099	0.0007533
9000	7931.48	4.92	187.53	10.24	0.0007103	0.0007533
10000	8730.20	5.10	187.69	10.79	0.0007065	0.0007533
11000	9516.72	5.27	187.80	11.32	0.0007013	0.0007533
12000	10294.06	5.42	187.85	11.85	0.0006915	0.0007533
13000	11065.89	5.57	187.90	12.36	0.0006842	0.0007533
14000	11831.76	5.72	187.94	12.83	0.0006827	0.0007533
15000	12595.16	5.84	187.97	13.31	0.0006747	0.0007533
16000	13333.92	5.96	188.04	13.77	0.0006690	0.0007533
17000	14065.70	6.08	188.05	14.23	0.0006626	0.0007533
18000	14787.08	6.18	188.05	14.69	0.0006569	0.0007533
19000	15503.77	6.28	188.06	15.12	0.0006504	0.0007533
20000	16215.88	6.40	188.06	15.50	0.0006532	0.0007533
22000	17613.16	6.61	188.11	16.27	0.0006520	0.0007533
24000	19008.67	6.79	188.11	17.06	0.0006421	0.0007533
26000	20447.29	6.97	188.11	17.81	0.0006393	0.0007533
28000	21899.20	7.16	188.11	18.53	0.0006398	0.0007533
30000	23244.47	7.21	188.11	19.50	0.0005952	0.0007533
32000	24738.45	7.51	188.11	19.91	0.0006406	0.0007533
34000	25908.92	7.51	189.10	20.74	0.0006049	0.0007533
36000	27095.28	7.64	192.13	21.24	0.0006088	0.0007533
38000	28255.18	7.79	192.13	21.71	0.0006185	0.0007533
40000	29313.11	7.87	193.73	22.20	0.0006263	0.0007533

Table B-1. Subreach 4 Averaged Channel Hydraulic Data

subreach 4		XS422-XS387				
Q Total	Q Chan	Vel Chan	Top Width Chan	Hydr Radius Chan	Frctn Slope	slope
(cfs)	(cfs)	(ft/s)	(ft)	(ft)	(Ft/ft)	(Ft/ft)
100	85.16	0.55	210.31	4.50	0.0003694	0.0005469
200	171.21	0.61	224.64	5.27	0.0005191	0.0005469
300	256.86	0.69	237.22	5.80	0.0005048	0.0005469
400	343.17	0.69	245.62	6.34	0.0004685	0.0005469
500	429.43	0.70	255.49	6.81	0.0004455	0.0005469
600	515.61	0.71	266.01	7.24	0.0004278	0.0005469
700	603.85	0.62	277.63	7.71	0.0001186	0.0005469
800	691.96	0.58	286.02	8.26	0.0000510	0.0005469
900	779.21	0.56	294.13	8.80	0.0000303	0.0005469
1000	866.54	0.54	298.05	9.48	0.0000201	0.0005469
1200	1035.52	0.49	306.54	11.23	0.0000087	0.0005469
1400	1200.97	0.50	309.10	12.40	0.0000067	0.0005469
1500	1285.59	0.53	312.65	12.20	0.0000072	0.0005469
1600	1370.19	0.55	313.19	12.27	0.0000079	0.0005469
1800	1538.38	0.60	313.75	12.44	0.0000093	0.0005469
2000	1708.55	0.67	314.25	12.49	0.0000111	0.0005469
2500	2127.42	0.80	314.56	12.80	0.0000152	0.0005469
3000	2546.30	0.93	314.78	13.03	0.0000198	0.0005469
4000	3367.76	1.16	315.47	13.56	0.0000285	0.0005469
5000	4154.66	1.45	312.29	14.83	0.0000316	0.0005469
6000	4848.63	1.63	314.07	16.39	0.0000274	0.0005469
7000	5530.57	1.65	314.38	18.32	0.0000223	0.0005469
8000	6526.38	1.87	317.15	15.38	0.0000603	0.0005469
9000	7294.46	2.02	317.30	15.79	0.0000675	0.0005469
10000	8053.00	2.16	317.47	16.11	0.0000751	0.0005469
11000	8799.57	2.29	317.65	16.46	0.0000820	0.0005469
12000	9540.45	2.39	317.76	16.74	0.0000895	0.0005469
13000	10294.89	2.51	317.78	17.02	0.0000968	0.0005469
14000	11078.32	2.67	318.84	17.06	0.0001090	0.0005469
15000	11859.80	2.81	318.86	17.32	0.0001164	0.0005469
16000	12602.81	2.93	318.88	17.56	0.0001236	0.0005469
17000	13345.65	3.05	318.91	17.78	0.0001314	0.0005469
18000	14120.54	3.17	318.93	17.99	0.0001388	0.0005469
19000	14839.60	3.28	318.96	18.19	0.0001460	0.0005469
20000	15554.38	3.39	318.98	18.39	0.0001531	0.0005469
22000	17009.57	3.61	319.02	18.76	0.0001677	0.0005469
24000	18443.88	3.81	319.06	19.15	0.0001808	0.0005469
26000	19843.16	4.00	319.09	19.52	0.0001928	0.0005469
28000	21223.01	4.18	319.11	19.84	0.0002063	0.0005469
30000	22591.76	4.36	319.11	20.18	0.0002180	0.0005469
32000	23981.75	4.54	319.11	20.48	0.0002306	0.0005469
34000	25379.85	4.72	319.11	20.81	0.0002437	0.0005469
36000	26737.63	4.89	319.11	21.10	0.0002580	0.0005469
38000	28040.80	5.05	319.11	21.40	0.0002682	0.0005469
40000	29321.61	5.20	319.11	21.71	0.0002773	0.0005469

Table B-1. XS384-XS227

Subreach 5 Averaged Channel Hydraulic Data

subreach 5						
Q Total	Q Chan	Vel Chan	Flow Width Chan	Hydraulic Depth Chan	Conv Actn Slope	slope
(cfs)	(cfs)	(ft/s)	(ft)	(ft)	(Ft/ft)	(Ft/ft)
100	95.76	1.05	93.19	2.48	0.0005006	0.0006785
200	191.71	1.33	103.22	2.86	0.0005615	0.0006785
300	287.49	1.53	108.77	3.17	0.0005891	0.0006785
400	383.16	1.69	113.85	3.42	0.0006011	0.0006785
500	473.79	1.79	117.35	3.65	0.0005836	0.0006785
600	568.19	1.90	120.55	3.86	0.0006148	0.0006785
700	660.64	1.97	124.92	4.03	0.0006152	0.0006785
800	754.29	2.06	127.77	4.22	0.0006109	0.0006785
900	847.59	2.13	130.86	4.38	0.0006063	0.0006785
1000	940.92	2.20	133.48	4.54	0.0006022	0.0006785
1200	1126.52	2.33	138.41	4.84	0.0005969	0.0006785
1400	1310.21	2.44	142.73	5.12	0.0005886	0.0006785
1500	1401.60	2.49	144.26	5.26	0.0005840	0.0006785
1600	1492.42	2.54	145.82	5.41	0.0005792	0.0006785
1800	1673.29	2.64	148.32	5.69	0.0005707	0.0006785
2000	1852.99	2.72	150.82	5.95	0.0005619	0.0006785
2500	2295.19	2.92	154.11	6.61	0.0005420	0.0006785
3000	2731.59	3.09	156.10	7.25	0.0005246	0.0006785
4000	3585.98	3.39	159.05	8.38	0.0005051	0.0006785
5000	4421.65	3.65	160.06	9.43	0.0004823	0.0006785
6000	5236.52	3.87	161.16	10.39	0.0004654	0.0006785
7000	6035.73	4.06	161.72	11.29	0.0004516	0.0006785
8000	6814.82	4.17	162.99	12.07	0.0004416	0.0006785
9000	7592.73	4.32	163.19	12.88	0.0004298	0.0006785
10000	8366.17	4.47	163.45	13.64	0.0004208	0.0006785
11000	9133.84	4.61	163.60	14.39	0.0004126	0.0006785
12000	9897.96	4.74	163.66	15.11	0.0004044	0.0006785
13000	10676.23	4.86	163.80	15.85	0.0003938	0.0006785
14000	11413.40	4.97	163.84	16.52	0.0003859	0.0006785
15000	12123.44	5.07	163.84	17.17	0.0003794	0.0006785
16000	12803.86	5.15	163.84	17.85	0.0003687	0.0006785
17000	13470.38	5.24	163.84	18.41	0.0003666	0.0006785
18000	14114.42	5.32	163.84	18.95	0.0003619	0.0006785
19000	14757.11	5.42	163.84	19.43	0.0003637	0.0006785
20000	15353.75	5.45	163.84	20.08	0.0003459	0.0006785
22000	16472.16	5.56	163.84	20.99	0.0003387	0.0006785
24000	17552.52	5.68	163.84	21.79	0.0003357	0.0006785
26000	18527.32	5.76	163.84	22.62	0.0003276	0.0006785
28000	19390.76	5.78	163.84	23.51	0.0003143	0.0006785
30000	20329.67	5.85	163.84	24.29	0.0003085	0.0006785
32000	21215.87	5.92	163.84	25.00	0.0003065	0.0006785
34000	22087.85	5.99	163.84	25.64	0.0002887	0.0006785
36000	22868.94	6.01	163.84	26.36	0.0002803	0.0006785
38000	23650.05	6.04	163.84	27.03	0.0002876	0.0006785
40000	24423.17	6.08	163.84	27.69	0.0002811	0.0006785

Table B-1. XS226-XS92
Subreach 6 Averaged Channel Hydraulic Data

subreach 6						
Q Total	Q Chan	Vel Chan	Flow Width Chan	Hydraulic Depth Chan	Conveyance Ratio	Energy Slope
(cfs)	(cfs)	(ft/s)	(ft)	(ft)	(Ft/ft)	(Ft/ft)
100	99.21	1.02	80.42	2.74	0.0003558	0.0004313
200	198.48	1.27	86.08	3.22	0.0003782	0.0004313
300	297.55	1.46	90.42	3.59	0.0003918	0.0004313
400	396.27	1.60	94.60	3.89	0.0004017	0.0004313
500	494.45	1.72	98.85	4.14	0.0004071	0.0004313
600	592.04	1.83	101.17	4.40	0.0004065	0.0004313
700	688.99	1.94	102.59	4.65	0.0004068	0.0004313
800	785.42	2.05	103.46	4.90	0.0004075	0.0004313
900	881.34	2.15	104.06	5.14	0.0004066	0.0004313
1000	976.58	2.24	104.59	5.37	0.0004058	0.0004313
1200	1164.82	2.41	105.53	5.80	0.0004057	0.0004313
1400	1350.47	2.55	105.83	6.21	0.0004053	0.0004313
1500	1442.41	2.62	105.94	6.41	0.0004054	0.0004313
1600	1533.68	2.69	106.99	6.57	0.0004092	0.0004313
1800	1714.69	2.81	107.38	6.94	0.0004087	0.0004313
2000	1892.73	2.92	107.46	7.29	0.0004077	0.0004313
2500	2328.54	3.18	107.64	8.10	0.0004071	0.0004313
3000	2753.96	3.40	107.87	8.85	0.0004061	0.0004313
4000	3571.11	3.76	109.61	10.12	0.0004090	0.0004313
5000	4350.05	4.06	109.62	11.27	0.0004086	0.0004313
6000	5101.27	4.32	109.62	12.30	0.0004076	0.0004313
7000	5820.16	4.55	109.62	13.22	0.0004069	0.0004313
8000	6506.76	4.75	109.62	14.04	0.0004068	0.0004313
9000	7177.80	4.94	109.62	14.82	0.0004052	0.0004313
10000	7823.78	5.11	109.62	15.53	0.0004070	0.0004313
11000	8454.04	5.27	109.62	16.22	0.0004076	0.0004313
12000	9078.30	5.42	109.62	16.87	0.0004101	0.0004313
13000	9709.46	5.56	109.62	17.53	0.0004096	0.0004313
14000	10306.15	5.69	109.62	18.14	0.0004109	0.0004313
15000	10917.52	5.83	109.62	18.74	0.0004116	0.0004313
16000	11504.76	5.95	109.62	19.33	0.0004123	0.0004313
17000	12062.82	6.04	109.62	19.95	0.0004074	0.0004313
18000	12625.83	6.17	109.62	20.43	0.0004130	0.0004313
19000	13195.99	6.30	109.62	20.82	0.0004170	0.0004313
20000	13739.77	6.40	109.62	21.27	0.0004189	0.0004313
22000	14819.68	6.61	109.62	22.20	0.0004214	0.0004313
24000	15898.31	6.82	109.62	23.00	0.0004280	0.0004313
26000	16940.38	7.01	109.62	23.81	0.0004321	0.0004313
28000	17971.25	7.19	109.62	24.58	0.0004350	0.0004313
30000	18985.64	7.36	109.62	25.30	0.0004389	0.0004313
32000	19948.49	7.49	109.62	26.06	0.0004372	0.0004313
34000	20884.14	7.62	109.62	26.77	0.0004366	0.0004313
36000	21802.31	7.74	109.62	27.45	0.0004365	0.0004313
38000	22709.64	7.87	109.62	28.12	0.0004366	0.0004313
40000	23593.08	7.98	109.62	28.80	0.0004353	0.0004313

Table B-1. Subreach 7 Averaged Channel Hydraulic Data

subreach 7		XS91-XS59				
Q Total	Q Chan	Vel Chan	Top Width Chan	Hydr Radius Chan	Frctn Slope	slope
(cfs)	(cfs)	(ft/s)	(ft)	(ft)	(Ft/ft)	(Ft/ft)
100	99.90	0.64	158.63	4.27	0.0002849	0.0000516
200	199.80	0.82	166.25	4.70	0.0003029	0.0000516
300	299.67	0.92	171.33	5.06	0.0002844	0.0000516
400	393.80	0.99	176.37	5.33	0.0002638	0.0000516
500	492.34	1.07	182.66	5.60	0.0002551	0.0000516
600	590.66	1.14	186.67	5.87	0.0002473	0.0000516
700	679.93	1.20	189.13	6.06	0.0002390	0.0000516
800	764.71	1.23	191.12	6.26	0.0002309	0.0000516
900	859.48	1.29	193.98	6.46	0.0002324	0.0000516
1000	953.80	1.35	197.50	6.62	0.0002389	0.0000516
1200	1120.92	1.42	202.02	6.86	0.0002506	0.0000516
1400	1304.94	1.51	205.58	7.20	0.0002516	0.0000516
1500	1396.78	1.55	207.10	7.34	0.0002535	0.0000516
1600	1476.32	1.59	208.47	7.47	0.0002555	0.0000516
1800	1657.40	1.68	211.46	7.72	0.0002597	0.0000516
2000	1836.50	1.75	214.60	7.98	0.0002604	0.0000516
2500	2276.27	1.94	219.63	8.56	0.0002643	0.0000516
3000	2710.16	2.10	222.92	9.12	0.0002644	0.0000516
4000	3568.47	2.41	224.74	10.10	0.0002736	0.0000516
5000	4418.41	2.69	226.35	10.94	0.0002854	0.0000516
6000	5253.62	2.93	227.04	11.72	0.0002954	0.0000516
7000	6078.82	3.16	228.18	12.40	0.0003083	0.0000516
8000	6893.03	3.38	229.32	13.01	0.0003212	0.0000516
9000	7706.84	3.59	229.34	13.62	0.0003324	0.0000516
10000	8491.44	3.76	229.34	14.19	0.0003386	0.0000516
11000	9269.50	3.93	229.34	14.73	0.0003442	0.0000516
12000	10069.94	4.10	229.34	15.23	0.0003516	0.0000516
13000	10837.13	4.26	229.34	15.72	0.0003578	0.0000516
14000	11615.51	4.41	229.34	16.19	0.0003645	0.0000516
15000	12372.18	4.56	229.34	16.63	0.0003715	0.0000516
16000	13142.84	4.72	229.34	17.05	0.0003811	0.0000516
17000	13886.74	4.86	229.34	17.43	0.0003888	0.0000516
18000	14613.82	4.99	229.34	17.80	0.0003951	0.0000516
19000	15351.96	5.12	229.34	18.16	0.0004014	0.0000516
20000	16066.35	5.24	229.34	18.51	0.0004070	0.0000516
22000	17475.01	5.46	229.34	19.16	0.0004176	0.0000516
24000	18885.68	5.68	229.34	19.77	0.0004285	0.0000516
26000	20267.01	5.89	229.34	20.35	0.0004392	0.0000516
28000	21624.75	6.10	229.34	20.90	0.0004496	0.0000516
30000	22967.55	6.29	229.34	21.42	0.0004600	0.0000516
32000	24339.76	6.51	229.34	21.93	0.0004730	0.0000516
34000	25762.69	6.74	229.34	22.41	0.0004948	0.0000516
36000	27117.04	6.92	229.34	22.88	0.0005059	0.0000516
38000	28442.17	7.11	229.34	23.32	0.0005164	0.0000516
40000	29714.33	7.27	229.34	23.76	0.0005242	0.0000516

Table B-1. XS58-XSA213
Subreach 8 Averaged Channel Hydraulic Data

subreach 8						
Q Total	Q Chan	Vel Chan	Top Width Channel	Hydraulic Depth Channel	Conveyance Factn Slope	slope
(cfs)	(cfs)	(ft/s)	(ft)	(ft)	(Ft/ft)	(Ft/ft)
100	96.73	1.09	79.04	1.96	0.0004066	0.0003403
200	192.33	1.26	89.31	2.44	0.0004649	0.0003403
300	286.96	1.39	95.79	2.84	0.0004897	0.0003403
400	380.67	1.51	100.09	3.18	0.0004882	0.0003403
500	472.51	1.64	101.69	3.50	0.0004900	0.0003403
600	559.66	1.75	102.23	3.77	0.0004920	0.0003403
700	647.78	1.86	102.62	4.04	0.0004957	0.0003403
800	734.95	1.96	102.99	4.30	0.0004999	0.0003403
900	817.35	2.03	103.41	4.54	0.0005015	0.0003403
1000	893.94	2.09	103.84	4.76	0.0004991	0.0003403
1200	1043.36	2.20	104.70	5.15	0.0004958	0.0003403
1400	1190.39	2.31	105.28	5.52	0.0004942	0.0003403
1500	1257.95	2.36	105.53	5.67	0.0004932	0.0003403
1600	1329.53	2.42	105.77	5.82	0.0004922	0.0003403
1800	1459.56	2.50	106.59	6.11	0.0004866	0.0003403
2000	1587.12	2.57	107.77	6.39	0.0004851	0.0003403
2500	1881.46	2.72	108.42	6.97	0.0004893	0.0003403
3000	2161.57	2.86	109.35	7.50	0.0004884	0.0003403
4000	2669.06	3.10	110.04	8.38	0.0004886	0.0003403
5000	3121.75	3.28	110.40	9.12	0.0004886	0.0003403
6000	3543.51	3.44	110.69	9.76	0.0004889	0.0003403
7000	3931.95	3.58	110.90	10.32	0.0004910	0.0003403
8000	4299.51	3.70	111.05	10.83	0.0004918	0.0003403
9000	4647.94	3.81	111.19	11.31	0.0004919	0.0003403
10000	4988.95	3.91	111.32	11.76	0.0004924	0.0003403
11000	5322.29	4.01	111.44	12.19	0.0004933	0.0003403
12000	5636.89	4.10	111.55	12.59	0.0004927	0.0003403
13000	5956.53	4.19	111.65	12.97	0.0004939	0.0003403
14000	6262.79	4.26	111.75	13.35	0.0004937	0.0003403
15000	6551.56	4.34	111.82	13.70	0.0004936	0.0003403
16000	6833.08	4.41	111.87	14.04	0.0004935	0.0003403
17000	7108.96	4.48	111.92	14.37	0.0004932	0.0003403
18000	7380.71	4.54	111.97	14.69	0.0004929	0.0003403
19000	7646.26	4.60	112.01	15.00	0.0004925	0.0003403
20000	7907.34	4.66	112.06	15.30	0.0004924	0.0003403
22000	8418.93	4.77	112.13	15.88	0.0004928	0.0003403
24000	8894.22	4.89	112.18	16.39	0.0004956	0.0003403
26000	9339.58	4.99	112.35	16.85	0.0004997	0.0003403
28000	9775.26	5.10	112.35	17.28	0.0005046	0.0003403
30000	10197.59	5.20	112.35	17.69	0.0005095	0.0003403
32000	10606.43	5.30	112.35	18.06	0.0005151	0.0003403
34000	11004.52	5.40	112.35	18.43	0.0005200	0.0003403
36000	11389.84	5.49	112.35	18.76	0.0005260	0.0003403
38000	11764.94	5.58	112.35	19.08	0.0005319	0.0003403
40000	12139.93	5.68	112.35	19.38	0.0005383	0.0003403

Table B-1

Subreach 9 Averaged Channel Hydraulic Data

subreach 9		XSA212-XSA187				
Q Total	Q Chan	Vel Chan	Flow Width Chan	Hydraulic Depth Chan	Conv Chan	slope
(cfs)	(cfs)	(ft/s)	(ft)	(ft)	(Ft/ft)	(Ft/ft)
100	98.06	0.88	119.51	2.47	0.0003319	0.0001371
200	195.36	1.07	130.43	2.89	0.0003746	0.0001371
300	292.14	1.19	138.42	3.23	0.0003888	0.0001371
400	386.86	1.29	144.19	3.51	0.0003878	0.0001371
500	481.69	1.40	149.67	3.78	0.0003908	0.0001371
600	570.24	1.49	153.35	3.99	0.0003968	0.0001371
700	660.36	1.57	156.27	4.20	0.0003992	0.0001371
800	748.35	1.65	158.83	4.42	0.0004011	0.0001371
900	836.42	1.72	160.96	4.62	0.0004036	0.0001371
1000	921.36	1.78	163.04	4.80	0.0004055	0.0001371
1200	1081.67	1.87	166.09	5.11	0.0004098	0.0001371
1400	1246.16	1.97	169.32	5.43	0.0004117	0.0001371
1500	1325.08	2.02	170.49	5.57	0.0004127	0.0001371
1600	1402.71	2.07	171.71	5.70	0.0004136	0.0001371
1800	1556.56	2.15	173.75	5.95	0.0004129	0.0001371
2000	1708.27	2.23	175.71	6.20	0.0004131	0.0001371
2500	2069.63	2.39	178.69	6.74	0.0004180	0.0001371
3000	2419.11	2.53	181.87	7.24	0.0004191	0.0001371
4000	3085.16	2.78	186.13	8.08	0.0004229	0.0001371
5000	3714.01	2.99	188.33	8.80	0.0004258	0.0001371
6000	4317.76	3.17	189.21	9.45	0.0004280	0.0001371
7000	4898.15	3.33	189.84	10.02	0.0004319	0.0001371
8000	5462.07	3.49	190.33	10.54	0.0004357	0.0001371
9000	6013.83	3.63	190.48	11.04	0.0004389	0.0001371
10000	6552.41	3.75	190.62	11.51	0.0004409	0.0001371
11000	7083.68	3.87	190.75	11.96	0.0004428	0.0001371
12000	7612.07	3.98	190.87	12.38	0.0004445	0.0001371
13000	8130.30	4.09	190.98	12.79	0.0004468	0.0001371
14000	8643.34	4.19	191.07	13.18	0.0004484	0.0001371
15000	9140.01	4.29	191.15	13.55	0.0004503	0.0001371
16000	9635.01	4.39	191.21	13.90	0.0004528	0.0001371
17000	10120.33	4.48	191.28	14.24	0.0004546	0.0001371
18000	10596.36	4.56	191.33	14.57	0.0004562	0.0001371
19000	11072.58	4.64	191.38	14.89	0.0004576	0.0001371
20000	11537.07	4.72	191.42	15.20	0.0004590	0.0001371
22000	12460.30	4.87	191.49	15.80	0.0004620	0.0001371
24000	13342.09	5.01	191.54	16.34	0.0004656	0.0001371
26000	14181.92	5.14	191.65	16.84	0.0004694	0.0001371
28000	14990.56	5.26	191.66	17.31	0.0004730	0.0001371
30000	15768.25	5.38	191.66	17.75	0.0004767	0.0001371
32000	16526.96	5.50	191.66	18.17	0.0004815	0.0001371
34000	17294.91	5.62	191.66	18.57	0.0004886	0.0001371
36000	18012.03	5.73	191.66	18.94	0.0004933	0.0001371
38000	18709.05	5.83	191.66	19.29	0.0004980	0.0001371
40000	19386.41	5.93	191.66	19.64	0.0005021	0.0001371

Table B-1 XSA186-XSA97

Subreach 10 Averaged Channel Hydraulic Data

subreach 10						
Q Total	Q Chan	Velocity Chan	Top Width Channel	Hydraulic Depth Chan	Enactn Slope	slope
(cfs)	(cfs)	(ft/s)	(ft)	(ft)	(Ft/ft)	(Ft/ft)
100	95.90	0.74	182.82	1.59	0.0003269	0.0004957
200	184.64	0.93	193.81	1.85	0.0003952	0.0004957
300	272.62	1.05	202.75	2.04	0.0004195	0.0004957
400	360.53	1.16	211.66	2.21	0.0004340	0.0004957
500	438.71	1.21	215.96	2.34	0.0004365	0.0004957
600	521.33	1.29	220.00	2.49	0.0004339	0.0004957
700	604.34	1.36	222.99	2.63	0.0004351	0.0004957
800	682.69	1.43	224.84	2.76	0.0004320	0.0004957
900	762.52	1.49	227.25	2.89	0.0004290	0.0004957
1000	841.51	1.55	228.76	3.02	0.0004252	0.0004957
1200	996.36	1.65	232.59	3.27	0.0004160	0.0004957
1400	1147.09	1.74	235.48	3.50	0.0004057	0.0004957
1500	1220.23	1.77	236.67	3.61	0.0004013	0.0004957
1600	1294.38	1.82	237.57	3.70	0.0004013	0.0004957
1800	1439.64	1.90	239.64	3.87	0.0004014	0.0004957
2000	1582.65	1.98	240.64	4.03	0.0004017	0.0004957
2500	1932.16	2.16	241.84	4.43	0.0004028	0.0004957
3000	2268.29	2.31	242.61	4.79	0.0004044	0.0004957
4000	2912.52	2.56	244.46	5.45	0.0004097	0.0004957
5000	3527.16	2.77	245.46	6.04	0.0004153	0.0004957
6000	4118.57	2.95	246.60	6.57	0.0004223	0.0004957
7000	4691.12	3.10	247.77	7.06	0.0004285	0.0004957
8000	5229.48	3.19	248.19	7.57	0.0004064	0.0004957
9000	5741.97	3.26	248.38	8.08	0.0003871	0.0004957
10000	6237.12	3.32	248.53	8.58	0.0003710	0.0004957
11000	6749.79	3.44	248.91	8.93	0.0003774	0.0004957
12000	7252.13	3.55	249.40	9.26	0.0003827	0.0004957
13000	7750.65	3.66	249.47	9.59	0.0003877	0.0004957
14000	8235.24	3.76	249.53	9.90	0.0003924	0.0004957
15000	8713.17	3.85	249.58	10.21	0.0003969	0.0004957
16000	9181.90	3.94	249.67	10.50	0.0004011	0.0004957
17000	9647.17	4.03	249.70	10.79	0.0004050	0.0004957
18000	10106.47	4.11	249.72	11.07	0.0004087	0.0004957
19000	10559.20	4.19	249.74	11.34	0.0004123	0.0004957
20000	11005.19	4.27	249.75	11.60	0.0004160	0.0004957
22000	11889.60	4.41	249.77	12.12	0.0004228	0.0004957
24000	12747.92	4.55	249.77	12.60	0.0004291	0.0004957
26000	13572.47	4.67	249.77	13.07	0.0004340	0.0004957
28000	14370.14	4.77	249.77	13.52	0.0004360	0.0004957
30000	15129.28	4.87	249.77	13.94	0.0004367	0.0004957
32000	15866.05	4.96	249.77	14.32	0.0004384	0.0004957
34000	16568.18	5.05	249.77	14.68	0.0004394	0.0004957
36000	17239.98	5.12	249.77	15.03	0.0004402	0.0004957
38000	17892.17	5.20	249.77	15.36	0.0004406	0.0004957
40000	18525.27	5.26	249.77	15.68	0.0004404	0.0004957

Table B-1. XSA94-XSA2

Subreach 11 Averaged Channel Hydraulic Data

subreach 11						
Q Total	Q Chan	Vel Chan	Top Width Chan	Hydr Radius Chan	Frctn Slope	slope
(cfs)	(cfs)	(ft/s)	(ft)	(ft)	(Ft/ft)	(Ft/ft)
100	99.45	0.53	156.90	2.77	0.0001690	0.0003017
200	197.88	0.70	168.11	2.98	0.0001869	0.0003017
300	294.92	0.83	174.27	3.21	0.0001919	0.0003017
400	390.51	0.94	176.30	3.44	0.0001941	0.0003017
500	484.58	1.03	177.99	3.66	0.0001957	0.0003017
600	577.32	1.11	180.10	3.86	0.0001969	0.0003017
700	669.12	1.19	180.96	4.06	0.0001985	0.0003017
800	760.13	1.26	181.64	4.26	0.0002000	0.0003017
900	850.06	1.33	182.24	4.45	0.0002016	0.0003017
1000	938.88	1.39	182.98	4.63	0.0002032	0.0003017
1200	1114.62	1.50	183.67	4.98	0.0002061	0.0003017
1400	1287.34	1.60	183.87	5.32	0.0002090	0.0003017
1500	1372.87	1.65	183.96	5.48	0.0002104	0.0003017
1500	1372.87	1.65	183.96	5.48	0.0002104	0.0003017
1500	1372.87	1.65	183.96	5.48	0.0002104	0.0003017
1500	1372.87	1.65	183.96	5.48	0.0002104	0.0003017
1500	1372.87	1.65	183.96	5.48	0.0002104	0.0003017
1500	1372.87	1.65	183.96	5.48	0.0002104	0.0003017
1500	1372.87	1.65	183.96	5.48	0.0002104	0.0003017
1500	1372.87	1.65	183.96	5.48	0.0002104	0.0003017
1500	1372.87	1.65	183.96	5.48	0.0002104	0.0003017
1500	1372.87	1.65	183.96	5.48	0.0002104	0.0003017
2500	2176.66	1.93	193.63	7.18	0.0001979	0.0003017
3500	2925.99	2.20	193.73	8.36	0.0002060	0.0003017
4500	3603.77	2.41	193.78	9.31	0.0002144	0.0003017
4500	3603.77	2.41	193.78	9.31	0.0002144	0.0003017
4500	3603.77	2.41	193.78	9.31	0.0002144	0.0003017
4500	3603.77	2.41	193.78	9.31	0.0002144	0.0003017
4500	3603.77	2.41	193.78	9.31	0.0002144	0.0003017
4500	3603.77	2.41	193.78	9.31	0.0002144	0.0003017
4500	3603.77	2.41	193.78	9.31	0.0002144	0.0003017
4500	3603.77	2.41	193.78	9.31	0.0002144	0.0003017
4500	3603.77	2.41	193.78	9.31	0.0002144	0.0003017
4500	3603.77	2.41	193.78	9.31	0.0002144	0.0003017
4500	3603.77	2.41	193.78	9.31	0.0002144	0.0003017
4500	3603.77	2.41	193.78	9.31	0.0002144	0.0003017
4500	3603.77	2.41	193.78	9.31	0.0002144	0.0003017
4500	3603.77	2.41	193.78	9.31	0.0002144	0.0003017
4500	3603.77	2.41	193.78	9.31	0.0002144	0.0003017
4500	3603.77	2.41	193.78	9.31	0.0002144	0.0003017
4500	3603.77	2.41	193.78	9.31	0.0002144	0.0003017
4500	3603.77	2.41	193.78	9.31	0.0002144	0.0003017
4500	3603.77	2.41	193.78	9.31	0.0002144	0.0003017
4500	3603.77	2.41	193.78	9.31	0.0002144	0.0003017
4500	3603.77	2.41	193.78	9.31	0.0002144	0.0003017

This page left blank intentionally.

Exhibit

Sensitivity Analysis of Sediment Transport Capacity Using Parker's Gravel-Sand-Mixed Transport Equation Combined with Engelund and Hansen's Sand Transport Equation

Draft
Sediment Mobilization Assessment Attachment

SAN JOAQUIN RIVER
RESTORATION PROGRAM

Draft
April 2011

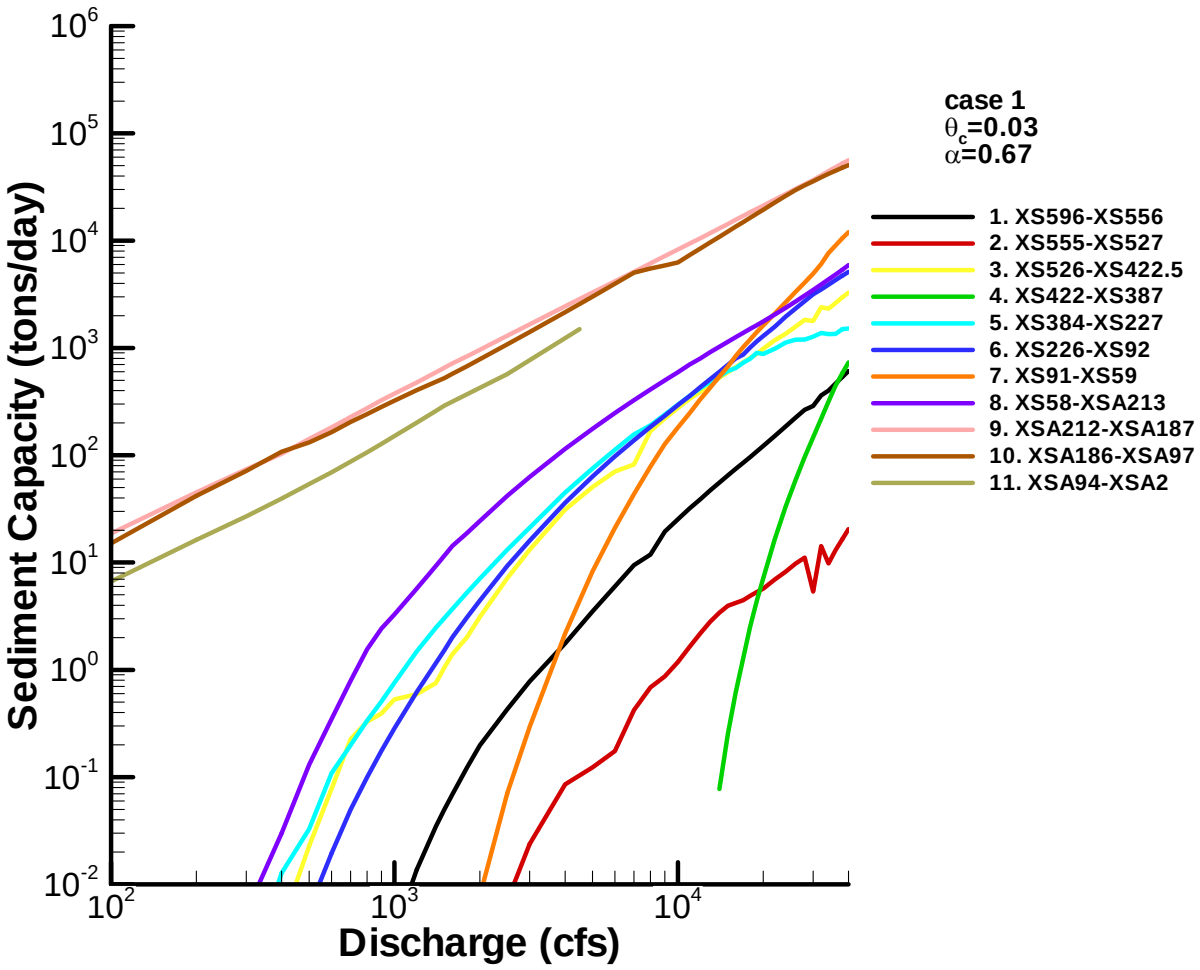
Sediment Capacity (tons/day)
Discharge (cfs)
case 1
θc=0.03
α=0.67
1. XS596-XS556
2. XS555-XS527
3. XS526-XS422.5
4. XS422-XS387
5. XS384-XS227
6. XS226-XS92
7. XS91-XS59
8. XS58-XSA213
9. XSA212-XSA187
10. XSA186-XSA97
11. XSA94-XSA2

Case 1

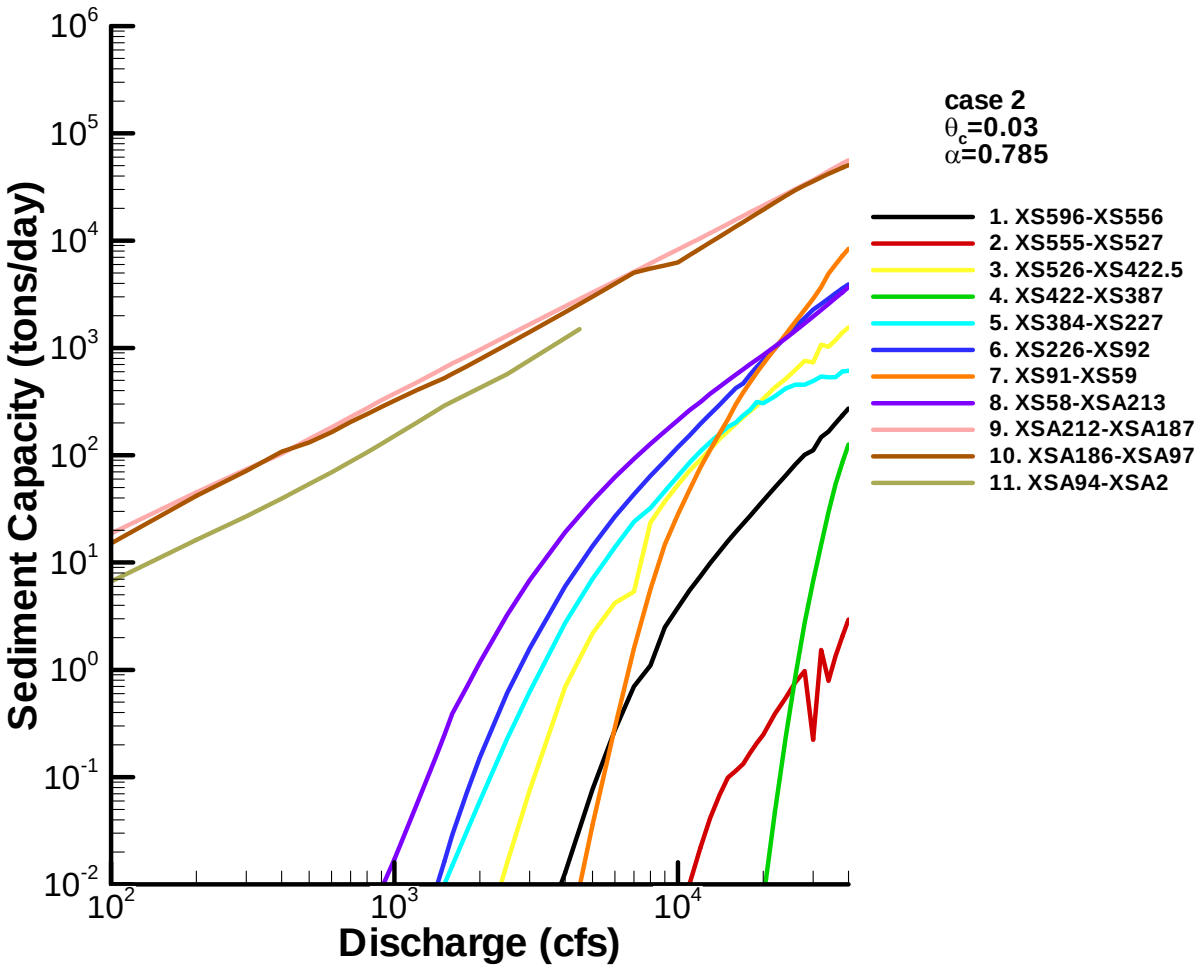
Sediment Capacity (tons/day)
Discharge (cfs)
case 2
θc=0.03
α=0.785
1. XS596-XS556
2. XS555-XS527
3. XS526-XS422.5
4. XS422-XS387
5. XS384-XS227
6. XS226-XS92
7. XS91-XS59
8. XS58-XSA213
9. XSA212-XSA187
10. XSA186-XSA97
11. XSA94-XSA2

Case 2

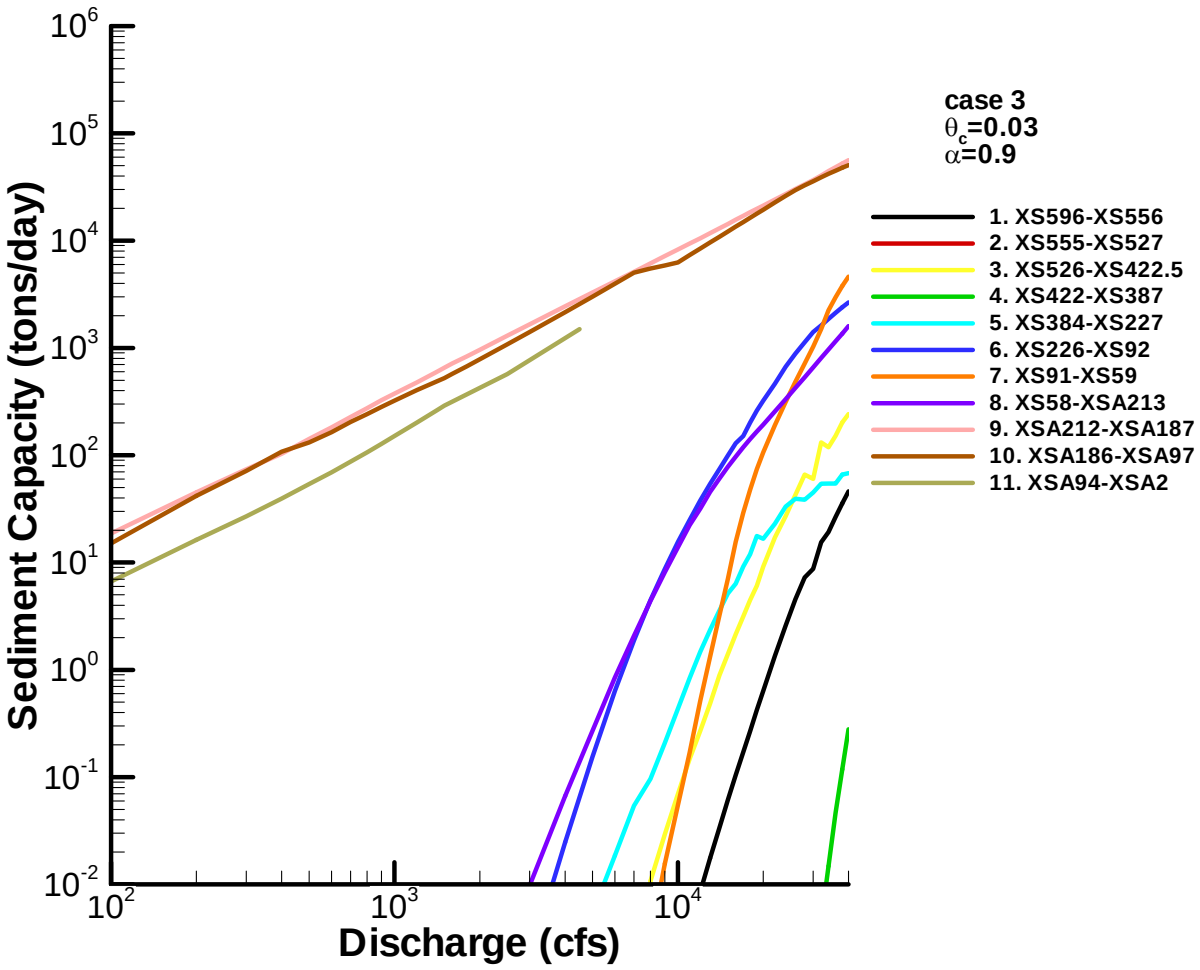
Sediment Capacity (tons/day)
Discharge (cfs)
case 3
θc=0.03
α=0.9
1. XS596-XS556
2. XS555-XS527
3. XS526-XS422.5
4. XS422-XS387
5. XS384-XS227
6. XS226-XS92
7. XS91-XS59
8. XS58-XSA213
9. XSA212-XSA187
10. XSA186-XSA97
11. XSA94-XSA2

Case 3

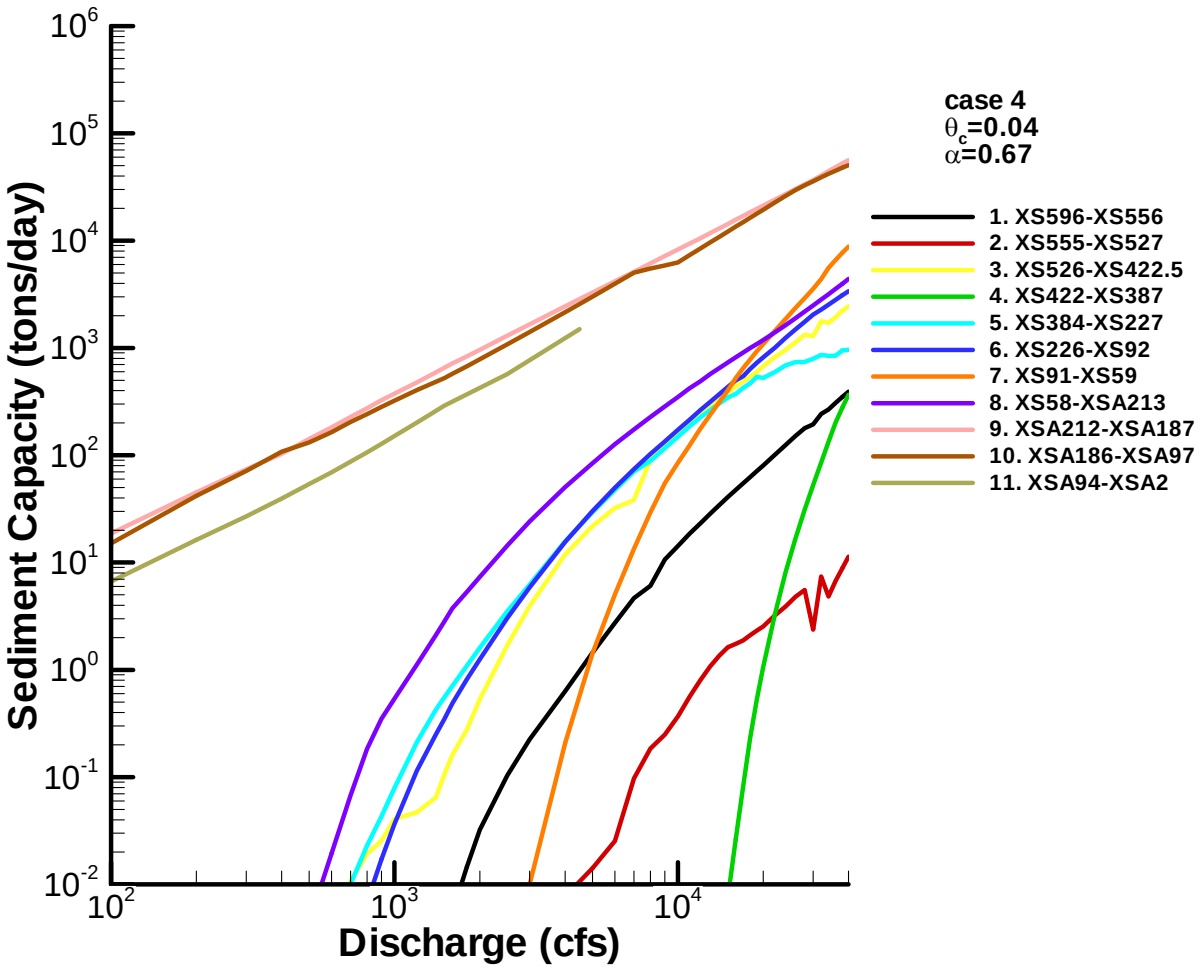
Sediment Capacity (tons/day)
Discharge (cfs)
case 4
θc=0.04
α=0.67
1. XS596-XS556
2. XS555-XS527
3. XS526-XS422.5
4. XS422-XS387
5. XS384-XS227
6. XS226-XS92
7. XS91-XS59
8. XS58-XSA213
9. XSA212-XSA187
10. XSA186-XSA97
11. XSA94-XSA2

Case 4

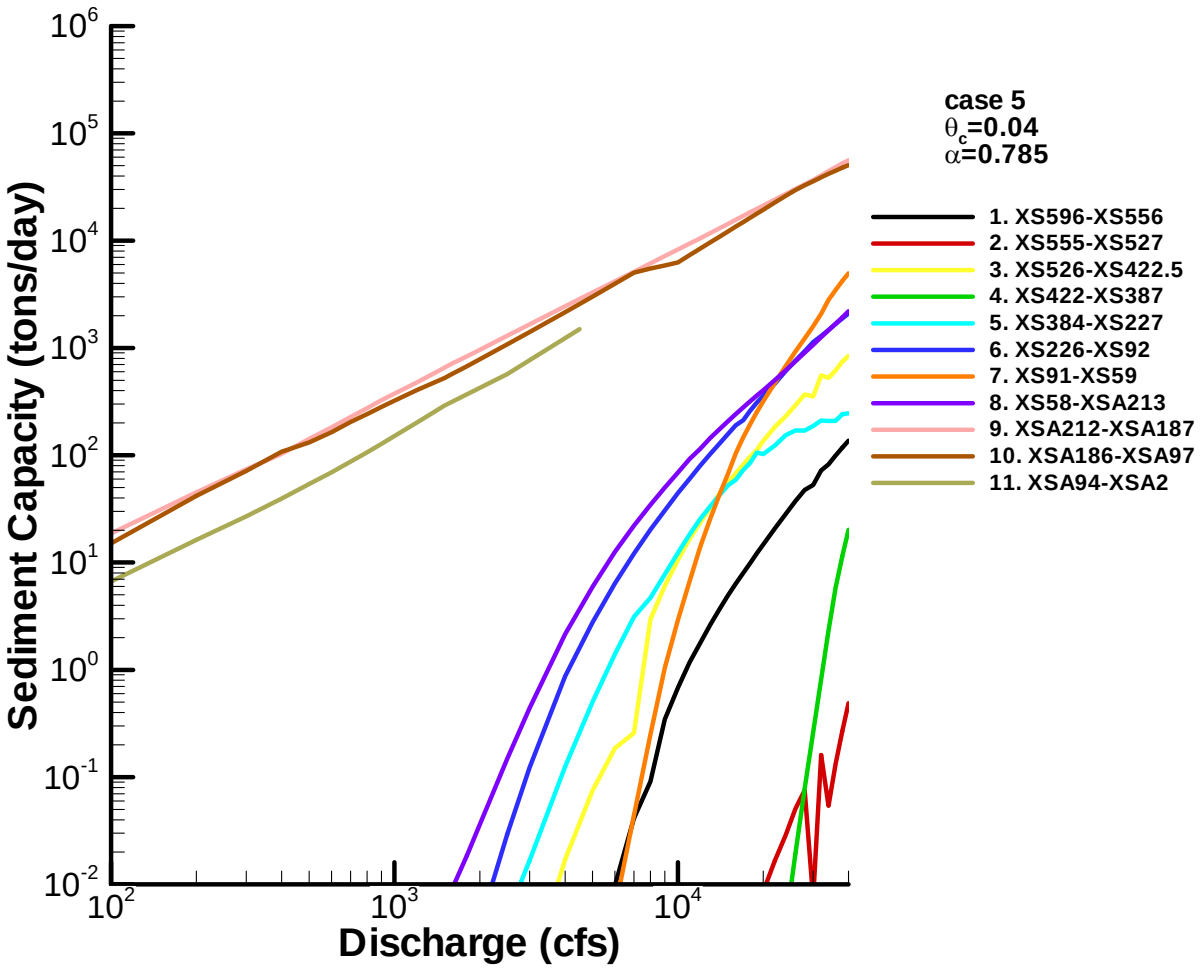
Sediment Capacity (tons/day)
Discharge (cfs)
case 5
θc=0.04
α=0.785
1. XS596-XS556
2. XS555-XS527
3. XS526-XS422.5
4. XS422-XS387
5. XS384-XS227
6. XS226-XS92
7. XS91-XS59
8. XS58-XSA213
9. XSA212-XSA187
10. XSA186-XSA97
11. XSA94-XSA2

Case 5

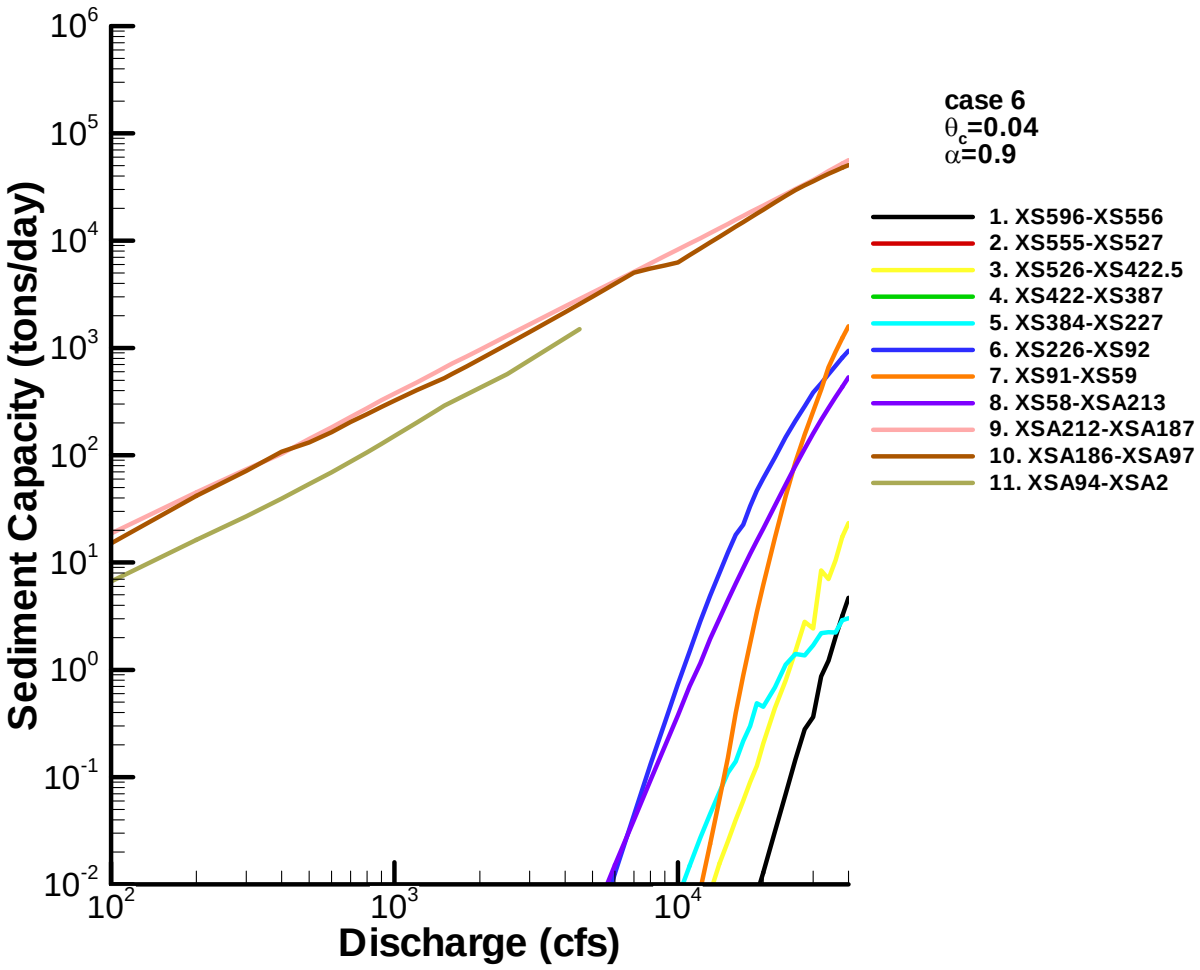
Sediment Capacity (tons/day)
Discharge (cfs)
case 6
θc=0.04
α=0.9
1. XS596-XS556
2. XS555-XS527
3. XS526-XS422.5
4. XS422-XS387
5. XS384-XS227
6. XS226-XS92
7. XS91-XS59
8. XS58-XSA213
9. XSA212-XSA187
10. XSA186-XSA97
11. XSA94-XSA2

Case 6

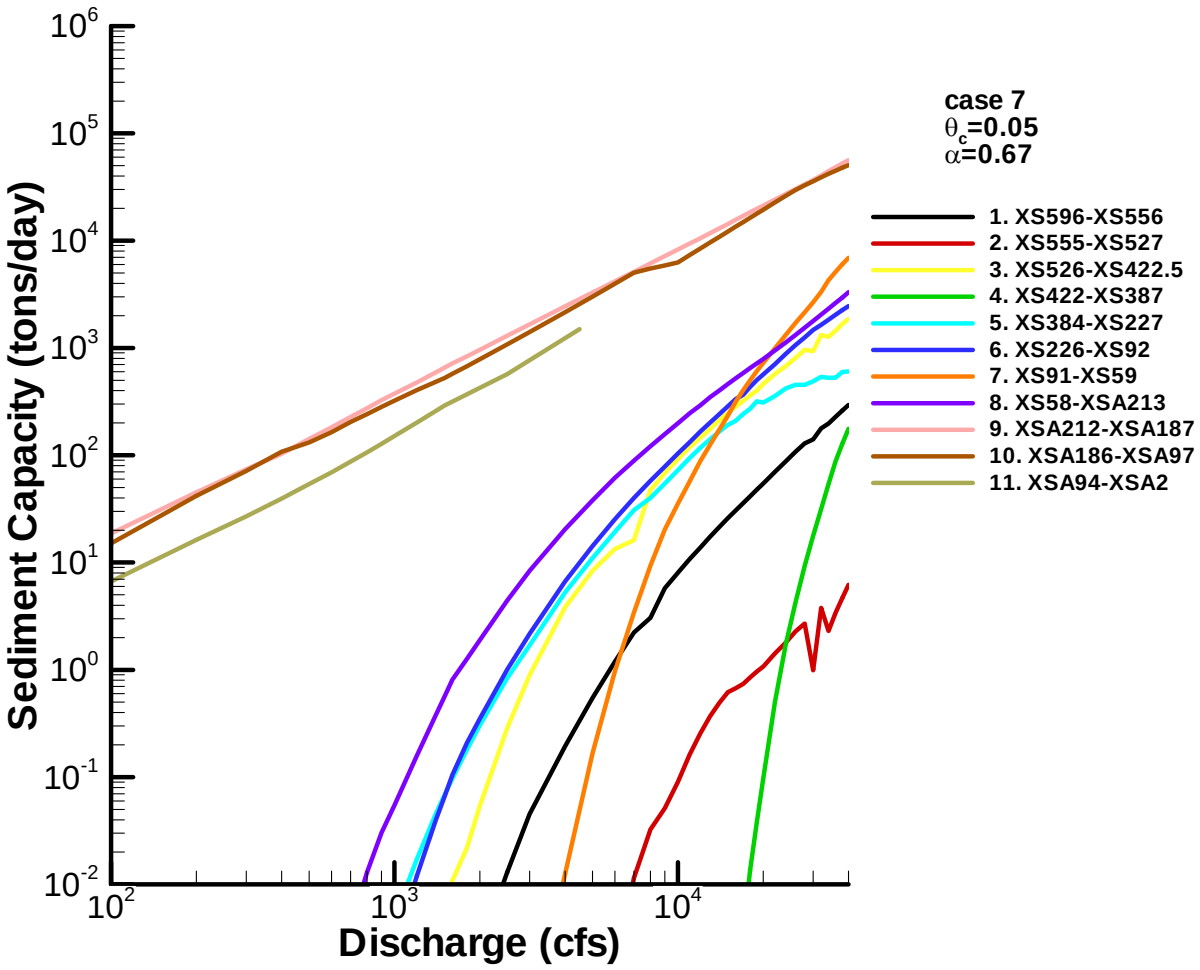
case 7
θc=0.05
α=0.67
1. XS596-XS556
2. XS555-XS527
3. XS526-XS422.5
4. XS422-XS387
5. XS384-XS227
6. XS226-XS92
7. XS91-XS59
8. XS58-XSA213
9. XSA212-XSA187
10. XSA186-XSA97
11. XSA94-XSA2
Sediment Capacity (tons/day)
Discharge (cfs)
10^6
10^5
10^4
10^3
10^2
10^1
10^0
10^-1
10^-2
10^2
10^3
10^4

Case 7

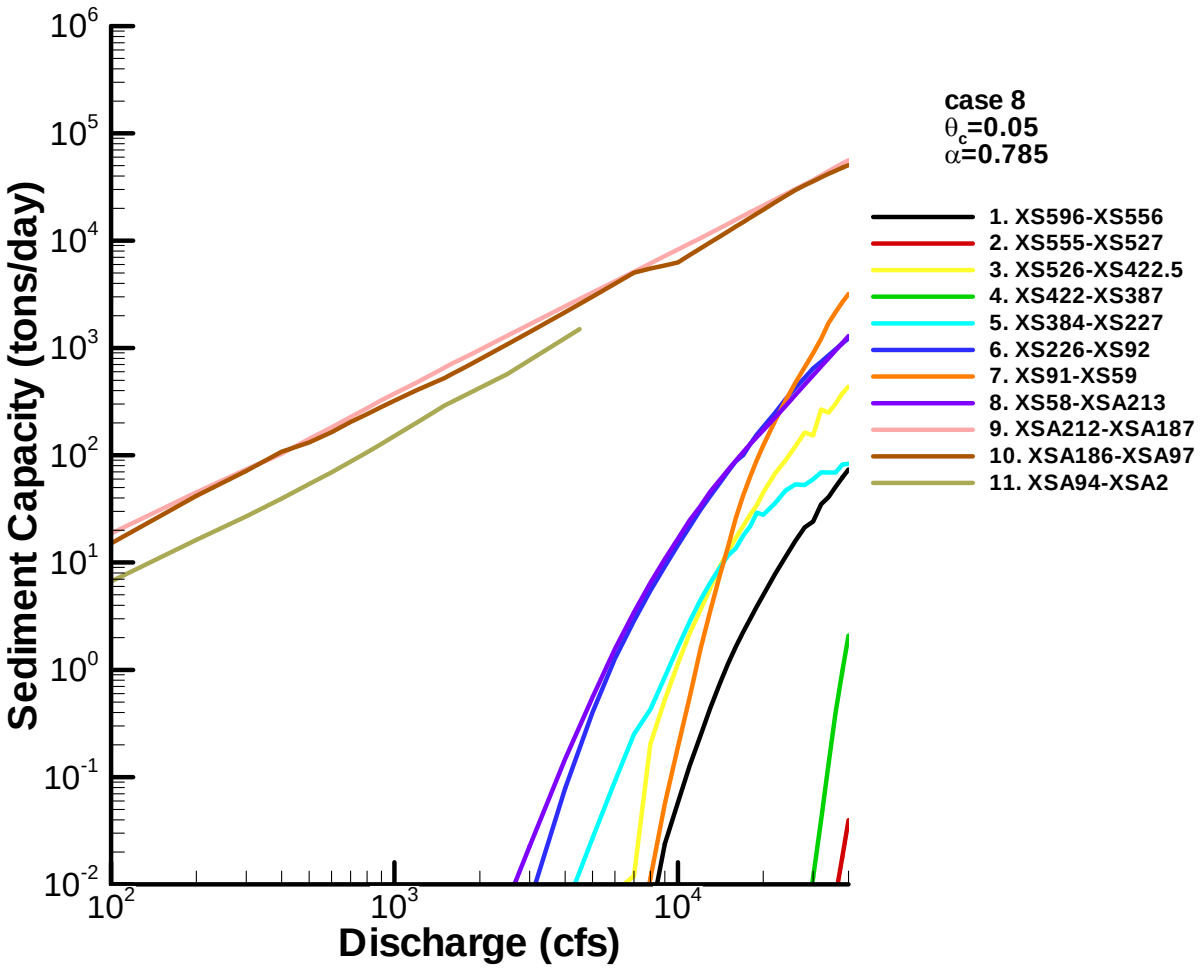
Sediment Capacity (tons/day)
Discharge (cfs)
case 8
θc=0.05
α=0.785
1. XS596-XS556
2. XS555-XS527
3. XS526-XS422.5
4. XS422-XS387
5. XS384-XS227
6. XS226-XS92
7. XS91-XS59
8. XS58-XSA213
9. XSA212-XSA187
10. XSA186-XSA97
11. XSA94-XSA2

Case 8

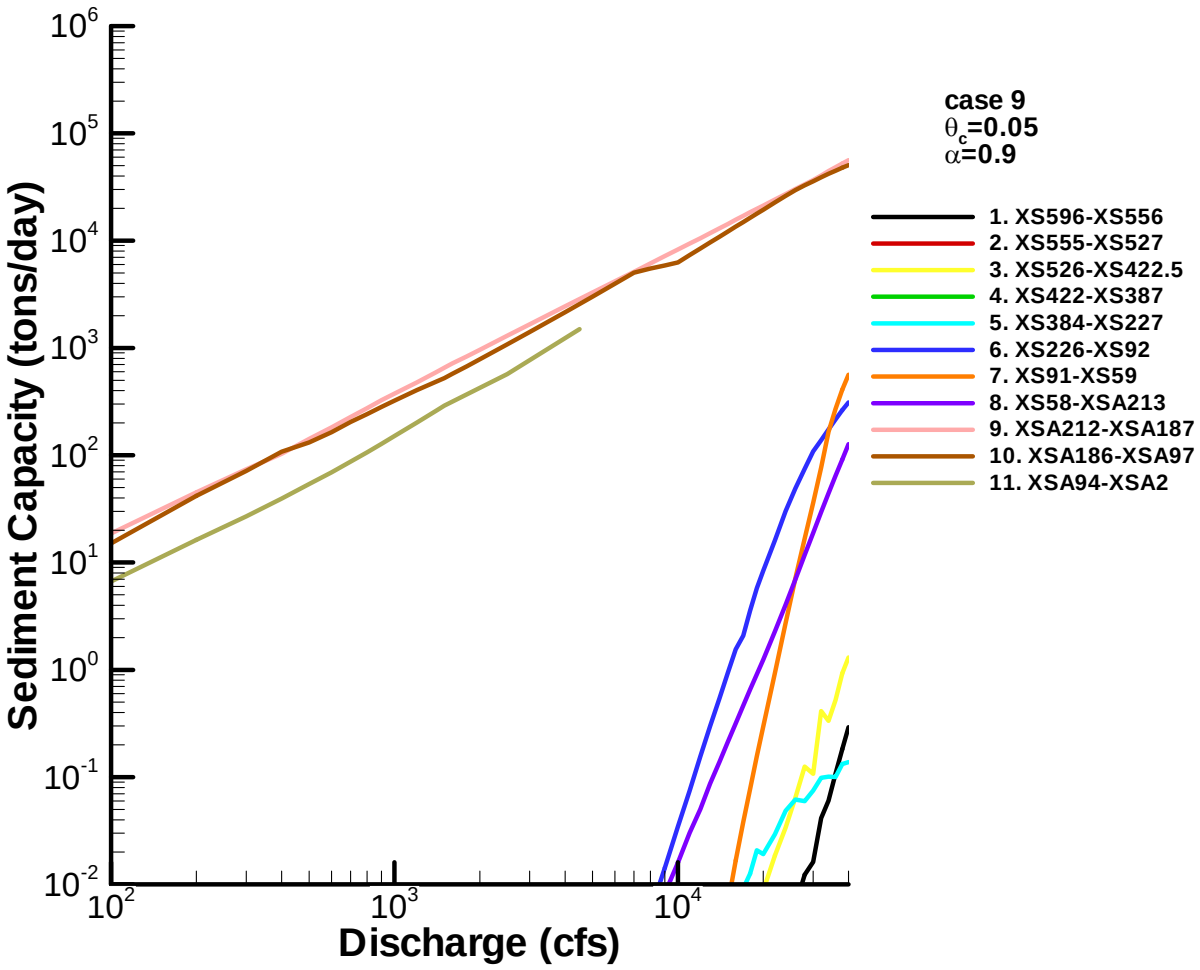
Sediment Capacity (tons/day)
Discharge (cfs)
case 9
θc=0.05
α=0.9
1. XS596-XS556
2. XS555-XS527
3. XS526-XS422.5
4. XS422-XS387
5. XS384-XS227
6. XS226-XS92
7. XS91-XS59
8. XS58-XSA213
9. XSA212-XSA187
10. XSA186-XSA97
11. XSA94-XSA2

Case 9

This page left blank intentionally.

Exhibit

Sensitivity Analysis of Annual Sediment Load Under Current Hydrology Using Parker's Gravel-Sand-Mixed Transport Equation Combined with Engelund and Hansen's Sand Transport Equation

Draft
Sediment Mobilization Assessment Attachment

Draft
April 2011

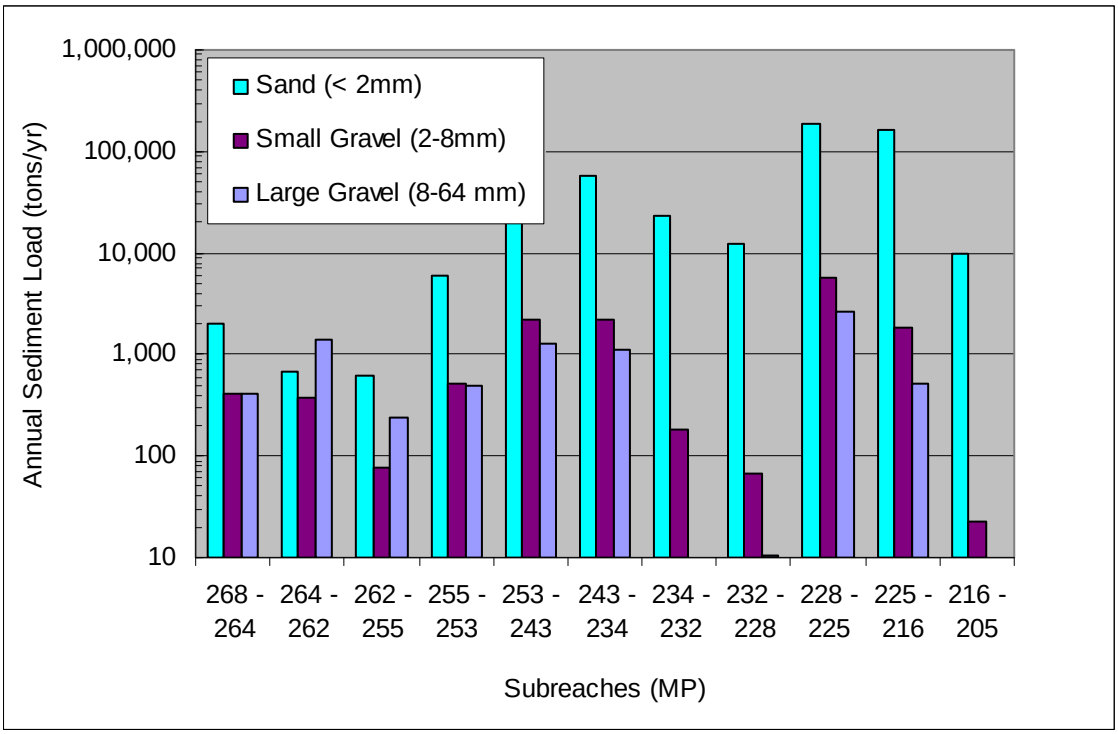

Case 1: $\theta_c = 0.03$ **and** $\alpha = 0.67$

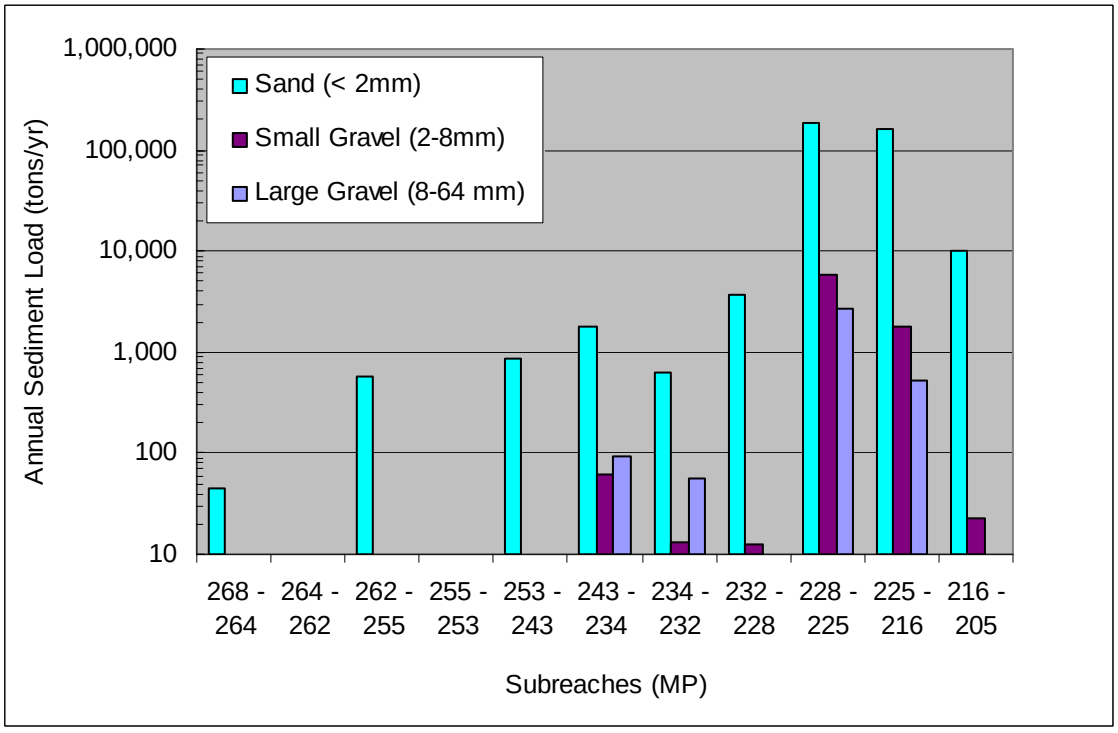

Case 2: $\theta_c = 0.03$ **and** $\alpha = 0.875$

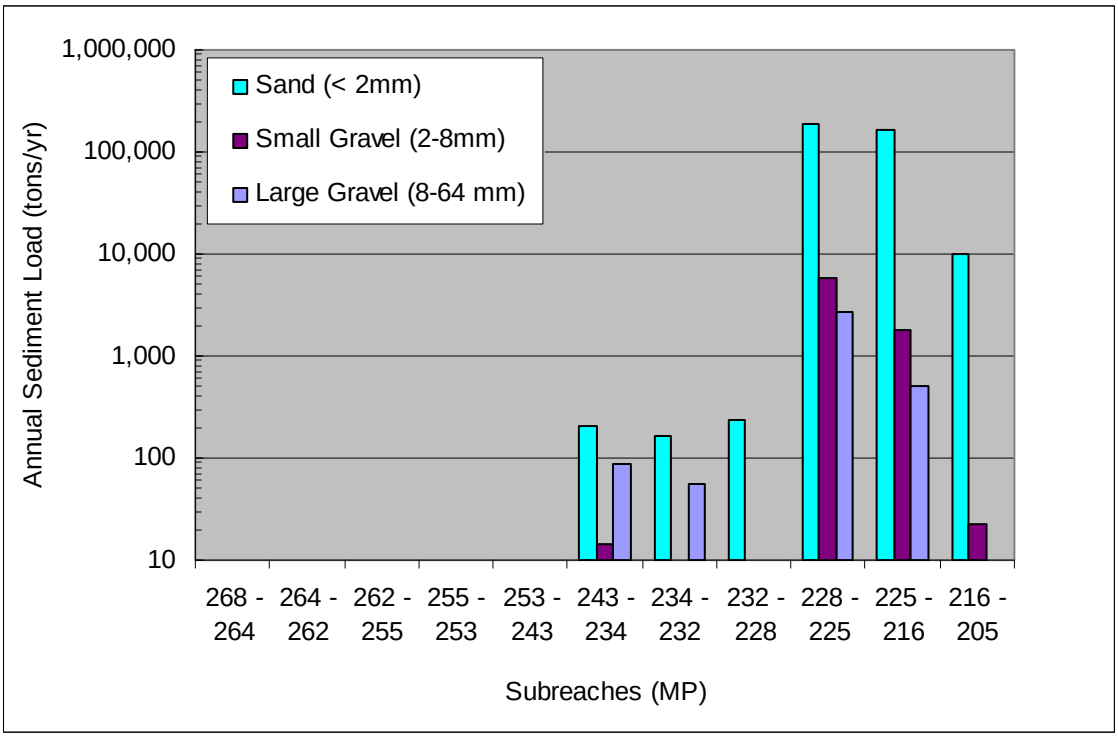

Case 3: $\theta_c = 0.03$ **and** $\alpha = 0.9$

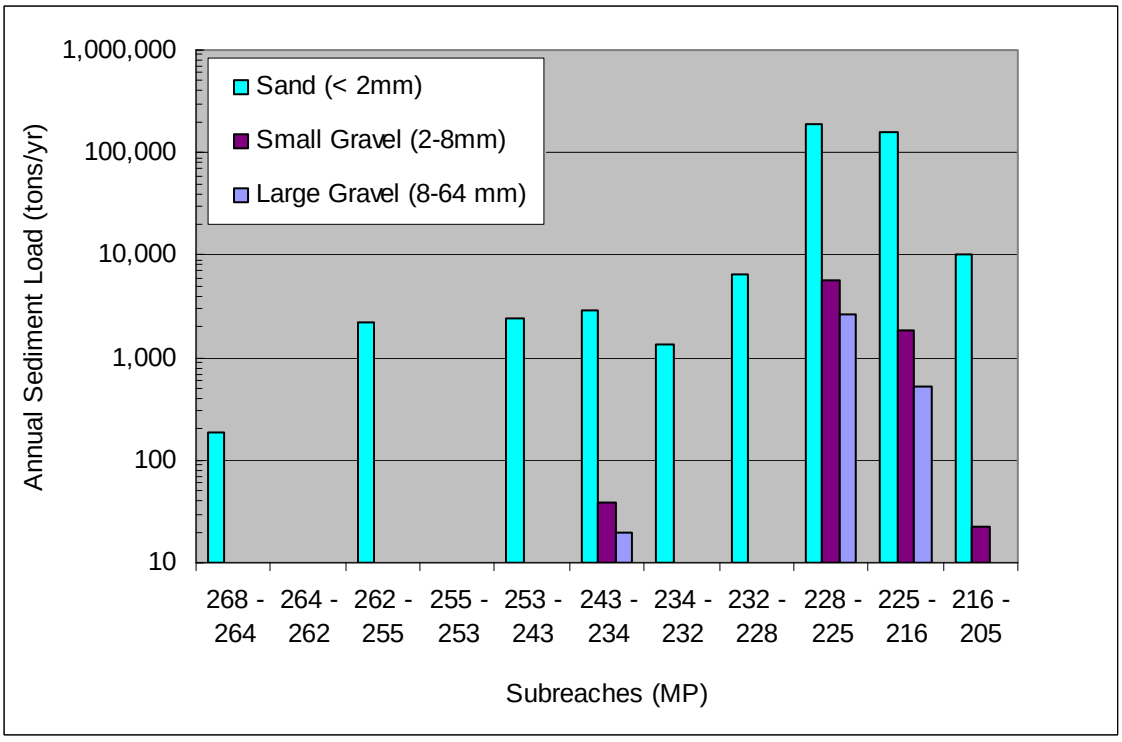

Case 4: $\theta_c = 0.04$ **and** $\alpha = 0.67$

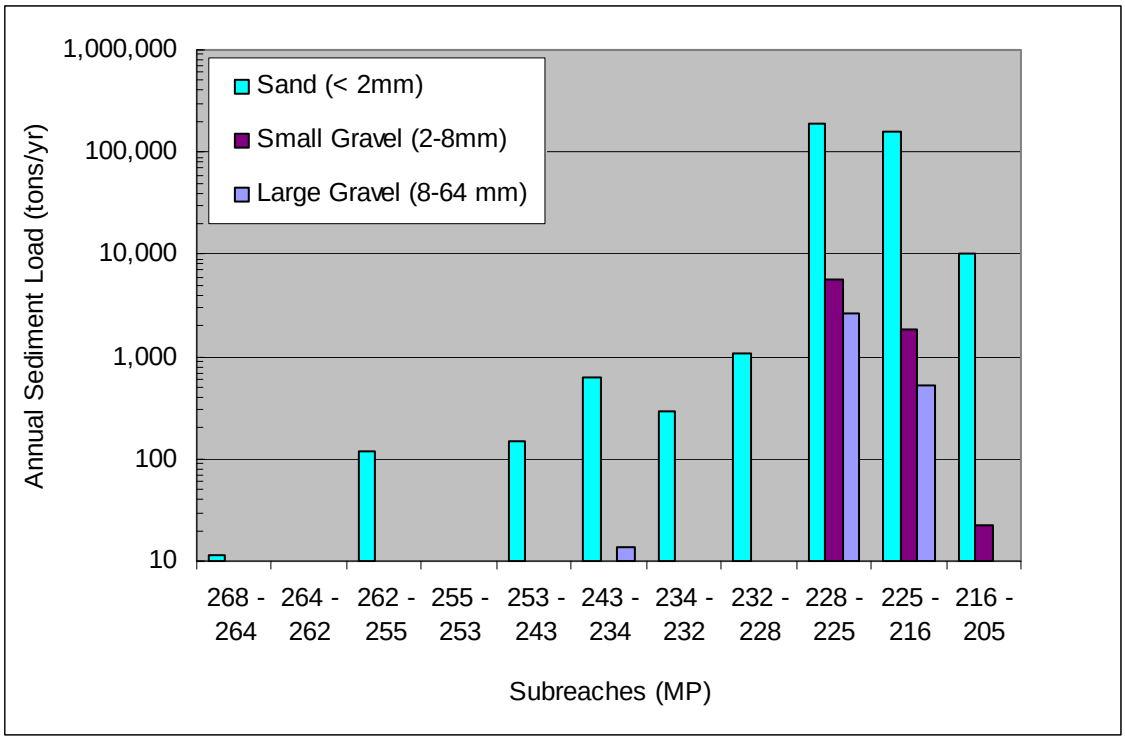

Case 5: $\theta_c = 0.04$ **and** $\alpha = 0.875$

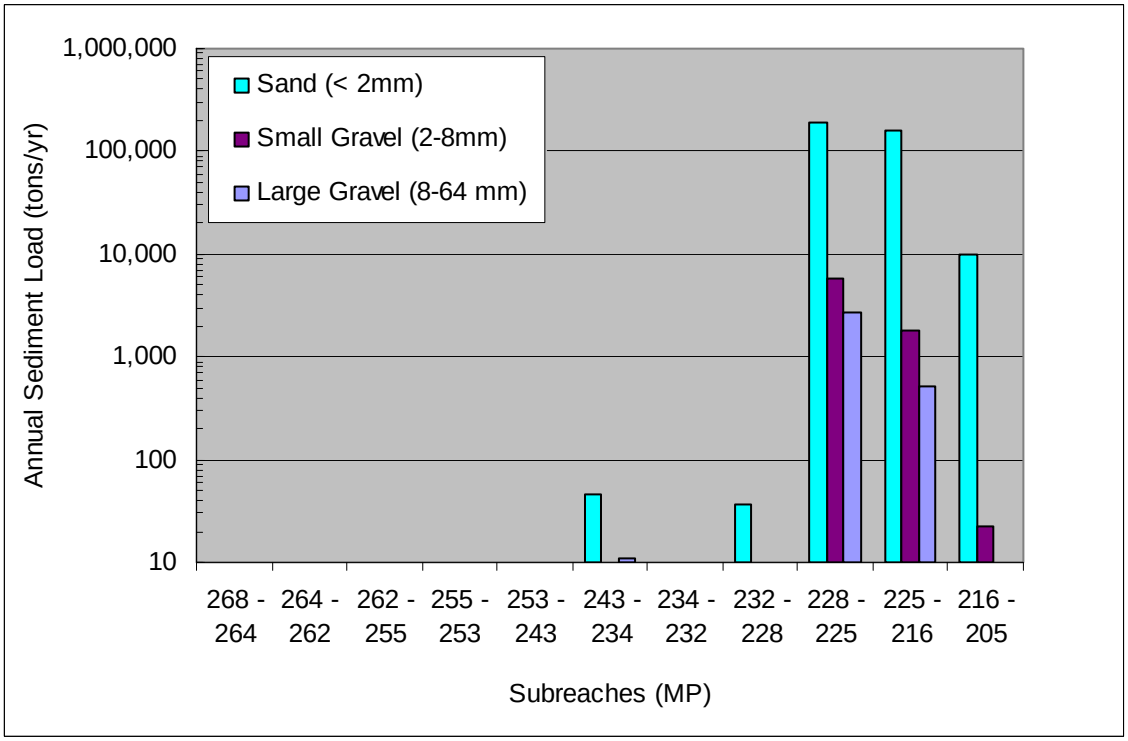

Case 6: $\theta_c = 0.04$ **and** $\alpha = 0.9$

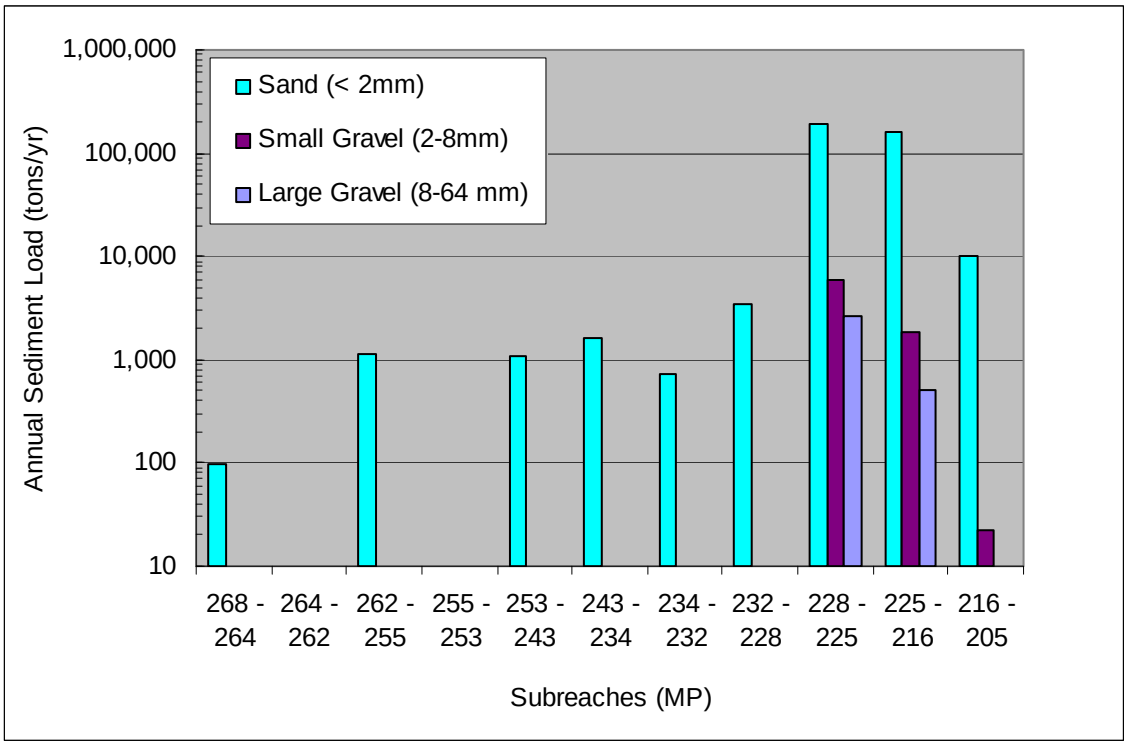

Case 7: $\theta_c = 0.05$ **and** $\alpha = 0.67$

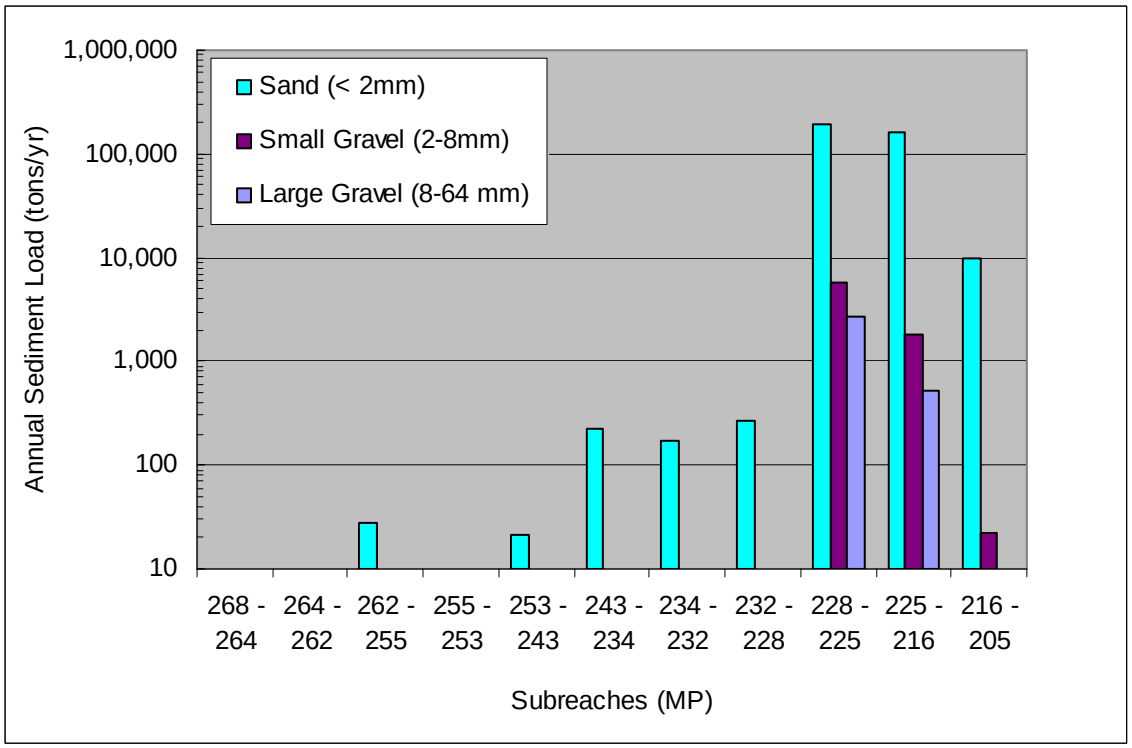

Case 8: $\theta_c = 0.05$ **and** $\alpha = 0.875$

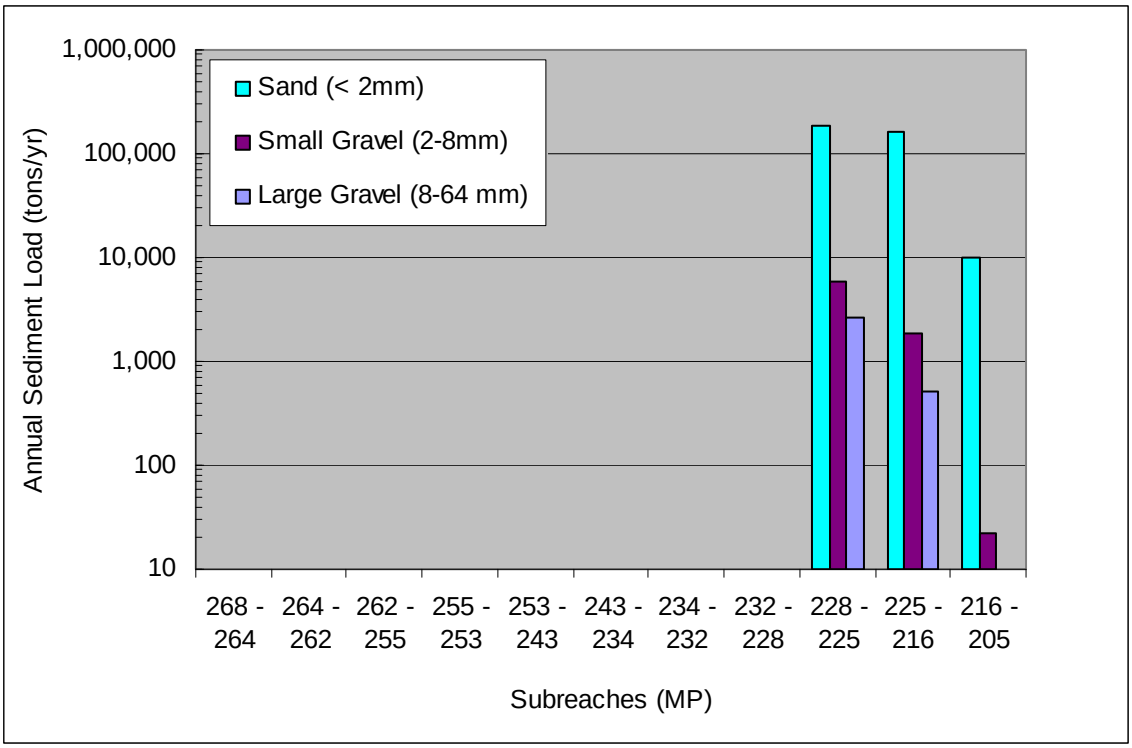

Case 9: $\theta_c = 0.05$ **and** $\alpha = 0.9$

This page left blank intentionally.

Attachment

Assessment of Sediment Transport and Channel Morphology on the San Joaquin River from Friant Dam to Mendota Dam

Draft
Geomorphology, Sediment Transport, and Vegetation Assessment Appendix

SAN JOAQUIN RIVER
RESTORATION PROGRAM

Draft
April 2011

Assessment of Sediment Transport and Channel Morphology on the San Joaquin River from Friant Dam to Mendota Dam

Report Prepared by:

Jianchun Huang, P.E., Ph.D., Hydraulic Engineer
Sedimentation and River Hydraulics Group, Technical Service Center

Signature:_____

Blair P. Greimann, P.E., Ph.D., Hydraulic Engineer
Sedimentation and River Hydraulics Group, Technical Service Center

Signature:_____

Peer Reviewed by:

Elaina Holburn, P.E., M.S., Hydraulic Engineer
Sedimentation and River Hydraulics Group, Technical Service Center

Signature:_____

Table of Contents

Exhibits

Tables

Figures

Abbreviations and Acronyms

1D	one-dimensional
ALS	Average Levee Setback
Caltrans	California Department of Transportation
CBP	Chowchilla Bypass downstream from Chowchilla Bifurcation Structure gage
cfs	cubic feet per second
CRF	San Joaquin River near Gravelly Ford gage
DTM	digital terrain model
MEI	Mussetter Engineering, Inc.
MIL	San Joaquin River below Friant Dam gage
MLS	Maximum Levee Setback
n	Manning's roughness coefficient
PEIS/R	Programmatic Environmental Impact Statement/Report
Reclamation	U.S. Department of the Interior, Bureau of Reclamation
RP	River Post
SJB	San Joaquin River downstream from Chowchilla Bifurcation Structure gage
SJRRP	San Joaquin River Restoration Program
SRH-1D	Sedimentation and River Hydraulics – One Dimensional
TSC	Technical Service Center

This page left blank intentionally.

1.0 Introduction

The Denver Technical Service Center (TSC) of the U.S. Department of the Interior, Bureau of Reclamation (Reclamation), was requested to perform an analysis of the sediment transport and channel morphology of the San Joaquin River between Friant Dam and the Merced River confluence. This report documents how the Sedimentation and River Hydraulics – One Dimensional (SRH-1D) hydraulic and sediment transport model (Huang and Greimann 2007) was used for this purpose. The assessment presented herein was conducted in support of the San Joaquin River Restoration Program (SJRRP) and is part of a larger analysis that focuses on the sediment transport and geomorphic characteristics of the San Joaquin River. A separate report documents further investigations of the sediment mobilization and reach-averaged sediment transport characteristics of the San Joaquin River from Friant Dam to the Merced River confluence (Huang and Greimann 2009b). This report is intended to support the Programmatic Environmental Impact Statement/Report (PEIS/R) for the SJRRP.

The current report covers two reaches. Project Reach 1 extends from Friant Dam to Gravelly Ford (River Post (RP) 267.5 to RP 229.0). Project Reach 2 extends from Gravelly Ford to Mendota Dam (RP 229.0 to RP 204.8) (Figure 1-1).

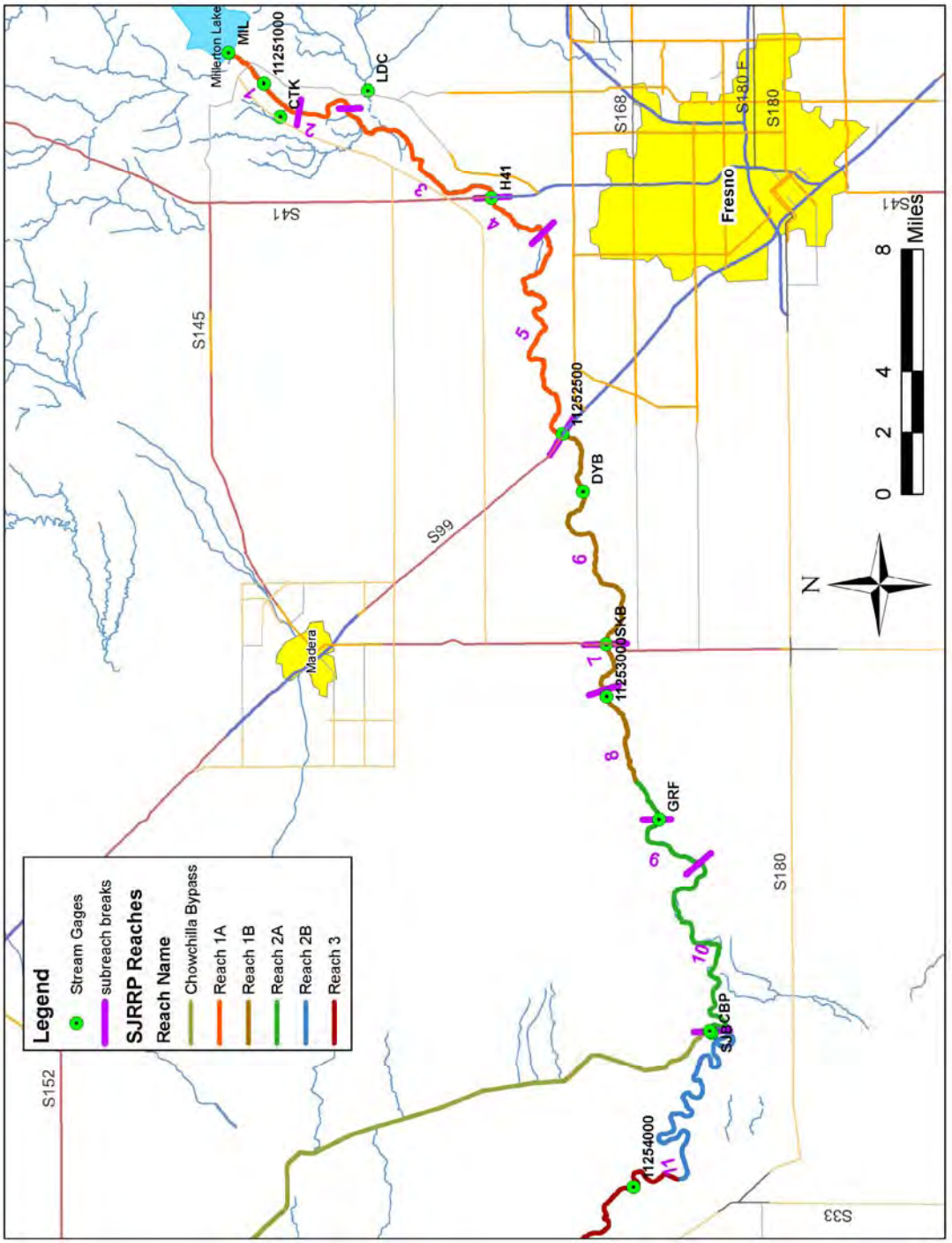

Figure 1-1.
Overview Map of Study Area (SJRRP Reaches 1 and 2)

1

2.0 Input Data

2.1 Hydrology

Three different hydrologic sets were analyzed in this report: Baseline Conditions, Project Conditions, and Historical Gage data.

The Baseline Conditions refer to the simulated flows in the San Joaquin River if current water operations were followed. CalSim II was used to develop the Baseline Conditions assuming that current water operations were followed and the Historical Conditions occur again. The monthly average flows from CalSim II were then downscaled to daily flows. These daily flows are also used in HEC5Q simulations of the river temperature. The details of the hydrologic modeling of the Baseline Conditions are given in the Appendix H of the PEIS/R.

The Project Conditions are also referred to as Alternative A in this report. These are the simulated flows in the San Joaquin River under the SJRRP and if the historic hydrology were to occur again. Details of the Baseline and Project scenarios are found in Appendix H of the PEIS/R. Two sets of Baseline and Project scenarios were developed: Future and Existing. For the purposes of this report, however, the Future and Existing scenarios are considered identical. This is based upon an analysis of the flow-duration curves that found no significant difference between the two scenarios. The Project Conditions assume that the maximum flow in Reach 4b1 will be 475 cubic feet per second (cfs).

The Historical Gage data was taken from U.S. Geological Survey stream gages shown in Figure 1-1. Of the gages shown in the figure, four gage stations provided Historical hydrology and are given in Table 2-1. The records for the other gages were not complete. Flow-duration curves were computed for each of these gages. The endpoint of the reaches used in the analysis did not always correspond to the gage locations. For these reaches, flow-duration curves were linearly interpolated from the gage values based upon the distance of the downstream end of the reach relative to the gage locations.

The flow-duration curves using the Historical Gage data, Baseline Conditions, and Alternative A are given in Figures 2-1, 2-2, and 2-3 for the Friant Dam, Gravelly Ford, and San Joaquin below Chowchilla stream gages, respectively. A common period from January 1, 1980, to May 31, 1997, was used to develop the flow-duration curves. This period of flow records was available for the gages shown in these figures. For the Friant Dam and Gravelly Ford stream gages, the Alternative A flows have a higher frequency of flows between 100 cfs and 2,300 cfs, compared to Baseline Conditions. Alternative A flows also show a slightly lower frequency of flows above 2,300 cfs. There is a significant increase in flows in the San Joaquin River below the Chowchilla Control Structure because the maximum release to the San Joaquin River was increased to 4,500

cfs, where under Baseline Conditions it is approximately 1,500 cfs, except when there are uncontrolled spills at Friant Dam.

Table 2-1.
Stream Gages Used to Derive Flow-Duration Curves

Description	Stream Gage ID	River Post (mile)	HEC-RAS XC	Agency
San Joaquin River Below Friant Dam	MIL	267.5	XS596	Reclamation
San Joaquin River near Gravelly Ford	GRF	227.5	XSA213	Reclamation
Chowchilla Bypass downstream from Chowchilla Bifurcation Structure	CBP	-	-	California Department of Water Resources
San Joaquin River downstream from Chowchilla Bifurcation Structure	SJB	216	XSA97	Reclamation

Note:
Historical (H) refers to gage used for historical flow analysis. Project (P) refers to gage used for future SJRRP flow analysis.
Key:
ID = Irrigation District

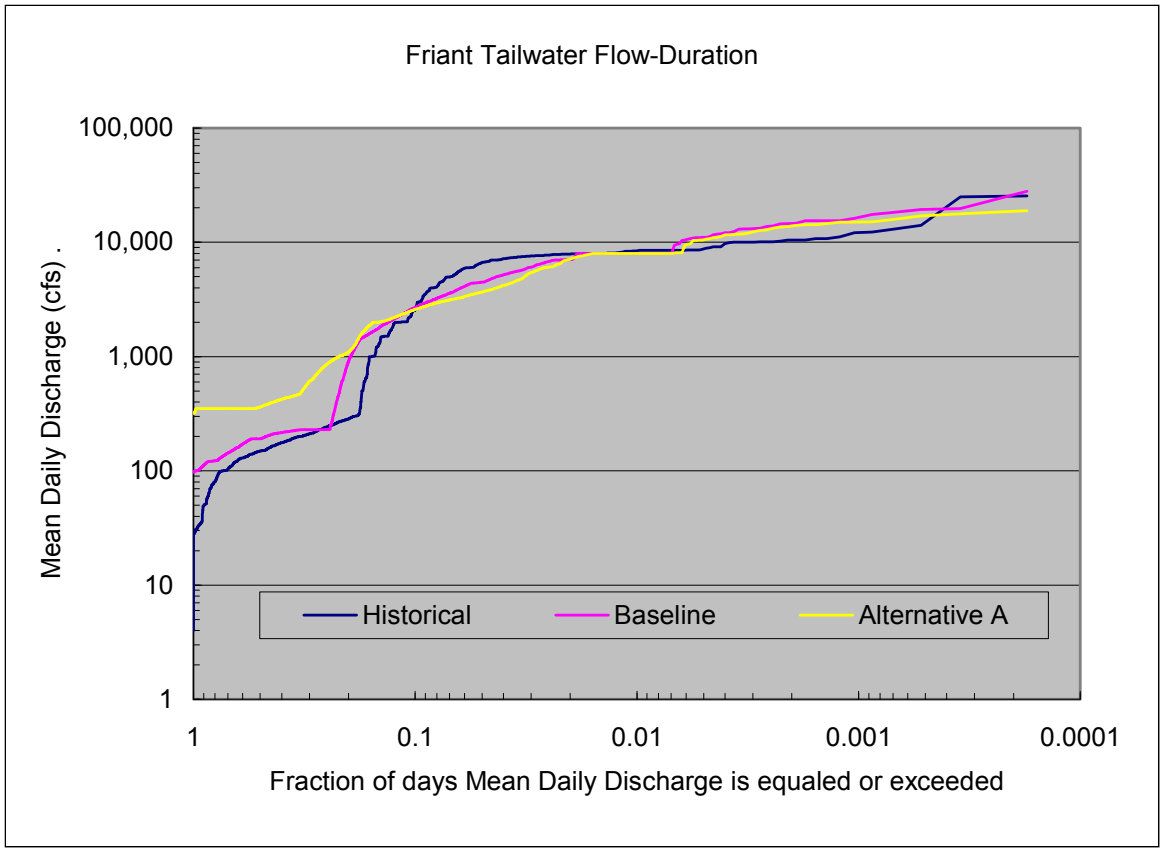

Note: The flow-duration curves are based upon daily average flow records from January 1, 1980, to May 31, 1997

Figure 2-1.
Flow-Duration Curves at Friant Dam

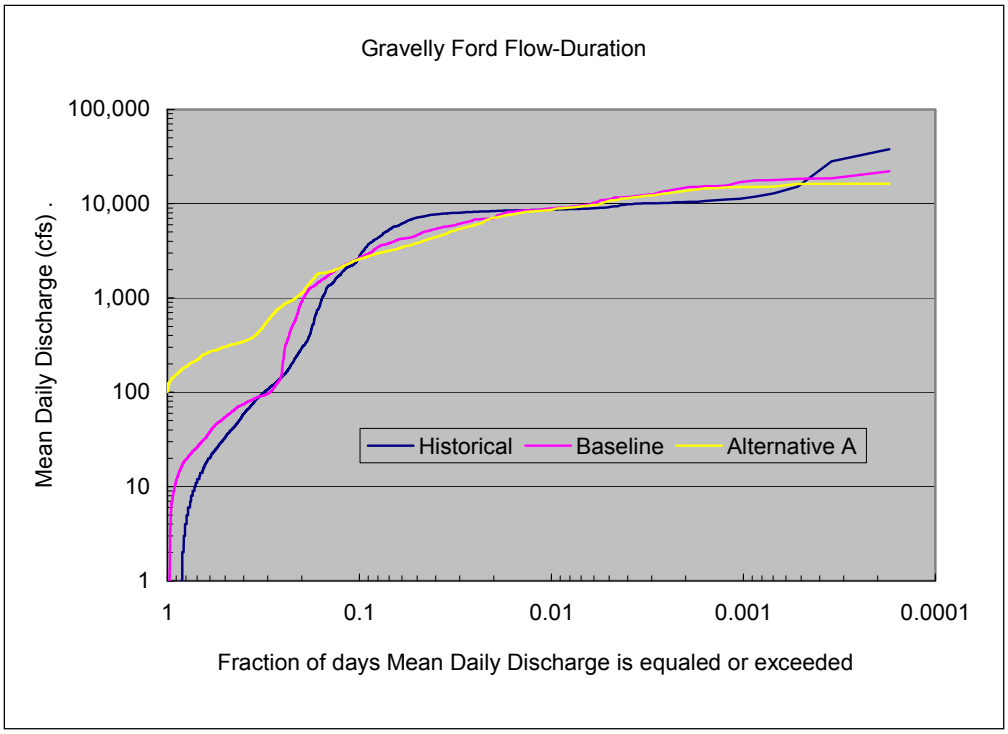

Note: The historical flow-duration curve is based upon daily average flow records from January 1, 1980, to May 31, 1997.

Figure 2-2.
Flow-Duration Curves at Gravelly Ford

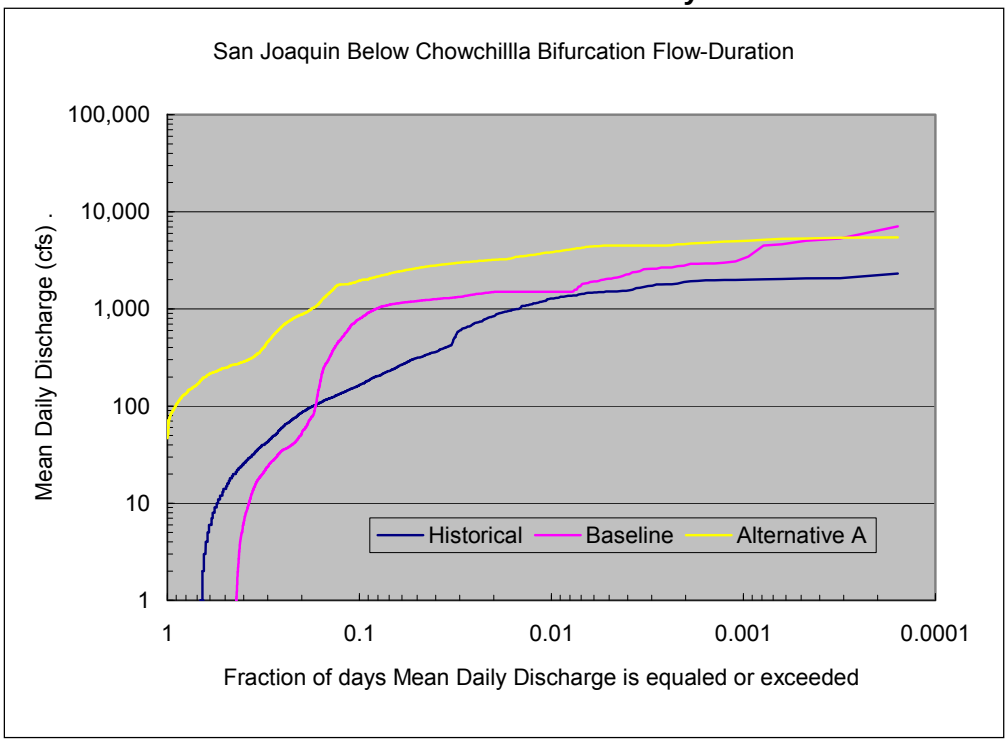

Figure 2-3.
Flow-Duration Curves on San Joaquin River Downstream from Chowchilla Bifurcation Structure from January 1, 1980, to May 31, 1997

2.2 Upstream Boundary Conditions

Sediment input from upstream and lateral point and not-point sources are required by the SRH-1D model. The upstream flow rate into the model was based on flows recorded at the gage station downstream from Friant Dam (XS596). Friant Dam was assumed to block all incoming sediment from upstream reaches, and therefore no sediment load was input at the upstream boundary.

2.3 Lateral Flow and Sediment Sources

Four gages were used for lateral flow calculation under Historical hydrology. Gages at San Joaquin River below Friant Dam (MIL) and San Joaquin River near Gravelly Ford (CRF) were used to determine flow rates at the upstream ends of Subreaches 1 and 9, respectively. Flows from the gages at the Chowchilla Bypass downstream from the Chowchilla Bifurcation Structure (CBP) and the San Joaquin River downstream from the Chowchilla Bifurcation Structure (SJB) were combined to represent the flow rate at the cross section upstream from the Chowchilla Bifurcation Structure (XSA 97). The San Joaquin River downstream from the Chowchilla Bifurcation Structure (SJB) was used to represent flow through all cross sections in Subreach 11. Flow rates at all the other subreaches were interpolated from existing data.

Lateral non-point flow sources were used to simulate the flow difference between each subreach. Flow differences between subreaches upstream from the Chowchilla Bifurcation Structure were mainly due to water losses by channel percolation; however, no sediment was added to or removed from the system. A negative point source was used to simulate the flow diversion at the Chowchilla Bifurcation Structure. The reduction in sediment from the San Joaquin River was calculated as proportional to the flow diversion at the Chowchilla Bypass Structure. The same sediment concentration was assumed for flow diverted to the bypass as flow routed through the river downstream from the bifurcation structure. Field measurements of sediment concentrations could be used in the future to validate or modify this assumption.

2.4 Cross-Section Geometry

HEC-RAS geometry data were provided by Mussetter Engineering, Inc. (MEI) (2002a) to Reclamation for all project reaches and bypasses. MEI first developed a HEC-2 hydraulic model, which was transferred into a HEC-RAS model. MEI used a total of 872 cross sections to represent the 63-mile reach from Friant Dam to Mendota Dam in Project Reaches 1 and 2. The HEC-RAS geometry data were derived from 1998 topographic and bathymetric surveys conducted by Ayres Associates, Inc. for Reclamation and U.S. Army Corps of Engineers (Ayres 1998, 1999). Intergraph Site Works, Version 7.01, in conjunction with Bentley Systems MicroStation, Version 7.00, was used to digitize cross-section geometry from the topographic data provided in digital terrain model (DTM) format.

River characteristics are represented by cross sections in a one-dimensional (1D) model. To reduce the model run time for the SRH-1D mobile bed model without substantially impacting reach-averaged results, the total number of cross sections was reduced. The study reach was represented with 143 cross sections out of the 872 total available HEC-RAS cross sections. One cross section was chosen from every six HEC-RAS cross sections for an average spacing of 2,316 feet and a maximum spacing of 6,260 feet.

The original HEC-RAS geometry used a looped channel network to model a side channel between RP 263.4 (XS543) and RP 262.1 (XS521), in which the side channel was blocked in the cross-section geometry of the main channel, and vice versa. In the SRH-1D model, this loop was eliminated, and multiple channels were represented within a single cross section. Even though SRH-1D supports looped channel networks, this function has not been fully tested for mobile bed calculations, and including loops greatly increases the model computation time. This study incorporated the main channel and side channel geometry into one cross section for flow and sediment calculations. Differences in the modeled water surface elevations between the HEC-RAS model with channel network and SRH-1D model without channel network were minor (see Exhibit B).

Depth-varied Manning's coefficients were used in the MEI HEC-RAS model to calibrate the water surface elevations across different flow rates and were only applied in some cross sections (MEI 2002a). SRH-1D does not implement the depth-varied Manning's coefficients modeled in the MEI HEC-RAS model. Instead, a simplified Manning's coefficient was developed for SRH-1D by averaging the depth-varied Manning's coefficients from the HEC-RAS model. In most cross sections where depth-varied coefficients were not applied, the Manning's roughness coefficient (n) was set to 0.035 for the main channel and 0.15 for the floodplain based on previous hydraulic calculations of MEI (2002).

In Reach 2b, channel geometry was modified to include a levee setback because Alternative A diverts more high flows into Reach 2b than under Historical or Baseline hydrologic conditions. The current levees in Reach 2b cannot contain flows exceeding 1,500 cfs. Two options of levee setbacks are currently under consideration: (1) Average Levee Setback (ALS), and (2) Maximum Levee Setback (MLS). HEC-RAS geometry for each option was provided by MEI to Reclamation with new locations and heights of setback levees. The levee setback options only affect the geometry in Reach 2b downstream from the Chowchilla Bifurcation Structure. In the Alternative A analysis, the effects of both the ALS and MLS options on sediment transport characteristics were investigated.

Within the current assessment, the 1998 geometry and 2008 sediment sizes were used in the simulations. Current geometry may be different from the 1998 geometry, but newer topographic data were not available for comparison at the time of this analysis. The available geometry data were sufficient to evaluate how the sediment transport characteristics and channel morphology may change under future hydrologic conditions.

2.5 In-Channel Structures

Bridges and culvert crossings are represented by stage-discharge rating curve tables in the SRH-1D model. The original bridges and culvert crossings data in HEC-RAS geometry files were obtained from the California Department of Transportation (Caltrans), the Southern Pacific Railroad, and the Atchison Topeka Santa Fe Railroad. These data, however, were not used directly in the SRH-1D model. HEC-RAS hydraulic analysis was first performed. Differences in the water surface elevations upstream and downstream from the structures were then computed from the HEC-RAS model for the flows of interest. Only structures affecting water surface elevations by 1 foot or more were considered in the SRH-1D model. Three structures were identified as significant, but the Lower Gravel Pit Crossing was no longer physically present and therefore not used as internal boundary condition. The other two structures, Ledger Island Bridge and Chowchilla Bypass Structure, were each represented by a rating curve table in the SRH-1D model (Exhibit A of this report). All the other structures were identified as insignificant and were not included in the SRH-1D model.

The calculated water surface profiles of the HEC-RAS model and the SRH-1D model were compared with the HEC-2 results reported by MEI (2002). Results are displayed in Exhibit B for nine profiles. Similar results were obtained for all three models. For low-flow release from Friant Dam (100 cfs), the average difference between SRH-1D and HEC-RAS calculated water surface elevations was 0.07 foot with a maximum value of 0.36 foot. For Friant dam releases of 4,000 cfs and 16,400 cfs, the average difference increases to 0.26 foot and 0.79 foot, respectively, and the maximum difference increases to 1.35 foot and 2.81 foot, respectively. The difference between the results of HEC-RAS and SHR-1D may result from fewer or simplified representation of hydraulic structures by a rating curve and simplified Manning's coefficient representation in SRH-1D compared with depth-varied Manning's coefficients in HEC-RAS.

2.6 Downstream Boundary Condition

The downstream boundary of the SRH-1D model is the Mendota Dam (XSA2, RP 204.6). During flows less then 1,500 cfs, the water surface elevation of Mendota Pool was set at an elevation of 152.7 feet (MEI 2002). For higher elevations, the pool elevation was estimated using a weir equation.

$$H = H_0 + \left(\frac{Q}{CB} \right)^{2/3} \tag{2.1}$$

Where: H = pool elevation at the dam
H0 = dam crest elevation = 153.1 feet with additional boards installed
Q = discharge
B = dam width (382 feet)
C = weir coefficient (= 3.0)

2.7 Surface Bed Material

Surface bed material data used in the sediment transport analysis were derived from surface samples collected in February 2008 (Reclamation 2008), 29 of which were located in Project Reaches 1 and 2. Stillwater Sciences has also collected pebble count data in Reach 1a (Stillwater Sciences 2003). However, the sediment transport model requires the fraction of material by weight in each size class present in the bed and therefore the Stillwater data were not used to compute the sediment transport and channel morphology. The fraction of bed material comprising each size class is given in Table 2-2. Sample 3-6 (XSA208) was collected on a sand patch in a gravel reach, and was averaged with samples 3-10 (XSA212) and 3-7 (XSA206) to represent the bed material at XSA208. Sample 3-18 (XSA151) was collected on a gravel patch in a sand reach, and was averaged with samples 3-17 (XSA169) and 3-19 (XSA135) to represent the bed material at XSA151. For cross sections where bed material samples were not available, SRH-1D automatically interpolates the surface bed material based upon linear channel distance from the nearest sediment samples.

Table 2-2.
Fraction of Sampled Bed Sediment Finer than Specified Sizes, as Used in the Sediment Transport Study

Site ID	XS-ID	RM	Location	0.063 mm	0.125 mm	0.25 mm	0.5 mm	1 mm
2-1	XS586	266.8	Friant Dam	0.0002	0.0001	0.0002	0.0003	0.0006
2-2	XS511	261.2	Defehr	0.0000	0.0000	0.0001	0.0001	0.0003
3-1	XS502	260.5	Reach 1A	0.0000	0.0000	0.0000	0.0000	0.0000
1-1	XS481	258.8	Vulcan 1	0.0000	0.0000	0.0001	0.0000	0.0002
1-2	XS458	257.5	Vulcan 2	0.0005	0.0003	0.0005	0.0005	0.0005
2-3	XS443	256.5	Finch	0.0040	0.0035	0.0206	0.0298	0.0192
3-2	XS421	255.2	Reach 1A	0.0005	0.0001	0.0003	0.0004	0.0012
3-4	XS383	252.7	Reach 1A	0.0034	0.0021	0.0124	0.0421	0.0950
1-3	XS344	250	Scout Island	0.0005	0.0003	0.0005	0.0005	0.0005
1-4	XS316	248.3	Hanson Ranch	0.0024	0.0013	0.0026	0.0059	0.0255
1-5	XS268	245.5	Fresno City Parks	0.0021	0.0008	0.0035	0.0145	0.0154
1-6	XS211	242.3	Naffziger	0.0006	0.0002	0.0006	0.0043	0.0172
3-21	XS126	236.2	Reach 1B	0.0041	0.0025	0.0076	0.0294	0.0686
2-4	XS95	234.2	Skaggs Bridge	0.0003	0.0000	0.0002	0.0009	0.0056
2-6	XS511	231.9	DS of Skaggs Gage	0.0153	0.0032	0.0202	0.0612	0.0130
2-5	XS37	231.1	Bellach	0.0006	0.0002	0.0011	0.0033	0.0061
3-11	XSA218	228.5	Reach 1B	0.0102	0.0036	0.0147	0.0315	0.1326
3-13	XSA217	228.3	Reach 1B	0.0028	0.0021	0.0072	0.0206	0.0284
3-10	XSA212	227.5	Reach 2A	0.0100	0.0067	0.0463	0.1287	0.1563
3-6	XSA208	226.9	Reach 2A	0.0138	0.0055	0.0218	0.1759	0.4048
3-7	XSA206	226.8	Reach 2A	0.0024	0.0005	0.0175	0.1007	0.1697
3-14	XSA177	224.1	Reach 2A	0.0827	0.0304	0.0481	0.1995	0.3496
3-17	XSA169	223.3	Reach 2A	0.0073	0.0072	0.0549	0.3499	0.392
3-18	XSA151	221.4	Reach 2A	0.0150	0.0064	0.0359	0.1211	0.1321
3-19	XSA135	219.7	Reach 2A	0.0156	0.0110	0.0592	0.4291	0.3917
3-20	XSA115	218	Reach 2A	0.0318	0.0128	0.0378	0.1778	0.4222
2-11	XSA111	217.5	Reach 2A	0.0153	0.0088	0.0540	0.3573	0.4185
2-10	XSA97	216.2	Chowchilla Structure	0.0259	0.0206	0.0709	0.2681	0.3835

Table 2-2.
Fraction of Sampled Bed Sediment Finer than Specified Sizes, as Used in the Sediment Transport Study (contd.)

Site ID	2 mm	4 mm	8 mm	16 mm	32 mm	64 mm	128 mm	256 mm
2-1	0.0007	0.0010	0.0020	0.0077	0.0318	0.1186	0.7499	0.0869
2-2	0.0003	0.0002	0.0003	0.0046	0.0479	0.3297	0.4895	0.1270
3-1	0.0000	0.0000	0.0068	0.0069	0.0274	0.2192	0.6027	0.1370
1-1	0.0002	0.0001	0.0002	0.0038	0.0646	0.2665	0.5898	0.0745
1-2	0.0003	0.0003	0.0001	0.0024	0.1898	0.7258	0.0790	0.0000
2-3	0.0240	0.0216	0.0269	0.0540	0.0903	0.2285	0.4776	0.0000
3-2	0.0010	0.0008	0.0013	0.0091	0.0617	0.4617	0.4619	0.0000
3-4	0.0865	0.0430	0.0820	0.1313	0.1934	0.2926	0.0162	0.0000
1-3	0.0003	0.0003	0.0001	0.0024	0.1898	0.7258	0.0790	0.0000
1-4	0.0210	0.0090	0.0124	0.0530	0.1024	0.4557	0.3087	0.0000
1-5	0.0096	0.0115	0.0176	0.0804	0.2405	0.5252	0.0789	0.0000
1-6	0.0210	0.0163	0.0454	0.1271	0.4268	0.3376	0.0029	0.0000
3-21	0.0423	0.0252	0.0458	0.1578	0.3400	0.2767	0.0000	0.0000
2-4	0.0126	0.0173	0.0333	0.1630	0.3685	0.3983	0.0000	0.0000
2-6	0.0017	0.0034	0.0233	0.1043	0.4218	0.3326	0.0000	0.0000
2-5	0.0065	0.0056	0.0111	0.1109	0.5747	0.2799	0.0000	0.0000
3-11	0.0870	0.0374	0.0701	0.1406	0.2144	0.2579	0.0000	0.0000
3-13	0.0257	0.0192	0.0380	0.1289	0.5052	0.2219	0.0000	0.0000
3-10	0.1346	0.0727	0.0756	0.1891	0.1732	0.0068	0.0000	0.0000
3-6	0.2914	0.0805	0.0045	0.0009	0.0009	0.0000	0.0000	0.0000
3-7	0.1539	0.0915	0.0943	0.2099	0.1596	0.0000	0.0000	0.0000
3-14	0.1289	0.0203	0.0173	0.0747	0.0451	0.0034	0.0000	0.0000
3-17	0.1653	0.0226	0.0008	0.0000	0.0000	0.0000	0.0000	0.0000
3-18	0.1238	0.1117	0.2004	0.2495	0.0041	0.0000	0.0000	0.0000
3-19	0.0825	0.0109	0.0000	0.0000	0.0000	0.0000	0.0000	0.0000
3-20	0.2513	0.0555	0.0096	0.0012	0.0000	0.0000	0.0000	0.0000
2-11	0.1326	0.0135	0.0000	0.0000	0.0000	0.0000	0.0000	0.0000
2-10	0.1805	0.0397	0.0081	0.0027	0.0000	0.0000	0.0000	0.0000

Key:
ID = Irrigation District
mm = millimeter
XS = cross section

2.8 Computational Parameters

The transport capacity was calculated with three different transport formulas: Parker's (1990) gravel transport equation combined with Engelund and Hansen's (1972) sand transport equation, Wilcock and Crowe's (2003) gravel-sand-mixed transport equation

combined with Engelund and Hansen's sand transport equation, and Wu et al.'s (2000) non-uniform sediment transport for gravel and sand.

A final required input parameter is the active layer thickness. The active layer concept is used to simulate channel armoring. In SRH-1D, the active layer thickness is equal to a constant times the diameter of the largest sediment size. The constant was set equal to 10, based on previous experience. A sensitivity analysis of the active layer thickness value was performed (Exhibit C).

2.9 Summary of Model Inputs

SRH-1D was used to simulate the sediment transport and channel morphology of the San Joaquin River between Friant Dam and Mendota Dam from 1980 to 1997. Model input included flow rates, sediment loads, channel roughness, initial channel geometry, and initial bed material. In addition, several computational parameters were required, including the active layer thickness and sediment transport formula.

HEC-RAS geometry provided by MEI (2002a) was transferred into SRH-1D format. To limit the computational time, one of every six cross sections was used in the sediment modeling. Based on previous hydraulic calculation of MEI (2002)the Manning's n was set to 0.035 for the main channel and 0.15 for the floodplain in most cross sections. In other cross sections, the coefficient was calculated by averaging the depth-varied Manning's n from the HEC-RAS model.

Non-uniform flow along the river was simulated with point and non-point sources in SRH-1D. Flow rates decreased significantly along the reach due to channel percolation and diversions. Hydrology data from four flow gage stations were used to interpolate the flow rates at the upstream and downstream ends of each subreach. The four gages stations are located downstream from Friant Dam (XS596), at Gravelly Ford (XSA213), on the Chowchilla Bypass downstream from Chowchilla Bifurcation Structure (CBP), and on the San Joaquin River downstream from Chowchilla Bifurcation Structure (XS94). Non-point flow sources were used to represent flow differences between the downstream and upstream end of each subreach. Flow upstream from the Chowchilla Bifurcation structures was determined by combining flows from the gages on the Chowchilla Bypass and the San Joaquin River, both downstream from the structure. A negative point source was used to represent the flow routed through the Chowchilla Bypass.

A rating curve table was used in SRH-1D model to simulate internal boundary conditions, such as bridges and culverts. The MEI model (MEI 2002) used 12 bridges and culverts as internal boundary conditions. Only three significantly influenced the hydraulics (i.e., resulted in a difference in water surface elevation of greater that 1 foot across the structure). Of the three structures, Lower Gravel Pit Crossing was no longer physically present and therefore was not used as internal boundary condition. Rating curve tables were used for the Ledger Island Bridge and Chowchilla Bypass Structure (Table A-1 in Exhibit A). The other structures were identified as hydraulically

insignificant for the purposes of this model and were not incorporated into the SRH-1D model.

Samples collected during the February 2008 data collection trip were used to determine the bed material gradations throughout the study reach. Thirteen size fractions were used ranging from silt to large cobble. For cross sections where bed material samples were not available, SRH-1D automatically interpolates the surface bed material.

3.0 Results

3.1 Sediment Transport Results

3.1.1 Historic Hydrology

SRH-1D was used to simulate the sediment transport and channel morphology using the historical flows from January 1, 1980, through May 31, 1997, which were obtained from gage stations. Figure 3-1 shows the bed profiles that were simulated under Historical hydrology with Parker's (1990) gravel transport equation combined with Engelund and Hansen's (1972) sand transport equation. The results from the model will be discussed from downstream to upstream.

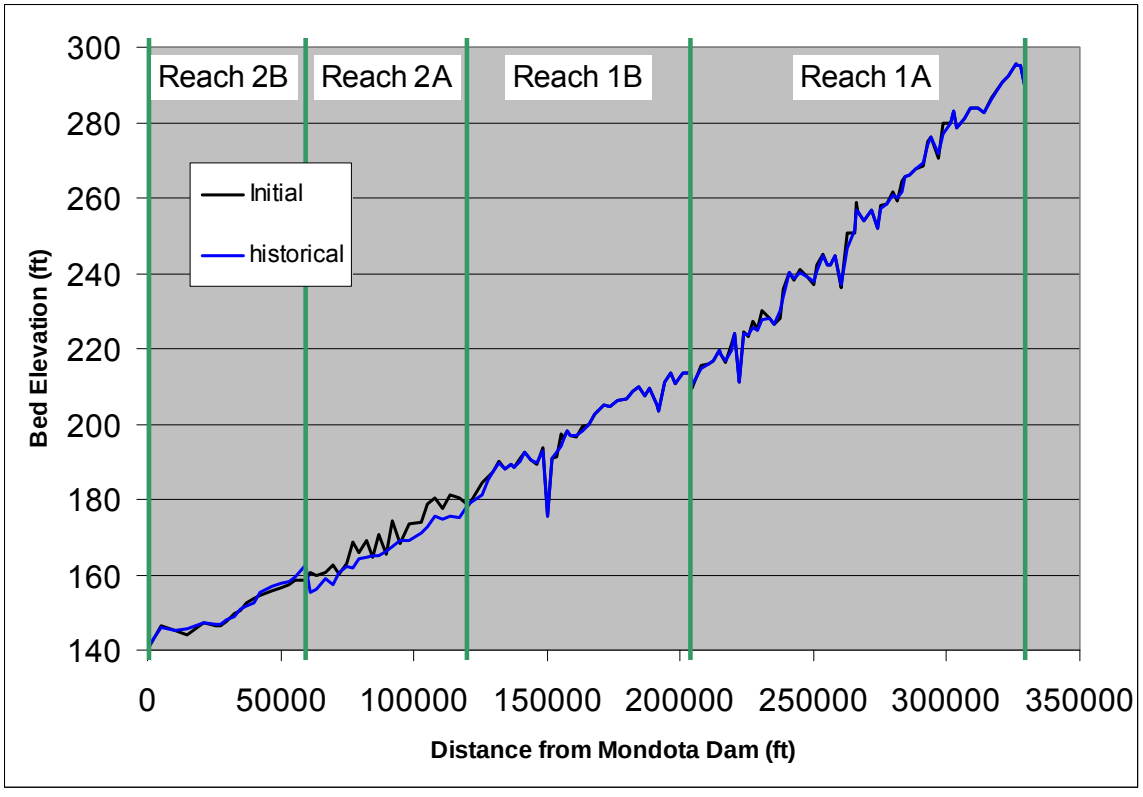

Figure 3-1.
Channel Bed Profiles Simulated with Historic Hydrology

Very minimal erosion and deposition occurred upstream from Gravelly Ford. The reach from Gravelly Ford to Chowchilla Bypass experienced erosion, as shown in Figure 3-2, which reached an average of 3.3 feet in 17.5 years. The model predicted deposition in the reach between Chowchilla Bypass and Mendota Pool. The average deposition was 0.54 foot in 17.5 years.

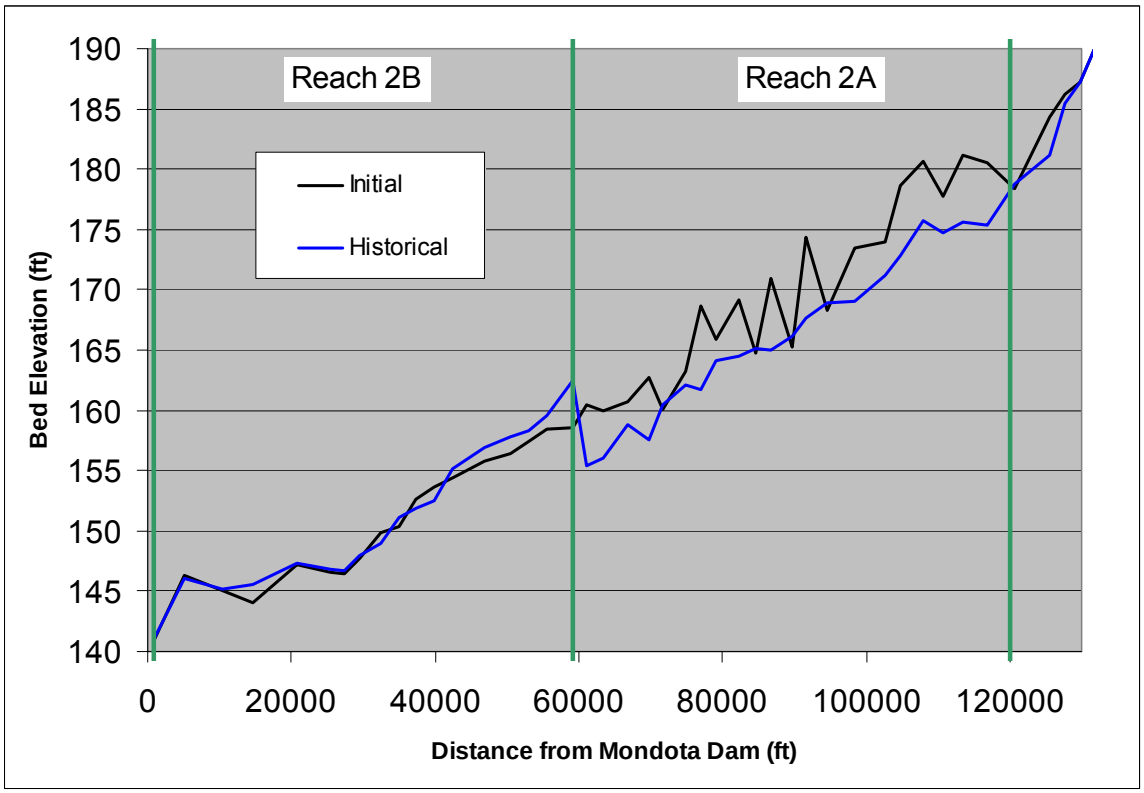

Figure 3-2.
Bed Profiles in Reach 2 Simulated with Historic Hydrology

Figure 3-3 illustrates the simulated mean sediment size under Historical hydrology. Sediment became coarser from Gravelly Ford to Chowchilla Bypass due to sediment erosion of the channel bed. No changes in sediment size were simulated upstream from Gravelly Ford. Just downstream from the Chowchilla Bypass, sediment size increased slightly. The increase in sediment size in this reach was due a coarsening of incoming sediment from upstream, and is not related to erosion and channel armoring.

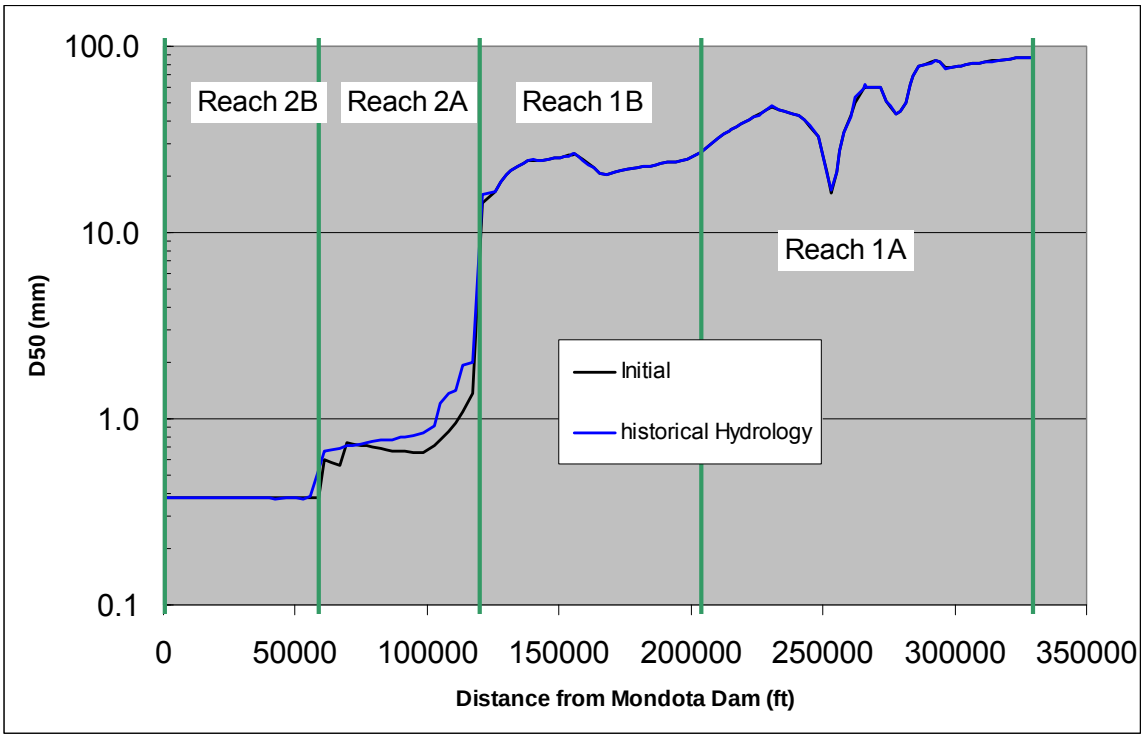

Figure 3-3.
Mean Sediment Size

Figure 3-4 depicts the locations of erosion and deposition of sand, small gravel, and large gravel at each cross section. Since the current SRH-1D model used one cross section in every six cross sections in the HEC-RAS geometry, the sediment erosion and deposition in each cross section represents what is expected to occur across six cross sections in the HEC-RAS geometry. Upstream from Gravelly Ford, erosion was generally observed in riffle locations, and deposition was noted in pool locations. Overall, an equilibrium state was reached in the gravel bedded portion of the study reach. Between Gravelly Ford and the Chowchilla Bypass, sand erosion occurred in all cross sections; gravels were eroded in some cross sections and deposited in others but in much smaller volumes than the sand. Downstream from the Chowchilla Bypass in Reach 2b, sand deposition occurred in most of the cross sections.

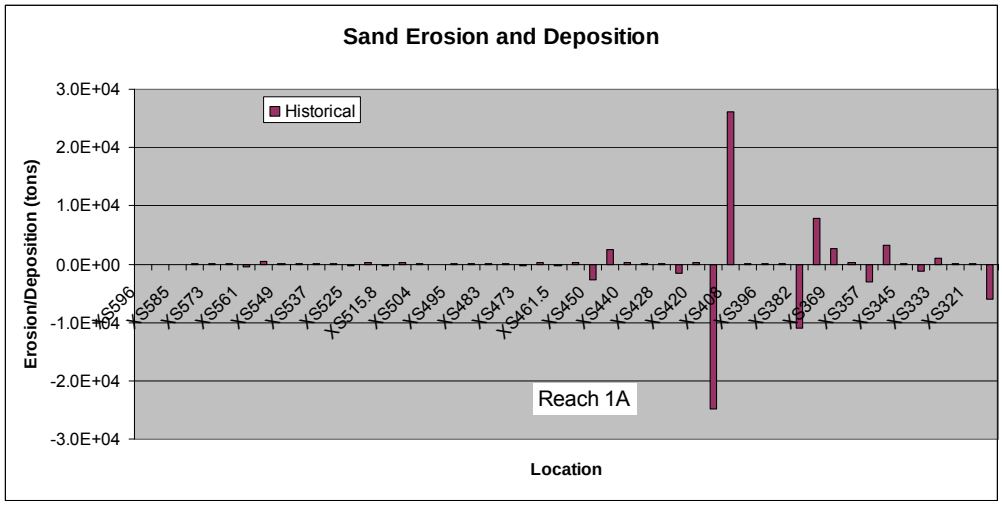

Figure 3-4(a).
Sand Erosion and Deposition with Upstream on the Left

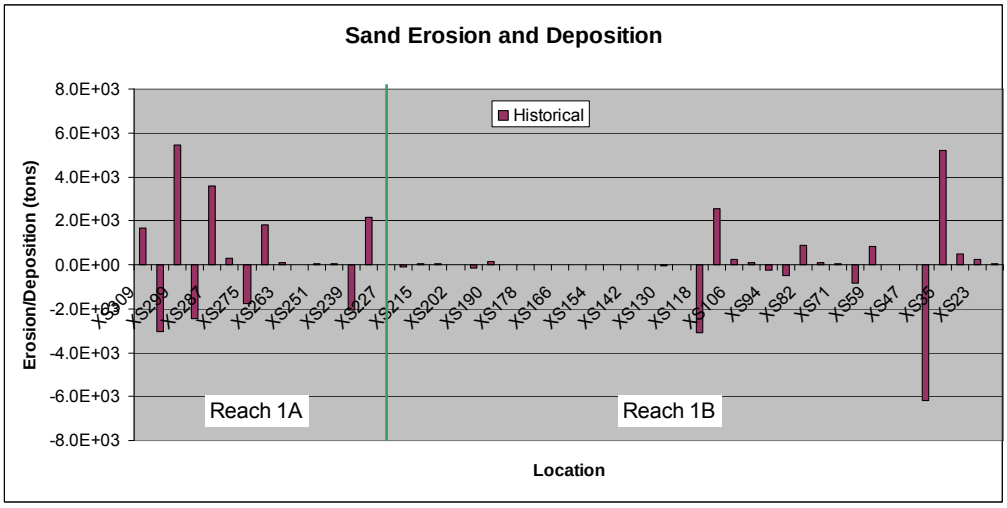

Figure 3-4(b).
Sand Erosion and Deposition with Upstream on the Left (contd.)

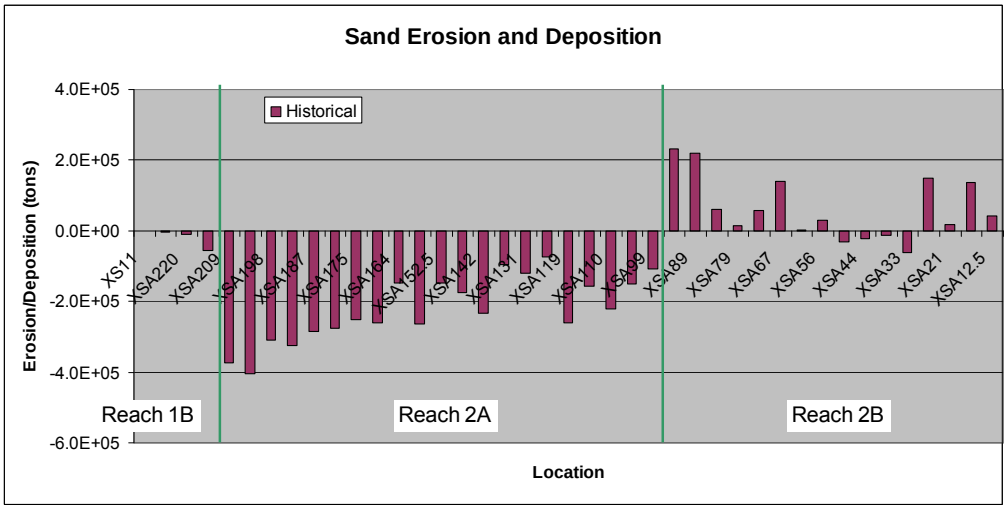

Figure 3-4(c).
Sand Erosion and Deposition with Upstream on the Left (contd.)

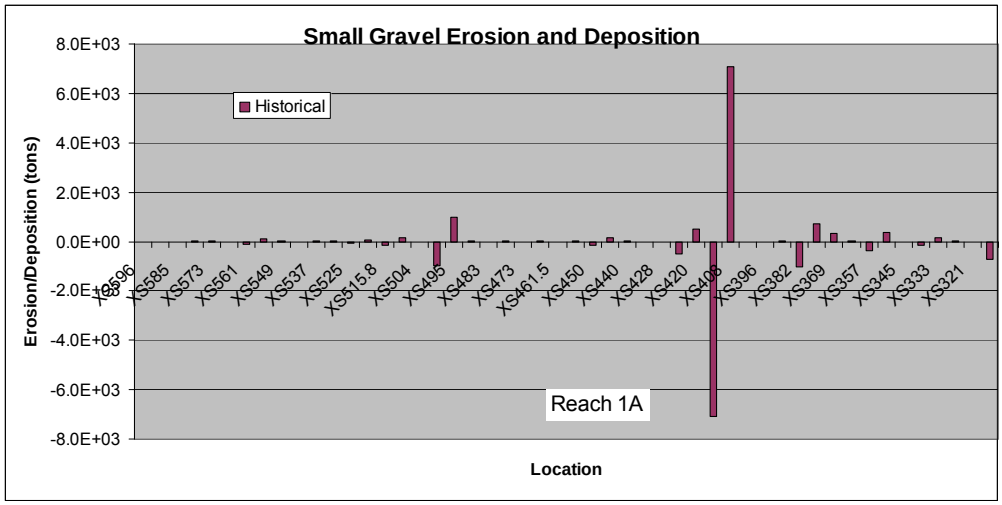

Figure 3-4(d).
Small Gravel Erosion and Deposition with Upstream on the Left

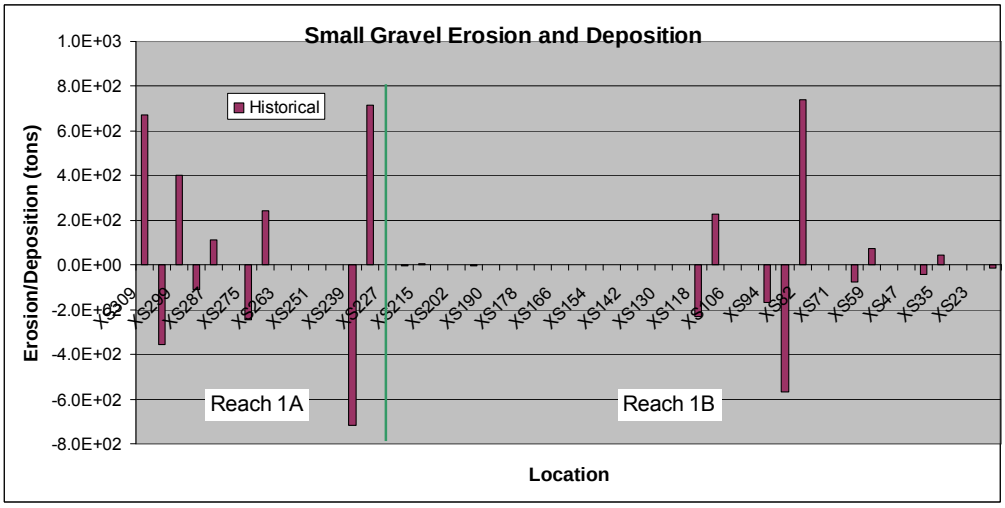

Figure 3-4(e).
Small Gravel Erosion and Deposition with Upstream on the Left (contd.)

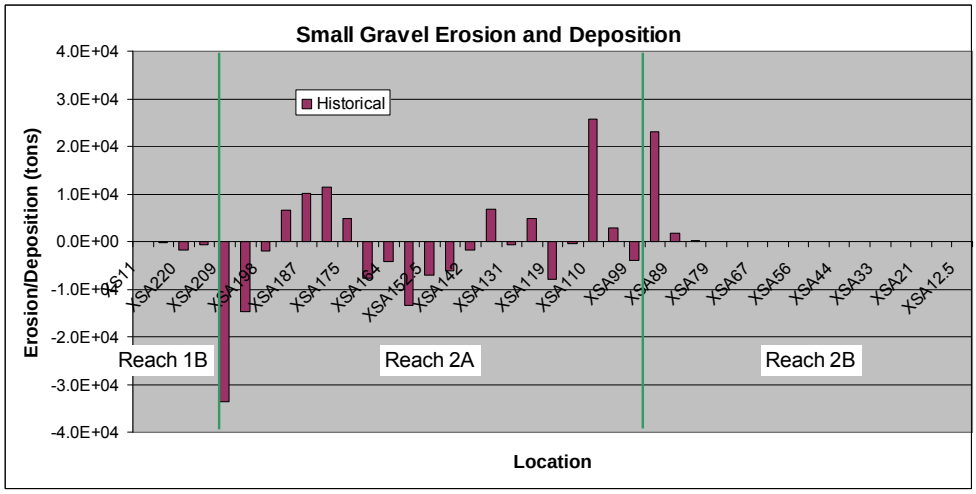

Figure 3-4(f).
Small Gravel Erosion and Deposition with Upstream on the Left (contd.)

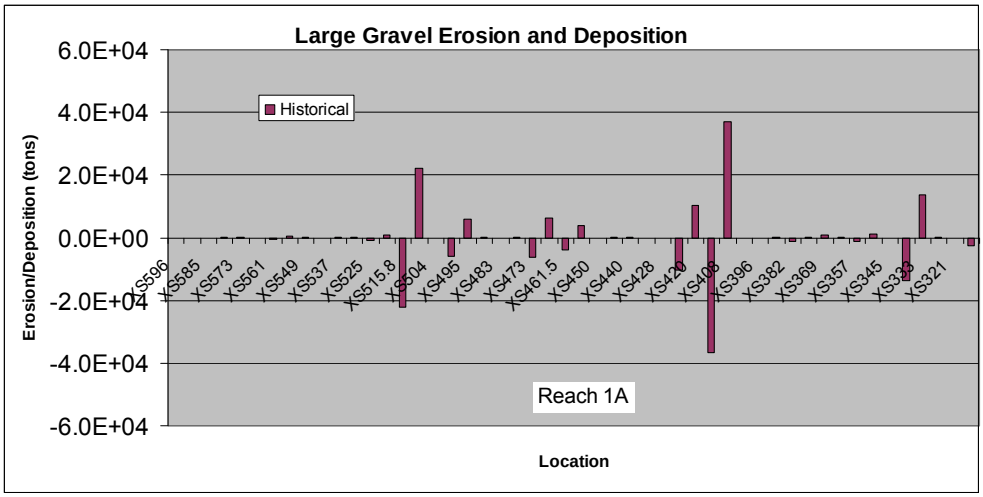

Figure 3-4(g).
Large Gravel Erosion and Deposition with Upstream on the Left

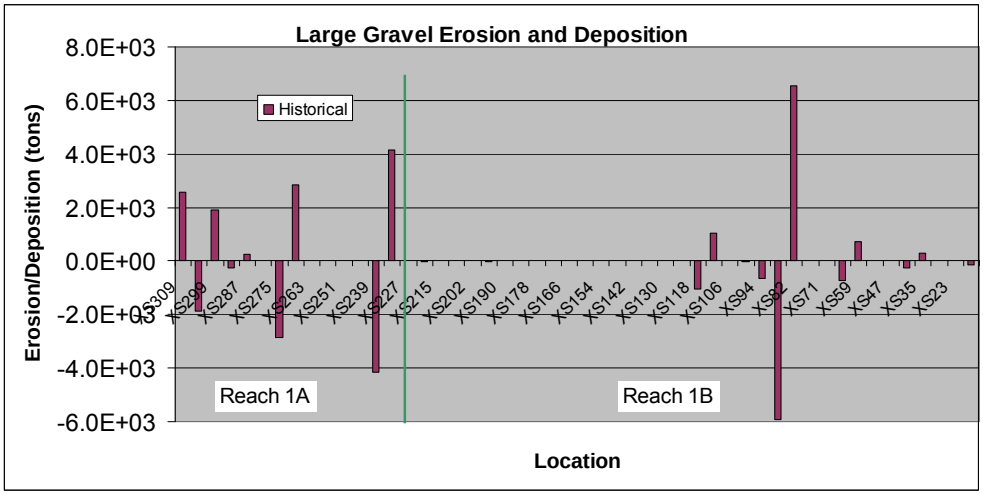

Figure 3-4(h).
Large Gravel Erosion and Deposition with Upstream on the Left (contd.)

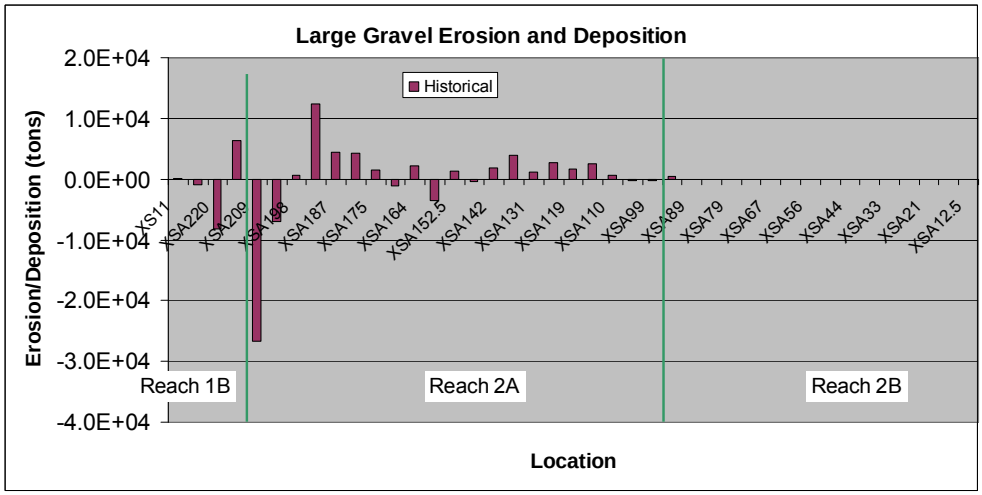

Figure 3-4(i).
Large Gravel Erosion and Deposition with Upstream on the Left (contd.)

3.1.2 Baseline Conditions

The simulated daily average flows under Baseline Conditions were obtained from MWH for the period from January 1, 1980, to September 30, 2003. The details behind the computation of these flows are found in Appendix H of the PEIS/R. SRH-1D was used to simulate the sediment transport and channel morphology beginning from 1998 channel geometry. Water Year 1997 was an extreme wet year and chance that the near-future river restoration program experiences a peak flow of this scale is low. Thus the Baseline hydrology was simulated based upon the period from January 1, 1980, through September 30, 2003, with and without Water Year 1997. A longer period of record was used in these simulations because the main purpose of these analyses is to compare Baseline Conditions to Project Conditions. The simulated daily average flows extended from January 1, 1980, through September 30, 2003; therefore, the full period was used when simulating the Baseline or Project conditions.

Figures 3-5 and 3-6 show the bed profiles that were simulated under Baseline Conditions with Parker's (1990) gravel transport equation combined with Engelund and Hansen's (1972) sand transport equation. Very minimal erosion and deposition occurs upstream from Gravelly Ford for both with and without Water Year 1997 hydrology. The reach from Gravelly Ford to Chowchilla Bypass experienced erosion, which reached an average of 3.1 feet in 24 years. Hydrology without Water Year 1997 results in 11 percent less erosion (2.8 feet) on average than with Water Year 1997. The reach between Chowchilla Bypass and Mendota Pool experienced deposition, which reached an average of 0.25 foot in 24 years. Hydrology without Water Year 1997 shows similar deposition (0.35 foot on average).

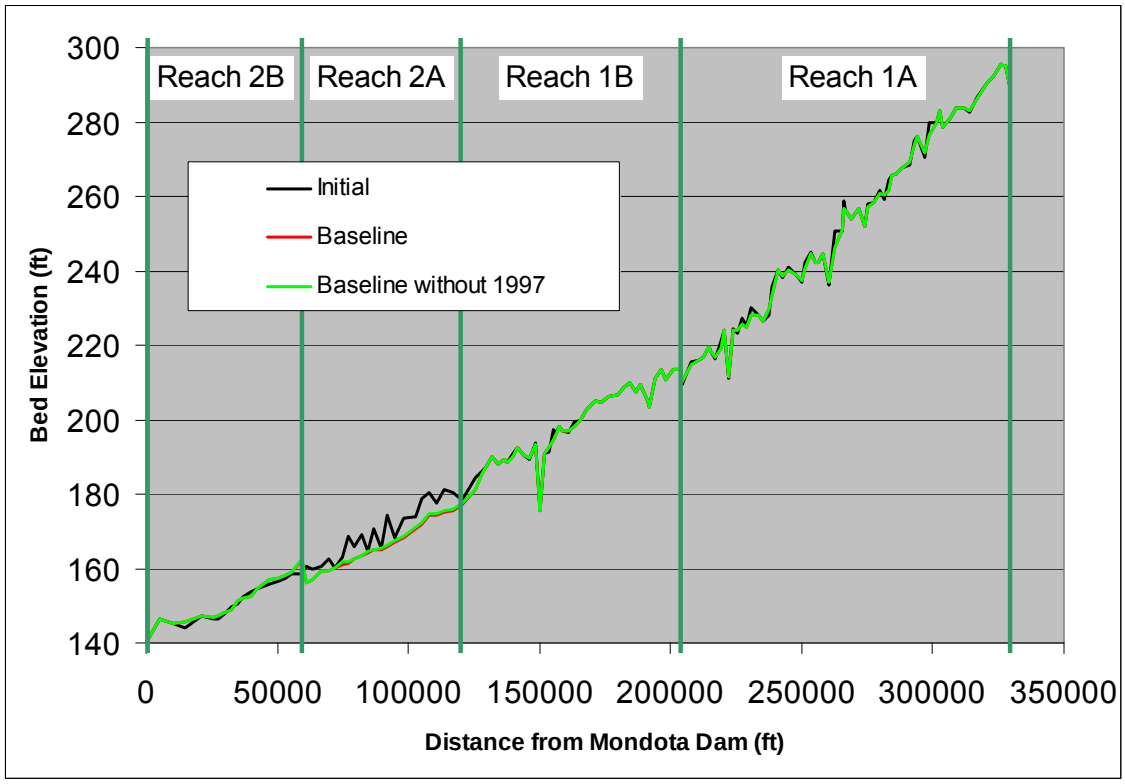

Figure 3-5.
Channel Bed Profiles Simulated Under Baseline Conditions

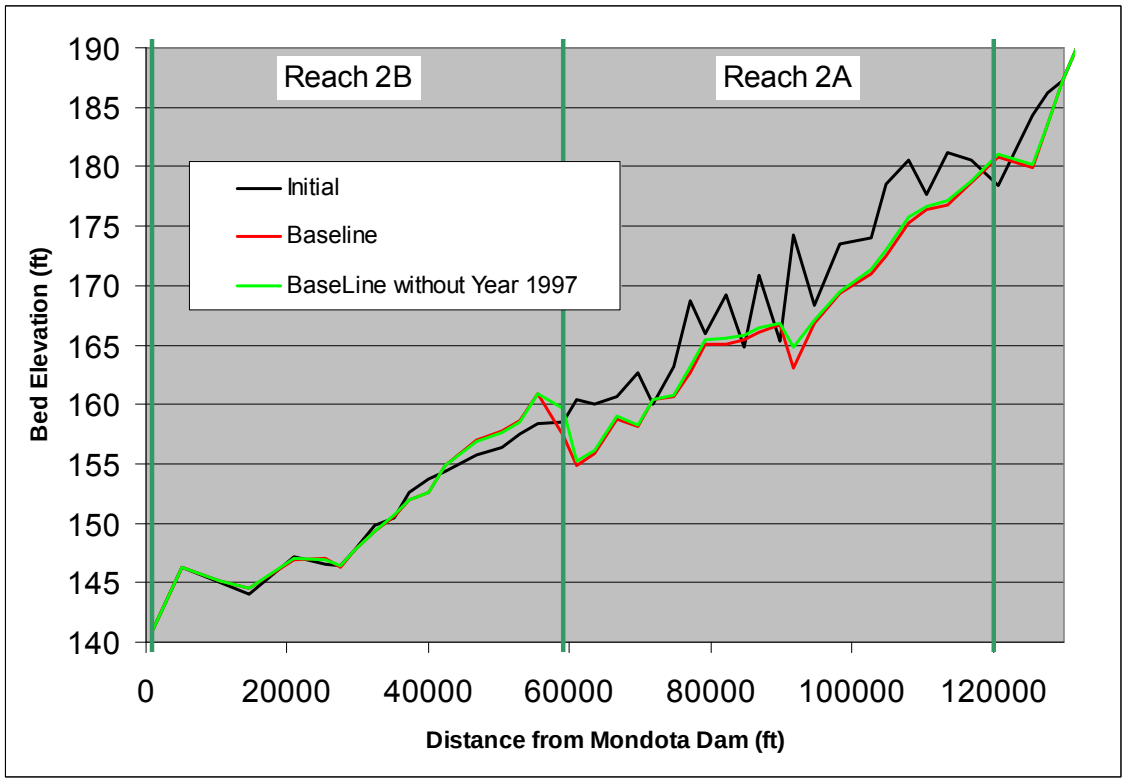

Figure 3-6.
Bed Profiles in Reach 2 Simulated with Baseline Hydrology

Figure 3-7 illustrates the simulated mean sediment size under Baseline hydrology with and without Water Year 1997. Sediment becomes coarser in Reach 2a from Gravelly Ford to Chowchilla Control Structure due to sediment erosion. Without high flows in Water Year 1997, slightly less erosion occurred in Reach 2a and the sediment is less coarse than that simulated using hydrology with Water Year 1997. No changes in sediment size are measured upstream from Gravelly Ford. Downstream from the Chowchilla Control Structure, sediment size increases slightly. The increase in sediment size in this reach is due to the coarsening of incoming sediment from upstream, and is not related to erosion and channel armoring.

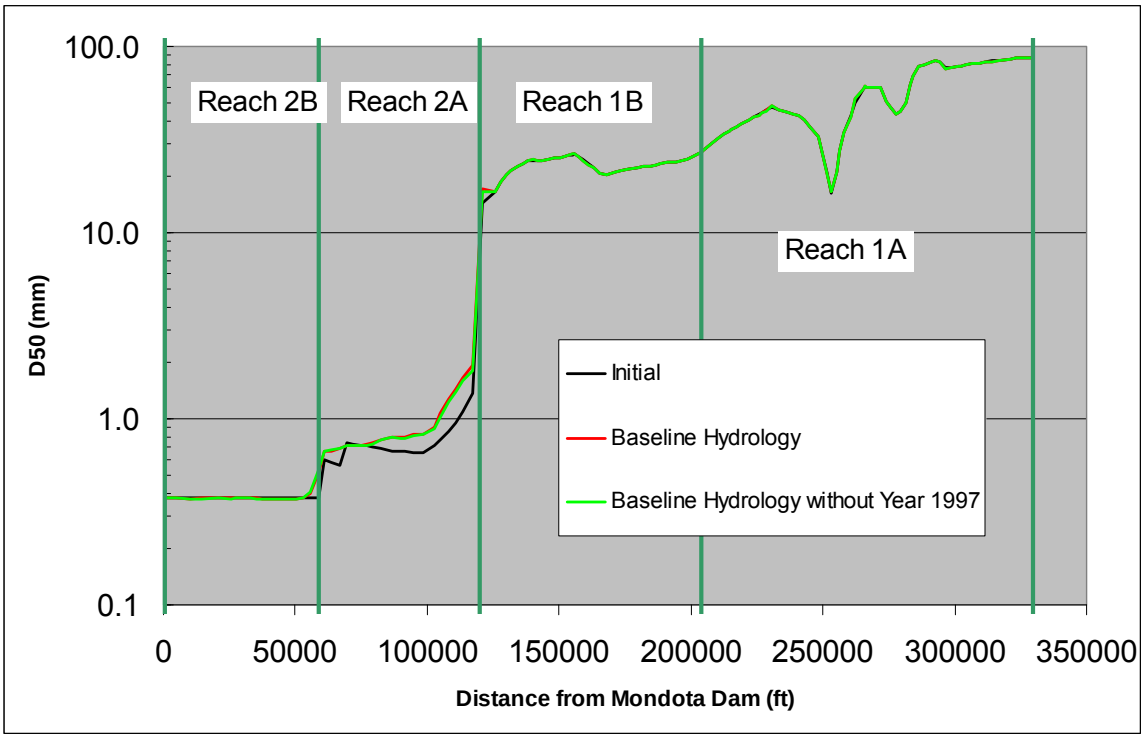

Figure 3-7.
Mean Sediment Size Simulated with Baseline Hydrology

Figure 3-8 depicts the locations of erosion and deposition of sand, small gravel, and large gravel at each cross section. Since the current SRH-1D model used one cross section in every six cross sections in the HEC-RAS geometry, the sediment erosion and deposition in each cross section represents what is expected to occur across six cross sections in the HEC-RAS geometry. Upstream from the Gravelly Ford, erosion is generally observed in riffle locations, and deposition is observed in pool locations. Overall, an equilibrium state is reached in the gravel bedded portion of the study reach. The simulations with and without Water Year 1997 show similar volumes of erosion and deposition. Between Gravelly Ford and the Chowchilla Bypass, sand erosion occurs in all cross sections, while gravels are eroded in some cross sections and deposited in others. Eliminating Water Year 1997 from the simulations results in slightly less erosion of sand and less erosion and deposition of gravel. However, the difference between including and not including this water year is not considered significant. Downstream from the Chowchilla Bypass, sand deposition occurred on most of the cross sections.

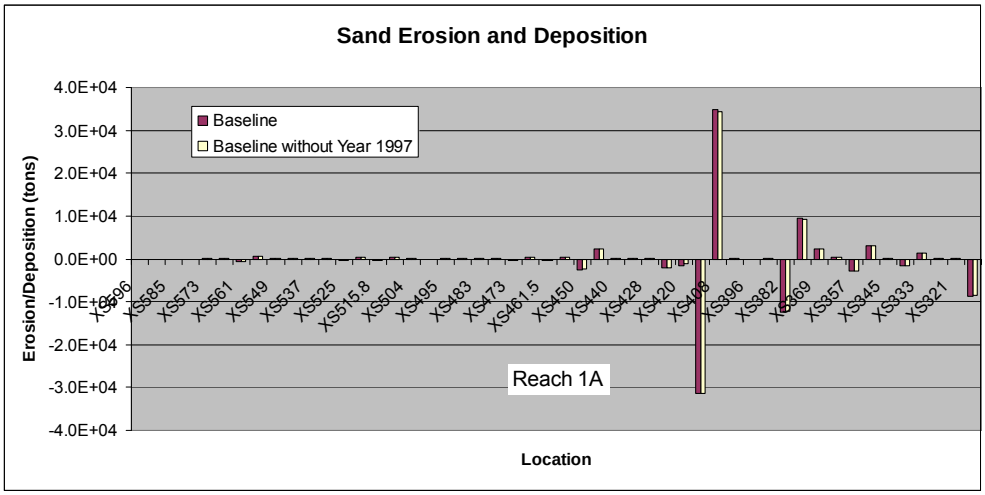

Figure 3-8(a).
Sand Erosion and Deposition with Upstream on the Left

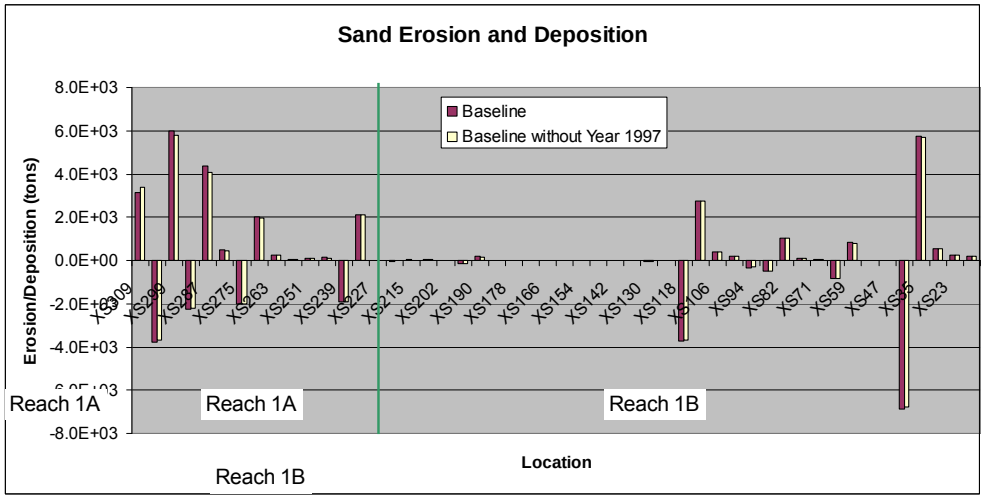

Figure 3-8(b).
Sand Erosion and Deposition with Upstream on the Left (contd.)

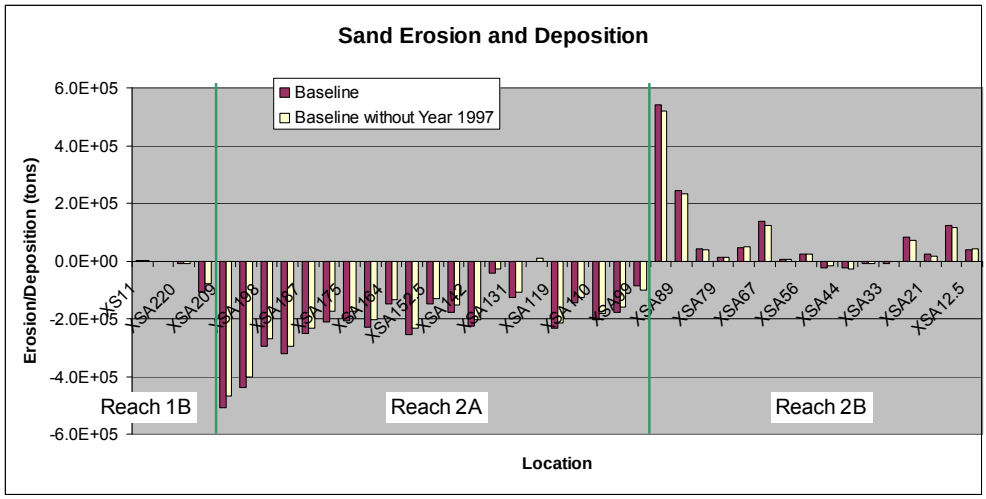

Figure 3-8(c).
Sand Erosion and Deposition with Upstream on the Left (contd.)

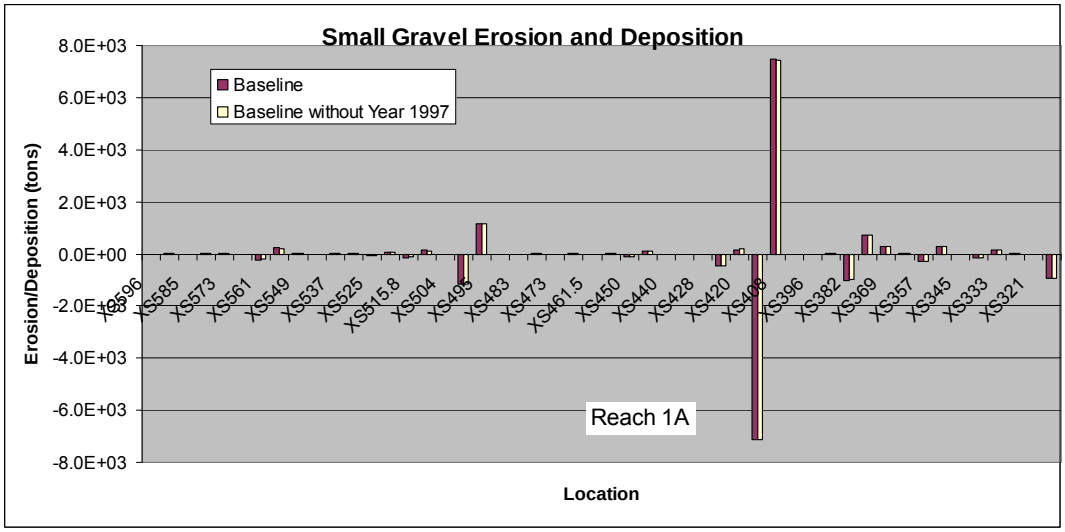

Figure 3-8(d).
Small Gravel Erosion and Deposition with Upstream on the Left

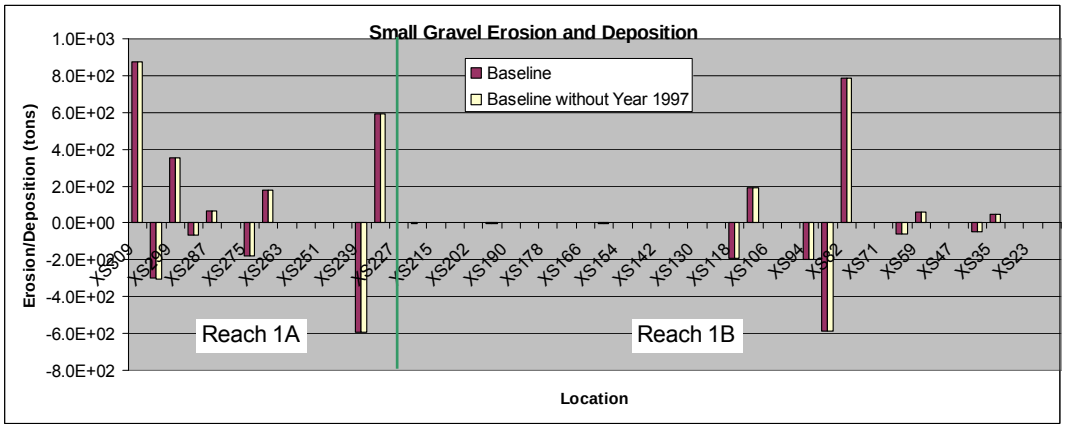

Figure 3-8(e).
Small Gravel Erosion and Deposition with Upstream on the Left (contd.)

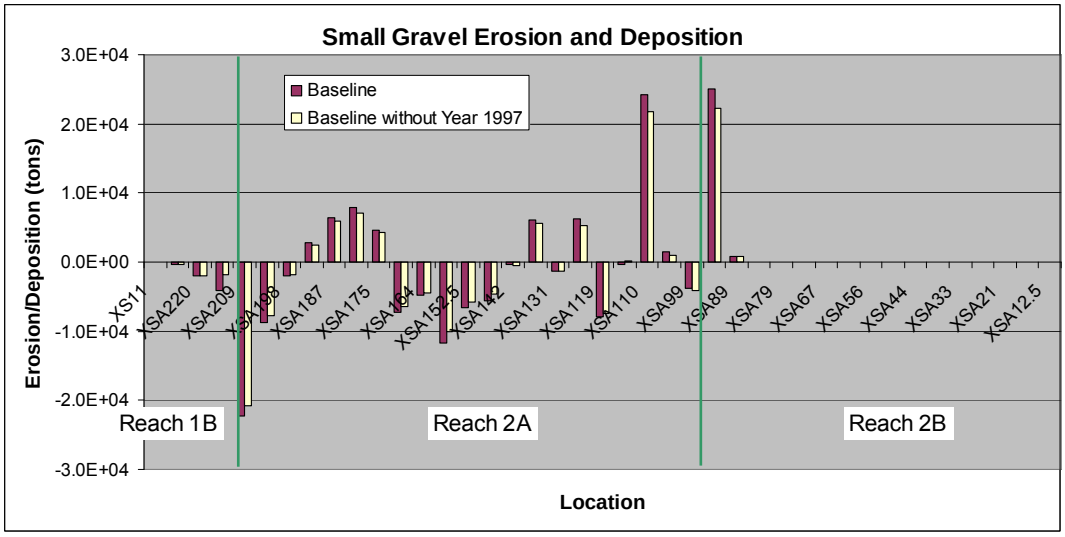

Figure 3-8(f).
Small Gravel Erosion and Deposition with Upstream on the Left (contd.)

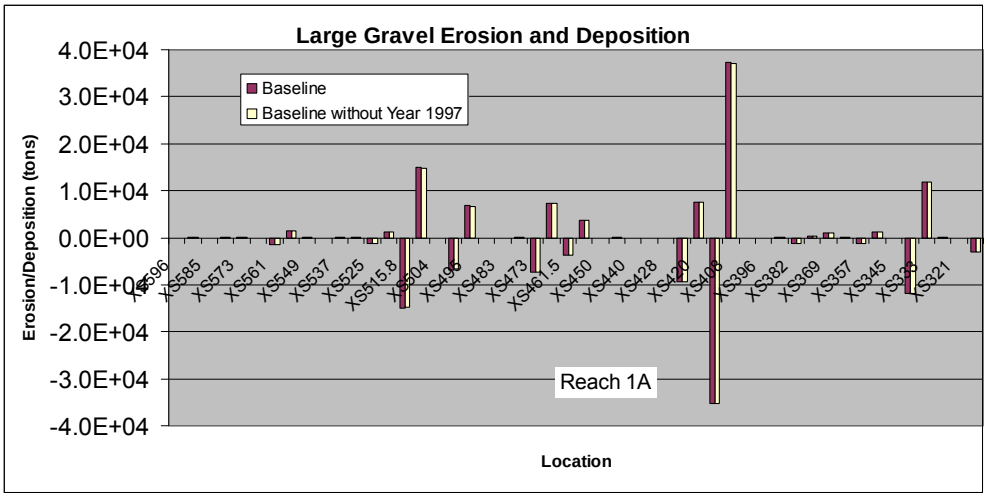

Figure 3-8(g).
Large Gravel Erosion and Deposition with Upstream on the Left

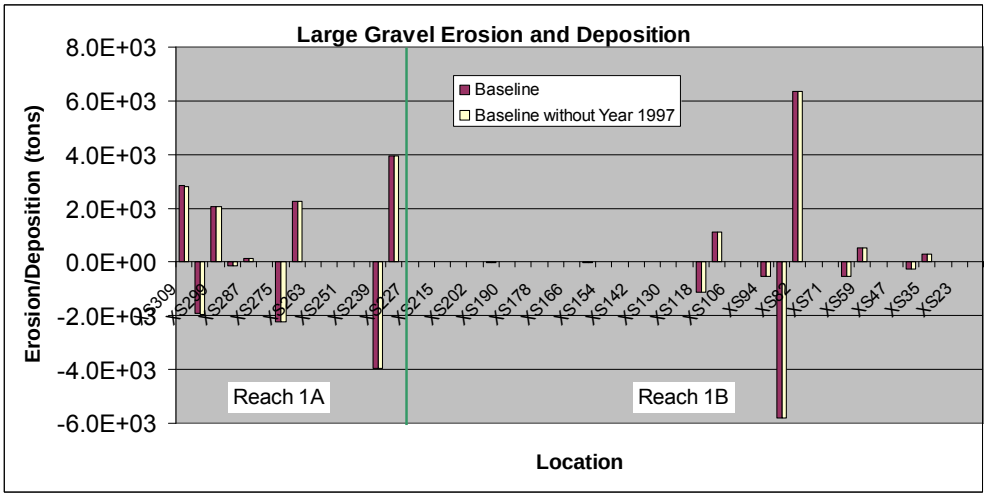

Figure 3-8(h).
Large Gravel Erosion and Deposition with Upstream on the Left (contd.)

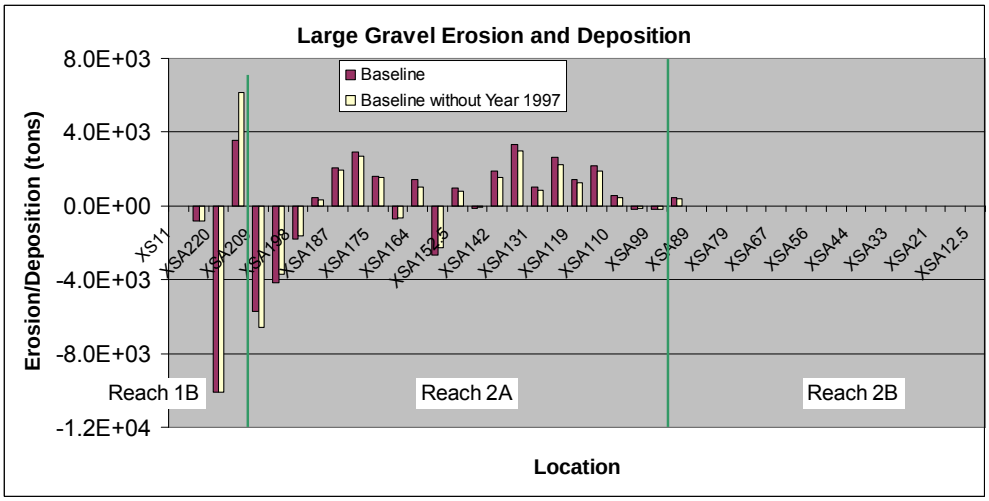

Figure 3-8(i).
Large Gravel Erosion and Deposition with Upstream on the Left (contd.)

3.1.3 Alternative A Hydrology with Levee Setbacks in Reach 2b

Alternative A hydrology from January 1, 1980, to September 30, 2003, was used to simulate the sediment transport and channel morphology with the 1998 channel geometry as the initial conditions. Levee setback was considered in Alternative A Hydrology to contain flows exceeding 1,500 cfs. Two options of levee setbacks are currently under consideration: (1) ALS, and (2) MLS. The levee setback options only affect the geometry in Reach 2b downstream from the Chowchilla Bifurcation Structure. In this analysis, the effects of both the ALS and MLS options on sediment transport characteristics were investigated.

Figures 3-9 and 3-10 show the bed profiles that were simulated under Alternative A hydrology with Parker's (1990) gravel transport equation combined with Engelund and Hansen's (1972) sand transport equation. Very minimal erosion and deposition occurs upstream from Gravelly Ford for Alternative A hydrology. The reach from Gravelly Ford to Chowchilla Bypass experiences erosion, which reaches an average of 2.1 feet in 24 years.

The reach between Chowchilla Bypass and Mendota Pool experiences deposition, which reaches an average of 0.37 foot and 0.22 foot in 24 years, for ALS and MLS, respectively. Compared with the Baseline hydrology, Alternative A hydrology increases the frequency of all flow ranges in Reach 2b. This reach shows about a fivefold increase in sand and small gravel transport capacity from Baseline Conditions (Huang and Greimann 2009a). The increase in transport capacity countered the increase in sediment delivery to the reach and Reach 2b has predicted to have less deposition in the main channel under Alternative A with MLS than under Baseline Conditions. Compared with the ALS option, MLS shows more deposition in the first few cross sections since more flow is distributed into the floodplain and the flow has less capacity to carry the incoming sediment there. Downstream cross sections in Reach 2b tended to experience less deposition under MLS than under ALS.

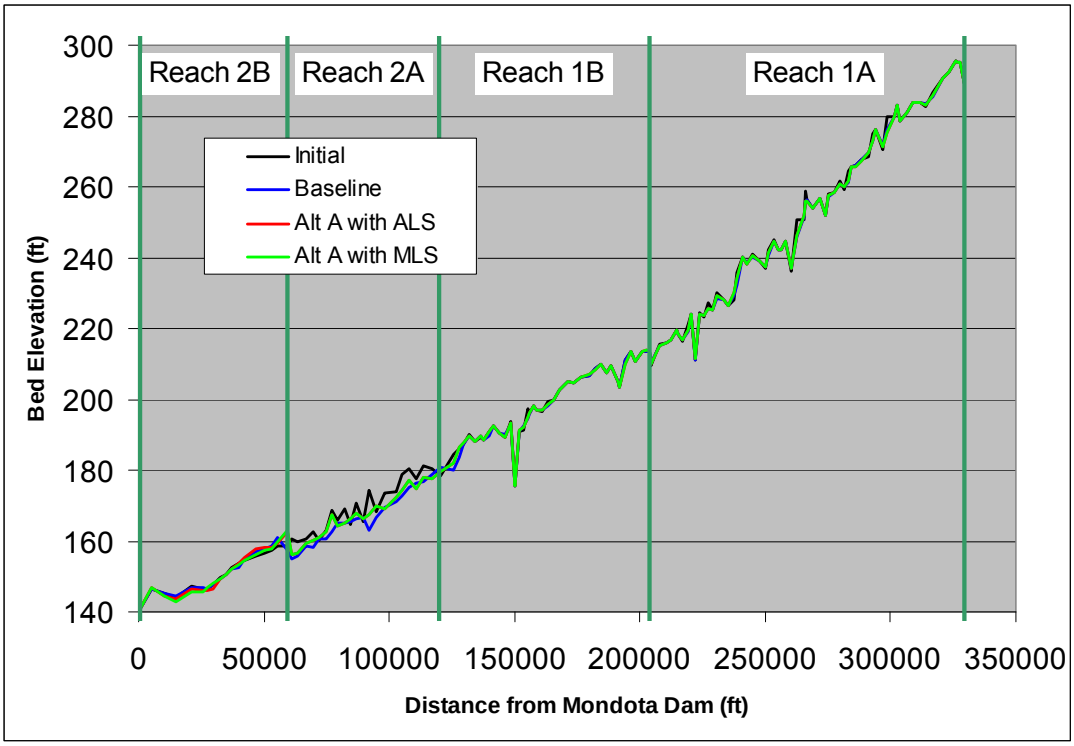

Figure 3-9.
Bed Profiles Simulated with Alternative A Hydrology

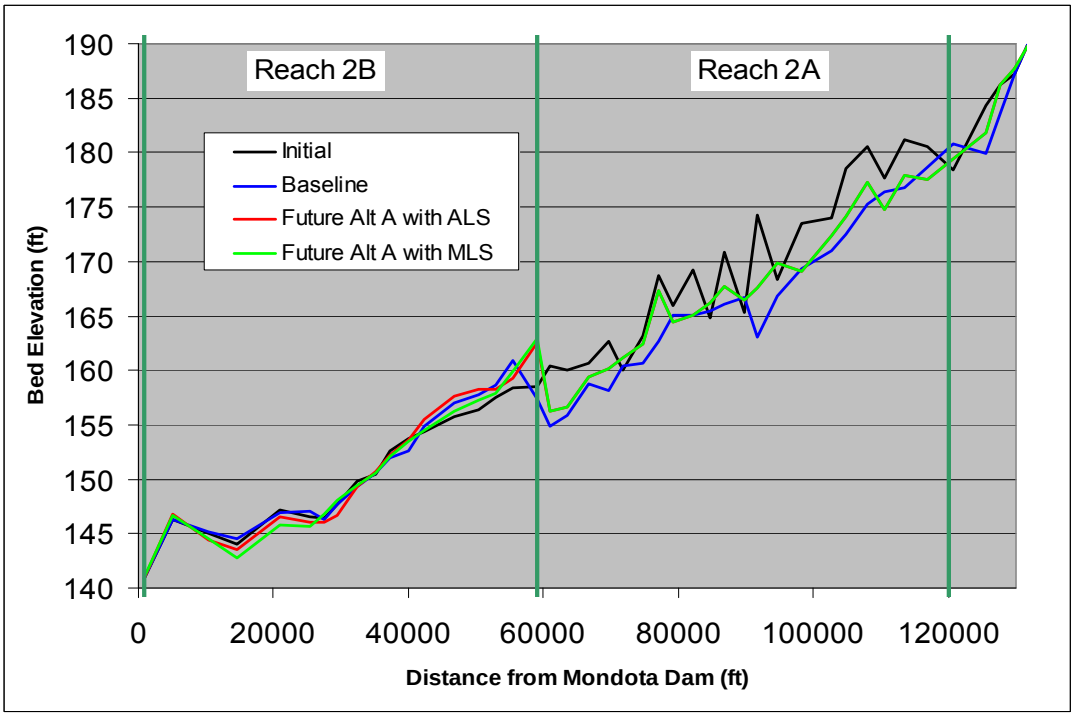

Figure 3-10.
Channel Bed Profiles in Reach 2 Simulated with Alternative A Hydrology

Figure 3-11 shows the simulated median bed material sediment size under Alternative A hydrology with ALS and MLS. No changes in sediment size were measured upstream from Gravelly Ford. Sediment became coarser in Reach 2a from Gravelly Ford to Chowchilla Bypass due to sediment erosion. Alternative A hydrology results in similar bed material in Reach 2a, compared with Baseline hydrology. Just downstream from the Chowchilla Bypass, the sediment size increased slightly.

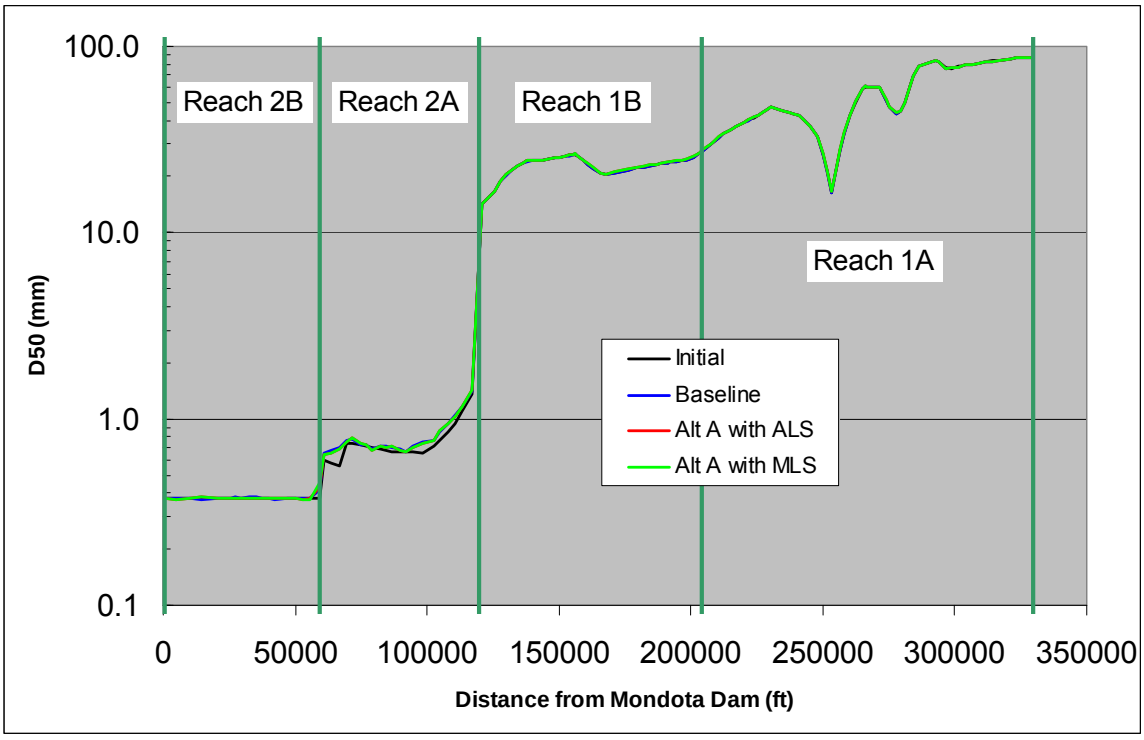

Figure 3-11.
Mean Sediment Size for Alternative A Hydrology

Figure 3-12 depicts the locations of erosion and deposition of sand, small gravel, and large gravel at each cross section. Upstream from Gravelly Ford, erosion was generally observed in riffle locations, and deposition was noted in pool locations. Overall, an equilibrium state was reached in the gravel bed portion of the study reach. Compared with Baseline hydrology, Alternative A hydrology resulted in less sand and small gravel erosion in riffle locations and also less sand and small gravel deposition in pool locations. A similar trend was identified for small gravel in Reach 1a; however, the trend was reversed in Reach 1b, where Alternative A hydrology resulted in more erosion and deposition of small gravel. For large gravel, Alternative A hydrology resulted in a small increase in erosion and deposition. This result was not supported by the annual sediment transport loads estimated by the reach-averaged sediment transport capacity. Erosion and deposition are restricted to areas of riffles and pools and on a reach-averaged basis, little transport actually occurred.

Between Gravelly Ford and the Chowchilla Bypass, sand erosion occurred in all cross sections; gravels were eroded in some cross sections and deposited in others. Compared to Baseline Conditions, Alternative A caused less sand erosion in most of the cross sections in Reach 2a. Also, Alternative A resulted in more small gravel erosion in riffle locations and deposition in pool locations. For large gravels, Alternative A hydrology usually caused more deposition as compared with Baseline Hydrology.

Downstream from the Chowchilla Bypass, sand deposition occurred at the cross section immediately downstream from the bypass. More deposition occurred in Reach 2b under Alternative A than under Baseline Conditions. However, most of this deposition was restricted to the widened floodplain. The main channel bed elevations actually increased less under Alternative A than under Baseline Conditions.

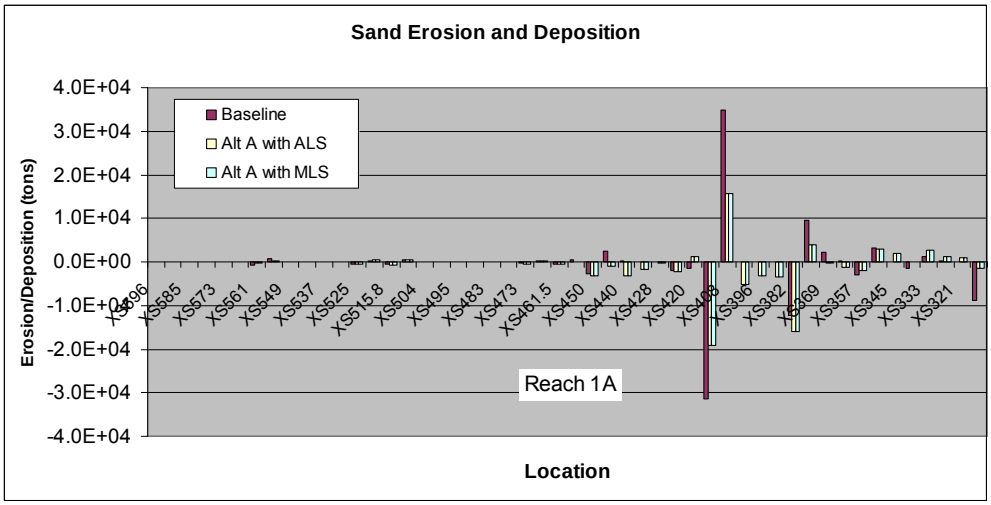

Figure 3-12(a).
Sand Erosion and Deposition with Upstream on the Left

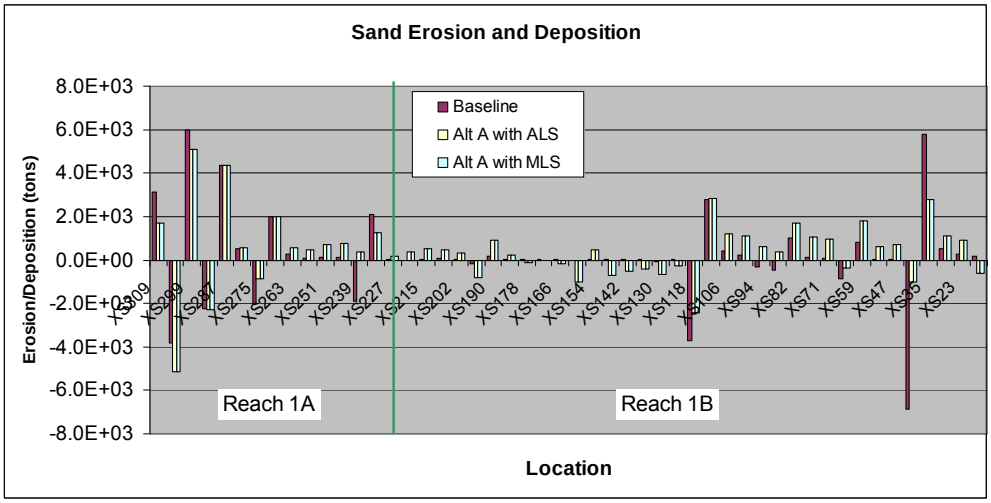

Figure 3-12(b).
Sand Erosion and Deposition with Upstream on the Left (contd.)

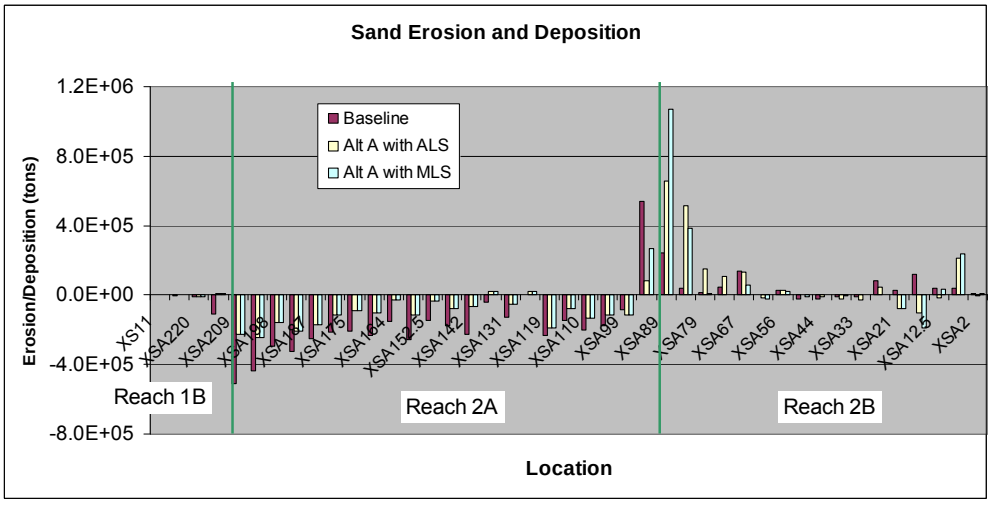

Figure 3-12(c).
Sand Erosion and Deposition with Upstream on the Left (contd.)

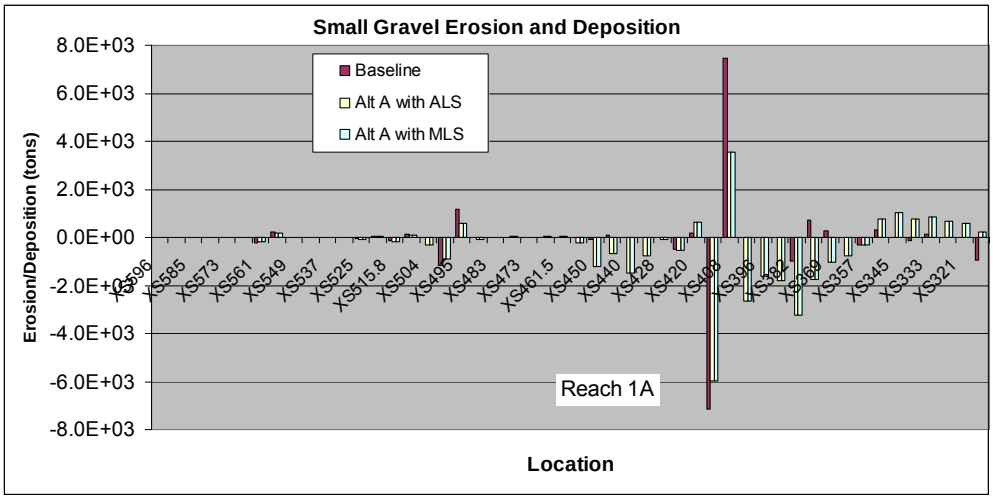

Figure 3-12(d).
Small Gravel Erosion and Deposition with Upstream on the left (contd.)

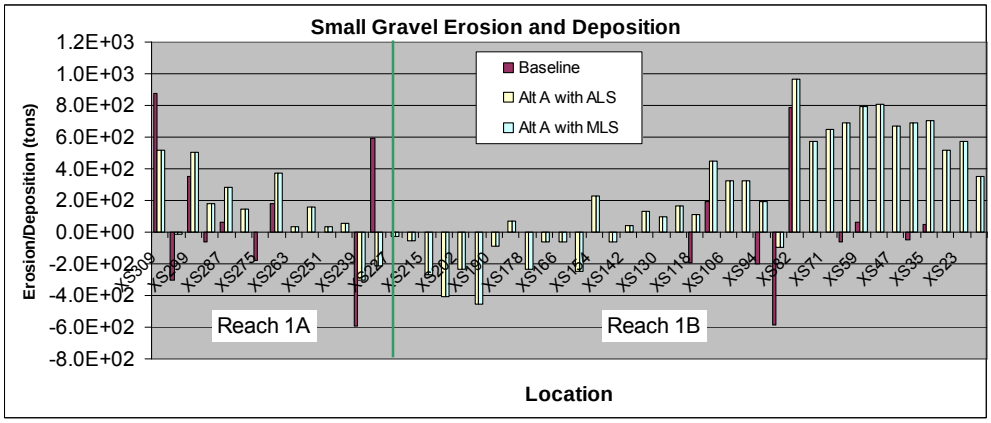

Figure 3-12(e).
Small Gravel Erosion and Deposition with Upstream on the left (contd.)

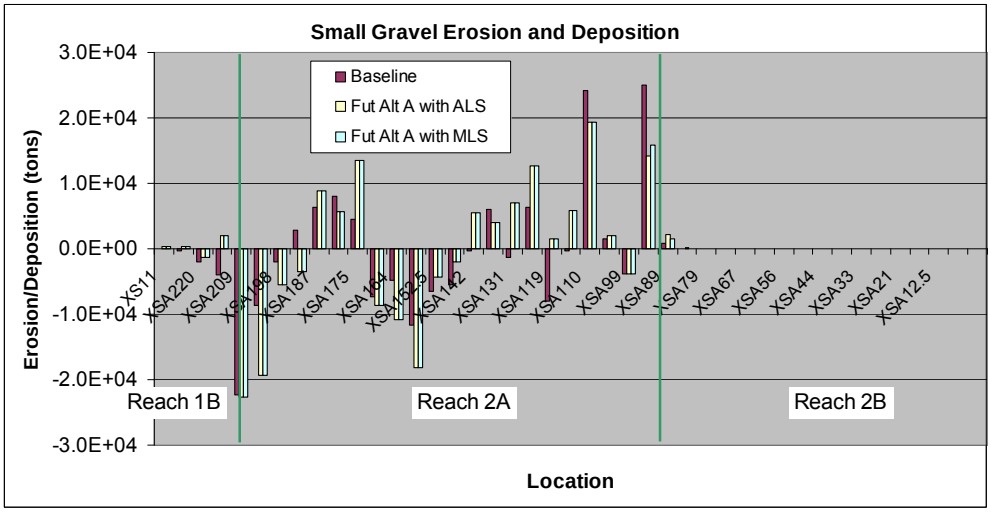

Figure 3-12(f).
Small Gravel Erosion and Deposition with Upstream on the Left (contd.)

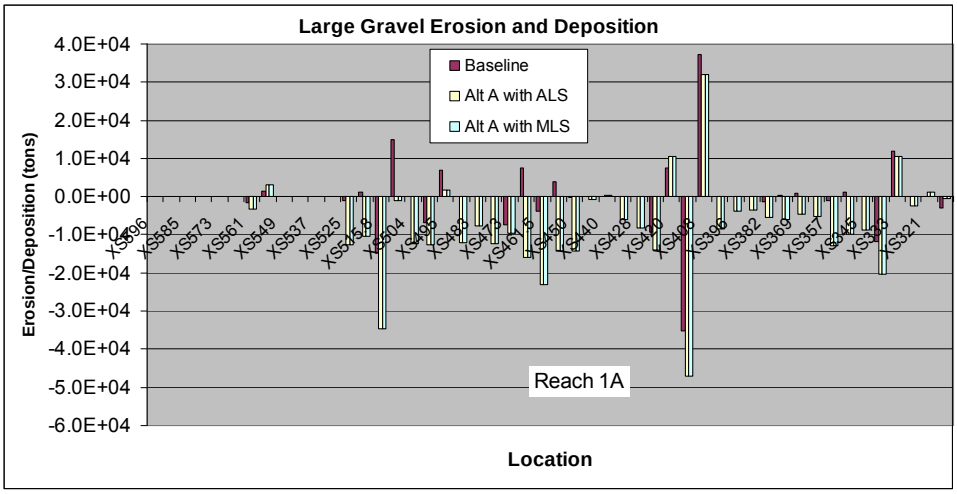

Figure 3-12(g).
Large Gravel Erosion and Deposition with Upstream on the Left (contd.)

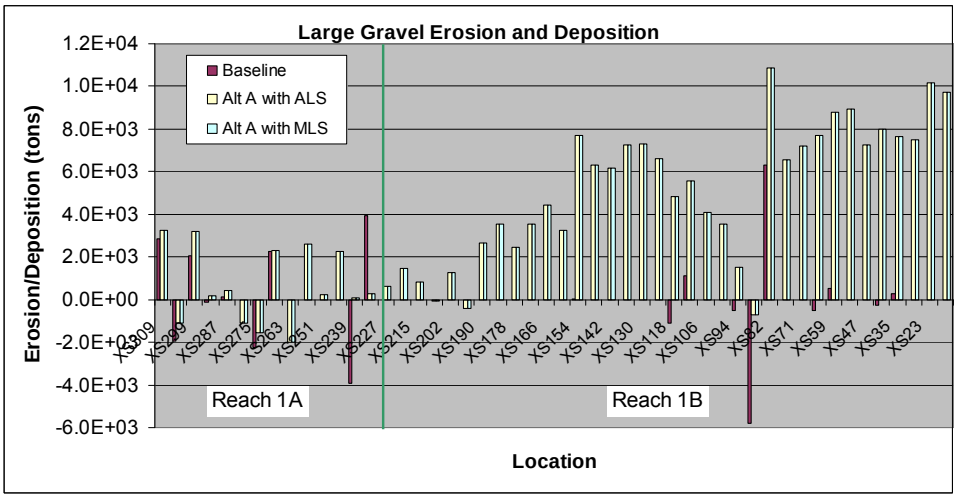

Figure 3-12(h).
Large Gravel Erosion and Deposition with Upstream on the Left (contd.)

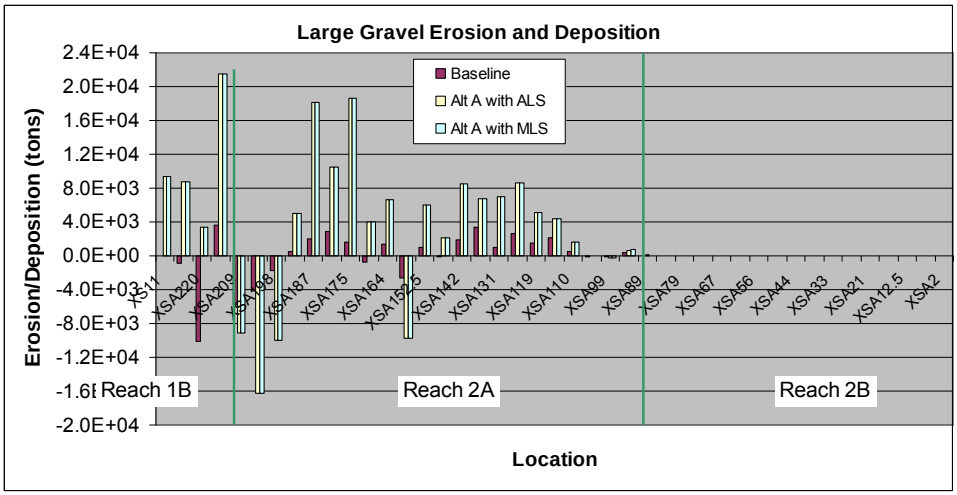

Figure 3-12(i).
Large Gravel Erosion and Deposition with Upstream on the Left (contd.)

Compared with the ALS option, the MLS scenario experienced greater volume of deposition at the very upstream and downstream cross sections of Reach 2b. No significant gravel erosion or deposition was predicted in this reach. Table 3-1 summarizes the depths of erosion and deposition predicted with the Baseline and Alternative A hydrologic conditions.

Table 3-1.
Summary of Results with Baseline and Alternative A Conditions

Hydrology	Baseline	Baseline with 1997	Alt A with ALS	Alt A with MLS
Reach 2a	3.1 ft Erosion	2.8 ft Erosion	2.1 ft Erosion	2.1 ft Erosion
Reach 2b	0.25 ft Deposition	0.35 ft Erosion	0.37 ft Deposition	0.22 ft Deposition

Key:
ALS = Average Levee Setback
Alt = Alternative
ft = feet
MLS = Maximum Levee Setback

3.2 Sensitivity Runs

Sensitivity analyses were conducted on several model inputs, including:

1. The number of bed material layers.
2. The active layer thickness.
3. The transport formula.
4. The roughness coefficient.
5. The number of cross sections.
6. Silt and sand gradations in Reach 1.

The sensitivity analyses were performed with the Historical hydrology. Results from the sensitivity runs are presented in Exhibit C and summarized in Table 3-2. Differences in model results in the first five parameters were only observed and presented between Gravelly Ford and the Chowchilla Bifurcation Structure. The analysis of the sixth parameter evaluated effects to Reaches 2A and 2B and was found to have minor effects to Reach 1.The following sections contain discussions relating to each parameter. A summary of the sensitivity runs is presented in Table 3-2.

3.2.1 Bed Material Layers

Bed material layers control the supply of bed material once the active layer undergoes erosion. When erosion occurs, the flow removes finer material from the active layer, and

the first inactive layer supplies material into the active layer. When deposition occurs, the active layer transfers material into the first inactive layer. The number of bed material layers is more sensitive when the system endures continuous cycles of erosion and deposition. The San Joaquin River experiences continuous erosion in the sand region where the armoring process is weak. The results suggest that the model is generally not sensitive to changes in the number of bed material layers. Three bed material layers result in a decrease in the average depth of erosion between Gravelly Ford and the Chowchilla Bifurcation Structure by 13.0 percent, compared with two layers. No difference was noted in the other reaches.

Table 3-2.
Summary of Sensitivity Runs

Run No.	Change	Effect on the Reach from Gravelly Ford to Chowilla Bifurcation Structure with Historic Hydrology
1	Original model run with Parker (1990) and Englund and Hansen (1972)	Erosion by an average depth of 3.30 ft
2	Changed number of bed material layers from 2 to 3	Decrease erosion depth by 13.0%
3	Increased active layer thickness by 100%	Increased erosion depth by 7.2%
4	Decreased active layer thickness by 50%	Decreased erosion depth by 2.1%
5	Wilcock and Crowe (2003) and Englund and Hansen (1972)	Increased erosion depth by 9.2%
6	Wu et al, 2000	Decreased erosion depth by 42.4%
7	Increased Manning's n by 20%	Increased erosion depth by 11.8%
8	Decreased Manning's n by 20%	Decreased erosion depth by 10.3%
9	All cross sections	Decreased erosion depth by 1.2%
10	Doubled silt and sand gradations in Reaches 1a and 1b	Increased erosion depth by 6.0%
11	Quadrupled silt and sand gradations in Reaches 1a and 1b	Decreased erosion depth by 15.3%

Key:
% = percent
ft = feet

3.2.2 Active Layer Thickness

The active layer thickness controls the amount of bed material available for erosion during any given time step. It also controls the armoring process. When erosion is taking place, the flow can remove finer material from the active layer at a faster rate than coarse material, which forms an armor layer. This armor layer decreases the amount of bed material mobilized. If degradation occurs, decreasing the active layer thickness increases the rate at which the armor layer forms. When the armor layer forms more quickly, the amount of material removed from the bed decreases. However, the model provides little evidence that an armor layer was formed in this area, and the active layer thickness has a minimal effect on sediment transport. Doubling the active layer thickness increases the average depth of erosion by 7.3 percent, and halving the thickness decreases the average depth of erosion by 2.1 percent. In the sand reach just downstream from Gravelly Ford,

increasing the active layer thickness slows the bed coarsening process, while decreasing the active layer thickness accelerates the coarsening process.

3.2.3 Transport Formula

Three methods were used, including (1) Parker's (1990) gravel transport equation combined with Engelund and Hansen's (1972) sand transport equation, (2) Wilcock and Crowe's (2003) gravel-sand-mixed transport equation combined with Engelund and Hansen's sand transport equation, and (3) Wu et al.'s (2000) non-uniform sediment transport for gravel and sand. Currently, we do not know which equation best predicts the sediment capacity in the San Joaquin River because no sediment load samples have been collected. Comparison of the results using the three transport capacity formulas indicates that the three formulas predicted nearly identical bed profiles in the gravel reach upstream from the Gravelly Ford. Between Gravelly Ford and the Chowchilla Bifurcation Structure, Parker's formula computed 3.30 feet erosion on average, whereas the Wilcock and Crowe's formula and Wu et al.'s formula computed 3.60 feet (9.1 percent more) and 1.90 feet (42 percent less) of erosion on average, respectively.

3.2.4 Roughness Coefficient

Manning's n in the main channel and floodplain were increased by 20 percent to 0.042 in the main channel and 0.18 in the floodplain, and decreased by 20 percent to 0.028 and 0.12, respectively. Coefficients in other cross sections, which were calculated by averaging the depth-varied roughness coefficients, were also changed accordingly. Results suggest that increasing the Manning's n by 20 percent increases the average depth of bed erosion by 11.8 percent between Gravelly Ford and the Chowchilla Bifurcation Structure. A 20 percent decrease in Manning's n decreases the average depth of bed erosion by 10.2 percent in this same reach.

3.2.5 Cross-Section Numbers

A simulation was performed using all available cross sections from the HEC-RAS model of MEI. Increasing the number of cross sections substantially increases the computational time in performing the hydraulic and sediment transport routines in SRH-1D simulation. An increased number of cross sections also requires a smaller time step to reach a stable solution due to reduced distances between cross sections. In the sensitivity analysis, the simulation with all cross sections required a time step of 0.05 hour instead of 0.25 hour when one in every six cross sections was used. The total computational time increased from 6 hours to 93 hours when every cross section was used. Results of the analysis indicate minimal differences between the two models. The model with all cross sections from the provided HEC-RAS geometry file resulted in erosion of 3.26 feet on average in Reach 2A, which is 1.2 percent less than results with one in every six cross sections.

3.2.6 Silt and Sand Gradations in Reaches 1A and 1B

While the sediment transport is principally controlled by coarse sediment on riffles, pools contain fine sediments that might be eroded during high flows. Because sediment samples were collected mainly on riffle locations in Reaches1A and 1B, model sensitivity to additional fine sediment input in these reaches was investigated. Silt and sand gradations were doubled and quadrupled in Reaches 1A and 1B and the results of the bed profiles in Reach 2a are shown Figure 3-13. This sensitivity analysis was intended to

examine the sediment transport and morphology of Reaches 2A and 2B when the silt and sand gradations in Reaches 1A and 1B were increased, and the gravel gradations were reduced accordingly. However, localized effects did occur in Reaches 1A and 1B, as illustrated in Figure C-11 of Exhibit C. The fine sediment introduced in Reach 1 reduced the median sediment sizes in Reaches 1A and 1B, which decreased the critical shear stress required for erosion and resulted in a net increase in erosion in these reaches. More fine sediment delivered from these upstream reaches to Reach 2A slowed the bed material coarsening process; increased fine sediment delivery also resulted in less erosion at the upstream end of Reach 2A than with original bed gradations and more erosion toward the downstream end of the reach.

By doubling the silt and sand gradations, approximately half of the cross sections experienced decreased erosion (primarily upstream from XSA158), and the remaining half experienced increased erosion. This resulted in an increase in the average depth of erosion of 6 percent (from an average depth of 3.1 feet to 3.3 feet) in Reach 2A. By quadrupling the silt and sand gradations in Reaches 1A and 1B, nearly 75 percent of the cross sections in Reach 2A experienced decreased erosion (upstream from XSA131), and the remaining cross sections experienced increased erosion. Quadrupling the fine sediment input resulted in a decrease in the average depth of erosion of 15 percent (from an average depth of 3.1 feet to 2.7 feet) in Reach 2A.

The additional fine sediment in Reaches 1A and 1B had minimal effects on Reach 2B. By doubling and quadrupling the silt and sediment gradations, the reach-averaged depth of deposition in Reach 2B decreased by approximately 0.2 foot for both cases.

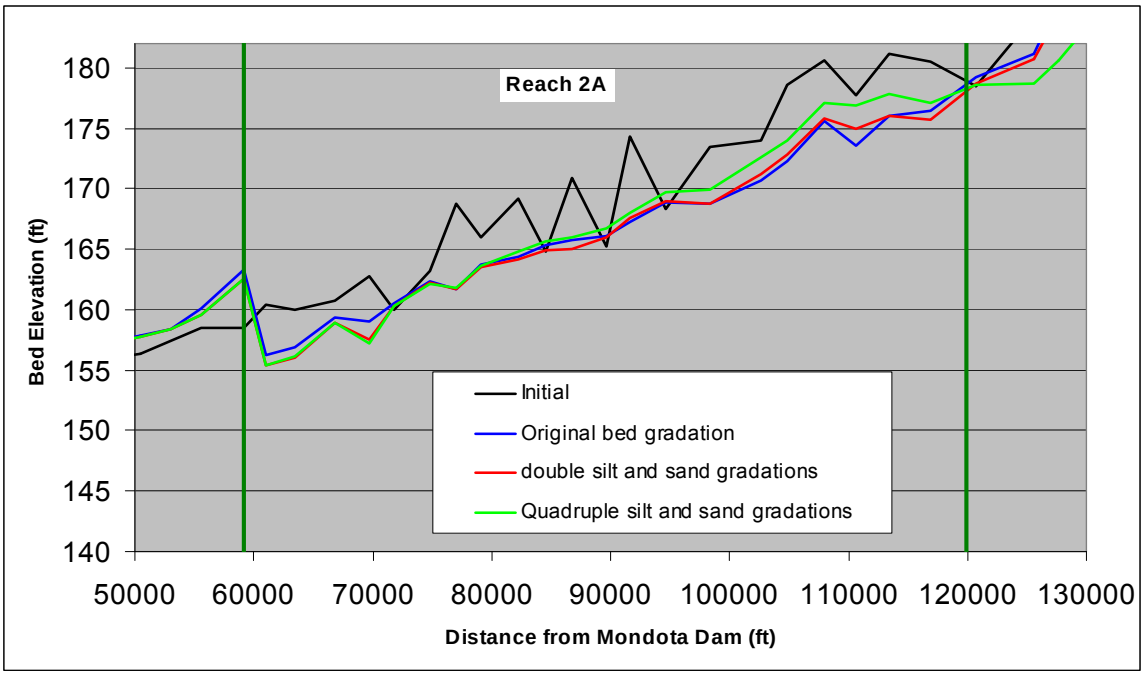

Figure 3-13.
Effects of Increased Fine Sediment in Reaches 1A and 1B on the Bed Elevations of Reach 2A

4.0 Summary of Modeling Results

SRH-1D was used to simulate the erosion and deposition under Historical hydrology, Baseline Conditions, and Alternative A (which is a potential with-project condition). The only difference among the scenarios is the water discharge. The other channel and sediment conditions are assumed identical among the scenarios.

Upstream from Gravelly Ford (Reach 1a and 1b), little erosion or deposition was notable under Historic Hydrology, Baseline Conditions, or Alternative A. Detailed investigation of erosion and deposition depth suggests that upstream from Gravelly Ford, some cross sections experienced erosion and some deposition, but overall, the reach is relatively stable and the water surface profiles remain stable.

Using Historical hydrology, the reach from Gravelly Ford to Chowchilla Bypass (Reach 2a) erosion eroded 3.3 feet on average over 17.5 years. Under the Baseline Conditions, the predicted erosion is 3.1 feet in 24 years. Alternative A hydrology, less erosion is predicted (2.1 feet in 24 years).

The model predicts deposition in the reach between Chowchilla Bypass and Mendota Pool (Reach 2b) under the all scenarios. The amount of average channel deposition predicted under Project Conditions varies between 0.22 and 0.38 foot over a 24-year simulation in Reach 2b. Most of the deposition occurs in the upper portion of Reach 2b. Under Alternative A, more channel deposition is predicted to occur with an ALS than with an MLS in Reach 2b. This is because more deposition occurs in the floodplain and less sediment is then available for deposition in the main channel. The amount of average channel deposition in Reach 2b relative to Baseline Conditions was slightly more for the ALS and similar for the MLS.

The model predicted that median sediment size in the bed would increase from Gravelly Ford to Chowchilla Bypass due to erosion of the bed material for all scenarios. There was not significant difference between the Baseline and Project conditions in their effect on bed material. No change in sediment size occurred upstream from Gravelly Ford. Just downstream from the Chowchilla Bypass, sediment size increased slightly due to the movement of coarser sands into that reach.

1

2 *This page left blank intentionally.*

5.0 References

Ayres Associates, Inc. 1998. Topographic and Bathymetric Surveys for the San Joaquin River from Friant Dam to Gravelly Ford (RM 267 to RM 229). Prepared for U.S. Bureau of Reclamation, Fresno, California.

Ayres Associates, Inc. 1999. Topographic and Hydrographic Surveys for the Sacramento and San Joaquin Comprehensive Study, California - Topographic and Hydrographic Surveying and Mapping for San Joaquin River, RM 40 to RM 230, Including Tributaries and Distributaries. Prepared for U.S. Army Corps of Engineers, Sacramento District. Sacramento, California.

Engelund, F., and E. Hansen. 1972. A monograph on sediment transport in alluvial streams, Teknish Forlag, Technical Press. Copenhagen, Denmark.

Huang, J., and B.P. Greimann. 2007. User's Manual for SRH-1D 2.0 (Sedimentation and River Hydraulics – One Dimension Version 2.0), Bureau of Reclamation, Technical Service Center (www.usbr.gov/pmts/sediment).

Huang, J., and B.P. Greimann. 2009. Sediment Mobilization Impacts of the San Joaquin River Restoration Project, Technical Report No. SRH-2009-17, Bureau of Reclamation, Technical Service Center, Denver, Colorado.

Huang, J., and B.P. Greimann. 2009b. Sediment transport and channel morphology model in the San Joaquin River from Mendota Dam to the Merced River confluence, California, Bureau of Reclamation, Technical Service Center, Denver, Colorado.

McBain & Trush, Inc. (eds.). 2002. San Joaquin River Restoration Study Background Report, prepared for Friant Water Users Authority, Lindsay, CA, and Natural Resources Defense Council. San Francisco, California

Mussetter Engineering, Inc. 2002a. "Hydraulic and Sediment Continuity Modeling of the San Joaquin River from Friant Dam to Mendota Dam, California," U.S. Bureau of Reclamation, Contract No. 98-CP-20-20060.

Mussetter Engineering, Inc. 2002b. "Hydraulic and Sediment-continuity Modeling of the San Joaquin River from Mendota Dam to the Merced River," U.S. Bureau of Reclamation, Contract No. 99-CP-20-2080.

Parker, G. 1990. "Surface based bedload transport relationship for gravel rivers," Journal of Hydraulic Research, Vol. 28(4), 417–436.

Stillwater Sciences. 2003. Restoration objectives for the San Joaquin River. Prepared for Friant Water Users Authority, Lindsay, CA, and Natural Resources Defense, Council. San Francisco, California.

U.S. Department of the Interior, Bureau of Reclamation (Reclamation). 2008. DRAFT San Joaquin River Bed Sediment Sampling Report From Friant Dam to Merced Confluence, Prepared by the Technical Service Center for the San Joaquin River Restoration Project, Mid-Pacific Region. Wilcock, P.R., and Crowe J.C. (2003). "Surface-Based Transport Model for Mixed-Size Sediment," Journal of Hydraulic Engineering, ASCE, 129(2): 120-128.

Wu, W., S.S.Y. Wang, and Y. Jia. 2000. "Nonuniform sediment transport in alluvial rivers," Journal of Hydraulic Research, Vol. 38(6):427-434.

Exhibit

Boundary Conditions Used in SRH-1D

Draft
Assessment of Sediment Transport and Channel Morphology on the San Joaquin River Restoration Program from Friant Dam to Mendota Dam Attachment

SAN JOAQUIN RIVER
RESTORATION PROGRAM

Draft
April 2011

Table A-1.
Water Surface Versus Discharge Tables for in-Channel Structures

Ledger Island Bridge		Chowchilla Bypass Structure	
Discharge (cubic feet per second)	Upstream Water Surface Elevation (feet)	Discharge (cubic feet per second)	Upstream Water Surface Elevation (feet)
85	284.59	1	160.73
177	285.02	6	160.73
477	285.71	277	161.79
977	286.72	759	163.34
1,977	288.07	1,740	165.10
3,977	290.02	3,717	165.04
7,977	293.20	7,691	164.63
11,977	295.74	11,673	167.38
16,377	298.00	16,058	170.10

This page left blank intentionally.

Exhibit

Computed Water Surface Profiles: San Joaquin River from Friant Dam to Mendota Dam

Draft
Assessment of Sediment Transport and Channel Morphology on the San Joaquin River Restoration Program from Friant Dam to Mendota Dam Attachment

SAN JOAQUIN RIVER
RESTORATION PROGRAM

Draft
April 2011

Table B 1.
Flow Discharges for Each Profile

Discharge(cfs)							
Profile Number	Friant Release	Subreach					
		1	2	3	4	5	6
		RM267.5	RM255.2	RM243.2	RM232.8	RM225.0	RM216.1
1	100	85	55	26	3	0	0
2	200	177	131	86	50	6	0
3	500	477	431	386	350	277	236
4	1,000	977	931	886	850	759	706
5	2,000	1,977	1,931	1,886	1,850	1,740	1,675
6	4,000	3,977	3,931	3,886	3,850	3,717	2,500
7	8,000	7,977	7,931	7,886	7,850	7,691	2,500
8	12,000	11,977	11,931	11,886	11,850	11,673	6,067
9	16,400	16,377	16,331	16,286	16,250	16,058	10,443

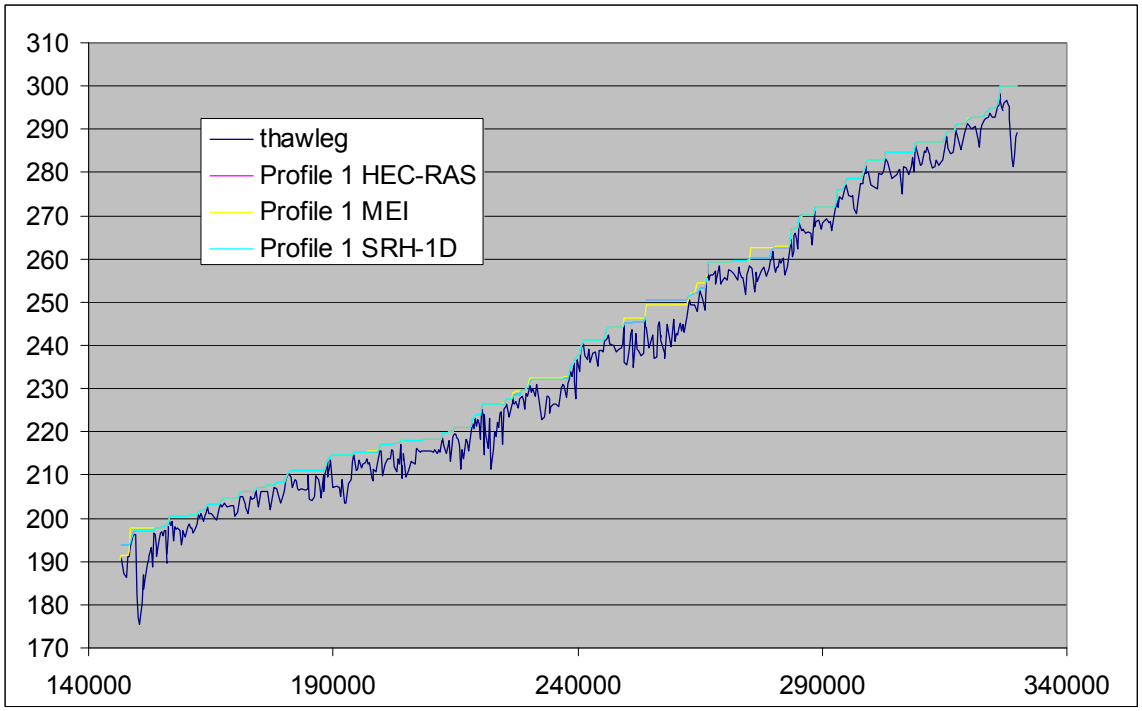

Profile 1 Friant to Gravelly Ford

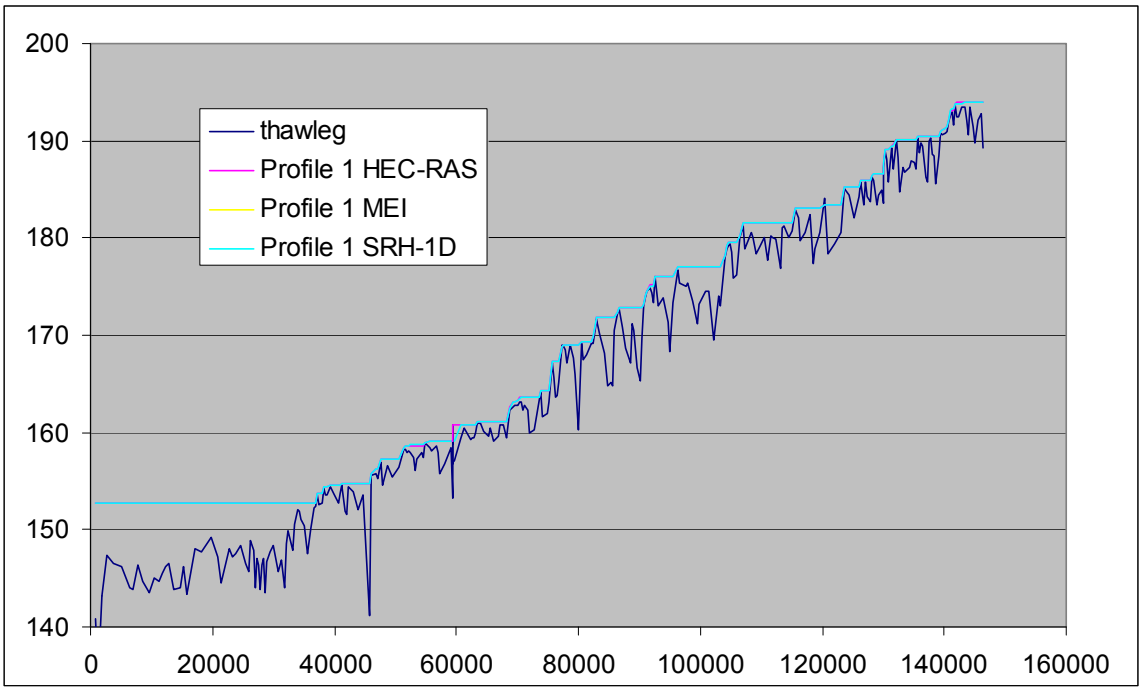

Profile 1 Gravelly Ford to Mendota

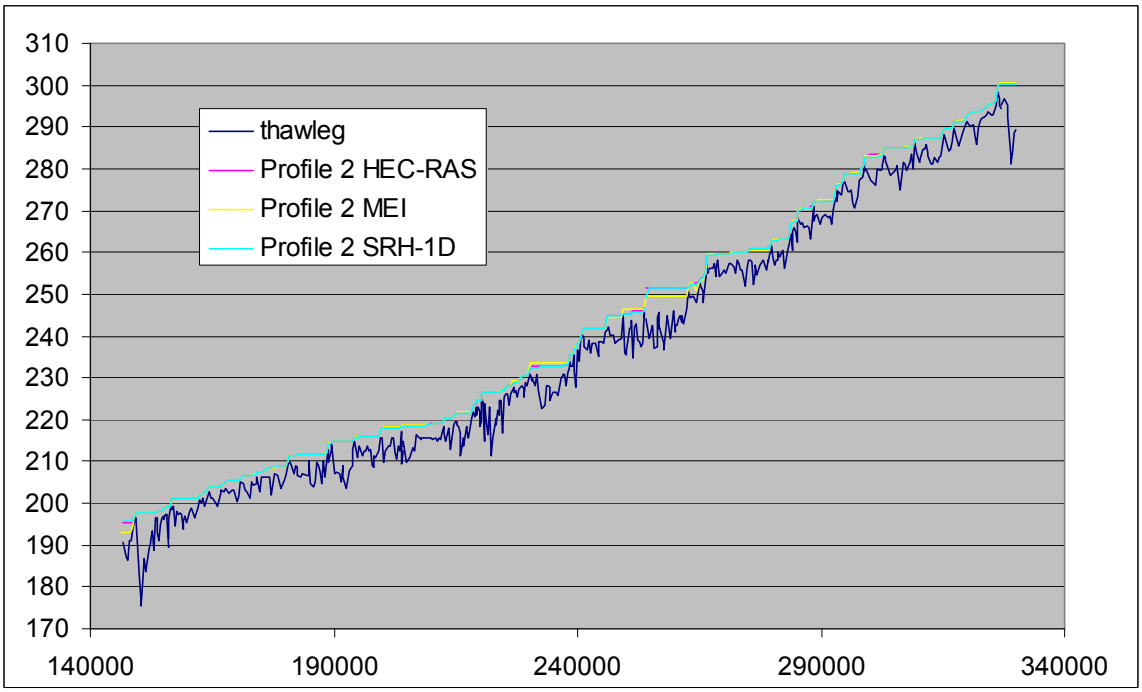

Profile 2 Friant to Gravelly Ford

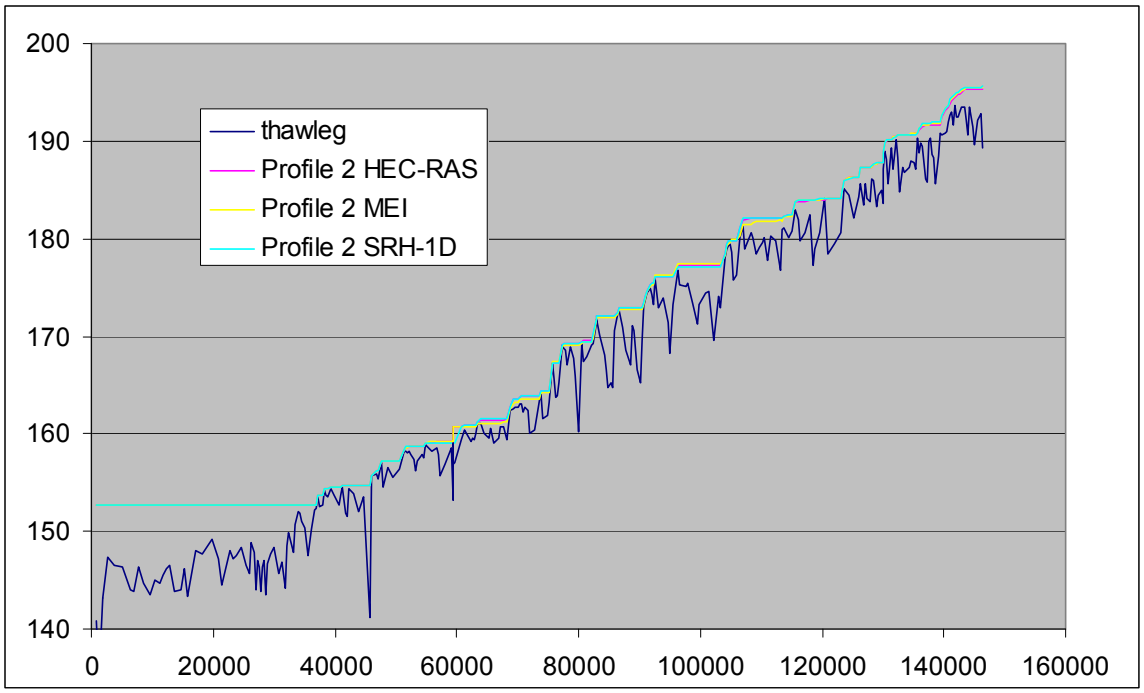

Profile 2 Gravelly Ford to Mendota

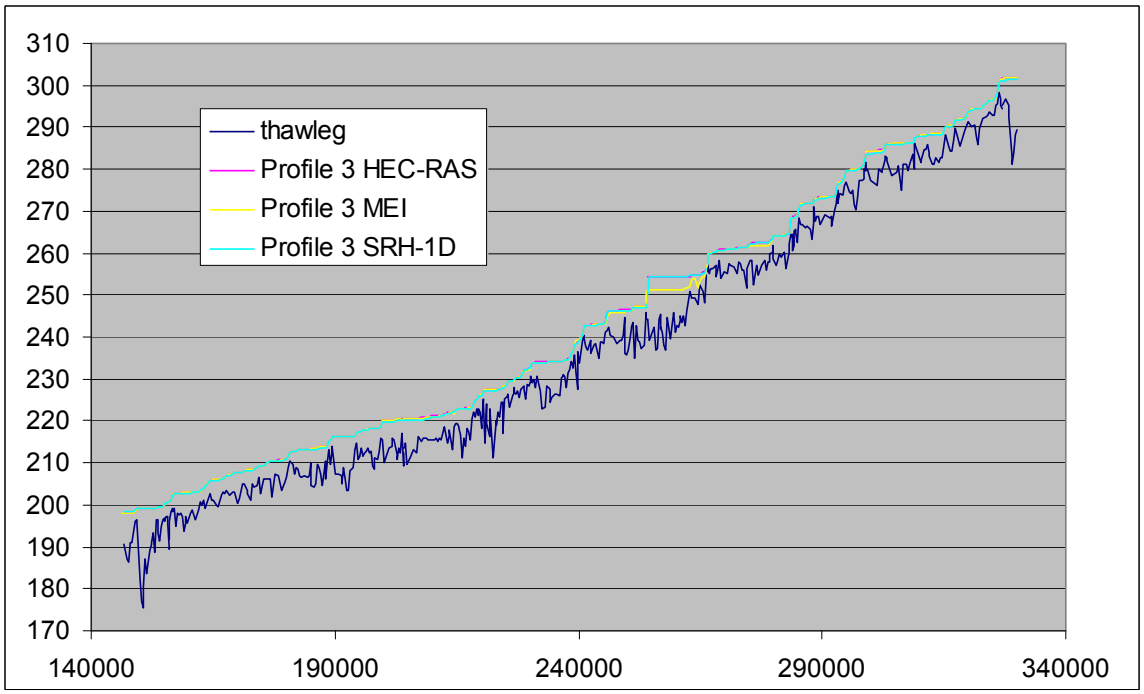

Profile 3 Friant to Gravelly Ford

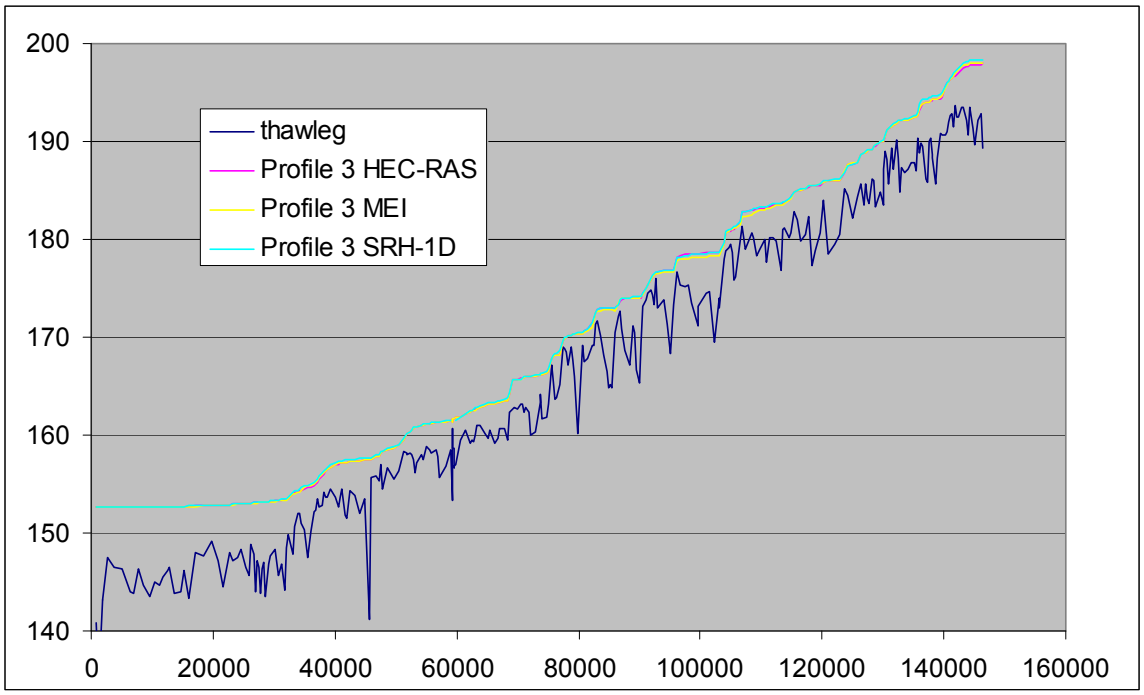

Profile 3 Gravelly Ford to Mendota

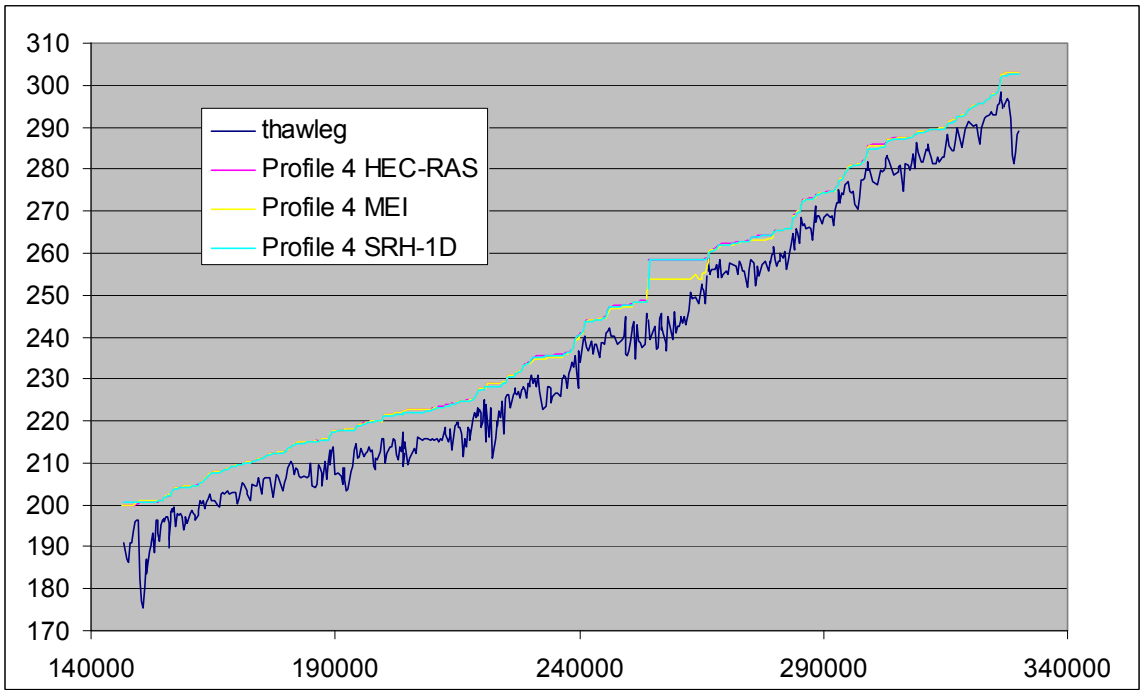

Profile 4 Friant to Gravelly Ford

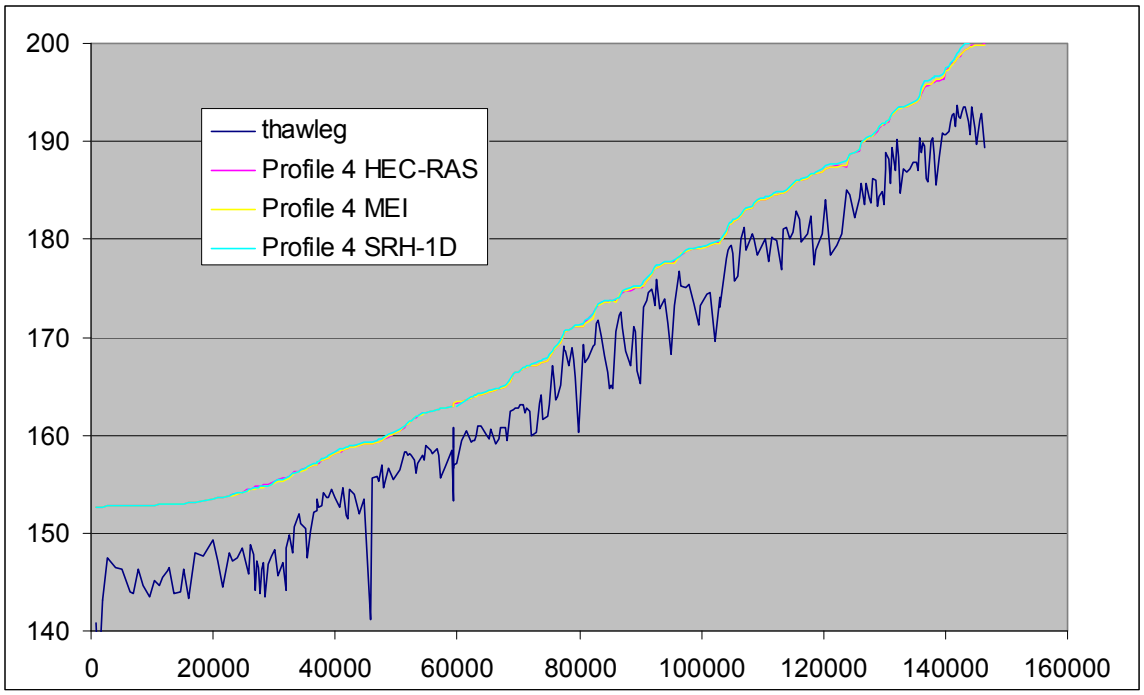

Profile 4 Gravelly Ford to Mendota

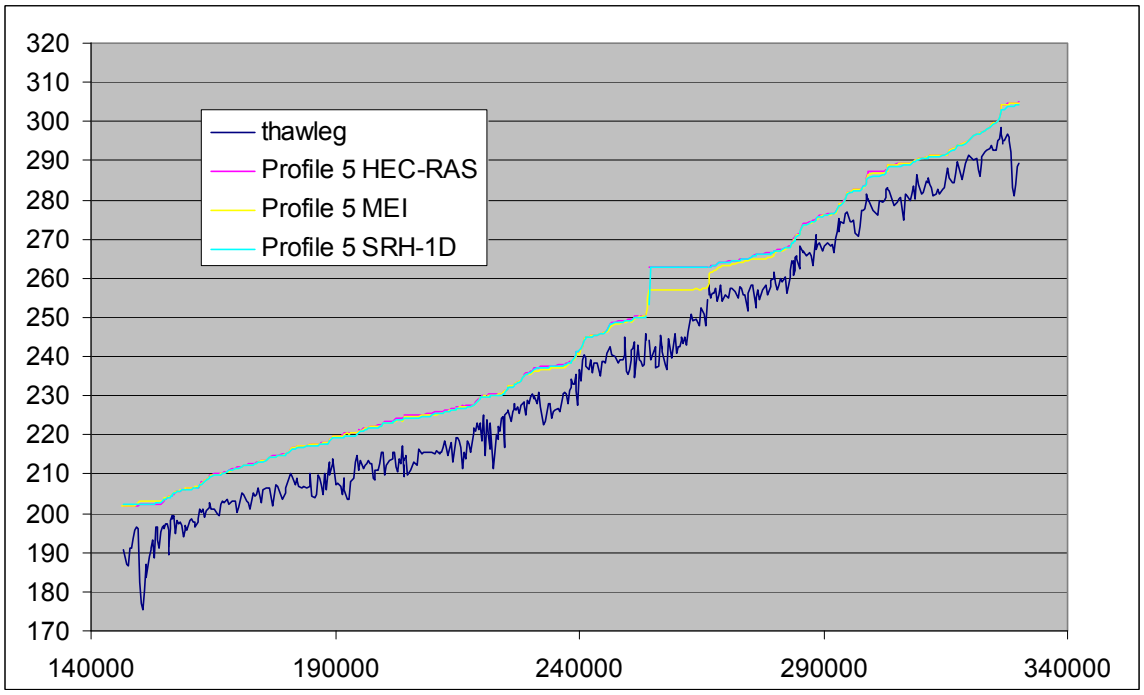

Profile 5 Friant to Gravelly Ford

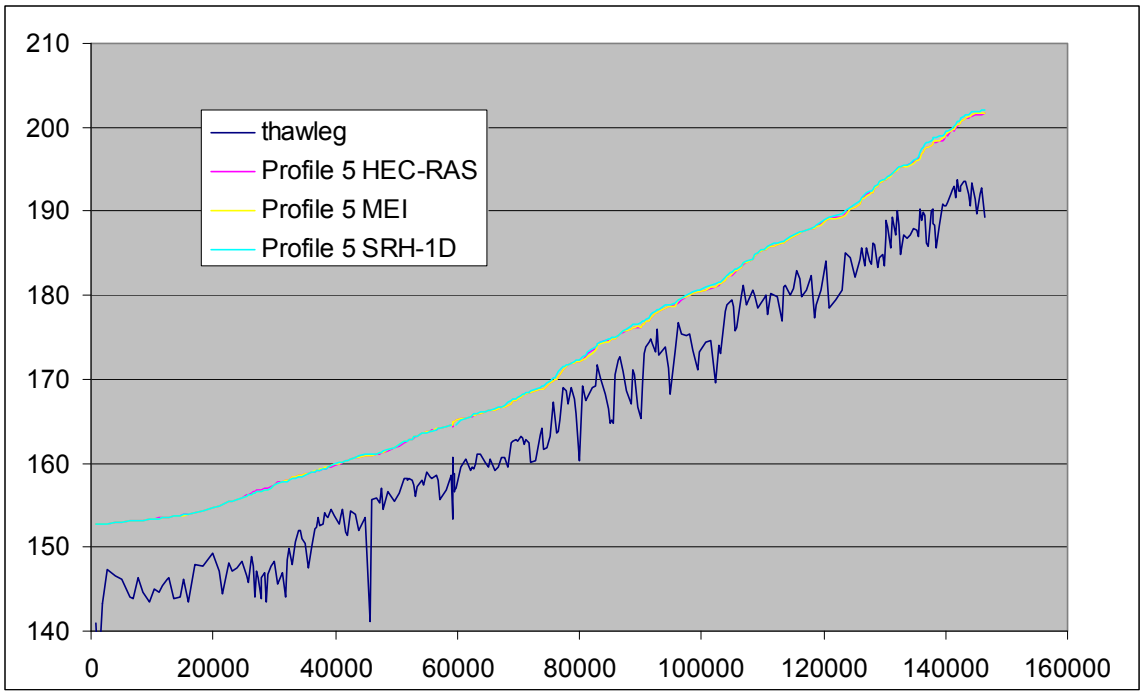

Profile 5 Gravelly Ford to Mendota

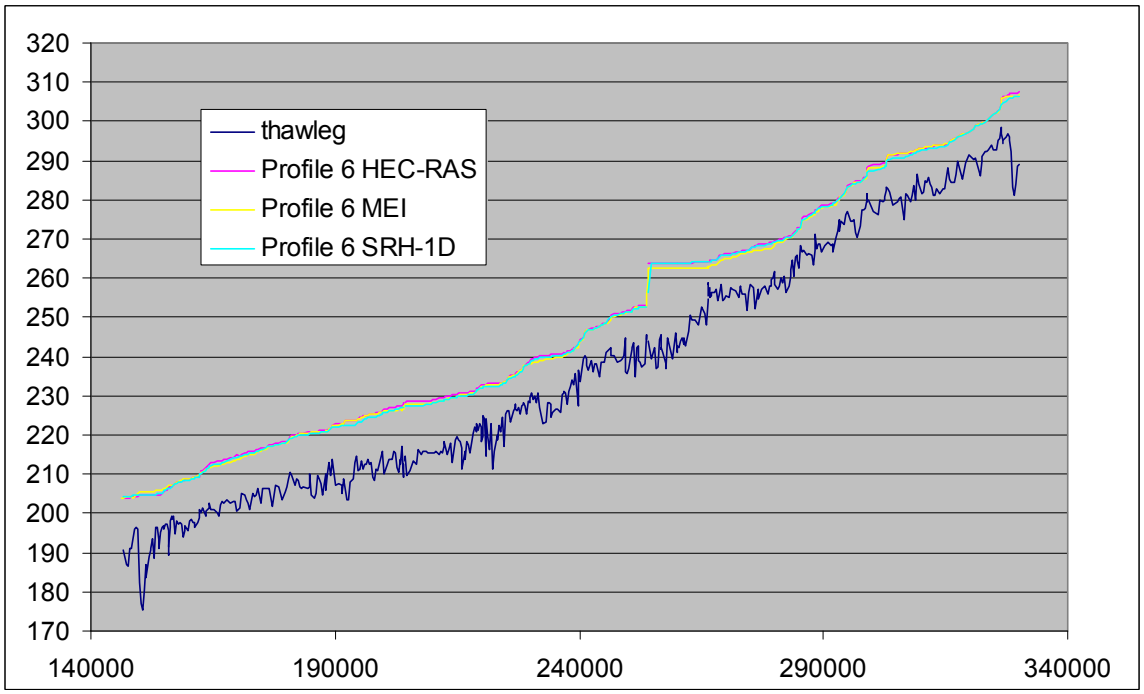

Profile 6 Friant to Gravelly Ford

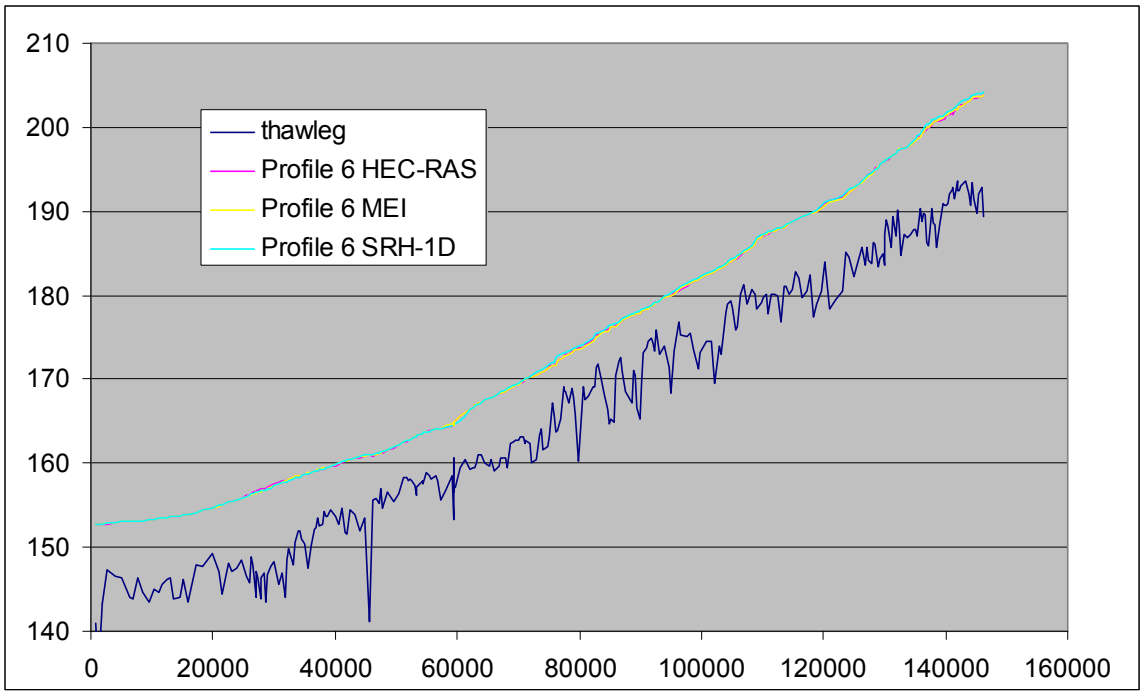

Profile 6 Gravelly Ford to Mendota

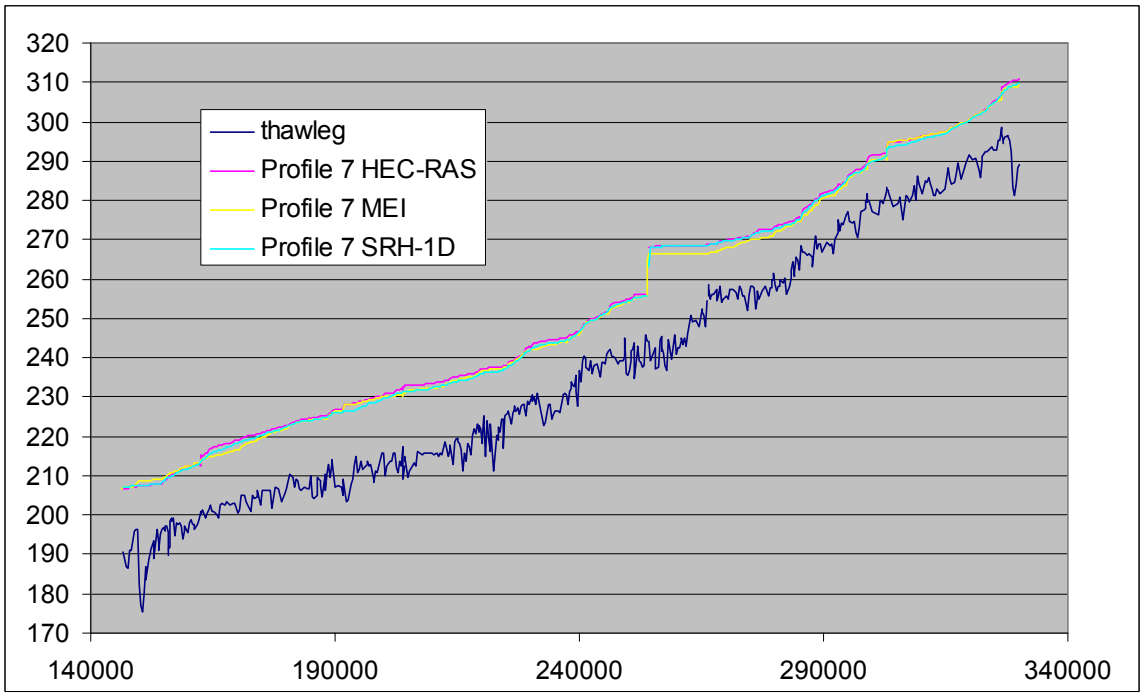

Profile 7 Friant to Gravelly Ford

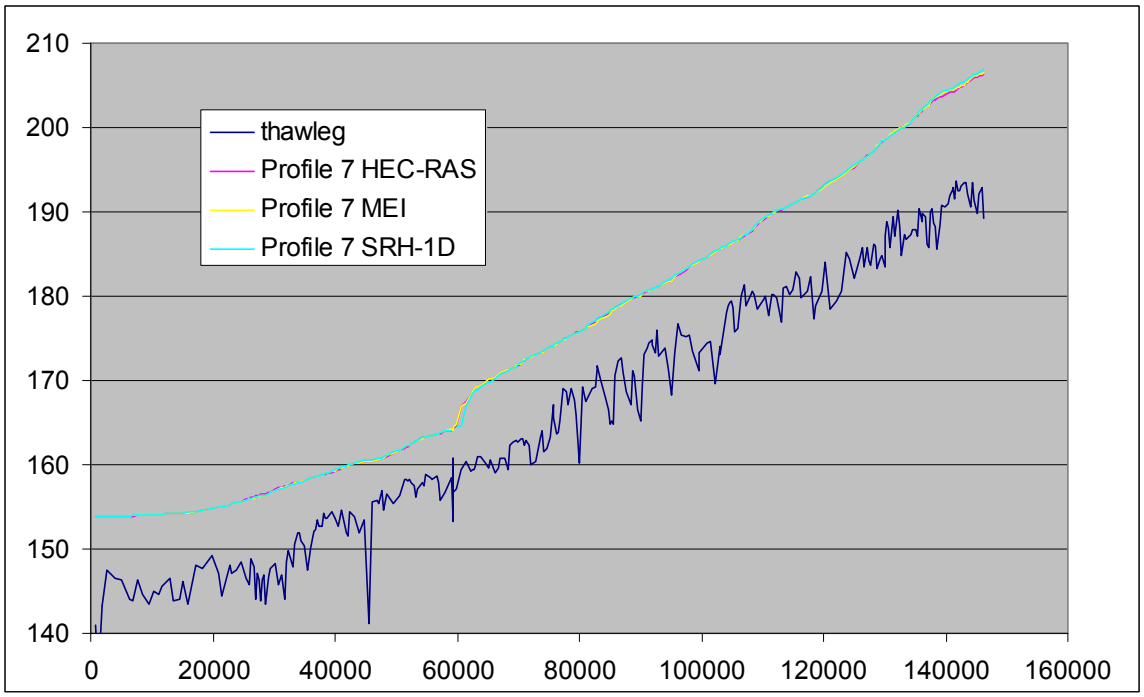

Profile 7 Gravelly Ford to Mendota

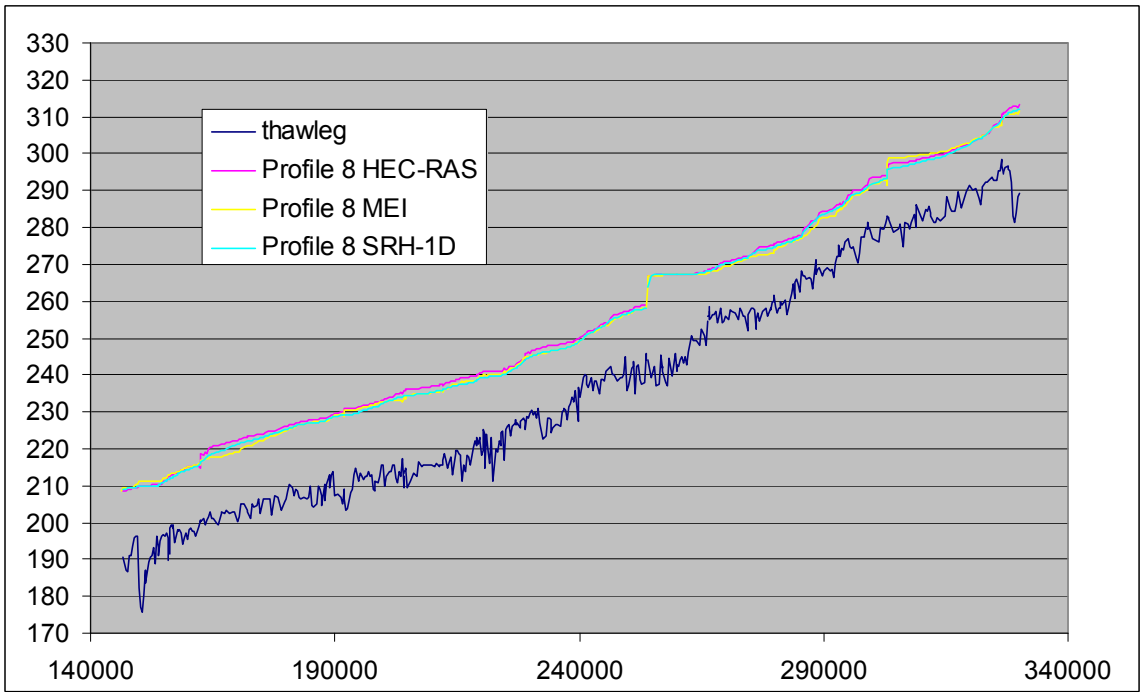

Profile 8 Friant to Gravelly Ford

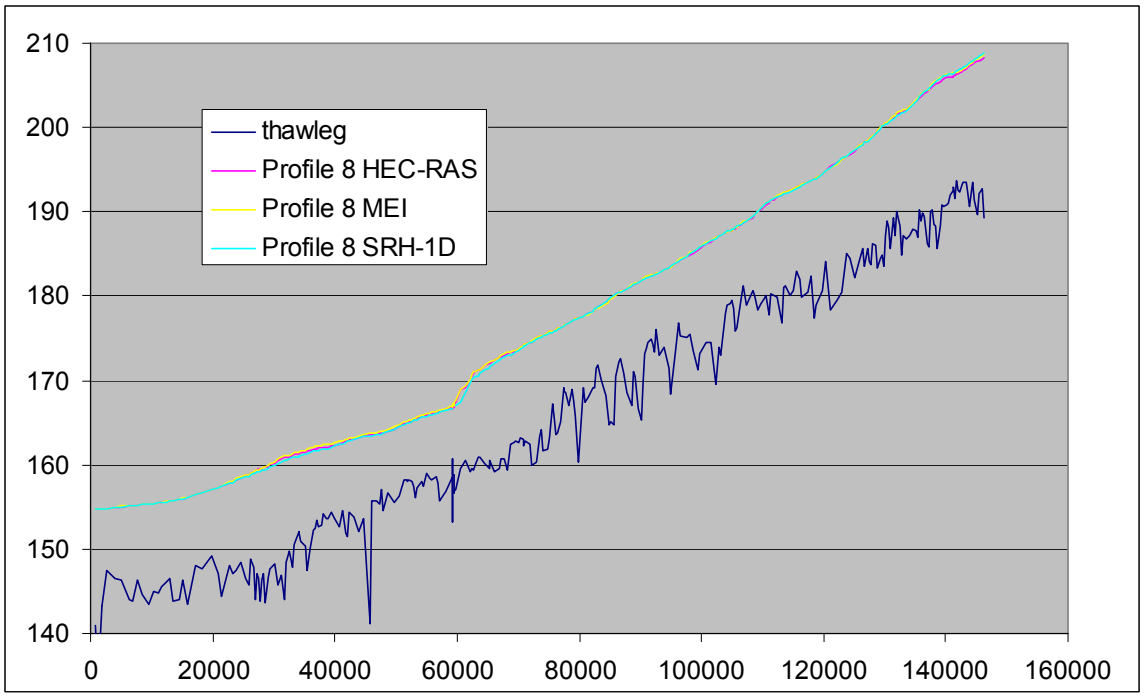

Profile 8 Gravelly Ford to Mendota

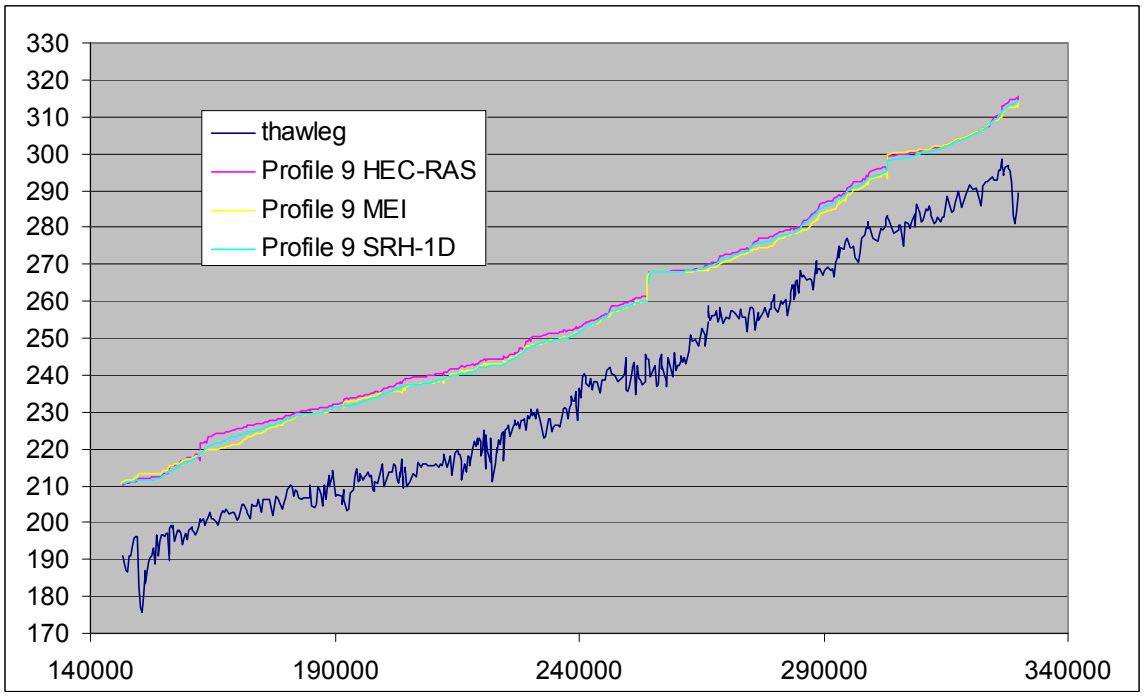

Profile 9 Friant to Gravelly Ford

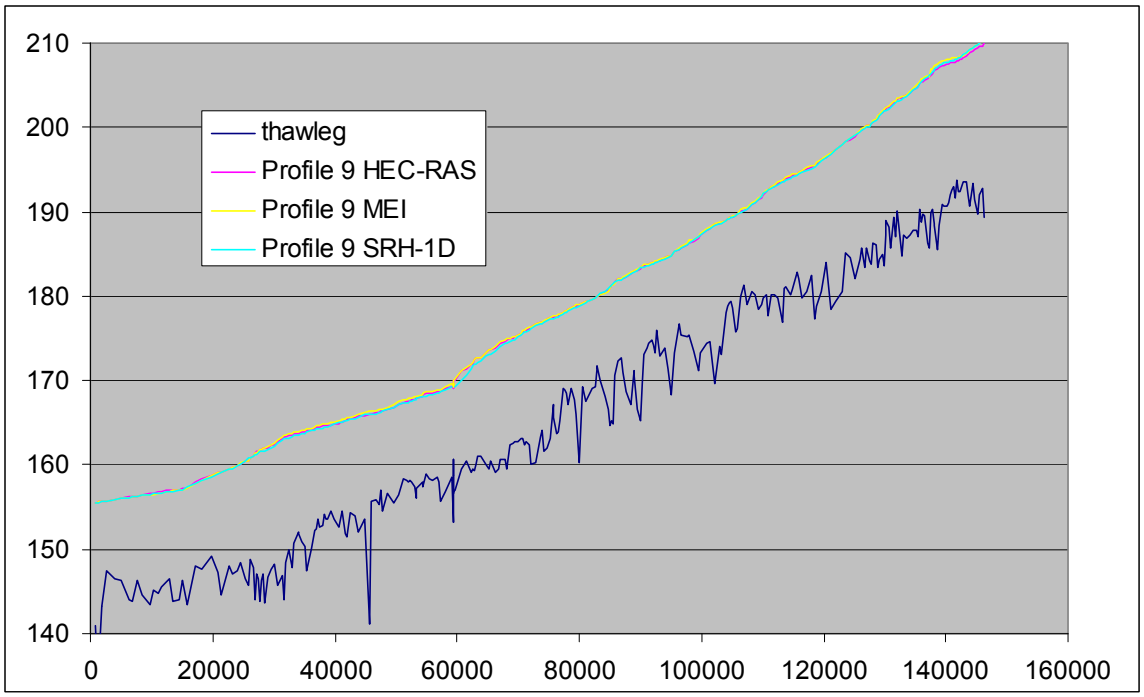

Profile 9 Gravelly Ford to Mendota

Exhibit

Sensitivity Analysis of Sediment Transport Modeling

Draft
Assessment of Sediment Transport and Channel Morphology on the San Joaquin River Restoration Program from Friant Dam to Mendota Dam Attachment

SAN JOAQUIN RIVER
RESTORATION PROGRAM

Draft
April 2011

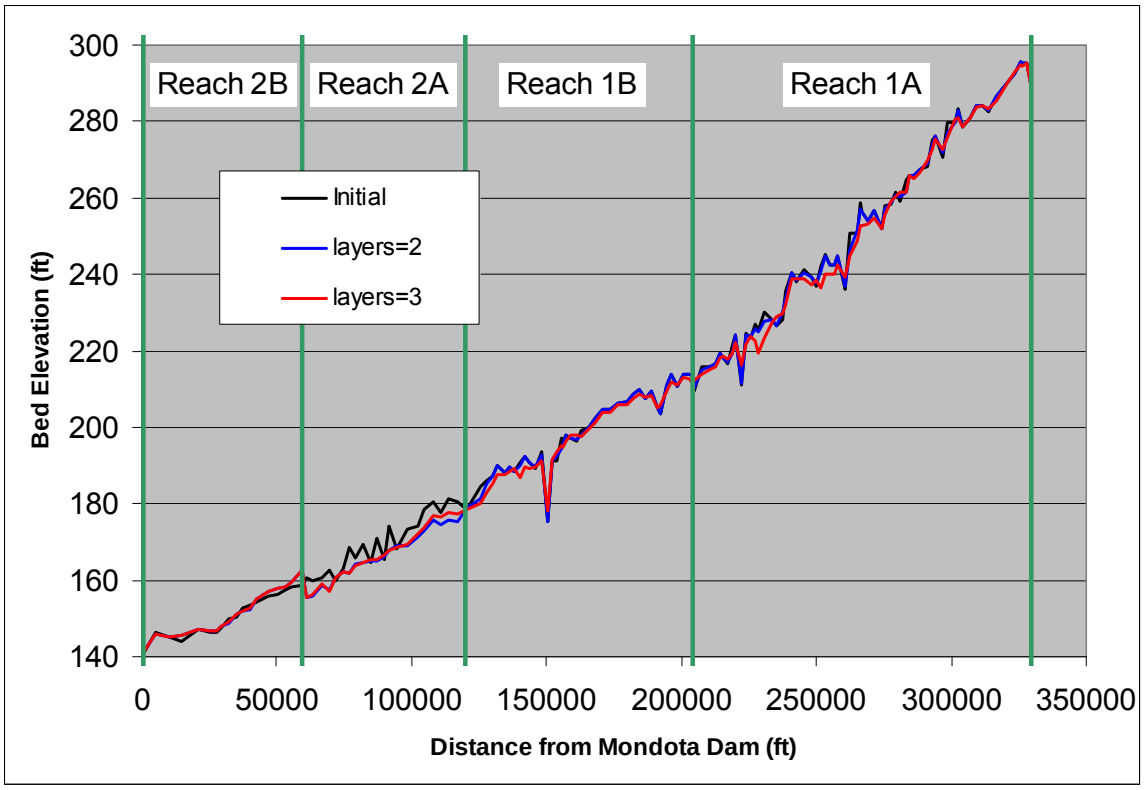

Figure C-1.
Bed Profiles Simulated with Different Bed Material Layers

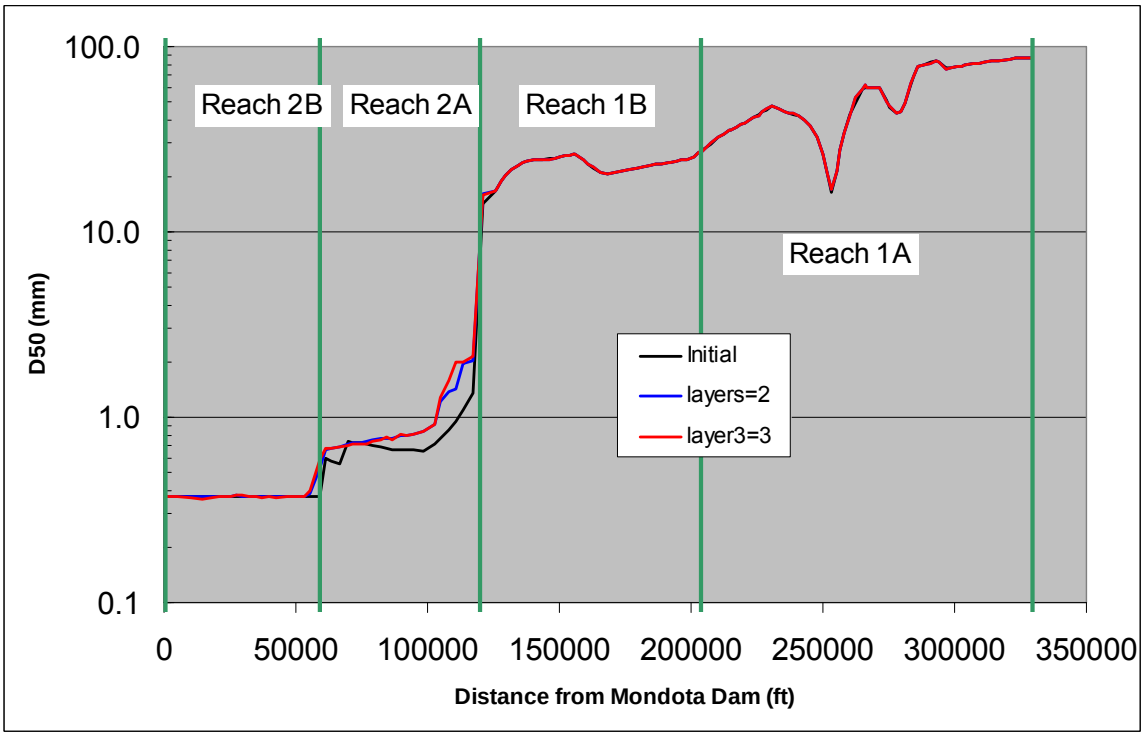

Figure C-2.
Mean Sediment Size Simulated with Different Bed Material Layers

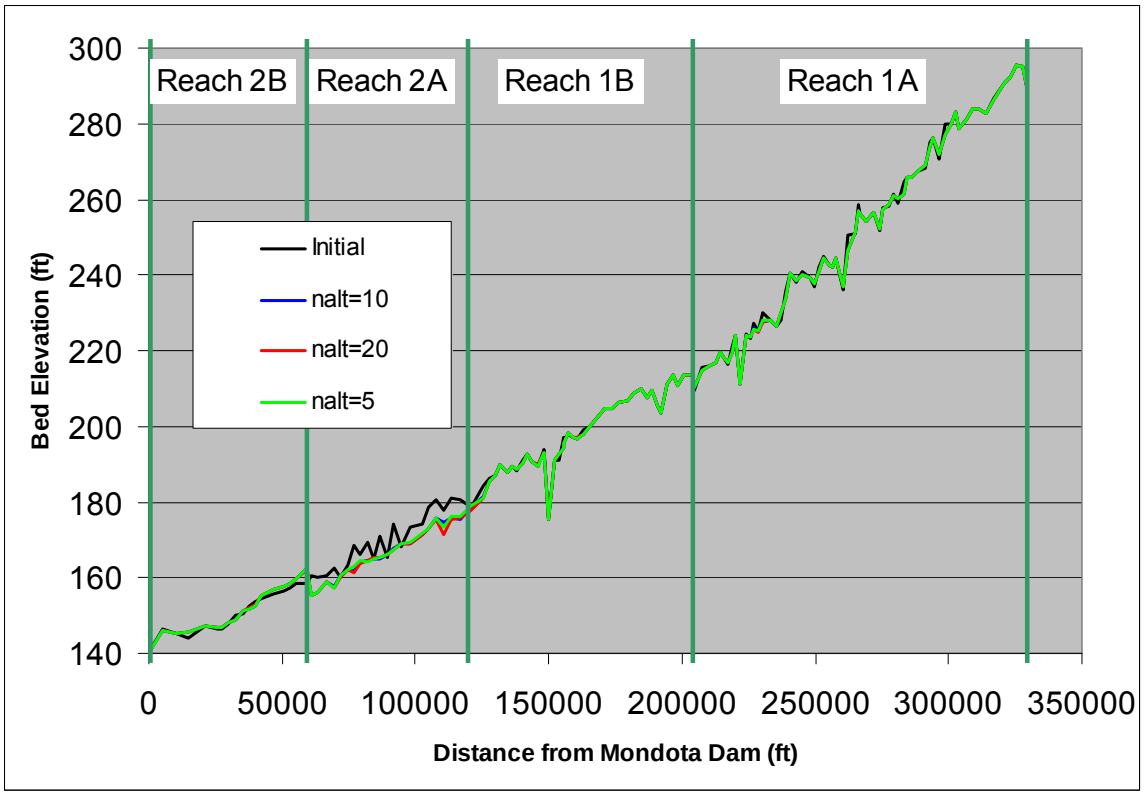

Figure C-3.
Bed Profiles Simulated with Different Active Layer Thicknesses

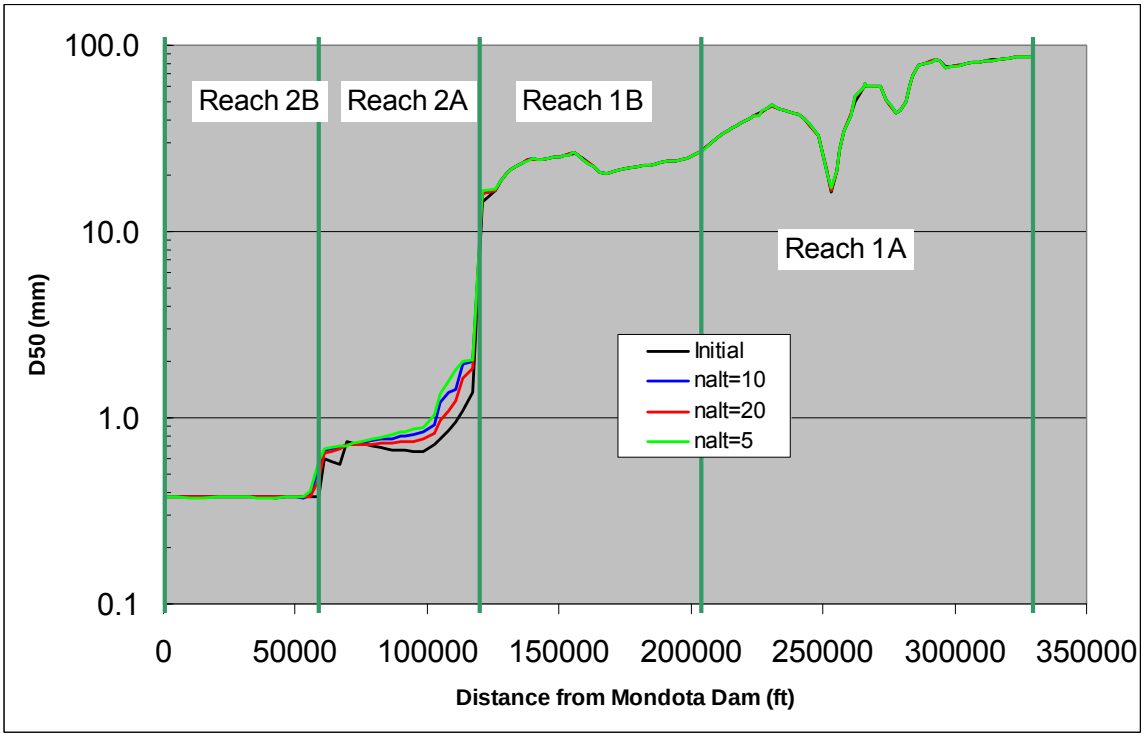

Figure C-4.
Mean Sediment Size Simulated with Different Active Layer Thicknesses

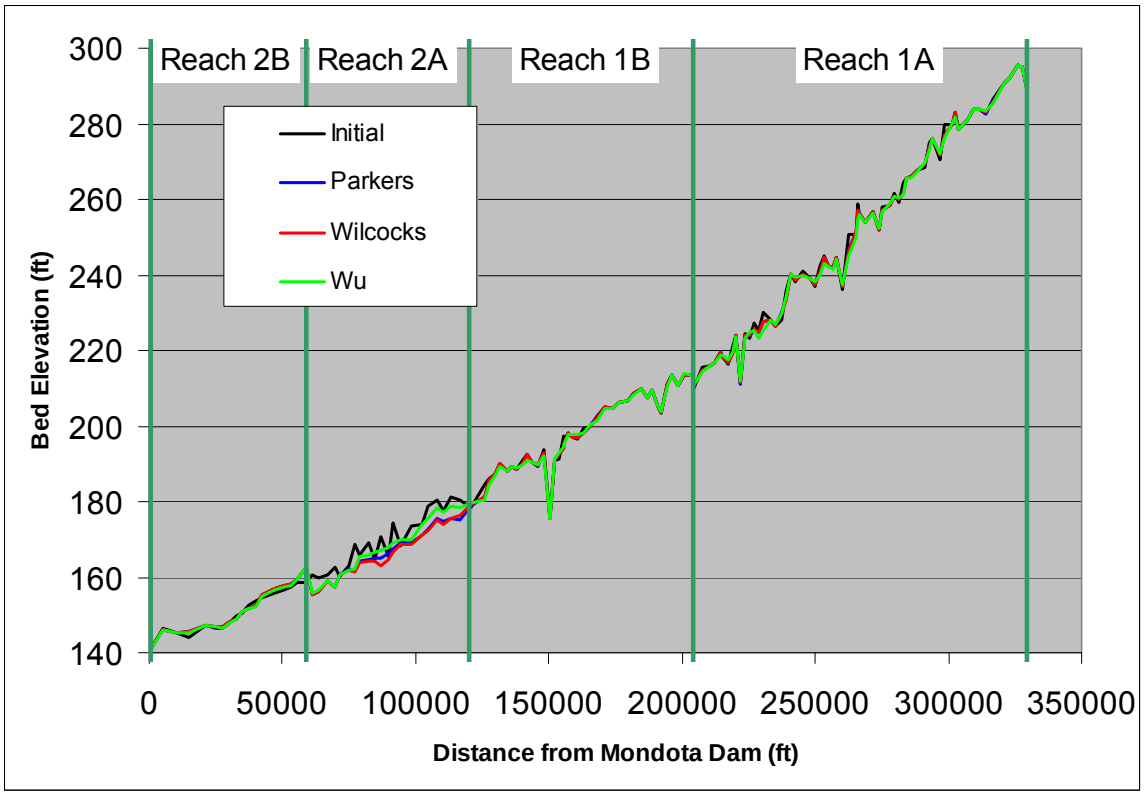

Figure C-5.
Bed Profiles Simulated with Different Sediment Transport Equations

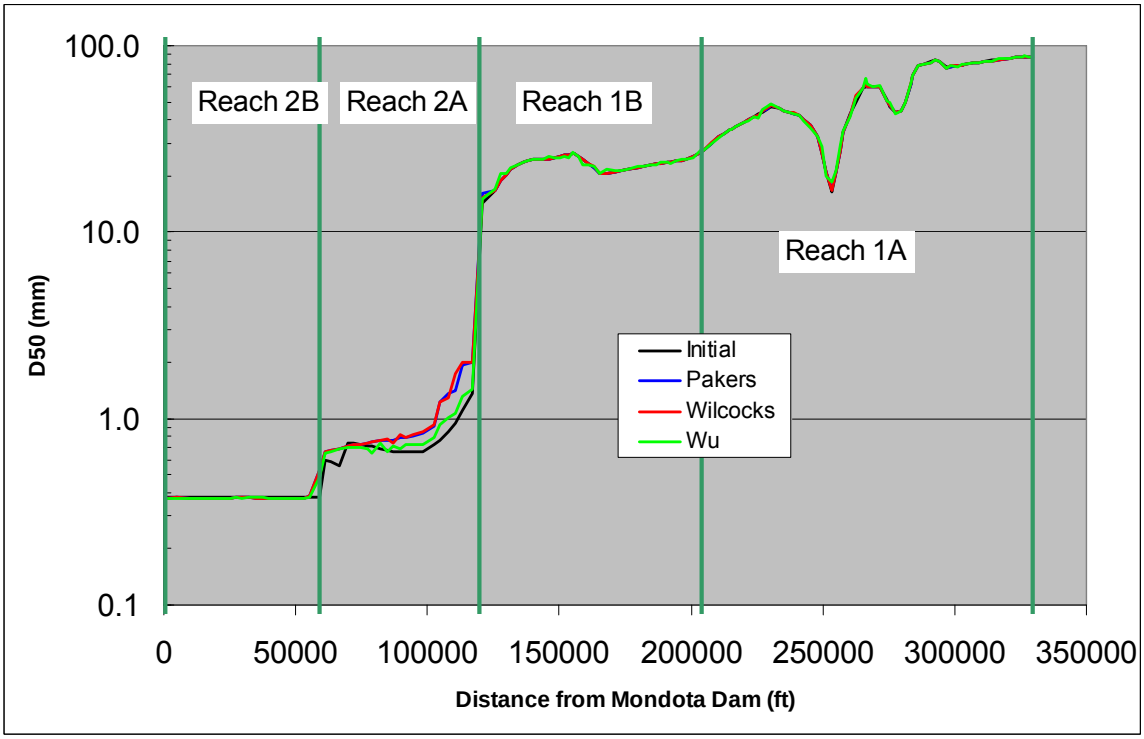

Figure C-6.
Mean Sediment Size Simulated with Different Sediment Transport Equations

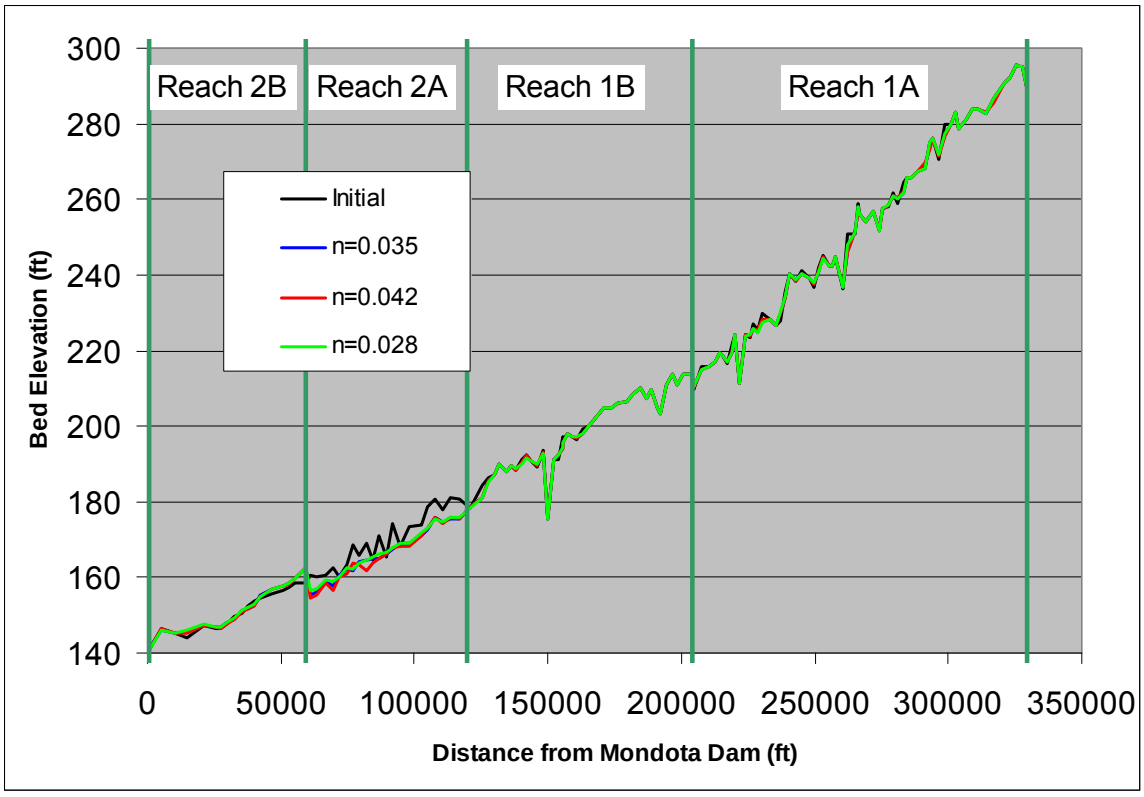

Figure C-7.
Bed Profiles Simulated with Different Manning's Roughness Coefficient

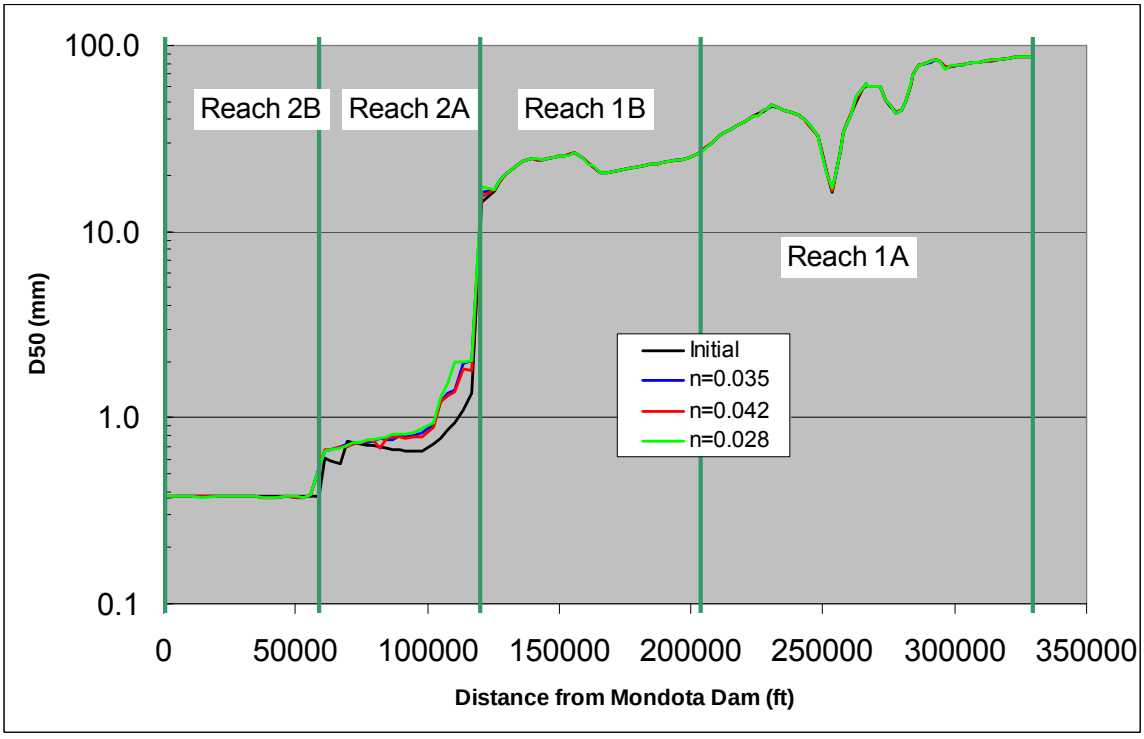

Figure C-8.
Mean Sediment Size Simulated with Different Manning's Roughness Coefficient

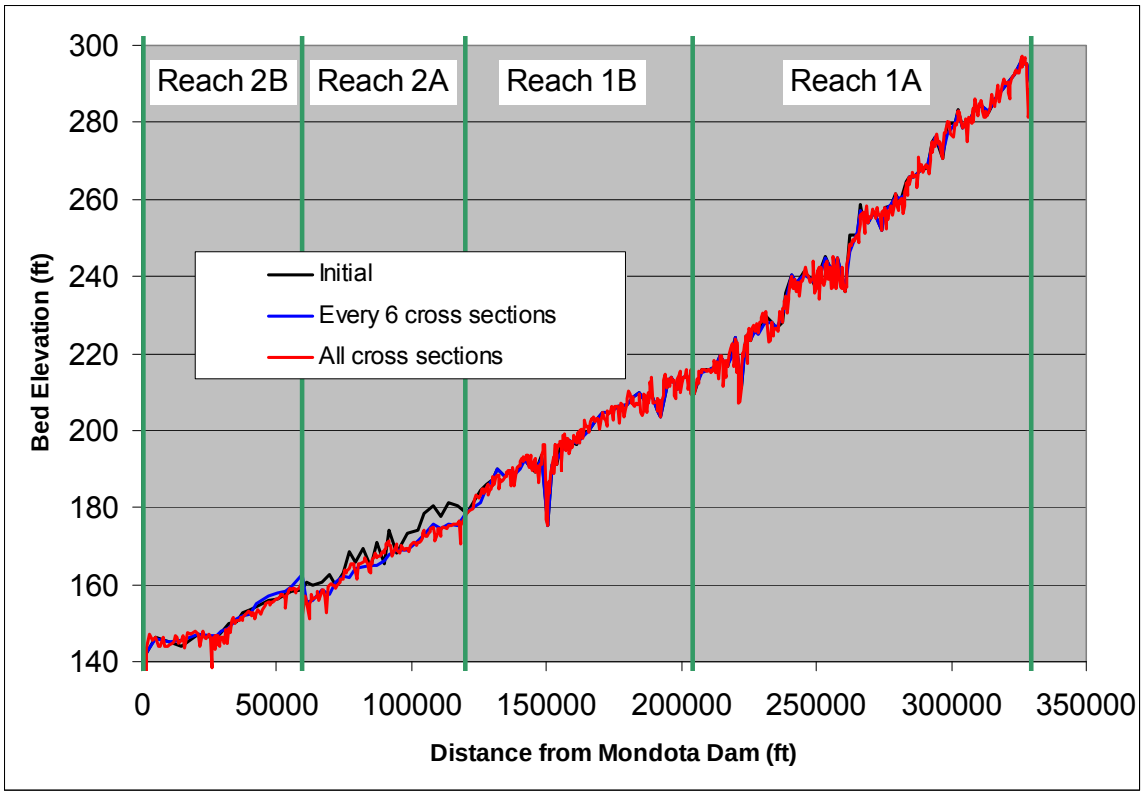

Figure C-9.
Bed Profiles Simulated with Different Cross-Section Numbers

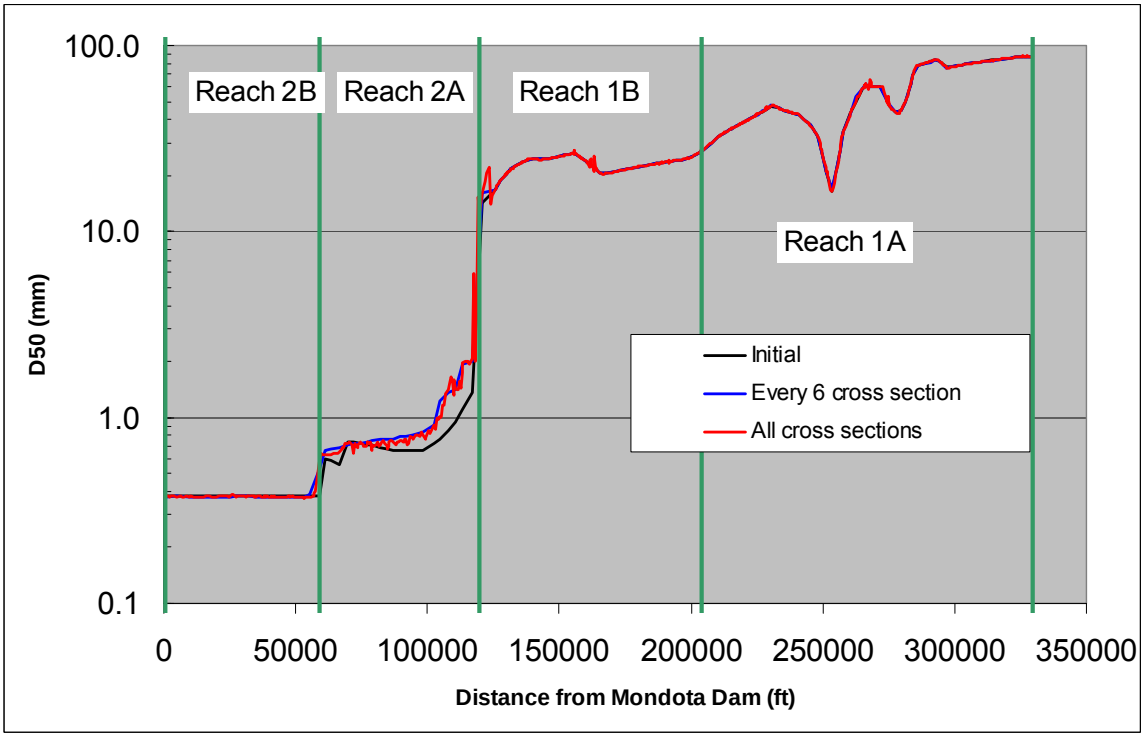

Figure C-10.
Mean Sediment Size Simulated with Different Cross-Section Numbers

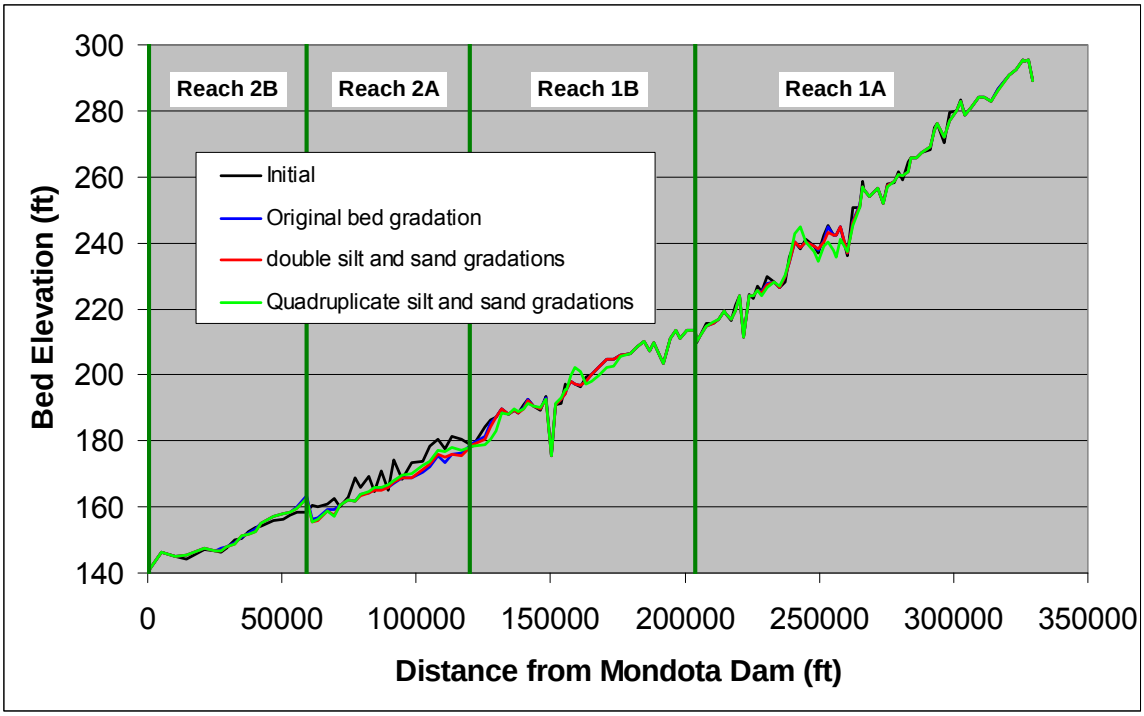

Figure C-11.
Bed Profiles Simulated with Different Silt and Sand Gradations

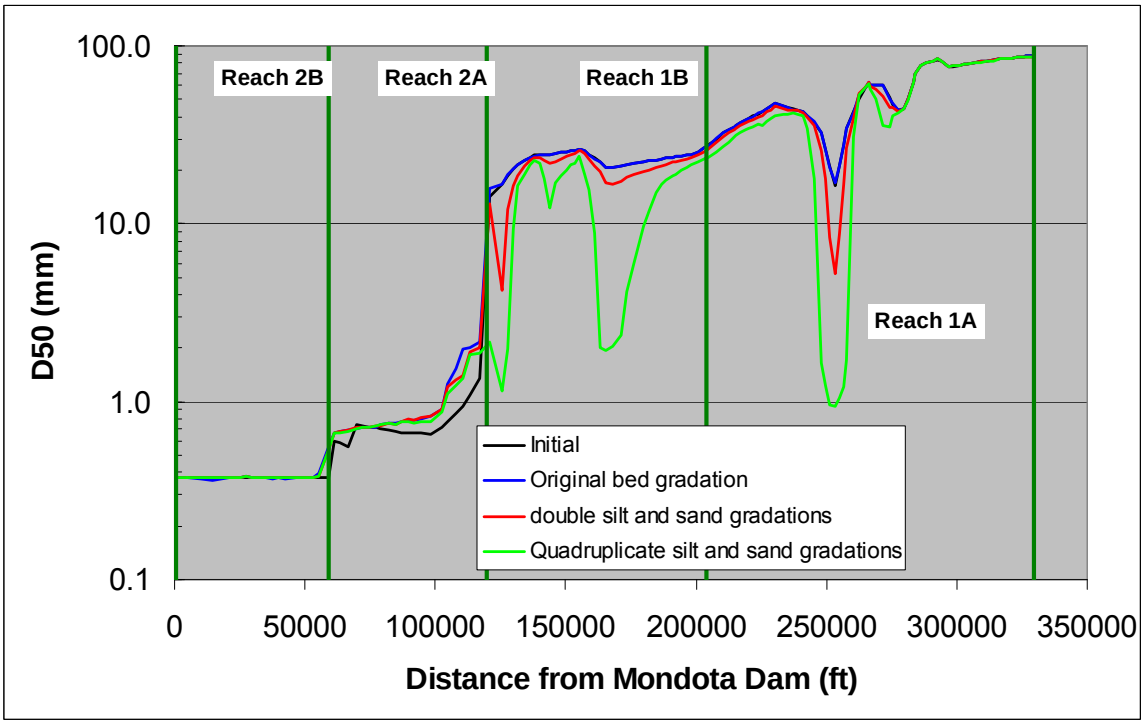

Figure C-12.
Mean Sediment Size Simulated with Different Silt and Sand Gradations

Attachment

Assessment of Sediment Transport and Channel Morphology on the San Joaquin River from Mendota Dam to the Merced River

Draft
Geomorphology, Sediment Transport, and Vegetation Assessment Appendix

SAN JOAQUIN RIVER
RESTORATION PROGRAM

Draft
April 2011

Assessment of Sediment Transport and Channel Morphology on the San Joaquin River from Mendota Dam to the Merced River

Report Prepared by:

Jianchun Huang, P.E., Ph.D., Hydraulic Engineer
Sedimentation and River Hydraulics Group, Technical Service Center

Signature:_____

Blair P. Greimann, P.E., Ph.D., Hydraulic Engineer
Sedimentation and River Hydraulics Group, Technical Service Center

Signature:_____

Peer Reviewed by:

Elaina Holburn, P.E., M.S., Hydraulic Engineer
Sedimentation and River Hydraulics Group, Technical Service Center

Signature:_____

Table of Contents

Exhibits

Tables

Figures

Abbreviations and Acronyms

ALS	Average Levee Setback
BBE	Bear Creek below Eastside Canal gage
Caltrans	California Department of Transportation
cfs	cubic feet per second
DTM	digital terrain model
ELN	El Nido gage
MLS	Maximum Levee Setback
n	Manning's roughness coefficient
Reach 3	San Joaquin River Mendota Dam to Sack Dam
Reach 4A	San Joaquin River Sack Dam to Sand Slough Control Structure
Reach 4B-1	San Joaquin River from Sand Slough Bypass to Mariposa Bypass
Reach 4B-2	San Joaquin River from Mariposa Bypass to Bear Creek
Reach 5-1	San Joaquin River Bear Creek to Salt Slough confluence
Reach 5-2	San Joaquin River Salt Slough to Mud Slough confluence
Reach 5-3	San Joaquin River Mud Slough to Merced River confluence
Reclamation	U.S. Department of the Interior, Bureau of Reclamation
River Post 41	Stockton
River Post 118.1	Merced River confluence
River Post 135.8	Bear Creek and the Eastside Bypass
River Post 147.3	Mariposa Bypass
River Post 168.5	Sand Slough Control Structure
River Post 173.9	Highway 152 Bridge
River Post 182.0	Sack Dam
River Post 204.7	Mendota Dam
RP	River Post
SJRRP	San Joaquin River Restoration Program
SJS	San Joaquin River near Stevinson gage

SRH-1D	Sedimentation and River Hydraulics – One Dimension Model
TSC	Technical Service Center
yr	year

1.0 Introduction

The Denver Technical Service Center (TSC) of the U.S. Department of the Interior, Bureau of Reclamation (Reclamation), was requested to perform an analysis of the sediment transport and channel morphology of the San Joaquin River between Friant Dam and the Merced River confluence. This report documents how the Sedimentation and River Hydraulics – One Dimension model (SRH-1D) (Huang and Greimann 2007) was used to evaluate these channel processes along the San Joaquin River between the Mendota Dam and the Merced River confluence. This assessment is in support of the San Joaquin River Restoration Program (SJRRP) and is part of a larger analysis that focuses on the sediment transport and geomorphic characteristics of the San Joaquin River.

The current study reach, as shown in Figure 1-1, covers Reach 3 from Mendota Dam (River Post (RP) 204.7) to Sack Dam (RP 182.0); Reach 4A from Sack Dam (RP 182.0) to the Sand Slough Control Structure (RP 168.5), Sand Slough Bypass, Eastside Bypass, and Mariposa Bypass; Reach 4B-1 from Sand Slough Bypass (RP 168.5) to Mariposa Bypass (RP 147.3); Reach 4B-2 from Mariposa Bypass (RP 147.3) to the confluence with Bear Creek and the Eastside Bypass (RP 135.8); and Reach 5 from the confluence with Bear Creek and the Eastside Bypass (RP 135.8) to the Merced River confluence (RP 118.1) (Figure 1-1). A separate report covers upstream Reaches 1 and 2 from Friant Dam to Mendota Dam (Huang and Greimann 2009b).

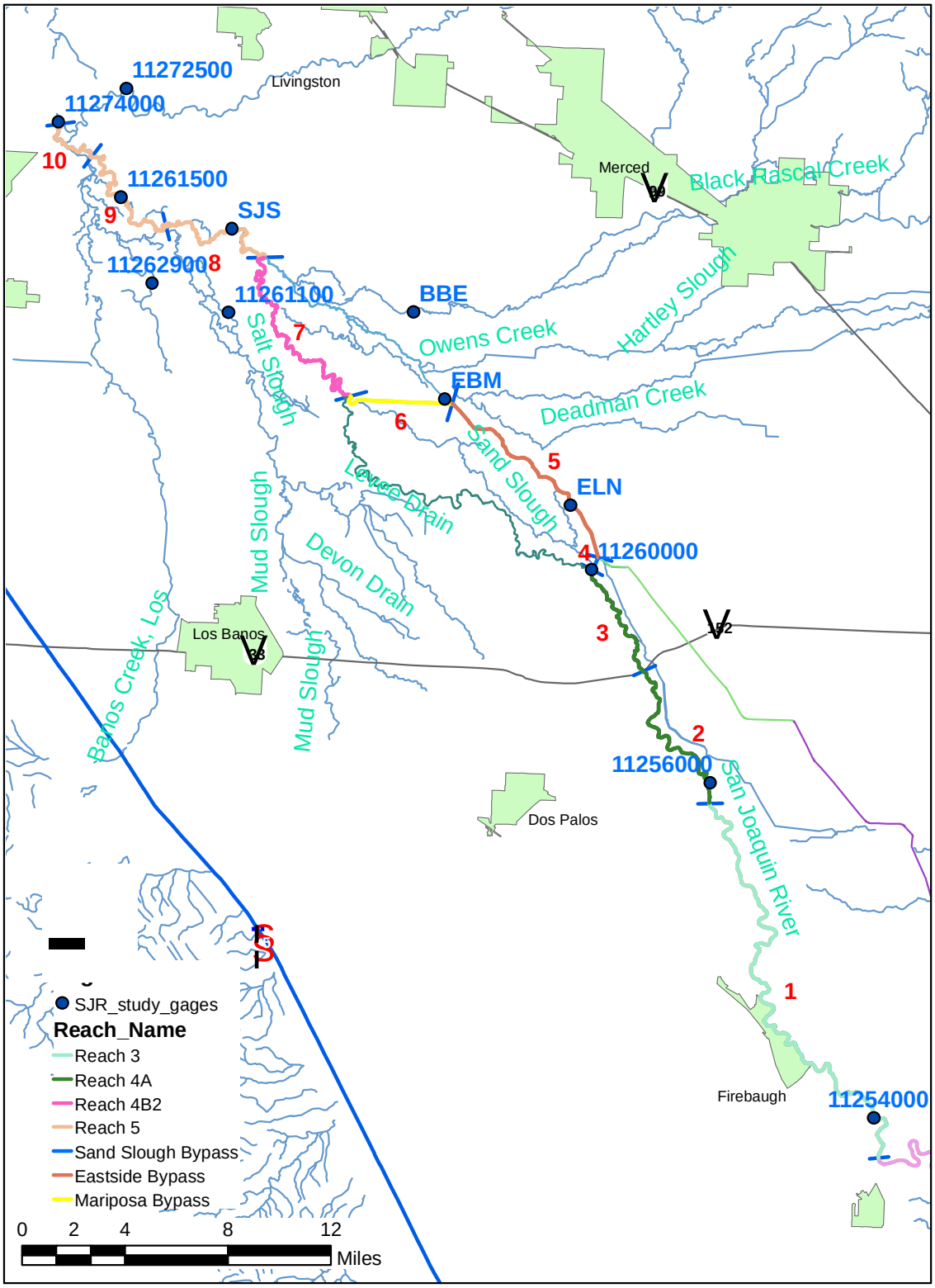

Figure 1-1.
Overview Map of Study Area (SJRRP Reaches 3, 4, 5 and Bypasses)

2.0 Input Data

2.1 Hydrology

Three primary hydrologic conditions were evaluated in this analysis: Historical, Baseline, and Alternative A. The Historical Conditions represent information from stream gage data and interpolated flows in locations where stream gage data were unavailable. Under Historical Conditions, no flow was conveyed through Reach 4B-1. However, two additional scenarios were examined with flow conveyance of a maximum of 475 cubic feet per second (cfs) and 4,500 cfs applying the Historical hydrology in all other reaches. The Baseline Conditions were simulated based on CalSim II analyses, and are documented in Appendix H, Modeling. Alternative A was also a CalSim II-simulated analysis developed to address river restoration. These scenarios are described in the following sections.

2.1.1 Historical Hydrology

Thirteen Existing and Historical stream gages are shown in Figure 1-1. Another unnamed gage located in the Mariposa Bypass near Crane Ranch was not used in the modeling effort. Descriptive information for each of these gages is provided in Table 2-1. The gage at the San Joaquin River near Mendota provided information from 1940 to 1954, 1974 to 1997, and 2000 to present. The gage at the San Joaquin River near Stevinson provided information from 1981 to present. Flows in other gages do not cover the same period; therefore, a common period from October 1, 1981, to September 30, 1997, was selected to represent Historical flows since a substantial amount of gage data were available during this time period.

Table 2-1.
Stream Gages Used to Derive Flow-Duration Curves

Description	Stream Gage ID	River Post	HEC-RAS XC	Agency	Period of Record
San Joaquin River near Mendota	11254000	202	XS730	USGS	1940 – 1954
				Reclamation	1974 – 1997 2000 – present
San Joaquin River near Dos Palos	11256000	181	XS464	USGS	1941 – 1954
				Reclamation	1986, 1987, 1995
San Joaquin River near El Nido	11260000	168	XS304	USGS	1940 –1949
Eastside Bypass near El Nido	ELN	N/A	N/A	DWR	1980 – present
Mariposa Bypass near Crane Ranch	N/A	N/A	N/A	DWR	1981 – 1994
Eastside Bypass below Mariposa Bypass	EBM	N/A	N/A	DWR	1980 – present
Bear Creek below Eastside Canal	BBE	N/A	N/A	DWR	1980 – present
San Joaquin River near Stevinson	SJS	133	XS199M	DWR	1981 – present
Salt Slough at Highway 165 near Stevinson	11261100	N/A	N/A	USGS	1986 – 1994, 1996 – present
				DWR	1980 – present
San Joaquin River at Fremont Ford Bridge	11261500	125	XS99M	USGS	1937 – 1989
Mud Slough near Gustine	11262900	N/A	N/A	USGS	1986 – present
Merced River near Stevinson	11272500	N/A	N/A	USGS	1941 – Present
San Joaquin River near Newman	11274000	118	XS1M	USGS	1912 – present

Key:
DWR = California Department of Water Resources
N/A = not applicable
Reclamation = U.S. Department of the Interior, Bureau of Reclamation
USGS = U.S. Geological Survey

Sack Dam allows for the diversion of water into Arroyo Canal. As such, the San Joaquin River downstream from Sack Dam yields lower base flows and lower peak flows than flows downstream from Mendota Dam and flows near Stevinson. Due to the return of high flows from the Eastside Bypass and seasonal flows from Bear Creek, the San Joaquin River near Stevinson in Reach 5 is characterized by higher peak flows than upstream at Mendota Dam. Base flows near Stevinson, however, are still lower than those downstream from Mendota Dam.

Flow-duration curves are provided in Figures 2-1 to 2-4. The Historical flow-duration curve is based upon records from October 1, 1980, to May 31, 1997.

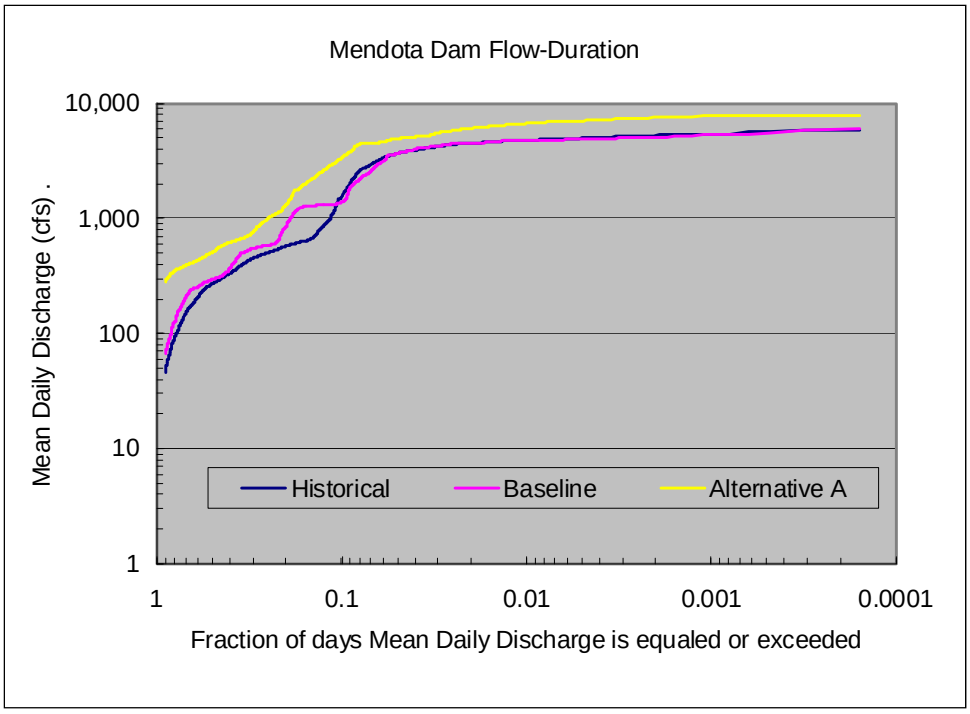

Note: The flow-duration curve is based upon daily average flow data from January 1, 1980, to May 31, 1997.

Figure 2-1.
Flow-Duration Curves on San Joaquin River Downstream from Mendota Dam

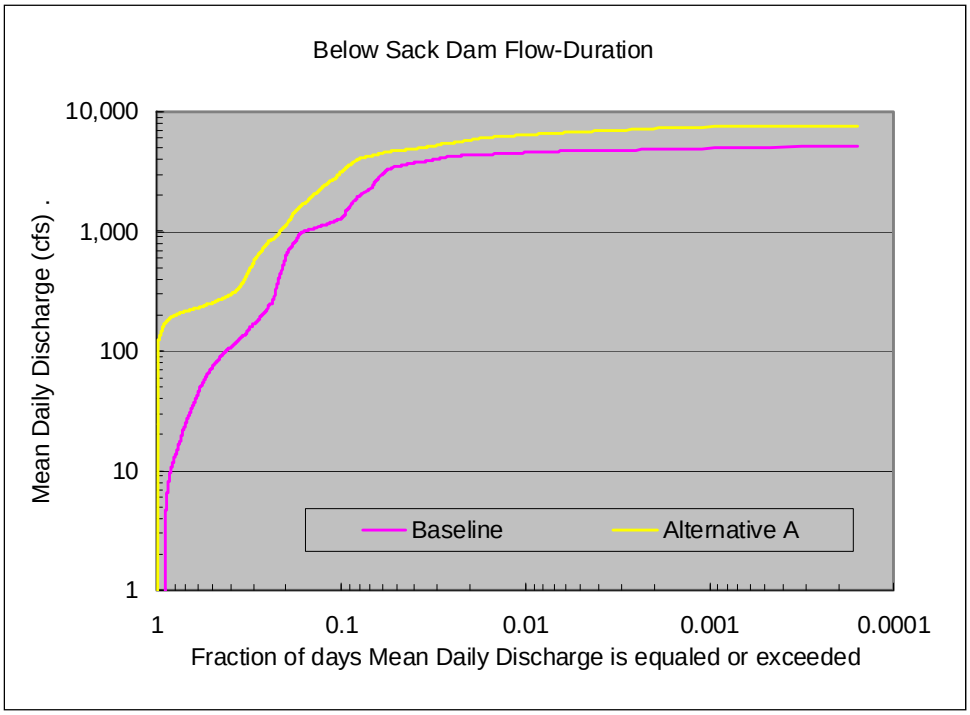

Note: The flow-duration curve is based upon daily average flow data from January 1, 1980, to May 31, 1997.

Figure 2-2.
Flow-Duration Curves on San Joaquin River Downstream from Sack Dam

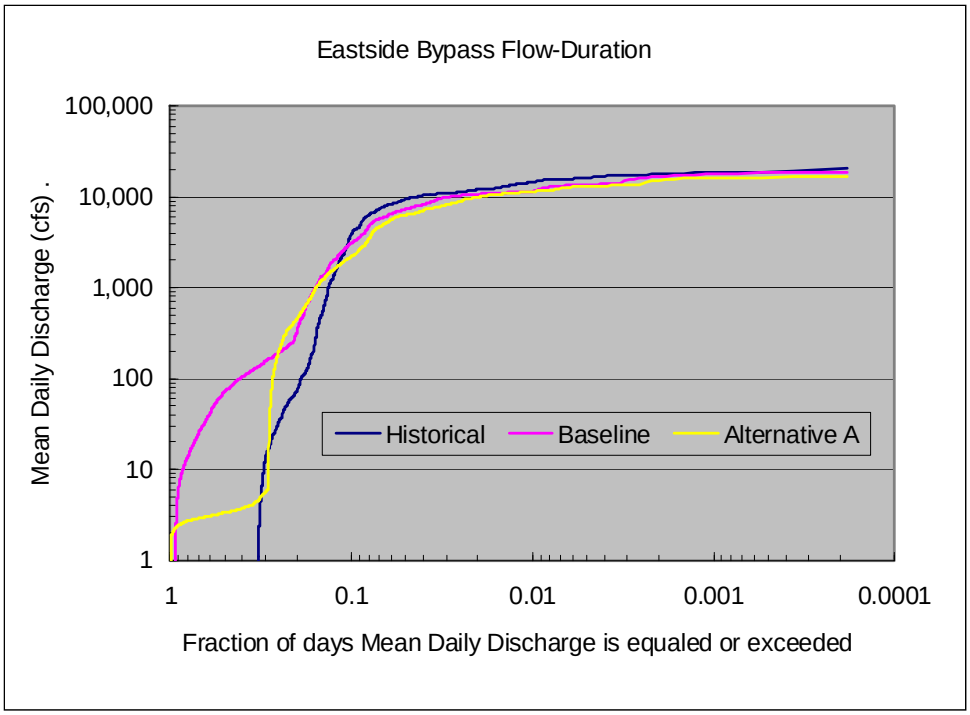

Note: The flow-duration curve is based upon daily average flow data from January 1, 1980, to May 31, 1997.

Figure 2-3.
Flow-Duration Curves on Eastside Bypass at El Nido

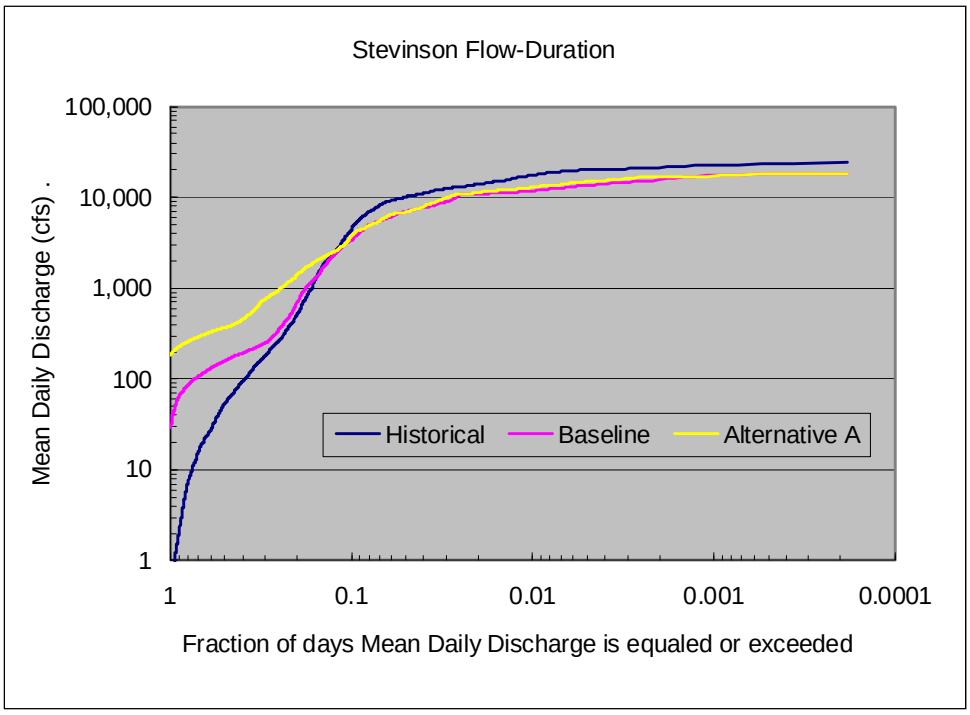

Note: The flow-duration curve is based upon daily average flow data from January 1, 1980, to May 31, 1997.

Figure 2-4.
Flow-Duration Curves on San Joaquin River at Stevinson Gage

2.1.2 Historical Hydrologic Conditions with Possible Flow Options in Reach 4B-1

The portion of Reach 4B upstream from Mariposa Bypass was referred to as Reach 4B-1 in this study. Although no project hydrology has been proposed for Reach 4B-1, two possible flow options through Reach 4B-1 were evaluated as part of this analysis. Under Historical Conditions, no flow was routed through Reach 4B-1. The first alternative evaluated was to convey a maximum of 475 cfs through Reach 4B-1, with all remaining flow routed through Sand Slough to the Eastside Bypass. The second alternative was to convey all flow up to a maximum of 4,500 cfs through Reach 4B-1 with all remaining flow routed to the Eastside Bypass. While these alternatives are not exclusive, they are used in this report to understand how potential flows through Reach 4B-1 could affect the geomorphology of other reaches. A different numerical model was set up that included Reaches 3, 4A-1, 4A-2, 4B-1, 4B-2, and 5, and the channel geomorphology in Reach 4B-1 was studied.

2.1.3 Baseline and Alternative A Hydrologic Scenarios

Numerical simulations were also performed with the Baseline and Alternative A hydrology conditions. For this report, Alternative A is also referred to as Project Conditions. There are potentially other hydrologic scenarios possible under Project Conditions, but Alternative A is considered to represent a most likely hydrologic representation of the flow conditions under the SJRRP.

There are considerable differences between the simulated Baseline Conditions and Historical Gage flows. In particular, the low flows under Baseline Conditions are significantly higher than the gage records indicate. For example, at El Nido gage on the Eastside Bypass, the simulated base flows are considerably higher than the Historical Gage records indicate. The probability of 100 cfs in the Eastside Bypass is more that 20 percent greater under Baseline Conditions than using Historical hydrology. However, data collection at the El Nido gage has been primarily focused upon high-flow events, and its accuracy in recording low-flow events is unknown.

2.2 Upstream Boundary Conditions

SRH-1D requires an incoming flow and sediment load at the upstream model boundary. Incoming flows to the model were based on the flow rate at gage stations downstream from the Mendota Dam (11254000). Since the Mendota Dam blocks most of the sediment contributed from upstream reaches, the model assumed that no sediment was conveyed through the upstream boundary. It was proposed to construct a new channel to divert the flow directly into the downstream of the Mendota Dam. The sediment loads upstream from the dam were calculated from the 1D model for Reaches 1 and 2 (Huang and Greimann 2009b) and were input upstream from the reach.

2.3 Lateral Flow Sources

To understand the hydraulics and sediment transport in the study reach, the San Joaquin River between Mendota Dam and the Merced River confluence was subdivided into 10 subreaches for the sediment transport analysis. At the Highway 152 Bridge (RP 173.9), Reach 4A was divided into two subreaches, Reaches 4A-1 and 4A-2. The portion of Reach 4B located upstream from the Mariposa Bypass was referenced as Reach 4B-1, while the downstream portion was referenced as Reach 4B-2. Reach 5 was divided into three subreaches to represent Reach 5 upstream from the Salt Slough confluence (Reach 5-1), from the Salt Slough confluence to the Mud Slough confluence (Reach 5-2), and from the Mud Slough confluence to the Merced River (Reach 5-3). The Sand Slough Bypass, the Eastside Bypass downstream from Sand Slough, and the Mariposa Bypass were each identified as a subreach. The spatial extent of each subreach is depicted in Figure 1-1, and the upstream and downstream limits are provided in Table 2-2.

Table 2-2.
Limits of Subreaches Used in the Sediment Capacity and Incipient Motion Analyses

	Project Reach	Sub-reach	Upstream Limit		Downstream Limit		Length (miles)
			Cross Section	River Post	Cross Section	River Post	
Mendota Dam to Sack Dam	3	1	XS764	204.68	XS477	182.00	22.4
Sack Dam to Highway 152 Bridge	4A-1	2	XS476	182.00	XS376	173.88	8.0
Highway 152 Bridge to Sand Slough Control Structure	4A-2	3	XS373	173.88	XS304	168.45	5.5
Sand Slough Bypass	Sand Slough Bypass	4	XS0.8ES	N/A	XS6ES	N/A	0.5
Eastside Bypass downstream from Sand Slough	Eastside Bypass	5	Start of Eastside Bypass	N/A	End of Eastside Bypass	N/A	8.9
Mariposa Bypass	Mariposa Bypass	6	Start of Mariposa Bypass	N/A	End of Mariposa Bypass	N/A	4.1
Mariposa Bypass to the confluence with Bear Creek and the Eastside Bypass	4B-2	7	XS36	147.25	XS235M	135.78	11.5
The confluence with Bear Creek and the Eastside to Salt Sough confluence	5-1	8	XS234M	135.78	XS147M	128.82	6.8
Salt Sough confluence to Mud Slough confluence	5-2	9	XS146M	128.82	XS47M	121.20	7.7
Mud Slough confluence to Merced River confluence	5-3	10	XS46M	121.20	XS1M	118.12	3.2

Key: N/A = not applicable

SRH-1D requires lateral flow sources to represent incoming flows from tributaries and flow diversions into irrigation canals. Flows in each subreach were estimated as follows:

- Mendota Dam to Sack Dam (Reach 3): The San Joaquin River near the Mendota gage (11254000) was used to represent flows in this subreach.

- Sack Dam to Sand Slough Control Structure (Reach 4A): When available, the San Joaquin River near Dos Palos gage (11256000) was used to represent the flows in this subreach. Flows during other periods were estimated using the assumption that all flow in the upstream river would be diverted into the Arroyo Canal up to the approximate canal capacity of 600 cfs. Flows exceeding 600 cfs were routed through this reach.

- Sand Slough Bypass: All flows from the San Joaquin River were distributed into this bypass. Flows through this reach are the same as flows in Reach 4A. Flows for future project conditions in the Sand Slough Bypass were calculated by flow continuity between incoming flows from the upper reach of the Eastside Bypass and Reach 4A and outgoing flows to the lower reach of the Eastside Bypass and Reach 4B. When flows in Reach 4A are less than 475 cfs, the Sand Slough may route flows from the Eastside Bypass to Reach 4B-1.

- Eastside Bypass from Sand Slough to Mariposa Bypass: Flow in this bypass was based on records from the Eastside Bypass near El Nido gage (ELN).

- Mariposa Bypass: Up to 8,500 cfs from Eastside Bypass were returned to the San Joaquin via Mariposa Bypass.

- San Joaquin River from Mariposa Bypass to Bear Creek (Reach 4B-2): Flows in this subreach were estimated by subtracting flows near the mouth of Bear Creek (recorded by the gage at Bear Creek below Eastside Canal (BBE)) from the recorded flows at the San Joaquin River near Stevinson gage (SJS).

- Bear Creek to Salt Slough (Reach 5-1): The San Joaquin River near Stevinson gage (SJS) was used to represent the flows in this subreach.

- Salt Slough to Mud Slough (Reach 5-2): When available, the San Joaquin River at Fremont Ford Bridge (11261500) was used to represent the flows in this subreach. Flows during some periods were estimated as the combination of the flows in Salt Slough, recorded at Salt Slough at HW165 near Stevinson (11261100), and flows at the San Joaquin River near Stevinson gage (SJS). When both data sets were not available, flows in this subreach were interpolated from the San Joaquin River near Stevinson gage (SJS) and the ratio of the cumulative flow volumes experienced for Reaches 5-1 and 5-2 across a common time period.

- Mud Slough to Merced River confluence (Reach 5-3): Flows in this subreach for Water Years 1986 through 1995 were estimated by subtracting the recorded flows at the Merced River near the Stevinson gage (11272500) from the recorded flows at the San Joaquin River near Newman (11274000). The ratio of accumulated

water volumes in these two gages for Water Years 1986 through 1995 and the recorded flows at the San Joaquin River near Newman were used to estimate the flows during other periods.

Flow differences were calculated between each subreach. In the study area, flow differences were mainly caused by flow diversions or tributary inflows, thus lateral point flows were used to simulate flow differences between each subreach.

2.4 Lateral Sediment Sources

2.4.1 Eastside Bypass

Under current conditions, flows from the Eastside Bypass upstream from the Sand Slough Bypass merge with flows from the Sand Slough Bypass just upstream from the Eastside Bypass near El Nido gage (ELN). Flow from the Eastside Bypass was input as a lateral point source by subtracting flow in the Sand Slough Bypass from the El Nido gage flow records.

The lateral sediment source from the Eastside Bypass was estimated based on the transport capacity of the bypass, as no sediment load measurement data were available for calibration. The transport capacity was calculated using the average hydraulic properties of the bypass and sediment samples collected in the bypass, as described below.

A separate HEC-RAS model was developed for this study for the Chowchilla Bypass and upstream reach from Eastside Bypass. A HEC-RAS geometry file was provided to Reclamation by MEI (2002). MEI first developed a HEC-2 hydraulic model, which was later transferred into a HEC-RAS model. Multiple flow profiles were modeled over a wide range of possible hydrologic conditions from 10 cfs to 70,000 cfs. The downstream boundary condition was determined by assuming normal depth at a slope of 0.000395. HEC-RAS hydraulic results, including main channel discharge, main channel velocity, main channel top width, hydraulic radius, and friction slope are shown in Table 2-3. Reach-averaged channel slopes were calculated from the difference in thalweg elevation between the upstream cross section and downstream cross section divided by the channel length.

Table 2-3.
Averaged Hydraulic Data in the Eastside Bypass Upstream from the Confluence of the Sand Slough Bypass

Q Total (cfs)	Main Channel Discharge (cfs)	Main Channel Velocity (ft/s)	Top Width (feet)	Hydraulic Radius (feet)	Friction Slope (ft/ft)	Slope (ft/ft)
10	**10**	**0.41**	**95**	**1.1**	**0.00020**	**0.000383**
20	20	0.51	104	1.2	0.00021	0.000383
30	30	0.58	108	1.3	0.00022	0.000383
40	40	0.63	112	1.4	0.00022	0.000383
50	50	0.67	115	1.5	0.00023	0.000383
60	60	0.69	120	1.6	0.00023	0.000383
70	70	0.72	124	1.6	0.00023	0.000383
80	80	0.74	127	1.7	0.00024	0.000383
90	90	0.75	129	1.7	0.00024	0.000383
100	100	0.77	131	1.8	0.00024	0.000383
200	200	0.91	145	2.2	0.00024	0.000383
300	300	1.05	155	2.5	0.00026	0.000383
400	400	1.16	163	2.8	0.00028	0.000383
500	500	1.27	168	3.0	0.00029	0.000383
600	600	1.34	173	3.2	0.00030	0.000383
700	700	1.42	176	3.3	0.00031	0.000383
800	800	1.50	178	3.5	0.00032	0.000383
900	900	1.57	181	3.7	0.00032	0.000383
1000	1,000	1.62	183	3.8	0.00033	0.000383
1,100	1,099	1.68	185	4.0	0.00033	0.000383
1,200	1,198	1.72	189	4.1	0.00033	0.000383
1,300	1,297	1.78	190	4.2	0.00033	0.000383
1,400	1,395	1.83	192	4.3	0.00034	0.000383
1,500	1,494	1.88	194	4.4	0.00034	0.000383
1,600	1,592	1.92	195	4.6	0.00034	0.000383
1,700	1,689	1.97	196	4.7	0.00034	0.000383
1,800	1,787	2.02	198	4.8	0.00034	0.000383
1,900	1,884	2.06	199	4.9	0.00035	0.000383
2,000	1,982	2.10	201	5.0	0.00035	0.000383
2,500	2,462	2.29	208	5.4	0.00036	0.000383
3,000	2,934	2.46	213	5.8	0.00037	0.000383
3,500	3,400	2.61	217	6.2	0.00038	0.000383
4,000	3,861	2.75	221	6.6	0.00038	0.000383
4,500	4,316	2.88	224	6.9	0.00039	0.000383
5,000	4,767	3.00	227	7.2	0.00039	0.000383
5,500	5,212	3.10	233	7.5	0.00040	0.000383
6,000	5,649	3.21	235	7.7	0.00040	0.000383
7,000	6,492	3.40	238	8.2	0.00041	0.000383
8,000	7,298	3.57	241	8.7	0.00042	0.000383
9,000	8,071	3.72	244	9.1	0.00043	0.000383
10,000	8,818	3.86	246	9.5	0.00044	0.000383

Table 2-3.
Averaged Hydraulic Data in the Eastside Bypass Upstream from the Confluence of the Sand Slough Bypass (contd.)

Total Discharge (cfs)	Main Channel Discharge (cfs)	Main Channel Velocity (ft/s)	Top Width (feet)	Hydraulic Radius (feet)	Friction Slope (ft/ft)	Slope (ft/ft)
15,000	12,040	4.39	248	11.3	0.00045	0.000383
20,000	14,802	4.78	248	12.7	0.00045	0.000383
25,000	17,310	5.06	248	14.0	0.00046	0.000383
30,000	19,824	5.35	248	15.2	0.00046	0.000383
35,000	22,191	5.60	248	16.2	0.00046	0.000383
40,000	24,515	5.84	248	17.1	0.00047	0.000383
45,000	26,801	6.06	248	18.0	0.00047	0.000383
50,000	29,033	6.26	248	18.8	0.00047	0.000383
55,000	31,190	6.42	248	19.7	0.00046	0.000383
60,000	33,353	6.59	248	20.5	0.00047	0.000383
65,000	35,476	6.75	248	21.2	0.00047	0.000383
70,000	37,543	6.86	248	22.1	0.00047	0.000383

Key:
cfs = cubic feet per second
ft/ft = feet rise per feet run
ft/s = feet per second

Surface bed material data were used to estimate the sediment load in the Eastside Bypass. Sediment samples collected in February 2008 (Reclamation 2008) provided five sample sites, 1-10, 1-7, 1-8, 1-9, and 2-20, located in the Eastside Bypass upstream from the Sand Slough Bypass confluence. The sediment size fractions at the five sample sites were averaged to get a representative sediment size fraction in the reach, as shown in Table 2-4.

Table 2-4.
Sampled Cumulative Bed Sediment Fraction Finer than Used in the Upstream Reach of the Eastside Bypass

Site ID	1-10	1-7	1-8	1-9	2-20	Average
0.063mm	3%	2%	1%	3%	2%	2%
0.125mm	4%	3%	2%	4%	2%	3%
0.25mm	9%	7%	5%	9%	12%	7%
0.5mm	35%	23%	30%	53%	58%	35%
1mm	58%	65%	64%	93%	87%	70%
2mm	81%	91%	92%	99%	98%	91%
4mm	98%	98%	100%	100%	100%	99%
8mm	100%	100%	100%	100%	100%	100%
16mm	100%	100%	100%	100%	100%	100%

Key:
% = percent
ID = Irrigation District
mm = millimeter

Averaged channel hydraulic data and averaged bed material data were used to estimate the sediment rating curve and sediment size fractions in the Eastside Bypass upstream from the Sand Slough Bypass confluence. Given the bed material size and averaged channel hydraulic data, SRH-Capacity, a program developed by Reclamation, was used to calculate the sediment transport capacity. Engelund and Hansen's (1972) formula was applied and the results are shown in Figure 2-5 (Exhibit B). The bed material of the Eastside Bypass upstream from the Sand Slough Bypass was composed mainly of sand; thus sediment size fractions experienced almost no change with increasing flow. This sediment transport capacity rating curve was used as a sediment point source at the confluence with the Eastside Bypass and Sand Slough Bypass.

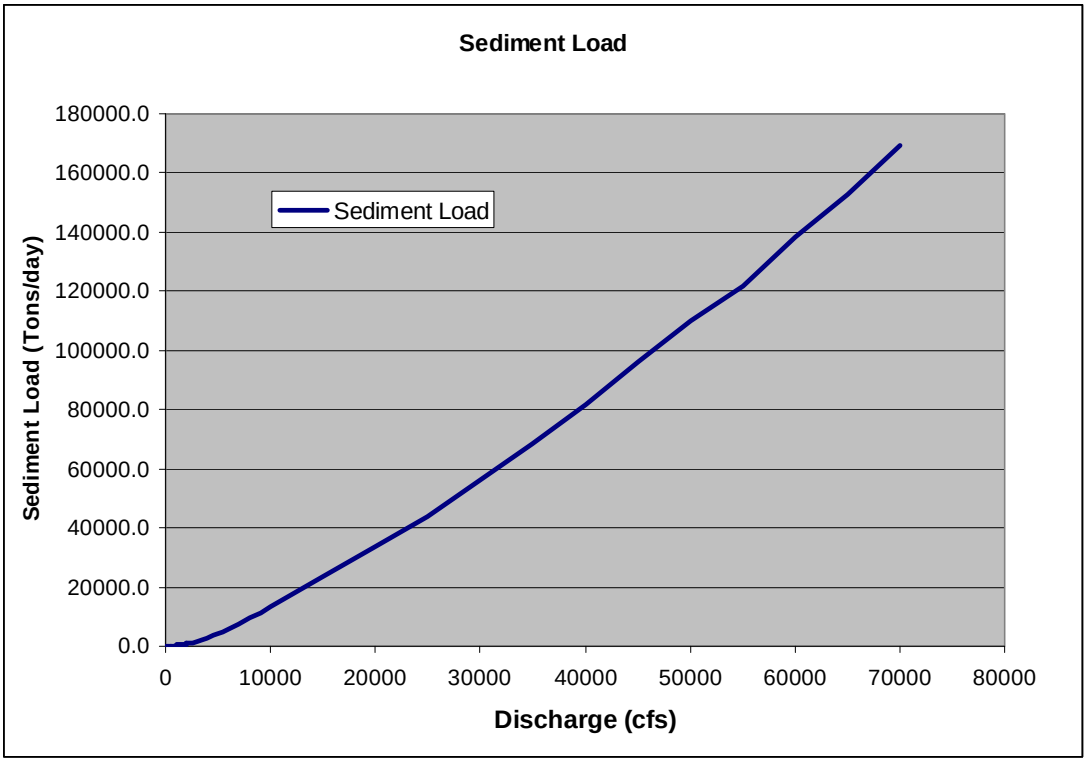

Figure 2-5.
Sediment Load Rating Curve Used as Lateral Input at Eastside Bypass

2.4.2 Lateral Sediment at Other Subreaches

No sediment data were available to account for the sediment distributed into canals or sediment incoming from tributaries in the other subreaches. Instead, the current study assumed that the flow distributed into irrigation channels and flow incoming from tributaries carried the same sediment concentrations and same size fractions as the flows at the corresponding locations in the channel. Future studies and sediment load monitoring may provide additional information to modify this assumption.

2.5 Cross-Section Geometry

HEC-RAS geometry data were provided by MEI (2002) to Reclamation for all cross sections from Friant Dam to the Merced River confluence, including all bypasses. MEI first developed a HEC-2 hydraulic model, which was later transferred into a HEC-RAS model. This study covers Reaches 3 and 4A, the Sand Slough Bypass, a portion of the Eastside Bypass, Mariposa Bypass, part of Reach 4B, and Reach 5. MEI developed 973 cross sections for the 79-mile reach from Mendota Dam to the Merced River confluence for previous investigations. The HEC-RAS geometry data were derived from 1998 topographic and bathymetric surveys conducted by Ayres Associates, Inc. for Reclamation and the U.S. Army Corps of Engineers (Ayres 1998, 1999). Intergraph Site Works, Version 7.01, in conjunction with Bentley Systems MicroStation, Version 7.00, was used to digitize cross-section geometry from the topographic data provided in digital terrain model (DTM) format.

One-dimensional modeling requires properly representing the general characteristics of the river, paying particular attention to locations where geometric properties (e.g., width, slope) change. To reduce the model run time for SRH-1D mobile bed model without substantially impacting reach-averaged results, the total number of cross sections was reduced. The entire study reach was represented with 163 cross sections out of the 973 total available HEC-RAS cross sections. One cross section was chosen from every six HEC-RAS cross sections for an average spacing of 2,511 feet and a maximum spacing of 5,445 feet. The original HEC-RAS geometry had no cross-section indices to represent the Eastside and Mariposa bypasses. These were added starting at the downstream end of each bypass as ES01 and MP01, respectively. Cross-sections MP12, MP14, MP46, and MP49 were also used for internal boundary conditions due to effects of structures on channel hydraulics.

SRH-1D does not implement the depth-varied Manning's coefficients modeled in the MEI HEC-RAS model (MEI 2002). In specific locations where the depth-varied Manning's roughness coefficient (n) was applied by MEI, a simplified Manning's coefficient was developed for SRH-1D by averaging the depth-varied Manning's coefficients from the HEC-RAS model. Based on previous hydraulic calculations of MEI (2002), the calibrated Manning's n was set at 0.045 for most of the main channel and 0.1 for most of the floodplain with vegetation. The SRH-1D model used the same values for Manning's n.

Within the current assessment, the 1998 geometry and 2008 sediment sizes were used to compare what would happen if Historical, Baseline, or Alternative conditions are experienced. Current geometry may be different from the 1998 geometry, but no newer topographic data were available for comparison at the time of this analysis. The available geometry were sufficient to evaluate how the sediment transport characteristics and channel morphology may differ if the river experiences the same hydrology as between 1981 and 1997, compared with proposed future hydrology.

2.6 In-Channel Structures

Bridges and culvert crossings are represented by stage-discharge rating curve tables in the SRH-1D model. The original bridges and culvert crossings data in HEC-RAS geometry file were obtained from the California Department of Transportation (Caltrans), the Southern Pacific Railroad, and the Atchison Topeka Santa Fe Railroad. These data, however, were not used directly in SRH-1D model. HEC-RAS hydraulic analysis was first performed. Differences in the water surface elevations upstream and downstream from the structures were computed from the HEC-RAS model. Only structures affecting water surface elevations by 1 foot or more were considered in SRH-1D model. Two grade-control structures in the Mariposa Bypass met these requirements and were represented by a rating curve table in SRH-1D model (Exhibit A). All the other structures were identified as not significant and were not modeled in the SRH-1D model.

2.7 Downstream Boundary Conditions

Downstream boundary conditions used in the SRH-1D model were calculated from HEC-RAS results in the reach along the San Joaquin River from the confluence with Bear Creek and the Eastside Bypass (RP 135.8) to Stockton (RP 41). The downstream channel slope at Stockton was set as 0.0001 foot rise per foot run. The water surface elevations calculated at Cross-Section XS1M near the Merced River confluence with the San Joaquin River was set as the downstream boundary and was input to the SRH-1D model as a rating curve table (Table 2-5).

2.8 Surface Bed Material

Surface bed material data used in the sediment transport analysis were derived from 12 surface samples collected between Mendota Dam and the Merced River confluence and one surface sample upstream from this reach. The bed material samples were collected in February 2008 (Reclamation 2008). The fraction in each size class is provided in Table 2-6. The sediment gradation of the channel at the upstream boundary of the model was interpolated from Sample 2-10 at XSA91 in Reach 2 and Sample 1-11 at XS372 in Reach 3. For cross sections where no bed material samples were available, SRH-1D automatically interpolates the surface bed material.

Table 2-5.
Rating Curving Table at the Downstream Boundary of the SRH-1D Model

Discharge (cfs)	Downstream water surface elevation at XS1M (feet)	Discharge (cfs)	Downstream water surface elevation at XS1M (feet)
10	46.14	1400	52.50
20	46.35	1500	52.80
30	46.51	1600	52.98
40	46.66	1700	53.18
50	46.80	1800	53.35
60	46.92	1900	53.53
70	47.04	2000	53.70
80	47.15	2500	54.61
90	47.25	3000	55.39
100	47.34	3500	56.27
200	48.02	4000	57.09
300	48.59	4500	57.81
400	49.07	5000	58.34
500	49.48	5500	58.80
600	49.88	6000	59.10
700	50.28	7000	59.76
800	50.63	8000	60.34
900	50.99	9000	60.90
1000	51.42	10000	61.17
1100	51.69	15000	62.26
1200	51.99	20000	63.41
1300	52.25	25000	64.35

Key:
cfs = cubic feet per second

Table 2-6.
Sampled Bed Sediment Fraction Finer Than and Representative Bed Material Size Gradations Used in the Sediment Transport Study

Site ID	XS ID	RM	Location	0.063 mm	0.125 mm	0.25 mm	0.5 mm	1 mm	2 mm	4 mm	8 mm
2-10	XSA97	216.2	Reach 2A	0.0259	0.0205	0.0709	0.2681	0.3835	0.1805	0.0396	0.0081
1-11	XS372	173.8	HY152 D/S	0.0243	0.0122	0.0557	0.2990	0.3781	0.1979	0.0328	0.0000
1-12	XS357	172.7	Menefee	0.0686	0.0154	0.1183	0.3826	0.2945	0.0809	0.0287	0.0111
1-13	XS331	170.6	Menefee	0.0395	0.0123	0.0187	0.2096	0.4823	0.2091	0.0266	0.0019
1-14	XS314	169.2	Menefee	0.0432	0.0375	0.1435	0.2870	0.3130	0.1585	0.0161	0.0012
2-19	Eastside Bypass		EB	0.0350	0.0562	0.6671	0.2182	0.0184	0.0041	0.0009	0.0000
2-12	Mariposa Bypass		Mariposa	0.7156	0.1693	0.0615	0.0300	0.0174	0.0037	0.0026	0.0000
2-13	Mariposa Bypass		Mariposa	0.4070	0.0624	0.1057	0.3188	0.0945	0.0085	0.0031	0.0000
3-25	XS305M	141.3	Reach 4B	0.1520	0.0355	0.0788	0.1863	0.3467	0.1750	0.0257	0.0000
3-24	XS305M	141.3	Reach 4B	0.0256	0.0149	0.1041	0.3207	0.3390	0.1292	0.0405	0.026
3-23	XS275M	139.0	Reach 4B	0.0288	0.0335	0.1500	0.2776	0.3335	0.1427	0.0340	0.0000
3-22	XS213M	134.2	Reach 5	0.3764	0.1259	0.2998	0.1454	0.0461	0.0058	0.0006	0.0000
1-15	XS1M	118.1	Newman Gage	0.0508	0.0677	0.2375	0.5154	0.1251	0.0021	0.0000	0.0014

Key:
ID = Irrigation District
mm = millimeter
RM = River Mile
xs = cross section

2.9 Computational Parameters

In SRH-1D, multiple sediment transport formulas are available for selection. The transport capacity was calculated with five different transport formulas: Engelund and Hansen's (1972) formula, modified Laursen's method (Madden 1993), Brownlie's method (1981), Yang's sand transport formula (1973), and Wu et al.'s (2000) non-uniform sediment transport method.

A final required input parameter is the active layer thickness. The active layer concept was used to simulate channel armoring. In SRH-1D, the active layer thickness is equal to a constant times the diameter of the largest sediment size. The constant was set equal to 10 based on previous experience. A sensitivity analysis of the active layer thickness value was performed (Exhibit D).

2.10 Summary of Model Inputs

SRH-1D was applied to simulate sediment transport and evaluation of changes in channel morphology of the San Joaquin River between Mendota Dam and the Merced River confluence. The analyses were based on historical flows between 1981 and 1997. Model input included flow rates, sediment loads, channel roughness, initial channel geometry, and initial bed material. In addition, several computational parameters were required, such as the active layer thickness and sediment transport formula.

HEC-RAS geometry provided by MEI (2002) was transferred into a useable format for SRH-1D. To limit the computational time, one of every six cross sections was selected for sediment modeling.

The SRH-1D model requires flows and sediment loads at the upstream model boundary and for all lateral sources. Incoming flows to the model were based on the flow rate at gage station downstream from the Mendota Dam. However, Mendota Dam was assumed to block all sediment contributions from upstream reaches. Non-uniform flow along the river was simulated with lateral sources in SRH-1D. Flow rates at the beginning of each subreach were determined from the nearest gages and based upon assumptions related to the system hydraulics. Flow differences between each subreach were due to irrigation diversions and tributary inputs and were therefore modeled as lateral flow sources. Incoming sediment from the Eastside Bypass upstream from the Sand Slough was simulated through a rating curve table, obtained from a separate sediment capacity model. Sediment contributed from other tributaries and sediment diverted into irrigation channels was assumed to have the same concentration as the flow in the main river.

A rating curve table was used in the SRH-1D model to simulate internal boundary conditions such as bridges and culverts. Although the MEI HEC-RAS model (MEI 2002) used 10 bridges and culverts as internal boundary conditions in the study reach, only two grade-control structures in the Mariposa Bypass significantly influenced the hydraulics (i.e., resulted in a difference in water surface elevation of greater that 1 foot across the structure). Each of these grade-control structures was modeled as an internal boundary

condition through a rating curve table in SRH-1D. All the other structures were identified as hydraulically insignificant for the purposes of this model and were not incorporated into the SRH-1D model.

Calculated water surface profiles of the HEC-RAS model were compared with the SRH-1D results. Results are displayed in Exhibit C for six profiles. Similar results were obtained for the two models. For uniform discharge of 100 cfs, the average difference between SRH-1D and HEC-RAS calculated water surface elevations was 0.53 foot with a maximum value of 2.3 feet. For Friant Dam releases of 1,000 cfs and 5,000 cfs, the average differences were 0.32 foot and 0.48 foot, respectively, and the maximum differences were 1.22 feet and 2.24 feet, respectively. Differences between the water surface elevations of HEC-RAS and SHR-1D may result from fewer cross sections, fewer or simplified representation of hydraulic structures by a rating curve and simplified Manning's coefficient representation in SRH-1D, compared with depth-varied Manning's coefficients in HEC-RAS.

Sediment samples collected during February 2008 were used to determine the bed material size fractions. Nine size fractions, ranging from silt to median gravel, represented the material present in the study area. Thirteen samples were used. For cross sections where no bed material samples were available, SRH-1D automatically interpolates the surface bed material.

This page left blank intentionally.

3.0 Results of Numerical Model with Eastside and Mariposa Bypass Geometry

To evaluate the flow and sediment division between the Eastside Bypass and Reach 4B-1, two separate models were developed. The first model routes flow from Mendota Dam to the confluence of the Merced River and includes Reaches 3 and 4A; Sand Slough, Eastside, and Mariposa bypasses; and Reaches 4B-2 and Reach 5. The second model, described in Section 4, also conveys flow through the same reach, but was used to examine potential changes to the sediment transport if flow is returned to Reach 4B-1 from the Sand Slough to the confluence with the Mariposa Bypass. The second model was only evaluated using Historical hydrology with modified flow into Reach 4B-1. Additional modeling of the flow into Reach 4B-1 could be used to refine the results presented here.

3.1 Historical Hydrology

Figure 3-1 shows the bed profiles that were simulated using Historical hydrology (no flow in Reach 4B-1) with Engelund and Hansen's (1972) sand transport equation. The model also predicted the sediment transport under scenarios using the Historical Gage data but assuming that a maximum of 475 cfs and 4,500 cfs are routed through Reach 4B-1 with remaining flows routed to the Eastside Bypass.

Reach 3 experienced an average depth of 0.84 foot erosion, and Reach 4A was considered stable. Varying the flows entering downstream from Reach 4B-1 did not affect the erosion or deposition of either Reach 3 or 4A.

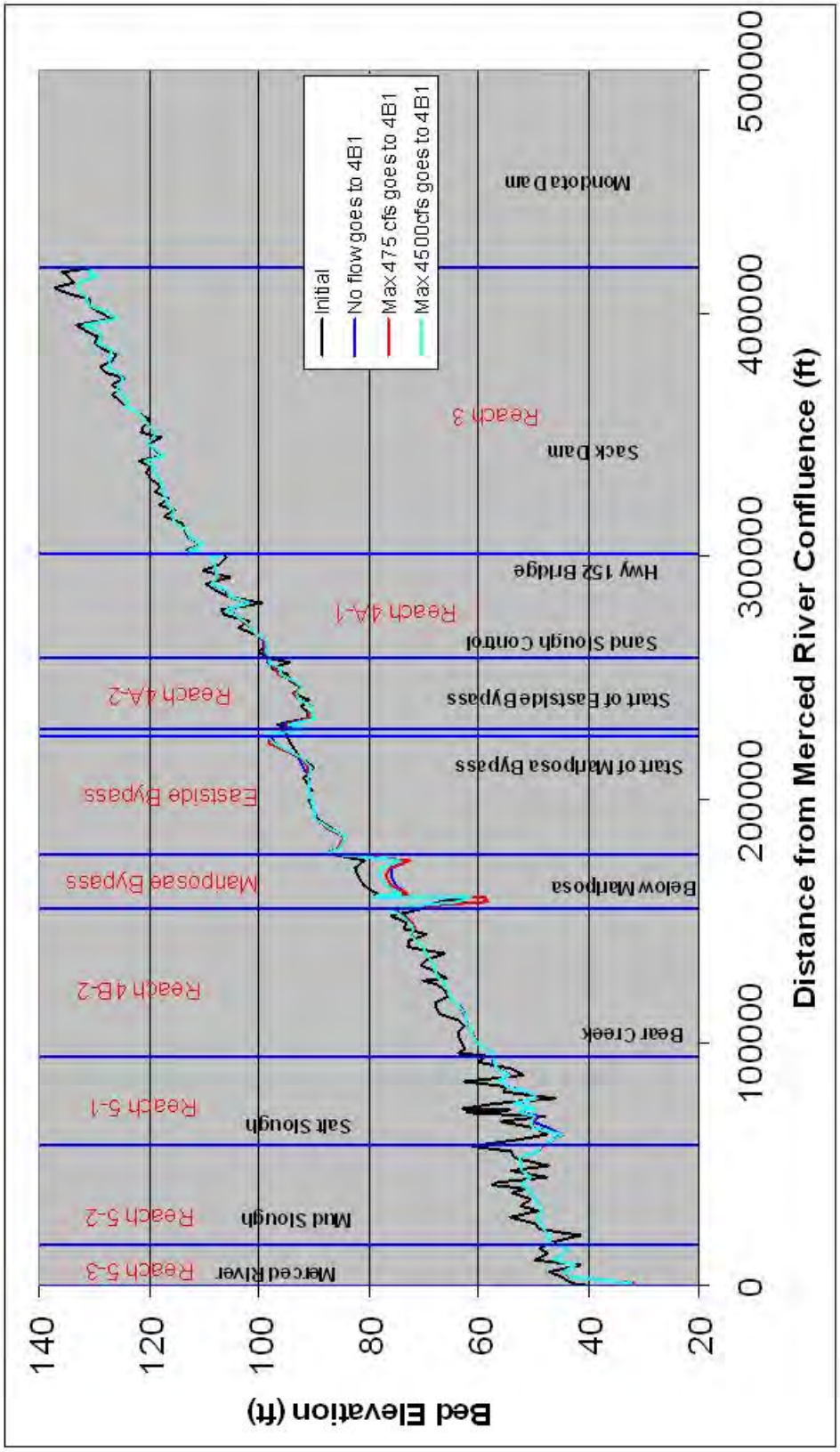

Figure 3-1.
Bed Profiles Simulated with Historical Hydrology

The Eastside Bypass experienced minor deposition (0.5 foot) using Historical hydrology and when only a maximum of 475 cfs was allowed into Reach 4B-1. When a maximum of 4,500 cfs was routed through Reach 4B-1, the average depth of deposition in the Eastside Bypass decreased to 0.3 foot. Predicted depths of deposition in the Eastside Bypass are dependent on sediment load from the upstream portion of the Eastside Bypass. Because this incoming sediment load was unknown, the accuracies of the predicted depths of deposition in the upstream portion of the Eastside Bypass are somewhat uncertain.

Results of the model suggest that the Mariposa Bypass experienced substantial erosion based on the Historical hydrology and current bed material. However, no stream gage information exists in the Mariposa Bypass and the simplified routing assumptions probably overestimate the amount of flow entering the Mariposa Bypass. Therefore, the erosion is likely over predicted for the Historical hydrology scenario. However, erosion through this reach was evidenced during a field trip to the site in July 2008, as illustrated in Figure 3-2. Two grade-control structures were installed in the Mariposa Bypass, likely to limit the channel erosion. This figure shows the grade-control structure at the downstream end of the bypass. The numerical model results indicate the degradation is anticipated even with the control imposed by the two structures. The model, however, does not consider resistance to erosion due to cohesion of the fine silt and clay and by vegetation. Field sediment samples in two sites of the Mariposa Bypass showed that the bypass contains 40 percent to 71 percent of silt and clay, which should increase resistance to erosion resulting from cohesive forces between sediment particles. For improved predictions of erosion in this reach, laboratory or field testing would be necessary to determine the critical shear stresses and erosion rates for surface erosion and potential mass erosion. Due to the limitation of the model to adequately account for these characteristics of erosion resistance, a coarser bed material gradation was assumed to be present in Mariposa Bypass. The sediment gradation of the Eastside Bypass (Site 2-19) was used to represent the material in the Mariposa Bypass. Under this condition, the Mariposa Bypass experienced an average of 3.6 feet erosion. When a maximum of 475 cfs were conveyed through Reach 4B-1 and remaining flow was routed through the Eastside Bypass, the average depth of erosion decreased to 3.4 feet (5 percent less). When a maximum of 4,500 cfs were allowed into Reach 4B-1 and remaining flow was routed through the Eastside Bypass, the average depth of erosion decreased to 2.2 feet (38 percent less).

Note: The photo was taken looking downstream on the left bank. The left bank of the channel shows evidence of erosion. The lower right corner of the photo shows part of the grade-control structure.

Figure 3-2.
Photo Taken in July 2008 near Downstream Grade-Control Structure in the Mariposa Bypass

Reach 4B-2 downstream from the Mariposa Bypass and Reach 5 experienced erosion under conditions of Historical hydrology and modified hydrology through Reach 4B-1. The flow and sediment loads were similar in these two project reaches under all three conditions. Reach 4B-2, which is downstream from the Mariposa Bypass, experienced an average of 1.4 feet of erosion. Reach 5-1, from the confluence with Bear Creek and the Eastside Bypass (RP 135.8) to the Salt Sough confluence, experienced an average depth of erosion of 3.1 feet. Reach 5-2, from the Salt Sough confluence to the Mud Slough confluence, experienced an average of 1.7 feet of erosion. And Project 5-3, from Mud Slough confluence to Merced River confluence, experienced an average depth of erosion of 4.1 feet. Computed erosion in Reach 5 was based on the assumption that flow incomings from Bear Creek, Salt Sough, and Mud Slough were of the same concentration as the San Joaquin River. Suspended sediment sampling in these tributaries across a wide range of flows could improve the prediction.

Figure 3-3 shows the simulated mean bed material size under all three hydrologic scenarios. The bed material tends to become coarser than current conditions throughout most of the study reach. The numerical model assumed no incoming sediment from reaches upstream from Mendota Dam due to a lack of sediment monitoring information. Measured sediment concentrations of flows from Mendota Dam would likely indicate that the flows do transport suspended sediments. If these loads were considered in the model, the predicted bed material sizes would likely be finer than those presented. The Eastside Bypass experienced sediment deposition with some coarse sediment contributions from Reach 4A and from the upstream portion of the Eastside Bypass. When more flow is routed into the Reach 4B-1, the sediment coarsening of the Eastside Bypass is less pronounced.

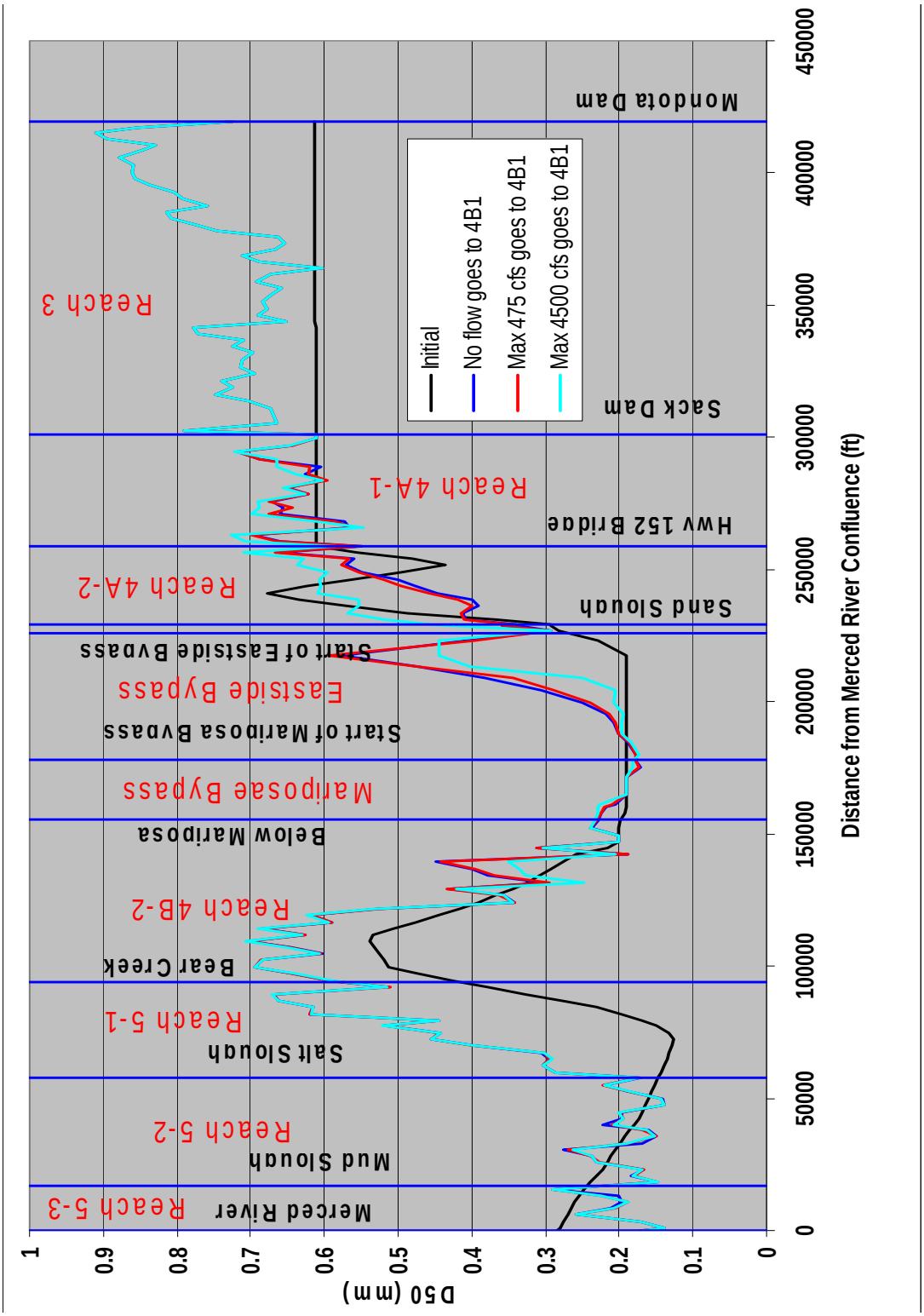

Figure 3-3.
Mean Sediment Size for Three Hydrologic Scenarios

Figures 3-4 and 3-5 show sand and gravel erosion and deposition at each cross section. Since the current SRH-1D model used one cross section to represent every six cross sections in the HEC-RAS geometry, the sediment erosion and deposition in each cross section represents what is expected to occur on average for every six cross sections in the HEC-RAS geometry. In Reaches 3 and 4A, erosion tends to occur in riffles and deposition in the pools. Net erosion was noted in Reach 3, and net deposition was noted in Reach 4A. The Eastside Bypass experienced both sand and gravel depositions. When 4,500 cfs was diverted into Reach 4B-1, a marked reduction in deposition was predicted, most notably at the upstream end of the bypass. The Mariposa Bypass experienced erosion of sand material. As more flow was diverted into Reach 4B-1, less erosion was predicted in the Mariposa Bypass. In Reaches 4B-2 and 5, erosion was primarily noted in riffles and deposition was present in pools. Overall, net erosion resulted in these two reaches. A summary of the modeled erosion and depositional patterns in each reach is presented in Table 3-1.

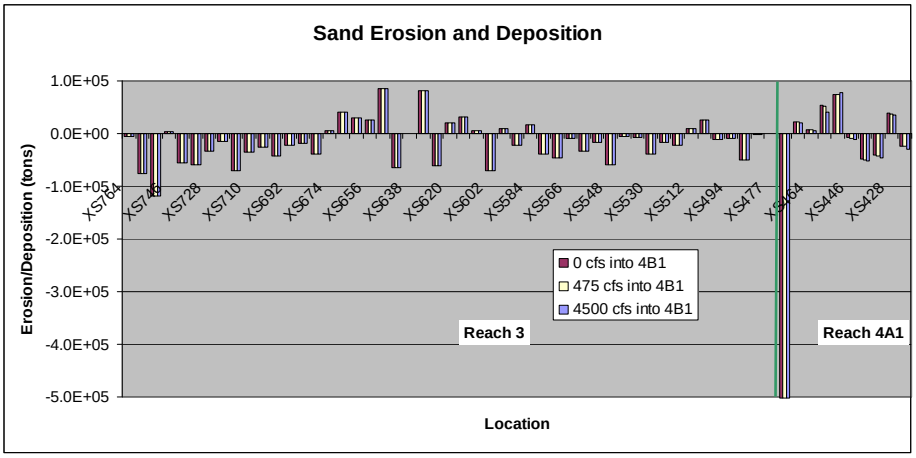

Note: Cross sections are presented from upstream (left) to downstream (right)

Figure 3-4 (a).

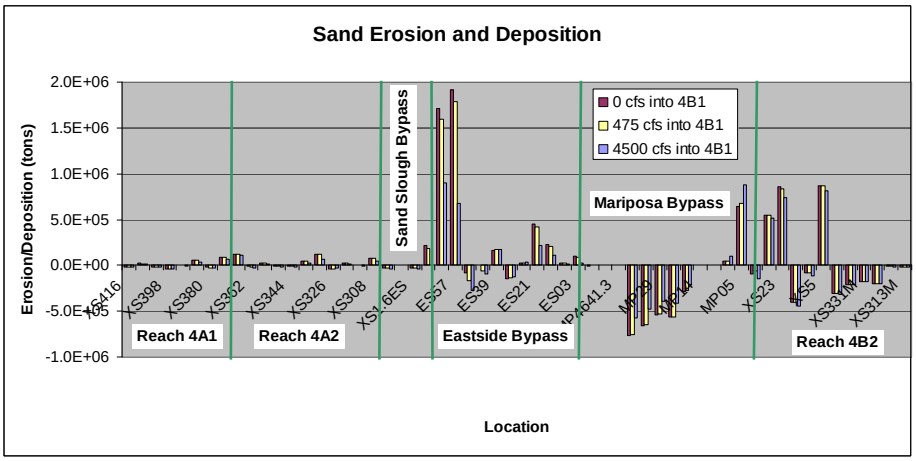

Note: Cross sections are presented from upstream (left) to downstream (right)

Figure 3-4 (b).

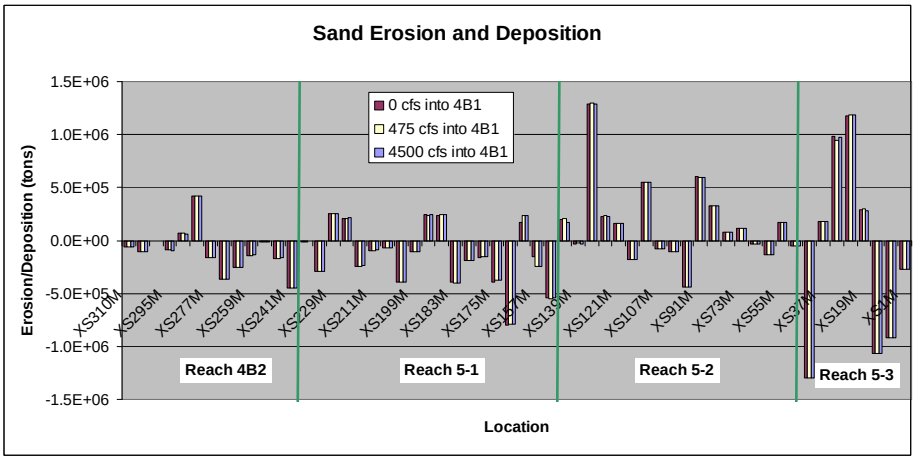

Note: Cross sections are presented from upstream (left) to downstream (right)

Figure 3-4 (c).
Sand Erosion and Deposition

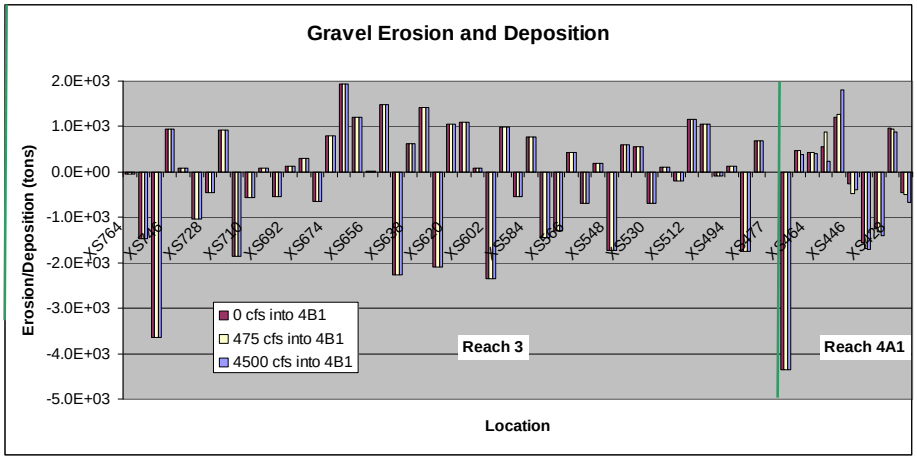

Note: Cross sections are presented from upstream (left) to downstream (right)

Figure 3-5 (a).

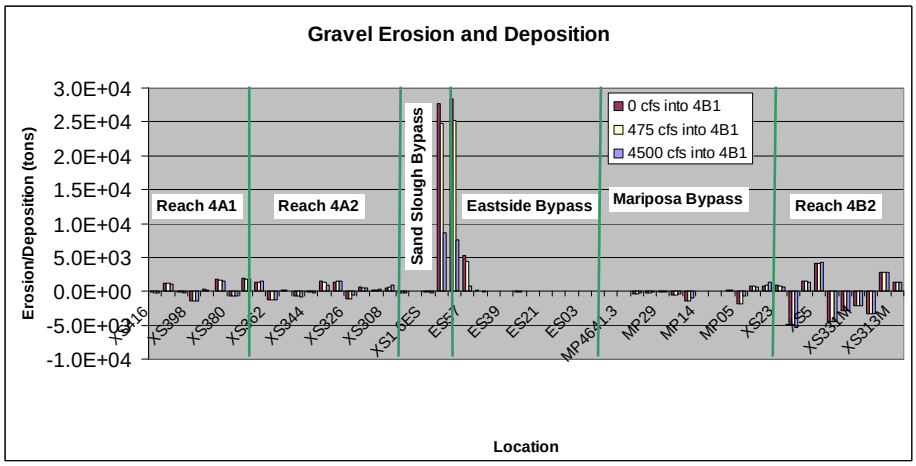

Note: Cross sections are presented from upstream (left) to downstream (right)

Figure 3-5 (b).

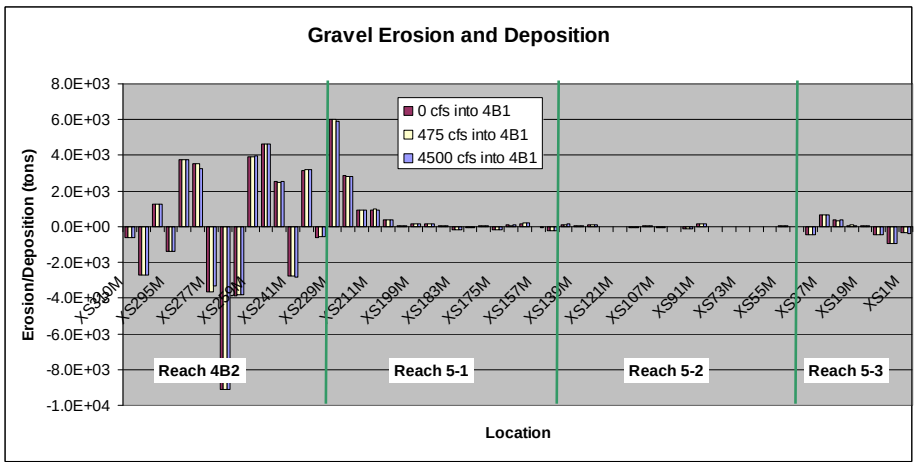

Note: Cross sections are presented from upstream (left) to downstream (right)

Figure 3-5 (c).
Gravel Erosion and Deposition

Table 3-1.
Summary of Results from Multiple Historical Hydrology Runs

Hydrology	Current Hydrology (0 cfs in Reach 4B-1)	Maximum 475 cfs into Reach 4B-1	Maximum 4,500 cfs into Reach 4B-1
Reach 3	Erosion 0.84 ft	Erosion 0.84 ft	Erosion 0.84 ft
Reach 4A	Stable	Stable	Erosion 0.26 ft
Eastside Bypass	Deposition 0.79 ft	Deposition 0.52 ft	Deposition 0.29 ft
Mariposa Bypass	Erosion 3.6 ft	Erosion 3.4 ft	Erosion 2.2 ft
Reach 4B-2	Erosion 1.4 ft	Erosion 1.4 ft	Erosion 1.4 ft
Reach 5-1	Erosion 3.2 ft	Erosion 3.1 ft	Erosion 3.0 ft
Reach 5-2	Erosion 1.8 ft	Erosion 1.8 ft	Erosion 1.7 ft
Reach 5-3	Erosion 4.2 ft	Erosion 4.2 ft	Erosion 4.1 ft

Key:
cfs = cubic feet per second
ft = feet

3.2 Baseline Hydrology

Simulated Baseline hydrology from January 1, 1980, to September 30, 2003, was used to perform the sediment transport and channel morphology simulations with the 1998 topography as the initial channel geometry. Water Year 1997 was a wet year with a high peak discharge. The chance that this high of a peak discharge occurs in the near future is low. Thus, the Baseline hydrology was simulated based upon the period from January 1, 1980, through September 30, 2003, with and without Water Year 1997.

Figure 3-6 shows the bed profiles that were predicted using Baseline hydrology with Engelund and Hansen's (1972) sand transport equation. Reach 3 experienced an average depth of 1.16 feet erosion. When the Baseline hydrology without the high flow in Water Year 1997 is simulated, the average depth of erosion in Reach 3 decreased to 0.07 foot. Reach 4A was relatively stable with minor deposition, with predicted average depths of deposition 0.10 foot and 0.15 foot with and without Water Year 1997, respectively.

The Eastside Bypass experiences erosion (1.56 feet) based on the Baseline hydrology. Without the high flow in Water Year 1997, the average depth of erosion in the Eastside Bypass decreases to 1.46 feet (7 percent less). Predicted depths of erosion in the Eastside Bypass are dependent on the incoming sediment load from the upstream portion of the Eastside Bypass. Because this incoming sediment load is unknown, the accuracies of the predicted depths of erosion in the bypass are limited by the assumption that the upstream portion of the Eastside Bypass is routing sediment at its sediment transport capacity.

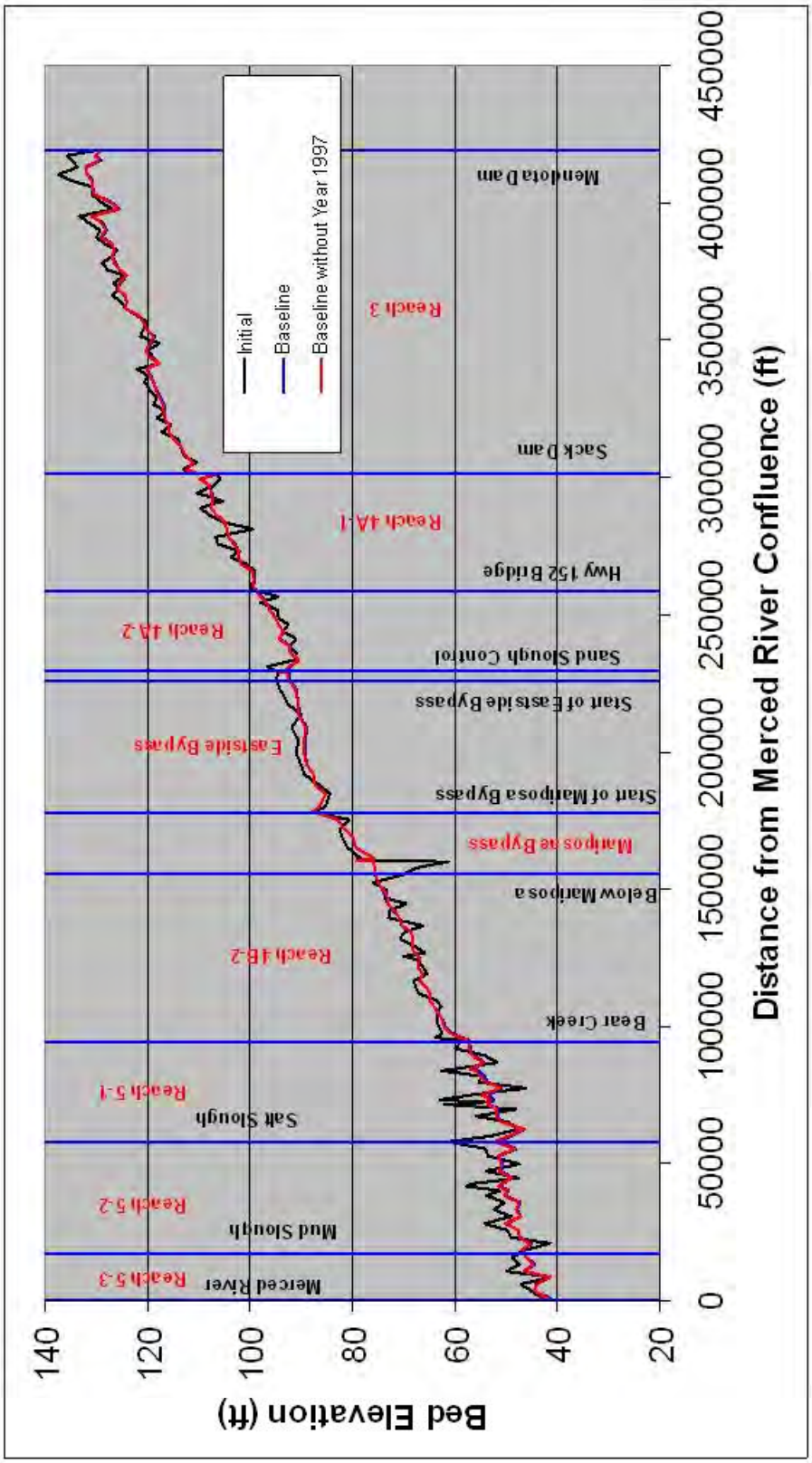

Figure 3-6.
Bed Profiles Simulated with Initial Conditions and Baseline Conditions with and Without Water Year 1997

Results of the model suggest that the Mariposa Bypass experienced erosion, but the erosion is not as significant as that simulated with Historical hydrology. The average erosion reaches 1.36 feet in 23 years using the simulated Baseline hydrology, while it reached 3.6 feet in 17 years with Historical hydrology. The main reason for the reduced erosion in this reach is that less water is diverted into the Mariposa Bypass in the Baseline hydrology, as compared with the assumed Historical hydrology. When the Baseline hydrology without Water Year 1997 is simulated, the average depth of erosion in the Mariposa Bypass decreased to 1.32 feet (3 percent less).

Reach 4B-2 downstream from the Mariposa Bypass experienced minor erosion (0.18 foot) under Baseline Conditions. Without the high flow in Water Year 1997, the average depth of deposition in Reach 4B-2 is similar in magnitude (0.20 foot).

Erosion was predicted in Reach 5 under Baseline Conditions. Reach 5-1, from the confluence with Bear Creek and the Eastside Bypass (RP 135.8) to Salt Sough confluence, experienced an average depth of erosion of 2.1 feet. Reach 5-2, from the Salt Sough confluence to the Mud Slough confluence, experienced an average of 2.7 feet of erosion. Reach 5-3, from the Mud Slough confluence to the Merced River confluence, experienced an average depth of erosion of 1.2 feet. Without Water Year 1997, the average depth of erosion reached 1.7 feet (19 percent less), 2.5 feet (9 percent less), and 1.1 feet (12 percent less) in Reaches 5-1, 5-2, and 5-3, respectively. Computed erosion in Reach 5 was based on the assumption that incoming flow from Bear Creek, the Salt Sough, and the Mud Slough were of same concentration as the San Joaquin River. Suspended sediment sampling in these tributaries across a wide range of flows could improve the prediction.

Figure 3-7 shows the simulated mean bed material size under Baseline Conditions with and without Water Year 1997. The bed material tends to become coarser than current conditions throughout most of the study reach.

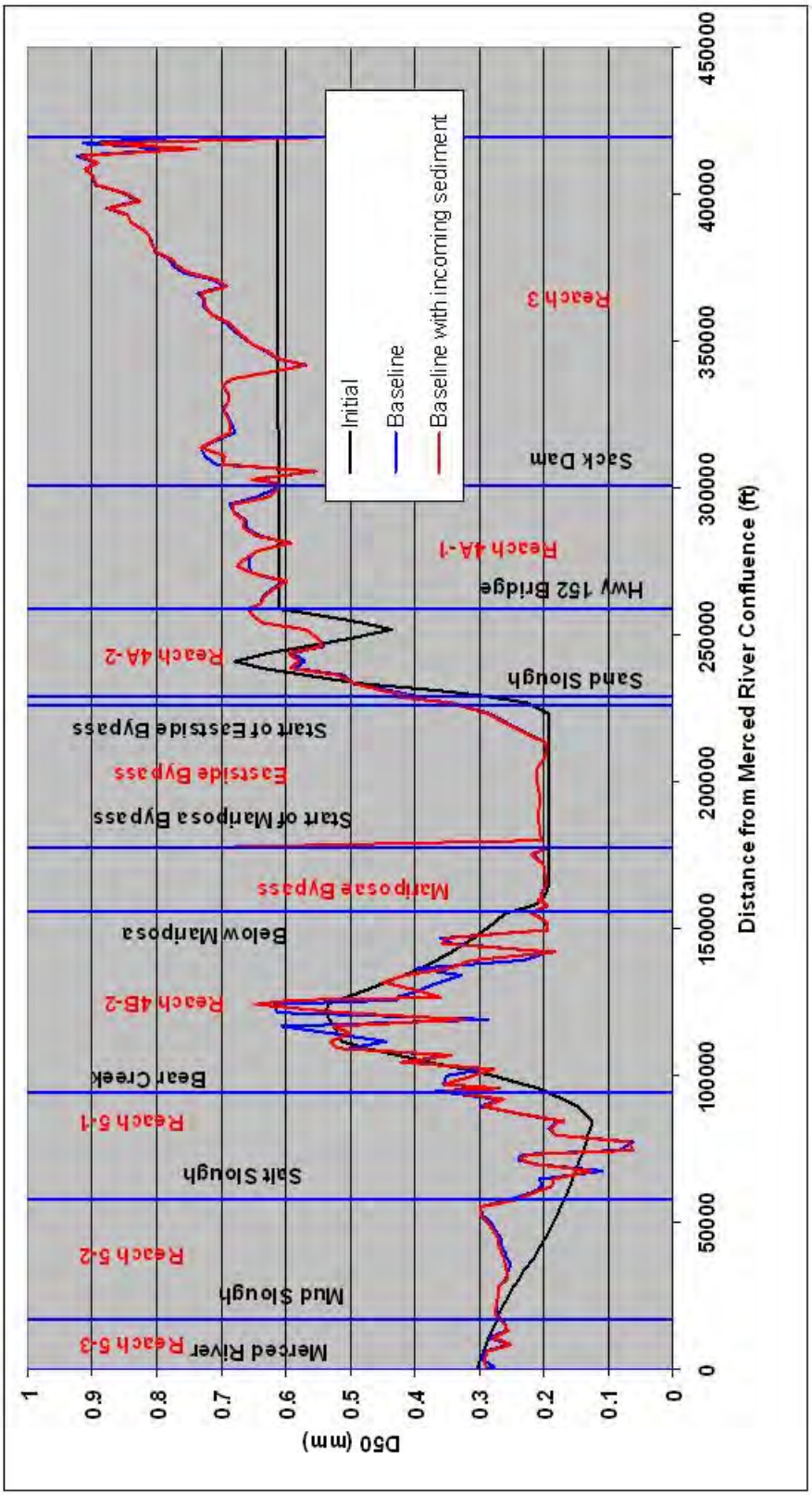

Figure 3-7.
Mean Sediment Size for Initial Conditions and Baseline Conditions

3.2.1 Conditions With and Without Incoming Sediment

Figures 3-8 and 3-9 show sand and gravel erosion and deposition at each cross section, respectively. Since the current SRH-1D model used one cross section to represent every six cross sections in the HEC-RAS geometry, the sediment erosion and deposition in each cross section represents what is expected to occur on average for every six cross sections in the HEC-RAS geometry. In Reaches 3 and 4A and the Eastside Bypass, erosion tends to occur in riffles and deposition in the pools. Net erosion was predicted in Reach 3 and the Eastside Bypass, and net deposition was predicted in Reach 4A. When simulated without Water Year 1997, a slight reduction in erosion or deposition was predicted. The Mariposa Bypass experienced a large amount of sand erosion at the upstream end of the reach. Even though the bed profile shows minor sediment deposition in Reach 4B-2, the erosion and deposition volumes offset each other, and the channel seems stable with erosion occurring in riffles and deposition in pools. In Reach 5, erosion occurred primarily in riffles, and deposition was present in pools. Overall, net sand erosion resulted in Reach 5, and net gravel deposition occurred at the upstream end of Reach 5-1.

A summary of average erosion/deposition depths is provided in Table 3-2.

Table 3-2.
Summary of Trends Identified from Multiple Baseline and Alternative Hydrology Runs

Hydrology	Baseline	Baseline with Incoming Sediment	Future Alternative A	Future Alternative A with Incoming Sediment and ALS	Future Alternative A with Incoming Sediment and MLS
Reach 3	Erosion 1.16	Erosion 1.19	Erosion 2.08	Erosion 2.04	Erosion 2.05
Reach 4A	Deposition 0.10	Deposition 0.12	Erosion 0.27	Erosion 0.26	Erosion 0.27
Eastside Bypass	Erosion 1.56	Erosion 1.58	Erosion 1.12	Erosion 1.12	Erosion 1.12
Mariposa Bypass	Erosion 1.36	Erosion 1.37	Erosion 1.20	Erosion 1.20	Erosion 1.20
Reach 4B-2	Erosion 0.18	Erosion 0.24	Erosion 0.96	Erosion 0.94	Erosion 0.94
Reach 5-1	Erosion 2.10	Erosion 1.90	Erosion 0.62	Erosion 0.72	Erosion 0.72
Reach 5-2	Erosion 2.68	Erosion 2.75	Erosion 3.68	Erosion 3.90	Erosion 3.90
Reach 5-3	Erosion 1.23	Erosion 1.06	Erosion 2.05	Erosion 1.77	Erosion 1.82

Note: All values in feet.

Key:
ALS = average levee setback
MLS = maximum levee setback

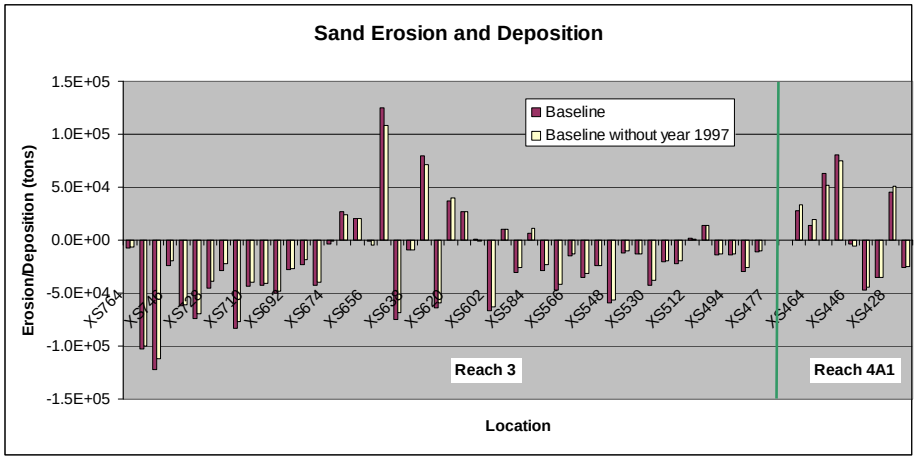

Note: Cross sections are presented from upstream (left) to downstream (right)

Figure 3-8 (a).

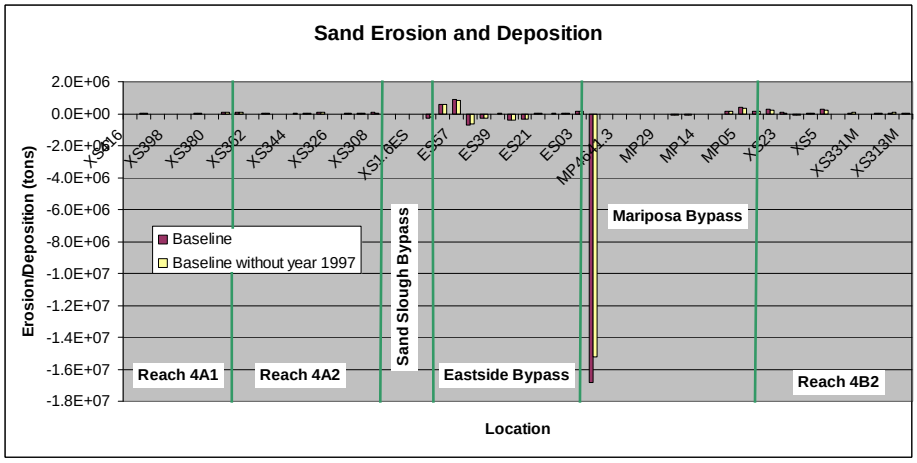

Note: Cross sections are presented from upstream (left) to downstream (right)

Figure 3-8 (b).

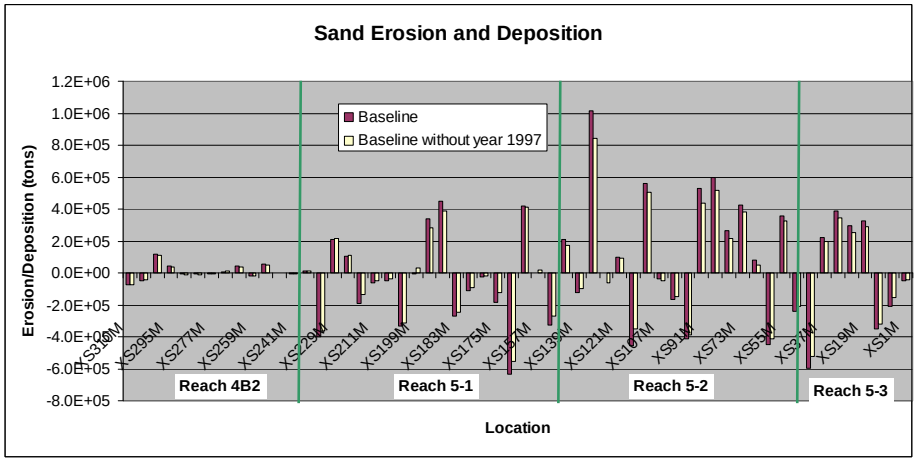

Note: Cross sections are presented from upstream (left) to downstream (right)

Figure 3-8 (c).
Sand Erosion and Deposition

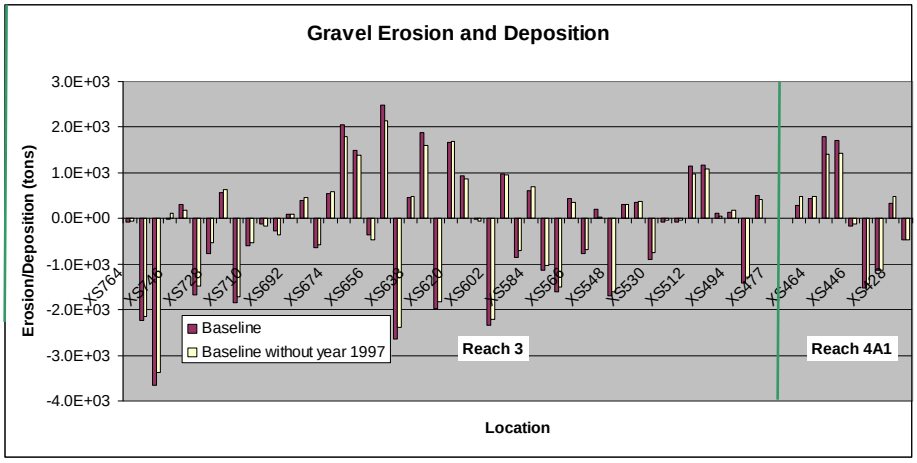

Note: Cross sections are presented from upstream (left) to downstream (right)

Figure 3-9 (a).

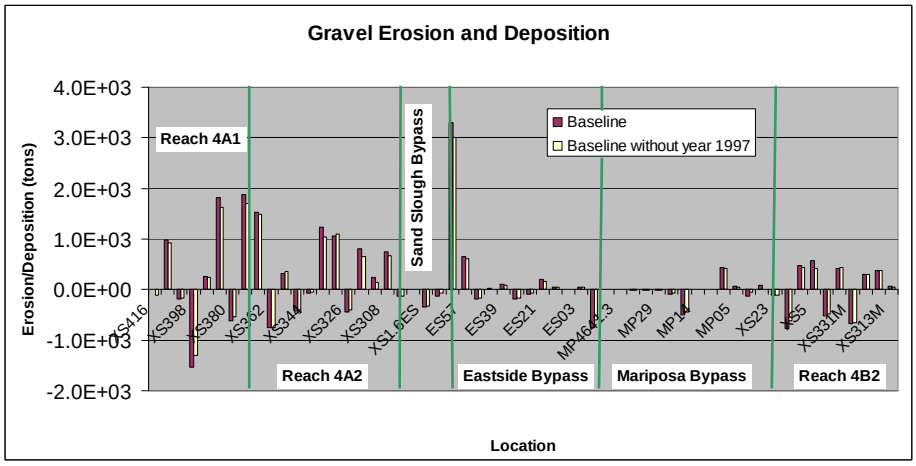

Note: Cross sections are presented from upstream (left) to downstream (right)

Figure 3-9 (b).

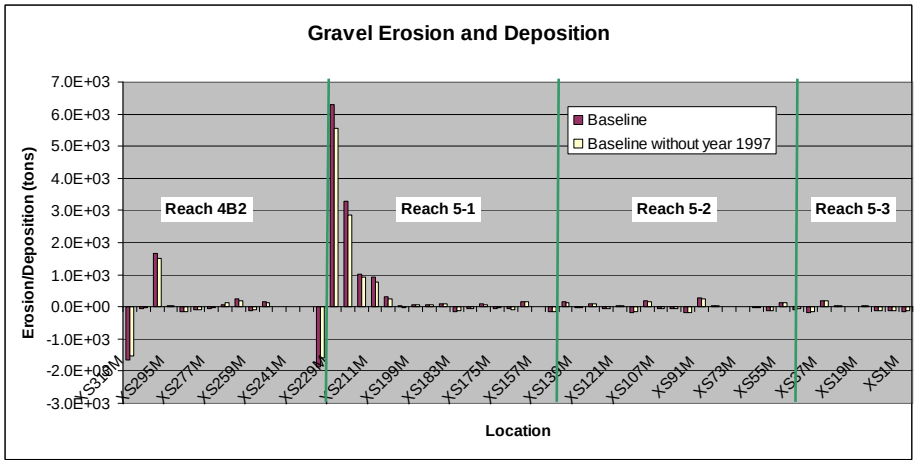

Note: Cross sections are presented from upstream (left) to downstream (right)

Figure 3-9 (c).
Gravel Erosion and Deposition

3.3 Alternative A Hydrology

Alternative A hydrology from January 1, 1980, to September 30, 2003, was used to perform the sediment transport and channel morphology simulations with the 1998 topography as the initial channel geometry.

Figure 3-10 shows the bed profiles that were simulated using Alternative A hydrology with Engelund and Hansen's (1972) sand transport equation. Reach 3 experienced an average depth of 2.1 feet of erosion, which is about twice the erosion predicted under Baseline Conditions. This increased erosion results from the more frequent occurrence of large flows through this reach, as compared with the Baseline hydrology.

Reach 4A remained relatively stable with minor erosion, which reaches an average depth of 0.27 foot. There is slightly more erosion under Alternative A than under Baseline Conditions because of the higher flows in Reach 4A under Alternative A.

The Eastside Bypass experienced erosion (1.1 feet) under Alternative A hydrology. The erosion rate is 29 percent less than that simulated with Baseline hydrology because less flow is diverted into the Eastside Bypass in the Alternative A hydrology. Predicted depths of erosion in the Eastside Bypass are dependent on the incoming sediment load from the upstream portion of the Eastside Bypass.

Results of the model suggest that the Mariposa Bypass experienced erosion based on the future Alternative A hydrology and current bed material. The erosion percentage is not as large as that simulated with Baseline hydrology. The average erosion reached 1.2 feet under the Alternative A hydrology, while it reached 1.4 feet with Baseline hydrology. Reduced erosion in this reach results from less water diverted into the Mariposa Bypass in the future Alternative A hydrology, as compared with the Baseline hydrology.

Reach 4B-2 downstream from the Mariposa Bypass experienced increased erosion (0.96 foot) with the future Alternative A hydrology compared with the minor erosion (0.2 foot) simulated with the Baseline hydrology. The difference is due to higher base flows in the reach under the Alternative A Conditions.

Erosion was predicted under Alternative A hydrology in Reach 5. Subreach Reach 5-1, from the confluence with Bear Creek and the Eastside Bypass (RP 135.8) to the Salt Sough confluence, experienced an average depth of erosion of 0.62 foot. Subreach Reach 5-2, from the Salt Sough confluence to the Mud Slough confluence, experienced an average of 3.7 feet of erosion. Subreach 5-3, from the Mud Slough confluence to the Merced River confluence, experienced an average depth of erosion of 2.1 feet. Computed erosion in Reach 5 was based on the assumption that flow from Bear Creek, Salt Sough, and Mud Slough had the same sediment concentrations as the San Joaquin River. Suspended sediment sampling in these tributaries across a wide range of flows could improve predictions.

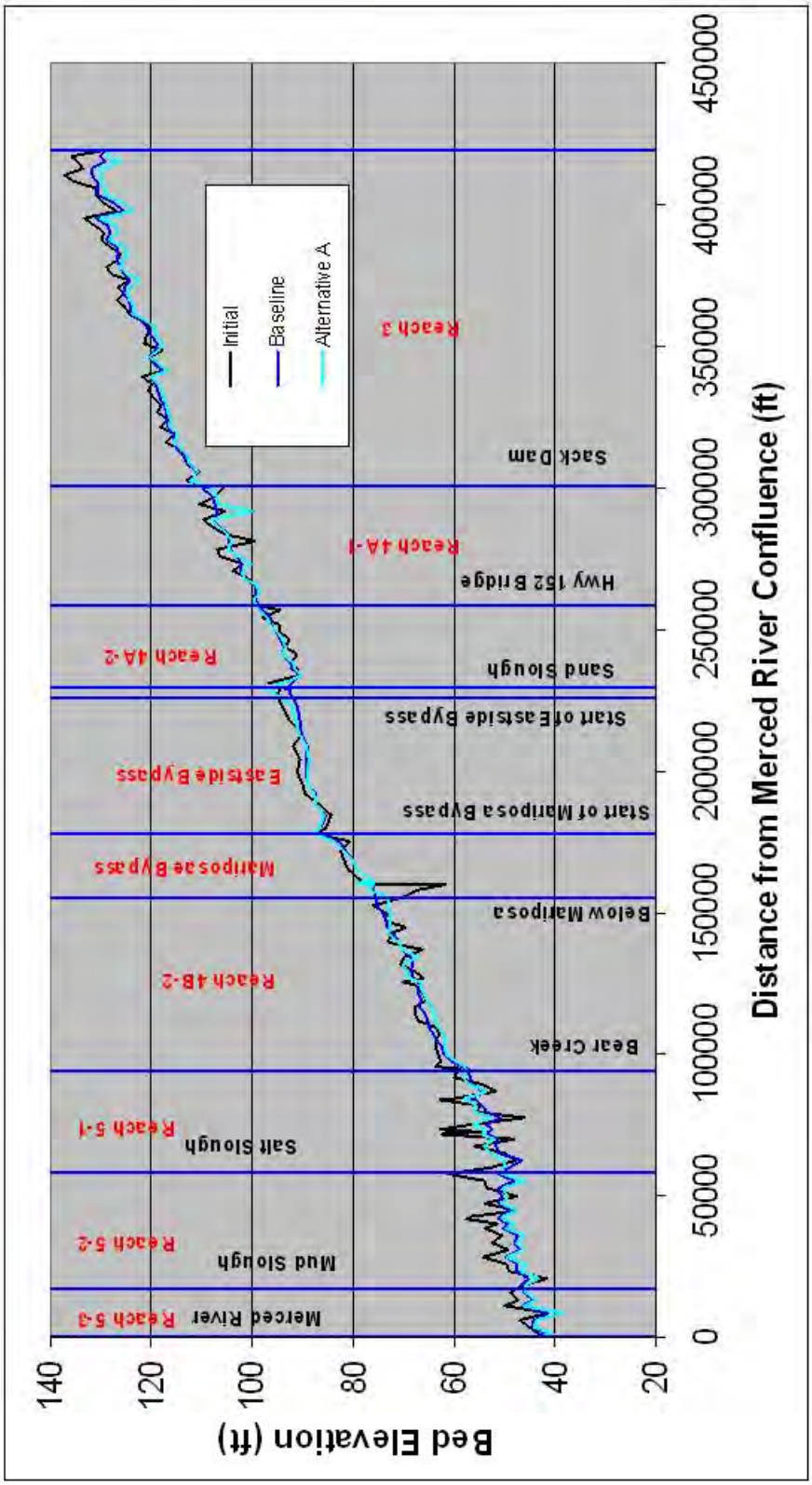

Figure 3-10.
Bed Profiles Simulated with Baseline Hydrology and Future Alternative A Hydrology

Figure 3-11 shows the simulated mean bed material size under Alternative A Conditions. Similar to Baseline Conditions, the bed material tends to become coarser than current conditions throughout most of the study reach. The only exception again occurred in Reach 4B-2 where sediment deposition was predicted and the bed material becomes finer at the upstream end of the reach due to fine sediment contributions from the Mariposa Bypass. Compared with the bed material sizes simulated with the Baseline hydrology, the predicted bed material sizes were coarser in Reaches 3, 4A, and 4B-2 where flow rates under Alternative A are generally higher than those of the Baseline hydrology. Bed material sizes simulated with the Alternative A hydrology were predicted to be similar in the bypasses to those predicted with the Baseline hydrology. In Reaches 5-2 and 5-3, the bed material sizes simulated with the Alternative A hydrology were finer than those predicted with the Baseline hydrology. The numerical model assumed no incoming sediment from reaches upstream from Mendota Dam due to a lack of sediment monitoring information. Measured sediment concentrations of flows from Mendota Dam would likely indicate that the flows do transport suspended sediments. If these loads were considered in the model, the predicted bed material sizes would likely be finer than those presented.

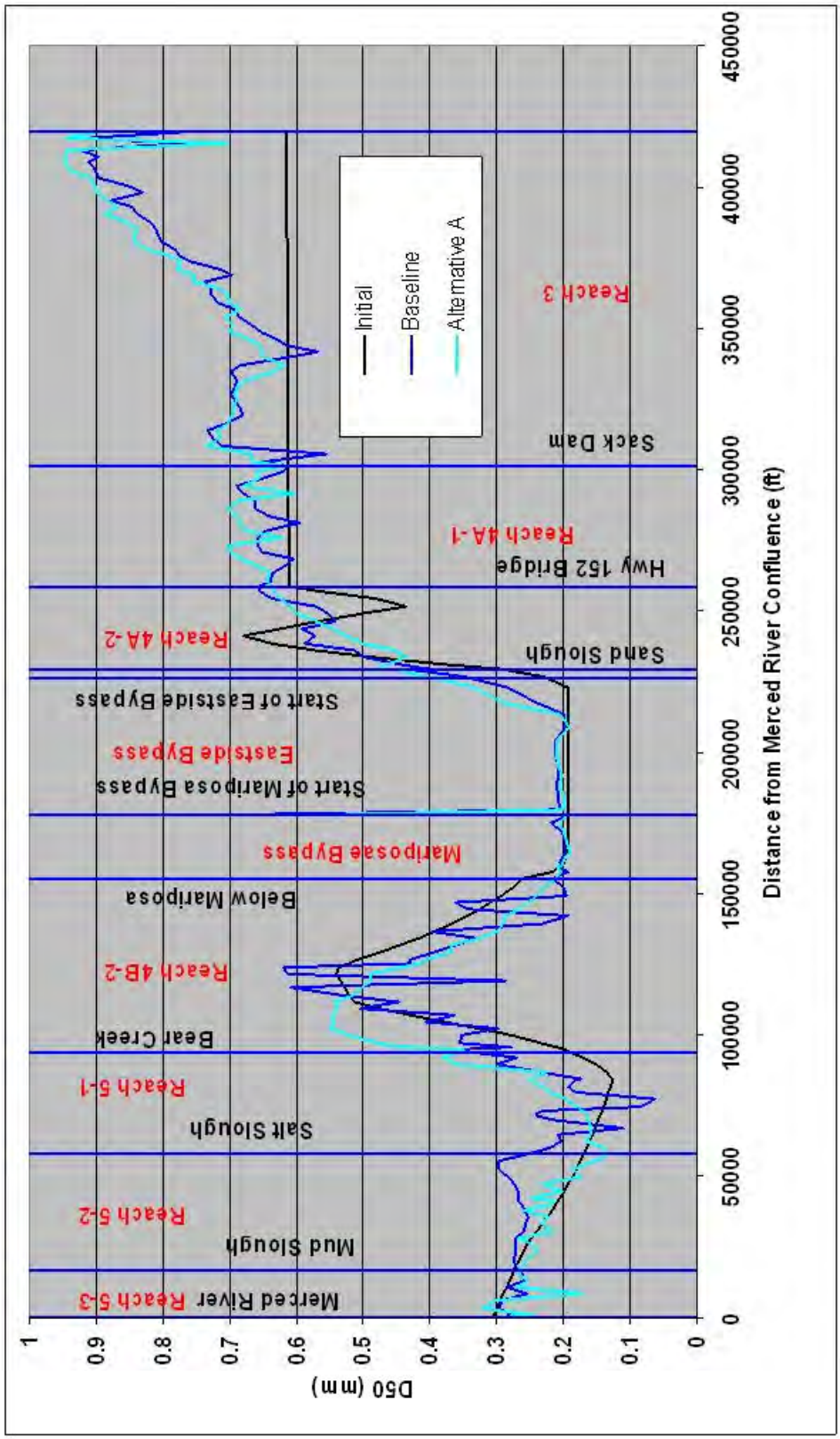

Figure 3-11.
Mean Sediment Sizes for the Initial Conditions and for Two Hydrologic Scenarios

Figures 3-12 and 3-13 display sand and gravel erosion and deposition at each cross section under the Alternative A hydrology scenario. In Reaches 3 and 4A and the Eastside Bypass, erosion tends to occur in riffles and deposition in the pools. Net erosion was predicted in Reach 3, and a stable channel was predicted in Reach 4A. Compared with results simulated with Baseline hydrology, the erosion and deposition volumes in Reaches 3 and 4A were larger due to higher flows with the Alternative A hydrology. Although the bed profile indicates sediment erosion in the Eastside Bypass, the erosion and deposition volumes offset each other. The Eastside Bypass appears relatively stable under Alternative A hydrology with erosion occurring in riffles and deposition in pools. Similar to the Baseline Conditions, the Mariposa Bypass experienced a large amount of sand erosion at the most upstream end of the reach. Reach 4B-2 experienced similar quantities of erosion and deposition and is relatively stable under all conditions evaluated. In Reach 5, erosion occurred primarily in riffles, and deposition was present in pools. Overall, Reach 5 is characterized by net sand erosion and by net gravel deposition at the upstream end of Reach 5-1. The erosion and deposition volumes were smaller than those compared with the Baseline hydrology in Reach 5. Reduced erosion and deposition in Reach 5 under Alternative A can be attributed to a reduction in the frequencies of high flows.

Summary of average erosion/deposition depths is provided in Table 3-2.

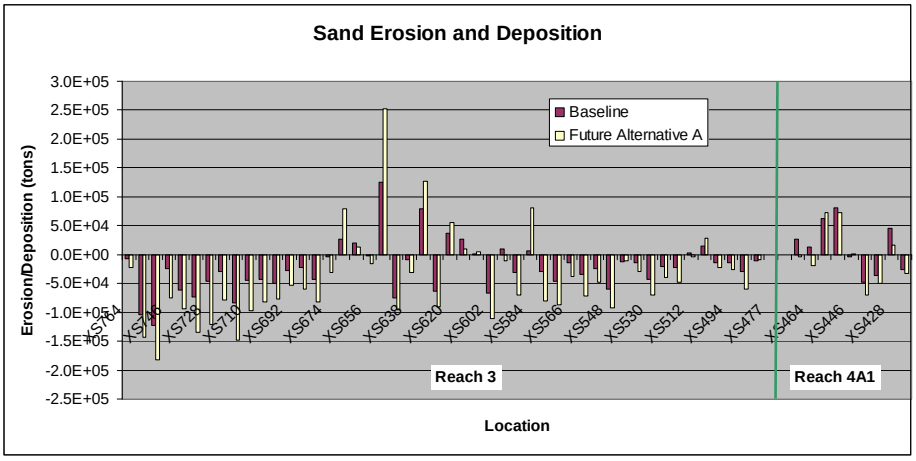

Note: Cross sections are presented from upstream (left) to downstream (right)

Figure 3-12 (a).

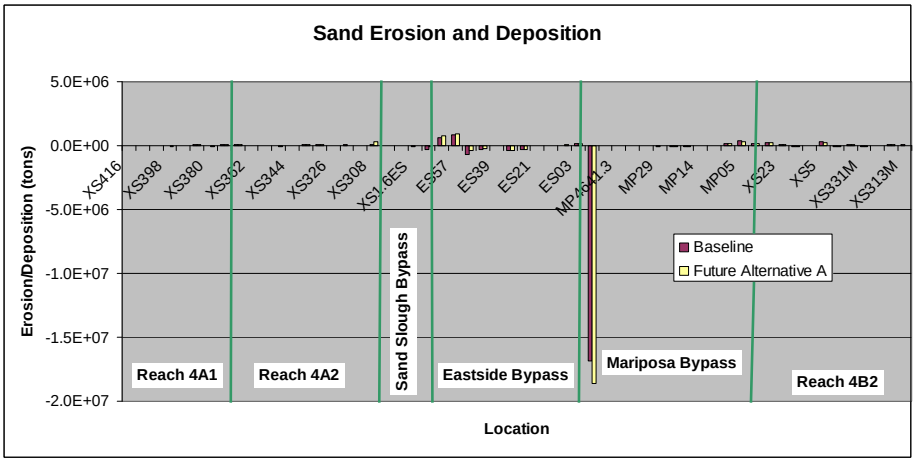

Note: Cross sections are presented from upstream (left) to downstream (right)

Figure 3-12 (b).

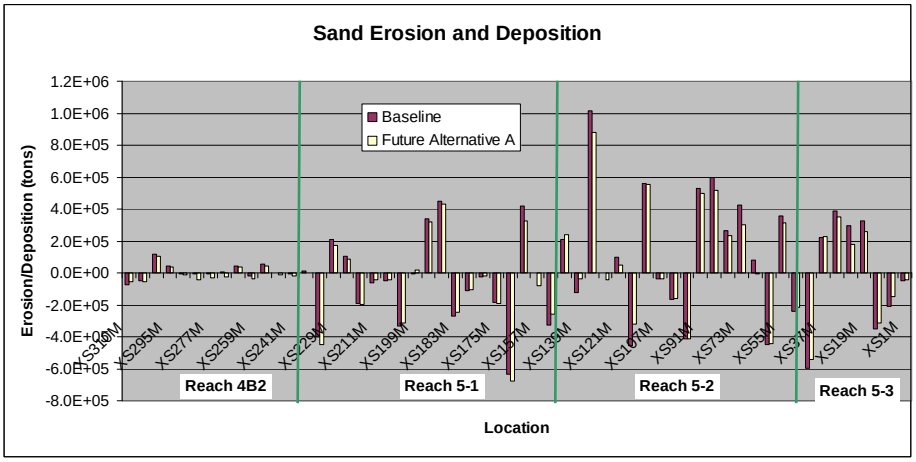

Note: Cross sections are presented from upstream (left) to downstream (right)

Figure 3-12 (c).
Sand Erosion and Deposition

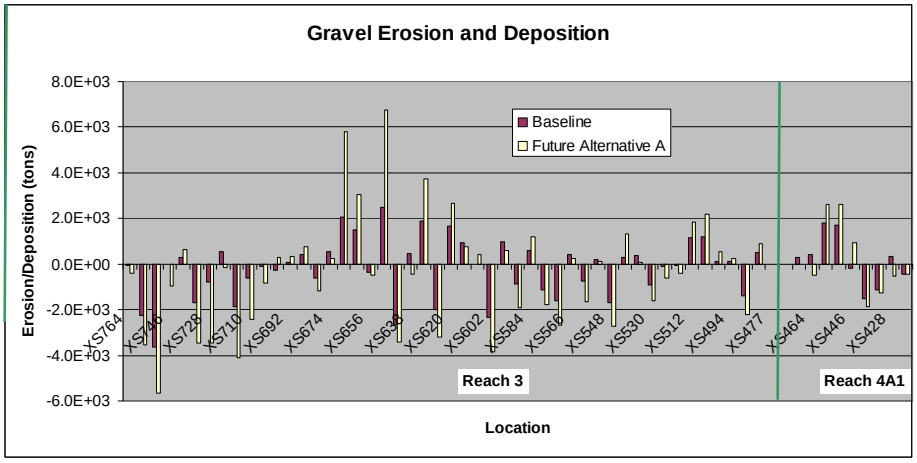

Note: Cross sections are presented from upstream (left) to downstream (right)

Figure 3-13 (a).

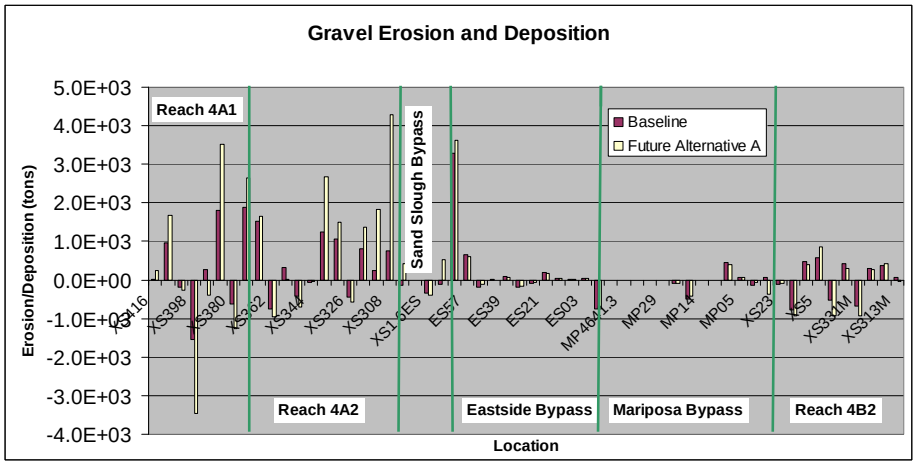

Figure 3-13 (b).

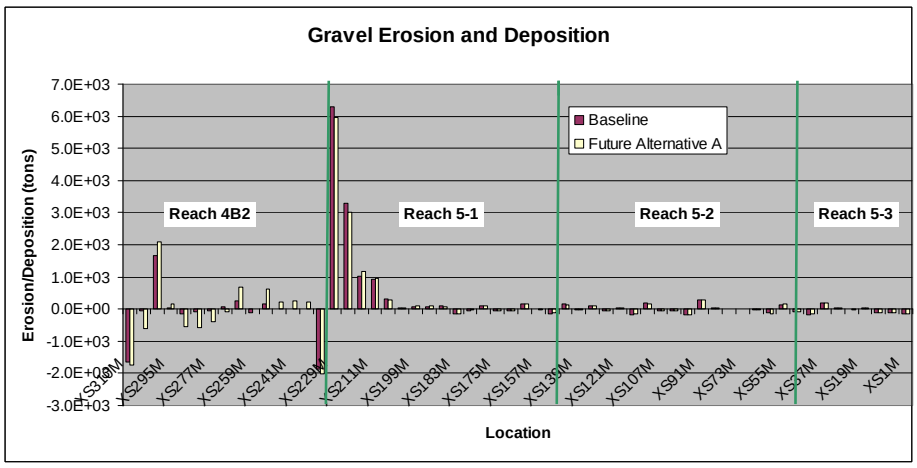

Note: Cross sections are presented from upstream (left) to downstream (right)

Figure 3-13 (c).
Gravel Erosion and Deposition

3.4 Evaluation of Incoming Sediment Loads at Mendota Dam with Baseline and Alternative Hydrology

The model was also used to evaluate potential changes on the sediment balance of the system if a bypass is constructed to route flow and sediment from Reach 2B to Reach 3 without going through the Mendota Pool. Sensitivity analyses were conducted on the Baseline and Alternative A hydrology, assuming that a bypass around Mendota Pool is constructed.

To determine the amount of sediment entering Reach 3, the sediment load at XSA16 was analyzed from the 1D sediment transport model that extends from Friant Dam to the Mendota Pool. A time series of sediment concentrations at XSA16 was output from the model and transferred into sediment loads in tons/day for each size class. The computed sediment loads were then input into the present model as the incoming sediment at the upstream end of Reach 3. Total sediment loads from January 2, 1980, to September 30, 2003, are summarized in Table 3-3 for Baseline hydrology and for Alternative A hydrology with two options of levee setbacks: Average Levee Setback (ALS) and Maximum Levee Setback (MLS).

Table 3-3.
Cumulative Sediment Loads at the Upstream Reach 3 from 1/2/1980 to 9/30/2003

	Lower Limit (mm)	Upper Limit (mm)	Baseline (tons)	Alt A with ALS (tons)	Alt A with MLS (tons)
Total	0.04	16	14,150	196,672	219,176
Silt	0.04	0.063	3,532	28,411	26,178
Very Fine Sand	0.063	0.125	508	6,103	6,499
Fine Sand	0.125	0.25	1,659	24,287	27,894
Medium Sand	0.25	0.5	7,421	118,170	139,079
Coarse Sand	0.5	1	972	18,057	18,396
Very Coarse Sand	1	2	57	1,619	1,112
Very Fine Gravel	2	4	1	26	17

Key:
ALS = average levee setback
Alt = Alternative
MLS = maximum levee setback
mm = millimeter

Compared with the Baseline hydrology, Alternative A hydrology is characterized by higher flows in Reach 2B downstream from the Chowchilla Bifurcation Structure. Under Alternative A Conditions, Reach 2B is expected to experience a fivefold increase in sand and small gravel transport capacity from Baseline Conditions (Huang and Greimann 2009a). The current levees in Reach 2B cannot confine flows exceeding 1,500 cfs. Levee modifications will be required to contain flows greater than 1,500 cfs. In a separate 1D sediment transport model from Friant Dam to Mendota Pool (Huang and Greimann 2009b), two options for levee setbacks were analyzed, and sediment loads were calculated for each. Both options convey similar sediment loads into the reach downstream from Mendota Dam. Sediment loads at XSA16 consist of relatively fine

sediments with 91 percent of the material finer than medium sand for Baseline hydrology and Alternative A hydrology.

Results indicate that if a diversion channel around Mendota Pool is designed to convey all incoming sediment from Reach 2B, the channel geometry in the reach downstream from Mendota Dam will not substantially change from the conditions predicted with the Alternative A hydrology without the diversion channel. The annual incoming sediment load is less than 600 tons/year (yr) for Baseline hydrology and 10,000 tons/yr for Alternative A hydrology and composed mostly of sediment finer that median sand. The difference between the simulated channel bed elevations with and without the Mendota Bypass is less than 10 percent or 0.1 foot. This difference is considered insignificant in a 1D sediment transport model. More notable differences are predicted in Reach 5-3, where the increase in incoming sediment reduces the erosion by 11 percent to 14 percent under Alternative A hydrology.

3.5 Sensitivity Runs on Historical Hydrology Runs and Sediment Transport Parameters

Results from the sensitivity runs are found in Exhibit D and summarized in Table 3-4. Sensitivity analyses were conducted using the Historical Gage information on four model inputs: the number of bed material layers, active layer thickness, transport formula, and roughness coefficient (n). The following sections contain discussions relating to each parameter. The comparison was mainly focused on the Mariposa Bypass, which yielded large amount of erosion.

Table 3-4.
Summary of Results of the Sensitivity Runs on Historical Hydrology Runs and Sediment Transport Parameters

Run No.	Simulation Description	Reach							
		3	4A	Mariposa Bypass	Eastside Bypass	4B-2	5-1	5-2	5-3
		E	Stable	E	D	E	E	E	E
1	Original Model run with Engelund	0.85 ft	Stable	2.8 ft	0.74 ft	1.3ft	1.9ft	1.5ft	4.1ft
2	Changed bed layers to 3	-1%	Stable	0%	4%	-5%	-9%	-5%	6%
3	Modified Laursen's	-69%	E 0.2 ft	-43%	67%	-54%	0%	-21%	5%
4	Brownlie	-38%	E 0.2 ft	-21%	38%	-47%	-12%	-54%	-59%
5	Yang 1973	-33%	E 0.2 ft	-34%	44%	-45%	-36%	-41%	-39%
6	Wu et al.	-61%	E 0.2 ft	-24%	40%	-48%	4%	-9%	-17%
7	Increased Manning's roughness by 20%	0%	Stable	0%	0%	0%	0%	0%	0%
8	Decreased Manning's roughness by 20%	12%	Stable	11%	-6%	0%	-1%	-5%	15%
9	Increased active layer thickness by 100%	4%	Stable	1%	1%	9%	8%	0%	2%
10	Decreased active layer thickness by 50%	-5%	Stable	-1%	5%	-9%	-3%	-13%	0%

Key:
D = Depositional reach
E = Erosional reach
ft = feet

3.5.1 Bed Material Layers

Bed material layers control the supply of bed material once the active layer undergoes erosion. When erosion occurs, the flow removes finer material from the active layer, and the first inactive layer supplies material into the active layer. When deposition occurs, the active layer transfers material into the first inactive layer. The bed material layers are more sensitive when the system endures continuous cycles of erosion and deposition. Erosion occurred most notably in the Mariposa Bypass and in Reach 5. Results suggest that the model is generally not sensitive to changes in the number of bed material layers. When three bed material layers were used as input in the model, the Mariposa Bypass yielded the same depths of erosion compared with the presence of two bed material layers. Three bed material layers resulted in a difference of less than 9 percent in terms of average erosions depths when compared with two bed material layers in Reach 5. The difference was about 5 percent in Reach 4B-2. Three bed material layers also resulted in coarser sediment overall; however, the difference was minimal.

3.5.2 Active Layer Thickness

The active layer thickness controls the amount of bed material available for erosion during any given time step and also controls the armoring process. The active layer is defined as a thin upper zone of constant thickness that is proportional to the geometric mean of the largest size class. The constant of proportionality is user defined. The active layer methodology assumes that all sediment particles of a given size class inside the

active layer are equally exposed to the flow. When erosion is taking place, the flow can remove finer material at a faster rate from the active layer than the coarse material, which forms an armor layer. This armor layer decreases the amount of bed material moved. If degradation occurs, decreasing the active layer thickness increases the rate at which the armor layer forms. When the armor layer forms more quickly, the amount of material removed from the bed decreases. The model provides little evidence that an armor layer was formed in this study reach, which is composed dominantly by sand, and the active layer thickness, therefore, has minimal effect on the sediment transport. In the Mariposa Bypass, doubling the active layer thickness increased the channel erosion by 1 percent, and halving the thickness decreases the channel erosion by 1 percent. Erosion depths in Reaches 3, 4B-2, and 5 followed the same directional trend, with maximum changes of 5 percent, 9 percent, and 13 percent, respectively. Reach 4A was stable with no net erosion or deposition, and the active layer thickness change did not affect the results. All active layer thicknesses result in a coarsening of the sediment in all reaches. However, increasing the active layer thickness results in less coarsening of sediment sizes, while decreasing the thickness generally results in greater coarsening of the bed material.

3.5.3 Transport Formula

Five methods are used to predict the sediment capacity in the San Joaquin River, including (1) Engelund and Hansen's method (1972), (2) modified Laursen's formula (Madden 1993), (3) Brownlie's method (1981), (4) Yang's sand transport formula (1973), and (5) Wu et al.'s formula (2000). Currently, we do not know which equation best predicts the sediment capacity because no sediment load samples have been collected. Comparison of the model results among transport capacity formulas consistently indicated erosion in Reach 3, the Mariposa Bypass, and Reaches 4B-2 and 5. All formulas predicted stable or minimal erosion in Reach 4A and deposition in the Eastside Bypass. However, the amount of erosion and deposition varies among each of the formulas. For example, within the Mariposa Bypass, the Engelund and Hansen's method computed most the erosion (2.8 feet), while the modified Laursen's formula computed the least (1.6 feet, 43 percent less). In the Eastside Bypass, Laursen's formula predicted the most deposition (1.3 feet), while Engelund and Hansen's method predicted the least (0.7 foot).

3.5.4 Roughness Coefficient

Manning's n in the main channel and floodplain were increased by 20 percent and decreased by 20 percent to evaluate the effect on model results. Changes in Manning's n did not modify the general trends of erosion predicted in Reach 3, the Mariposa Bypass, and Reaches 4B-2 and 5, nor the deposition predicted in Reach 4A and the Eastside Bypass. The relationship between Manning's n and sediment transport is complex. In some instances, increasing n causes an increase in the channel shear stress, which may result in an increase in the sediment transport capacity. In other cases, increasing n decreases channel velocity, which may cause a decrease in sediment transport capacity. In the Mariposa Bypass, increasing Manning's n by 20 percent resulted in the same erosion of 0.85 foot on average, while decreasing n by 20 percent caused a decrease in bed erosion by 11 percent. In Reach 3, differences in the average depth of erosion reached 0 percent and 12 percent by increasing and decreasing n by 20 percent, respectively. Reach 4A was stable with all roughness coefficients. The Eastside Bypass was stable with minimal deposition with all roughness coefficients. By increasing and decreasing n by 20 percent in Reaches 4B-2 and 5, the average change in the depth of erosion was within 15 percent.

4.0 Results of Numerical Model with Reach 4B-1 Geometry

A separate SRH-1D model was used to evaluate the sediment transport in Reach 4B-1. The model extends from the Mendota dam to Merced River confluence, but contains no bypasses. The model investigated geomorphic changes assuming the alternative flow options of a maximum of 475 cfs and 4,500 cfs routed through Reach 4B-1. Flows exceeding these values for each option were assumed to be conveyed through the Eastside Bypass.

The boundary conditions for this model were the same boundary conditions previously described for the model with the Sand Slough, and Eastside and Mariposa bypasses. The upstream boundary was defined by flows at the gage San Joaquin River near Mendota (11254000). The downstream water surface elevations near the Merced River confluence were input as a rating curve table (Table 2-5), which was calculated from a separate HEC-RAS model extending from the confluence with Bear Creek and the Eastside Bypass (RP 135.8) to Stockton (RP 41). No sediment was assumed to be delivered from reaches upstream from Mendota Dam.

Channel geometry for Reach 4B-1 was developed from a HEC-RAS geometry file provided by MEI (2002a) and transferred into SRH-1D format. Channel geometry was not modified to represent any levees along the channel banks. Both the HEC-RAS and SRH-1D models assume vertical walls are present to limit the lateral flow extent when the water surface elevation overtops the elevation of the cross-section endpoints. A flow of 4,500 cfs results in water surface elevation exceedance at every cross section in Reach 4B-1. Future levee design by the California Department of Water Resources to protect near-river properties should be incorporated in future modeling runs to more accurately predict sediment transport and geomorphic channel change in this reach. Results presented herein are preliminary and do not represent the influence of possible levees.

Two bridges located in Reach 4B-1 were represented as internal boundary conditions through rating curve tables in the SRH-1D model. A separate HEC-RAS model was developed to calculate water surfaces elevation upstream from the bridges, the results of which are provided in Exhibit A.

No bed material data were collected in this reach. Although one surface bed material sample (Site 3-26) was collected in February 2008 (Reclamation 2008) in this reach, this sample did not adequately represent the bed material in this reach due to the high percentage of organics and the geomorphic location of the sample (a backwater pool at the downstream end of the reach). Consequently, the bed material in Reach 4B-1 was interpolated from sediment samples in Reaches 4A and 4B-2.

Model results indicate that Reach 4B-1 generally experienced erosion when flows were routed into this reach (Figure 4-1). The average depth of erosion reached 0.4 foot for a flow of 475 cfs. Most of the erosion for the maximum flow of 475 cfs occurs in the

downstream portion of the reach and is due to erosion in Reach 4B-2. Reach 4b-1 is considered stable for a maximum flow of 475 cfs. For the scenario with a maximum flow of 4,500 cfs into Reach 4b-1 there is 1.9 feet of average channel erosion predicted. Most of the erosion was in the upstream and downstream portions of the reach. The erosion in the downstream portion of the reach was due to the base level lowering in Reaches 4b2 and 5. There is also erosion upstream from the reach caused by the higher flows being discharged to the reach. Because Reach 4a is degrading, this reach is also expected to degrade in the future if flows are sufficiently high. The benefit of erosion in this reach is that the flow capacity of the reach is expected to increase with time. Some channel erosion would be expected as the channel forms to accommodate the higher flows.

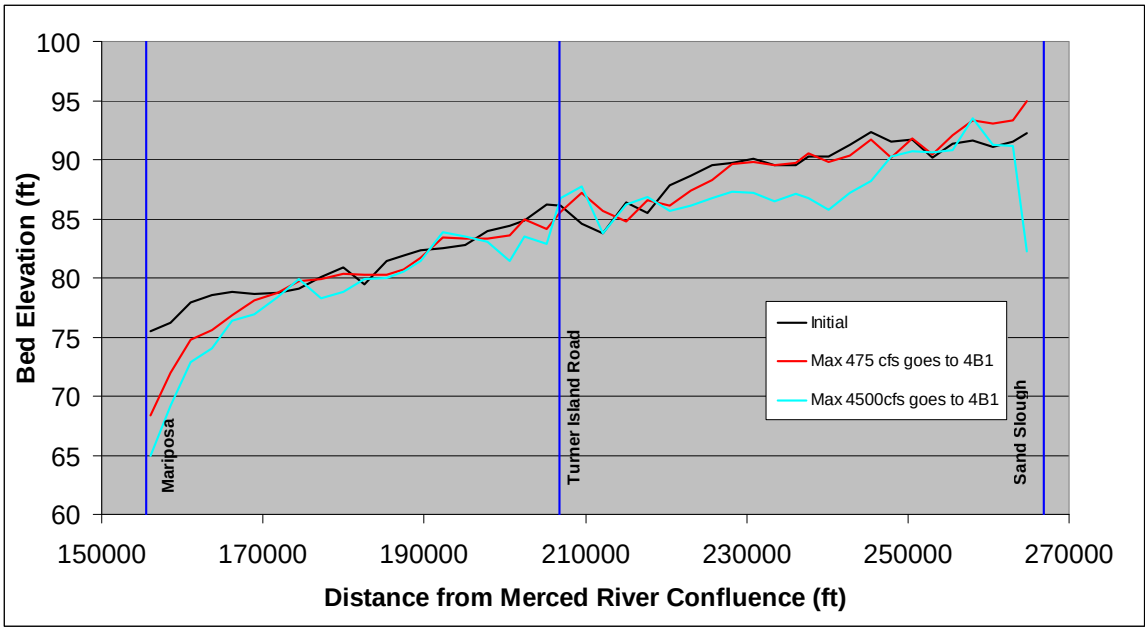

Figure 4-1.
Bed Profiles in Reach 4B-1

In most of the cross sections, sediment coarsening occurred when flows were conveyed through this reach (Figure 4-2). This prediction is limited by the assumption that the median sediment size in this reach was assumed from the bed material in upstream and downstream reaches. Future sediment samples collected in Reach 4B-1 may validate this assumption or provide refined information for use in this estimation.

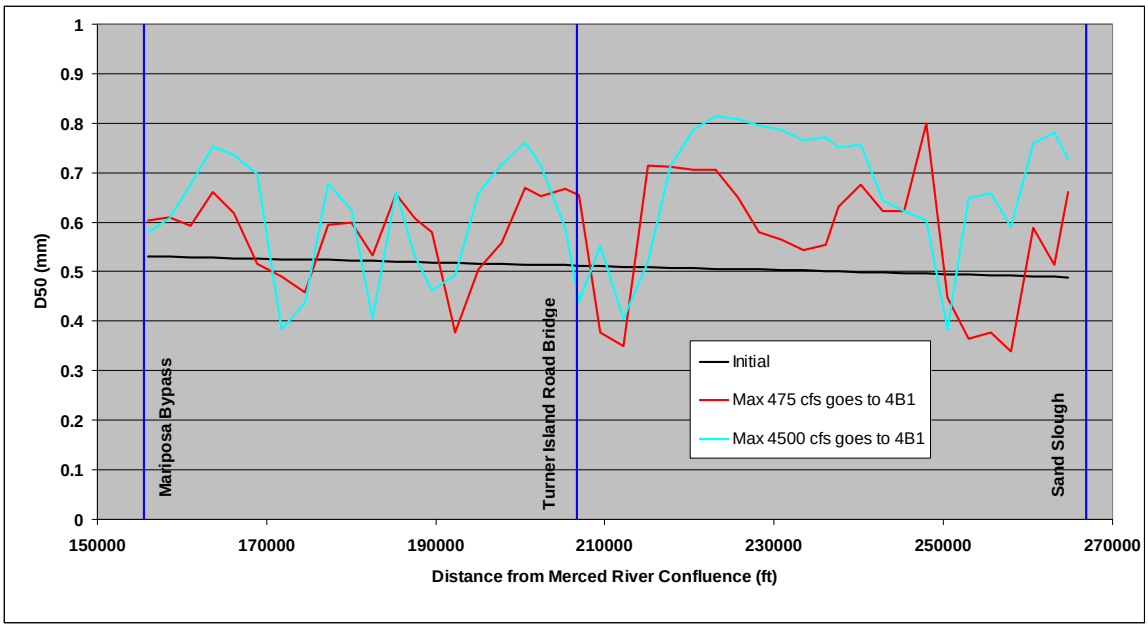

Figure 4-2.
Mean Sediment Sizes in Reach 4B-1

This page left blank intentionally.

5.0 Summary of Model Results

Bed profiles in the San Joaquin River were simulated under Historical hydrology from Mendota Dam to the confluence with the Merced River. Two different flow capacities of Reach 4B-1 were considered: 475 cfs and 4,500 cfs. Under all hydrologic conditions, Reach 3 experienced minor erosion and Reach 4A was stable. More substantial erosion occurred in the Mariposa Bypass and Reaches 4B-2 and 5, while substantial deposition occurred in the Eastside Bypass. Of particular note are the changes to the Mariposa Bypass geomorphic conditions resulting from the alternative flow scenarios. Based on Historical Conditions, the Mariposa Bypass experienced an average of 3.5 feet erosion. When flows are routed through Reach 4B-1, the average depth of erosion in the Mariposa Bypass decreased to 3.4 feet (6 percent less) and 2.2 feet (39 percent less) for flows of 475 cfs and 4,500 cfs, respectively.

Bed profiles were also simulated under Baseline and Alternative A hydrologic scenarios. Under Baseline Conditions, Reach 3 experienced erosion and Reach 4A was stable with minor deposition. Under Alternative A, Reach 3 experienced a twofold increase in erosion compared with Baseline Conditions, and Reach 4a experienced minor erosion instead of minor deposition. Erosion and deposition predicted in Reach 4a were minor, and the reach was relatively stable. The Eastside and the Mariposa bypasses experienced similar erosion under both hydrologic scenarios. However, the erosion rates are smaller under Alternative A than Baseline Conditions because less flow diverted into the bypass under the Alternative A hydrology. Reaches 4B-2 and 5 experienced erosion under both Baseline and Alternative A conditions.

Other notable findings include changes to the sediment sizes throughout the study reach. Using Historical hydrology, downstream from the Highway 152 Bridge, bed material tended to coarsen. Minimal changes in sediment size were modeled upstream from Sack Dam. Under Baseline and Alternative A hydrological conditions, the bed material tends to become coarser than current conditions throughout most of the study reach. Compared with the bed material size simulated with the Baseline hydrology, the Alternative A Conditions predicted coarser bed material sizes in Reaches 3, 4A, and 4B-2, similar bed material sizes in the bypasses and Reach 5-1, and finer bed material in Reaches 5-2 and 5-3.

Detailed results of erosion and deposition volumes in each cross section were presented. In Reaches 3 and 4A, erosion tends to occur in riffles and deposition in the pools. Net erosion was modeled in Reach 3, and a stable channel was modeled in Reach 4A under all hydrological conditions evaluated. Alternative A hydrology resulted in greater volumes of erosion and deposition in Reaches 3 and 4A compared with results simulated with Baseline hydrology due to higher flows under Alternative A hydrology.

Under the Historical hydrology, the Eastside Bypass experienced a net volume of deposition, while the Mariposa Bypass experienced substantial sand erosion. When flows

are routed through Reach 4B-1, smaller volumes of deposition and erosion were predicted in the Eastside Bypass and the Mariposa Bypass, respectively.

Baseline and Alternative A hydrological conditions result in similar trends of erosion in the Eastside and Mariposa bypasses. Through Reaches 4B-2 and 5, net erosion occurred with most erosion occurring in riffles and deposition in pools. One-dimensional models typically overestimate the amount of erosion occurring in riffles and the amount of deposition occurring in pools. While the overall trends of each reach are expected to be accurate, the computed depths and volumes at individual cross sections may be slightly greater than what is actually experienced.

Model results indicate that Reach 4B-1 generally experienced erosion when flows were routed into this reach. The average depth of erosion reached 0.4 foot for a flow of 475 cfs and 1.9 feet for a flow of 4,500 cfs.

The model was also used to evaluate potential effects on the sediment balance of the system if a bypass is constructed to route flow and sediment from Reach 2B to Reach 3 without going through the Mendota Pool. The construction of the bypass will increase the amount of sediment entering Reach 3. However, the effect of this increase in sediment load is considered to be small and does not noticeably affect the downstream channel geometry.

This modeling effort was based upon multiple assumptions due to the lack of detailed information related to suspended sediment and bed material in some reaches. Collecting this additional information could improve the accuracies of predicted results.

6.0 References

Ayres Associates, Inc. 1998. Topographic and Bathymetric Surveys for the San Joaquin River from Friant Dam to Gravelly Ford (RM 267 to RM 229). Prepared for U.S. Bureau of Reclamation, Fresno, California.

———. 1999. Topographic and Hydrographic Surveys for the Sacramento and San Joaquin Comprehensive Study, California - Topographic and Hydrographic Surveying and Mapping for San Joaquin River, RM 40 to RM 230, Including Tributaries and Distributaries. Prepared for U.S. Army Corps of Engineers, Sacramento District, Sacramento California.

Brownlie, W.R. 1981. Prediction of flow depth and sediment discharge in open channels, Report KH-R-43A, W.M. Keck Laboratory of Hydraulics and Water Resources, Division of Engineering and Applied Science, California Institute of Technology, Pasadena, California.

Engelund, F., and E. Hansen. 1972. A monograph on sediment transport in alluvial streams, Teknish Forlag, Technical Press, Copenhagen, Denmark.

Huang, J., and B.P. Greimann, 2007. User's Manual for SRH-1D 2.0 (Sedimentation and River Hydraulics – One Dimension Version 2.0), Bureau of Reclamation, Technical Service Center (www.usbr.gov/pmts/sediment).

———. 2009a. Sediment Mobilization Impacts of the San Joaquin River Restoration Project, Technical Report No. SRH-2009-17, Bureau of Reclamation, Technical Service Center, Denver, Colorado.

———. 2009b. Sediment Transport and Channel Morphology Impacts of the San Joaquin River Restoration Project from Friant Dam to Mendota Dam, Technical Report No. SRH-2009-18, Bureau of Reclamation, Technical Service Center, Denver, Colorado.

Madden, E.B. 1993. Modified Laursen Method for Estimating Bed-Material Sediment Load, U.S. Army Corps of Engineers, U.S. Army Engineer Waterways Experiment Station, Contract report HL-93-3.

Mussetter Engineering, Inc. 2002a. "Hydraulic and Sediment Continuity Modeling of the San Joaquin River from Friant Dam to Mendota Dam, California," U.S. Bureau of Reclamation, Contract No. 98-CP-20-20060.

———. 2002b. "Hydraulic and Sediment-continuity Modeling of the San Joaquin River from Mendota Dam to the Merced River," U.S. Bureau of Reclamation, Contract No. 99-CP-20-2080.

U.S. Department of the Interior, Bureau of Reclamation (Reclamation), 2008. DRAFT San Joaquin River Bed Sediment Sampling Report From Friant Dam to Merced Confluence, Prepared by the Technical Service Center for the San Joaquin River Restoration Project, Mid-Pacific Region.

Wu, W., S.S.Y. Wang, and Y. Jia. 2000. "Nonuniform sediment transport in alluvial rivers," Journal of Hydraulic Research, Vol. 38(6):427-434.

Yang, C.T. 1973. "Incipient motion and sediment transport," Journal of Hydraulic Division, ASCE, Vol. 99(10), 1679-1704.

Exhibit

Boundary Conditions Used in SRH-1D Mendota Dam to Merced River

Draft
Assessment of Sediment Transport and Channel Morphology on the San Joaquin River from Mendota Dam to Merced River Attachment

SAN JOAQUIN RIVER
RESTORATION PROGRAM

Draft
April 2011

Table A-1.
Water Surface Elevations Versus Discharge for Two Grade-Control Structures in the Mariposa Bypass

Discharge (cubic feet per second)	Upstream Water Surface Elevation at MP49 (feet)	Upstream Water Surface Elevation at MP14 (feet)
10	92.56	80.24
20	92.60	80.30
30	92.62	80.34
40	92.65	80.39
50	92.68	80.42
60	92.70	80.46
70	92.72	80.49
80	92.74	80.52
90	92.76	80.55
100	92.78	80.58
200	92.94	80.81
300	93.08	80.99
400	93.20	81.16
500	93.32	81.30
600	93.42	81.44
700	93.52	81.61
800	93.61	81.95
900	93.71	82.27
1,000	93.8	82.56
1,100	93.88	82.83
1,200	93.96	83.08
1,300	94.04	83.31
1,400	94.12	83.54
1,500	94.19	83.74
1,600	94.27	83.93
1,700	94.34	84.11
1,800	94.41	84.29
1,900	94.48	84.45
2,000	94.55	84.61
2,500	94.88	85.31
3,000	95.19	85.91
3,500	95.48	86.39
4,000	95.75	86.78
4,500	96.02	87.11
5,000	96.28	87.39
5,500	96.53	87.64
6,000	96.77	87.87
7,000	97.23	88.31
8,000	97.67	88.72
9,000	98.09	89.09

Table A-1.
Water Surface Elevations Versus Discharge for Two Grade-Control Structures in the Mariposa Bypass (contd.)

Discharge (cubic feet per second)	Upstream Water Surface Elevation at MP49 (feet)	Upstream Water Surface Elevation at MP14 (feet)
10,000	98.49	89.43
15,000	100.97	90.97
20,000	101.91	92.32
25,000	102.78	93.52
30,000	106.17	94.75
35,000	106.81	96.29
40,000	107.43	97.86
45,000	108.04	99.25
50,000	108.62	100.06
55,000	109.19	100.76
60,000	109.75	101.52
65,000	110.29	102.32
70,000	110.82	103.12

Table A-2.
Water Surface Elevations Versus Discharge for Two Bridge Structures in Project

Discharge (cubic feet per second)	Upstream water surface elevation at XS302.8 (feet)	Upstream water surface elevation at XS157 (feet)
10	96.51	87.68
20	96.68	87.88
30	96.83	88.01
40	96.96	88.14
50	97.08	88.26
60	97.20	88.37
70	97.30	88.48
80	97.41	88.60
90	97.50	88.71
100	97.60	88.82
200	98.40	89.79
300	99.11	90.50
400	99.88	91.03
500	100.32	91.47
600	100.82	91.84
700	101.35	92.19
800	101.87	92.49
900	102.40	92.77
1,000	102.94	93.04
1,100	103.49	93.29
1,200	104.05	93.51
1,300	104.62	93.72
1,400	105.19	93.92
1,500	105.79	94.10
1,600	106.41	94.27
1,700	107.06	94.44
1,800	107.72	94.73
1,900	108.41	94.85
2,000	109.10	94.93
2,500	111.68	95.39
3,000	112.08	95.74
3,500	112.33	96.14
4,000	112.54	96.54
4,500	112.74	97.12

This page left blank intentionally.

Exhibit

Lateral Sediment Incoming from the Upper Reach of Eastside Bypass

Draft
Assessment of Sediment Transport and Channel Morphology on the San Joaquin River from Mendota Dam to Merced River Attachment

SAN JOAQUIN RIVER
RESTORATION PROGRAM

Draft
April 2011

Table B-1.
Sediment Rating Curve and Size Fraction Finer than in the Upper Reach of the Eastside Bypass

flow	Sediment load	Bed sediment fraction finer than								
(cfs)	(tons/day)	0.063mm	0.125mm	0.25mm	0.5mm	1mm	2mm	4mm	8mm	16mm
10	0.7	0	0.0528	0.1550	0.4649	0.2458	0.0682	0.0125	0.0007	0.0000
20	1.5	0	0.0528	0.1550	0.4649	0.2457	0.0682	0.0126	0.0008	0.0001
30	2.4	0	0.0528	0.1550	0.4649	0.2457	0.0682	0.0125	0.0008	0.0000
40	3.4	0	0.0528	0.1550	0.4649	0.2458	0.0682	0.0125	0.0008	0.0000
50	4.4	0	0.0528	0.1550	0.4649	0.2457	0.0682	0.0125	0.0008	0.0000
60	5.3	0	0.0528	0.1550	0.4649	0.2457	0.0682	0.0125	0.0008	0.0000
70	6.3	0	0.0528	0.1550	0.4649	0.2458	0.0682	0.0125	0.0008	0.0000
80	7.2	0	0.0528	0.1550	0.4649	0.2458	0.0682	0.0125	0.0008	0.0000
90	8.1	0	0.0528	0.1550	0.4649	0.2457	0.0682	0.0125	0.0008	0.0000
100	9.1	0	0.0528	0.1550	0.4649	0.2458	0.0682	0.0125	0.0008	0.0000
200	20.4	0	0.0528	0.1550	0.4649	0.2458	0.0682	0.0125	0.0008	0.0000
300	38.8	0	0.0528	0.1550	0.4649	0.2458	0.0682	0.0125	0.0008	0.0000
400	62.9	0	0.0528	0.1550	0.4649	0.2458	0.0682	0.0125	0.0008	0.0000
500	93.8	0	0.0528	0.1550	0.4649	0.2458	0.0682	0.0125	0.0008	0.0000
600	124.9	0	0.0528	0.1550	0.4649	0.2458	0.0682	0.0125	0.0008	0.0000
700	160.8	0	0.0528	0.1550	0.4649	0.2458	0.0682	0.0125	0.0008	0.0000
800	203.1	0	0.0528	0.1550	0.4649	0.2458	0.0682	0.0125	0.0008	0.0000
900	245.7	0	0.0528	0.1550	0.4649	0.2458	0.0682	0.0125	0.0008	0.0000
1000	287.0	0	0.0528	0.1550	0.4649	0.2458	0.0682	0.0125	0.0008	0.0000
1100	331.2	0	0.0528	0.1550	0.4649	0.2458	0.0682	0.0125	0.0008	0.0000
1200	376.3	0	0.0528	0.1550	0.4649	0.2458	0.0682	0.0125	0.0008	0.0000
1300	427.1	0	0.0528	0.1550	0.4649	0.2458	0.0682	0.0125	0.0008	0.0000
1400	481.7	0	0.0528	0.1550	0.4649	0.2458	0.0682	0.0125	0.0008	0.0000
1500	539.2	0	0.0528	0.1550	0.4649	0.2458	0.0682	0.0125	0.0008	0.0000
1600	598.8	0	0.0528	0.1550	0.4649	0.2458	0.0682	0.0125	0.0008	0.0000
1700	662.2	0	0.0528	0.1550	0.4649	0.2458	0.0682	0.0125	0.0008	0.0000
1800	728.7	0	0.0528	0.1550	0.4649	0.2458	0.0682	0.0125	0.0008	0.0000
1900	799.3	0	0.0528	0.1550	0.4649	0.2458	0.0682	0.0125	0.0008	0.0000
2000	871.1	0	0.0528	0.1550	0.4649	0.2458	0.0682	0.0125	0.0008	0.0000
2500	1270.8	0	0.0528	0.1550	0.4649	0.2458	0.0682	0.0125	0.0008	0.0000
3000	1743.5	0	0.0528	0.1550	0.4649	0.2458	0.0682	0.0125	0.0008	0.0000
3500	2277.9	0	0.0528	0.1550	0.4649	0.2458	0.0682	0.0125	0.0008	0.0000
4000	2867.5	0	0.0528	0.1550	0.4649	0.2458	0.0682	0.0125	0.0008	0.0000
4500	3505.7	0	0.0528	0.1550	0.4649	0.2458	0.0682	0.0125	0.0008	0.0000
5000	4202.6	0	0.0528	0.1550	0.4649	0.2458	0.0682	0.0125	0.0008	0.0000
5500	4954.7	0	0.0528	0.1550	0.4649	0.2458	0.0682	0.0125	0.0008	0.0000
6000	5746.4	0	0.0528	0.1550	0.4649	0.2458	0.0682	0.0125	0.0008	0.0000
7000	7462.2	0	0.0528	0.1550	0.4649	0.2458	0.0682	0.0125	0.0008	0.0000
8000	9350.2	0	0.0528	0.1550	0.4649	0.2458	0.0682	0.0125	0.0008	0.0000
9000	11333.7	0	0.0528	0.1550	0.4649	0.2458	0.0682	0.0125	0.0008	0.0000
10000	13377.8	0	0.0528	0.1550	0.4649	0.2458	0.0682	0.0125	0.0008	0.0000
15000	23425.7	0	0.0528	0.1550	0.4649	0.2458	0.0682	0.0125	0.0008	0.0000
20000	33759.5	0	0.0528	0.1550	0.4649	0.2458	0.0682	0.0125	0.0008	0.0000
25000	43981.8	0	0.0528	0.1550	0.4649	0.2458	0.0682	0.0125	0.0008	0.0000
30000	56228.9	0	0.0528	0.1550	0.4649	0.2458	0.0682	0.0125	0.0008	0.0000
35000	68473.5	0	0.0528	0.1550	0.4649	0.2458	0.0682	0.0125	0.0008	0.0000
40000	81854.1	0	0.0528	0.1550	0.4649	0.2458	0.0682	0.0125	0.0008	0.0000
45000	95908.0	0	0.0528	0.1550	0.4649	0.2458	0.0682	0.0125	0.0008	0.0000
50000	110039.6	0	0.0528	0.1550	0.4649	0.2458	0.0682	0.0125	0.0008	0.0000
55000	121601.7	0	0.0528	0.1550	0.4649	0.2458	0.0682	0.0125	0.0008	0.0000
60000	138246.9	0	0.0528	0.1550	0.4649	0.2458	0.0682	0.0125	0.0008	0.0000
65000	152856.3	0	0.0528	0.1550	0.4649	0.2458	0.0682	0.0125	0.0008	0.0000
70000	169100.0	0	0.0528	0.1550	0.4649	0.2458	0.0682	0.0125	0.0008	0.0000

This page left blank intentionally.

Exhibit

Computed Water Surface Profiles: Mendota Dam to Merced River

Draft
Assessment of Sediment Transport and Channel Morphology on the San Joaquin River from Mendota Dam to Merced River Attachment

SAN JOAQUIN RIVER
RESTORATION PROGRAM

Draft
April 2011

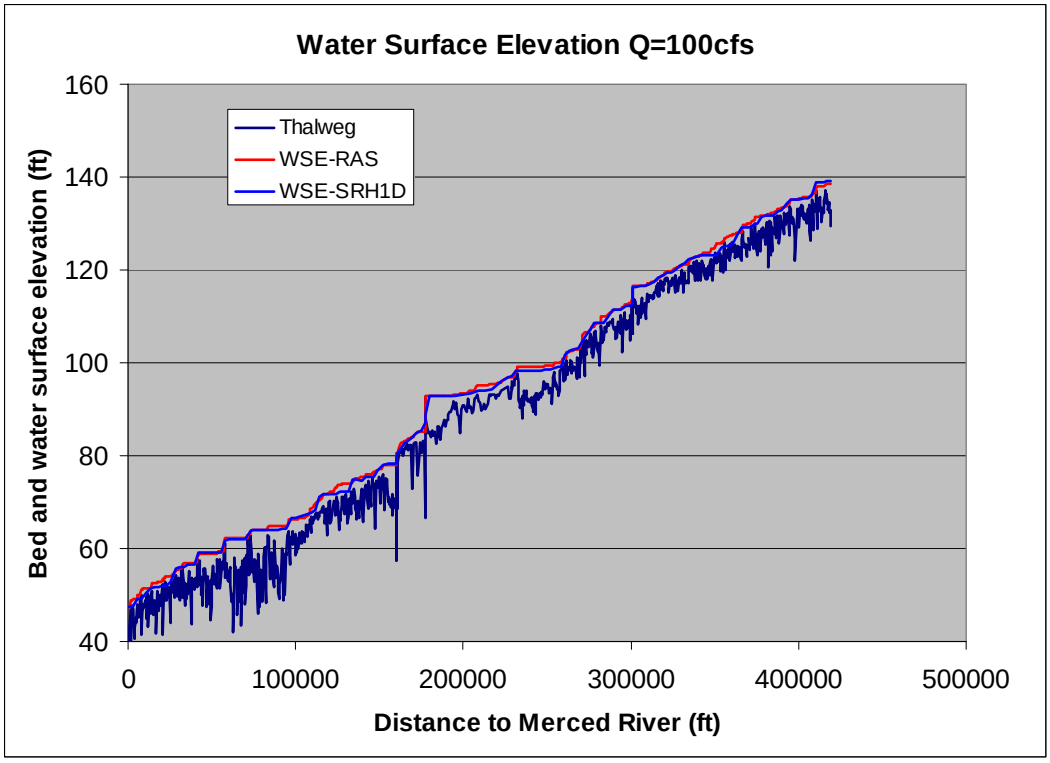

Profile 1 with Uniform Discharge of 100 cfs

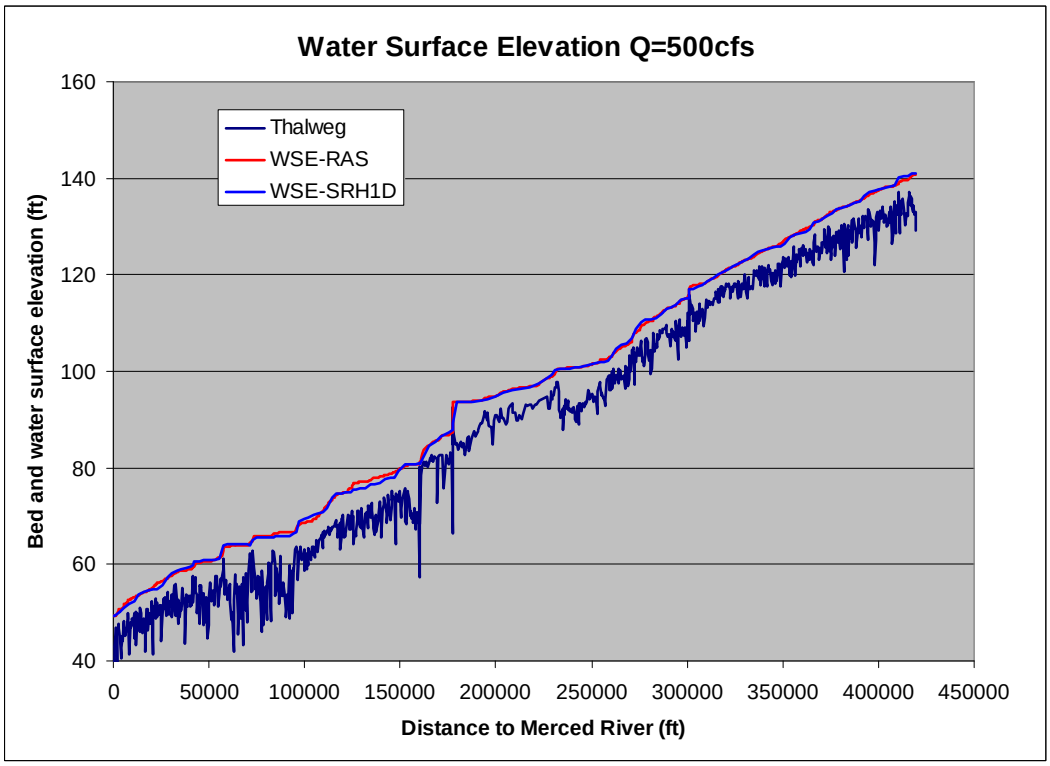

Profile 2 with Uniform Discharge of 500 cfs

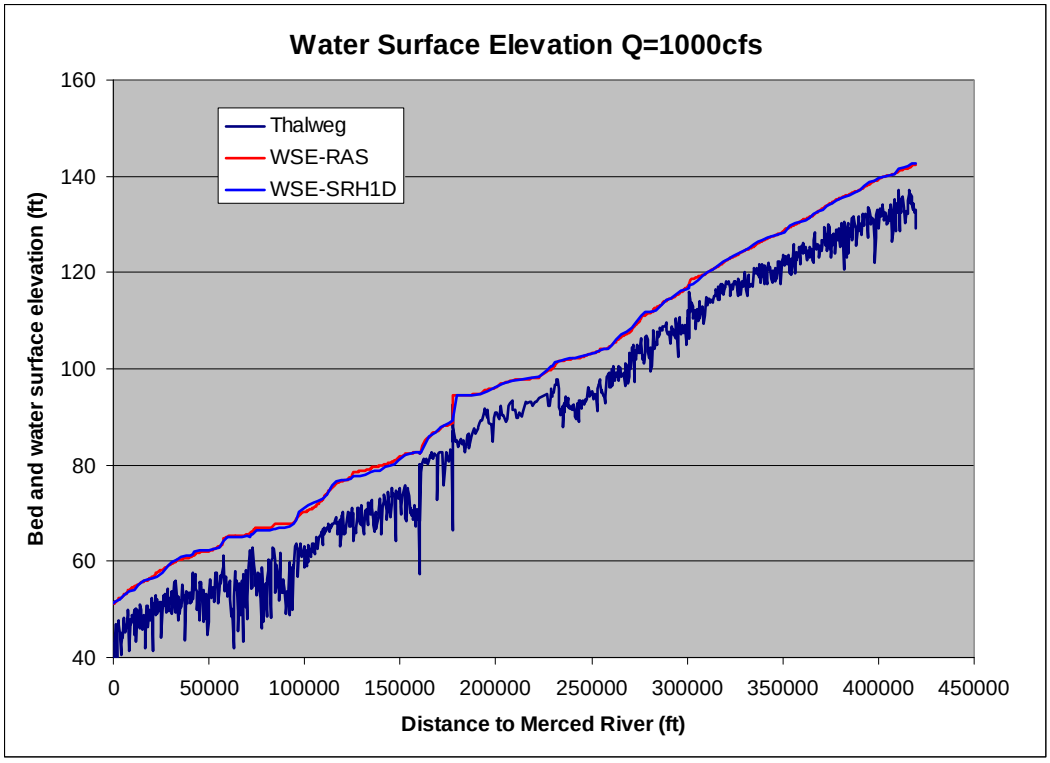

Profile 3 with Uniform Discharge of 1,000 cfs

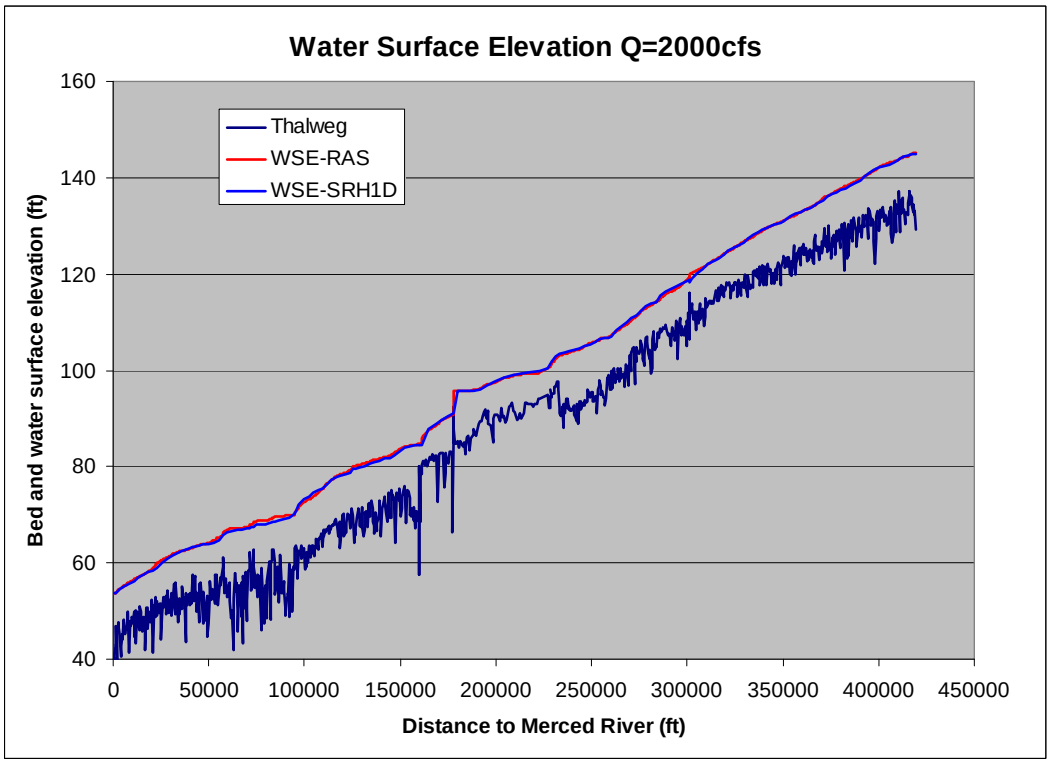

Profile 4 with Uniform Discharge of 2,000 cfs

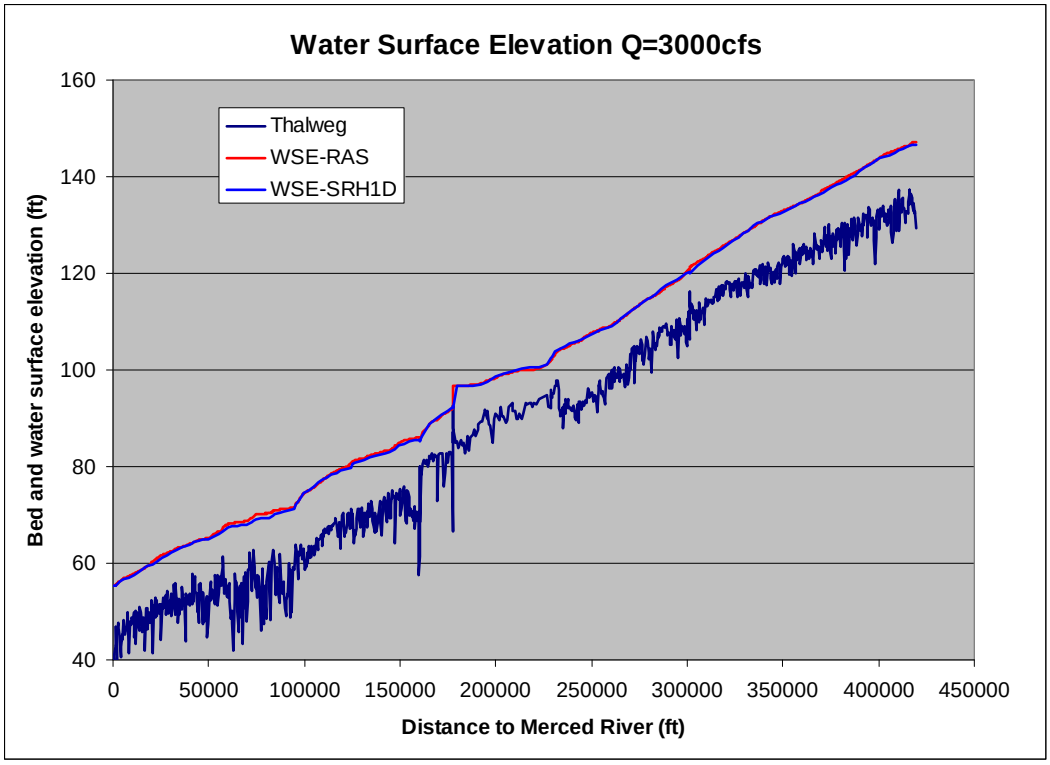

Profile 5 with Uniform Discharge of 3,000 cfs

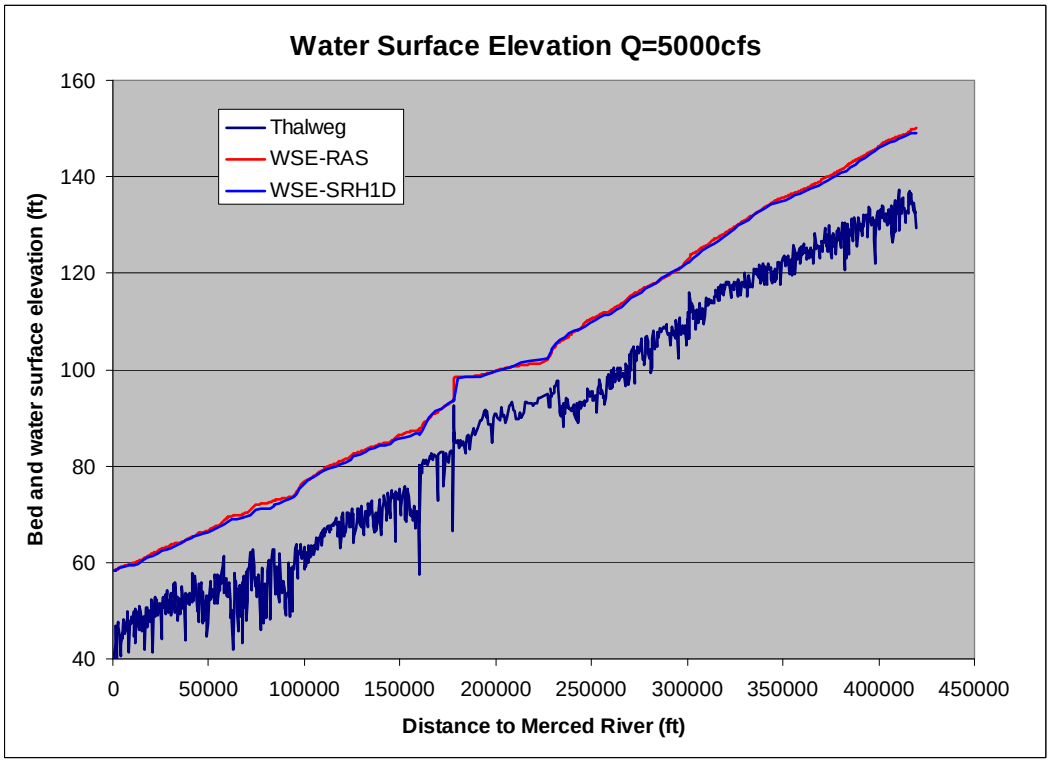

Profile 6 with Uniform Discharge of 5,000 cfs

This page left blank intentionally.

Exhibit

Sensitivity Analysis on Historical Hydrology Runs and Sediment Transport Parameters

Draft
Assessment of Sediment Transport and Channel Morphology on the San Joaquin River from Mendota Dam to Merced River Attachment

SAN JOAQUIN RIVER
RESTORATION PROGRAM

Draft
April 2011

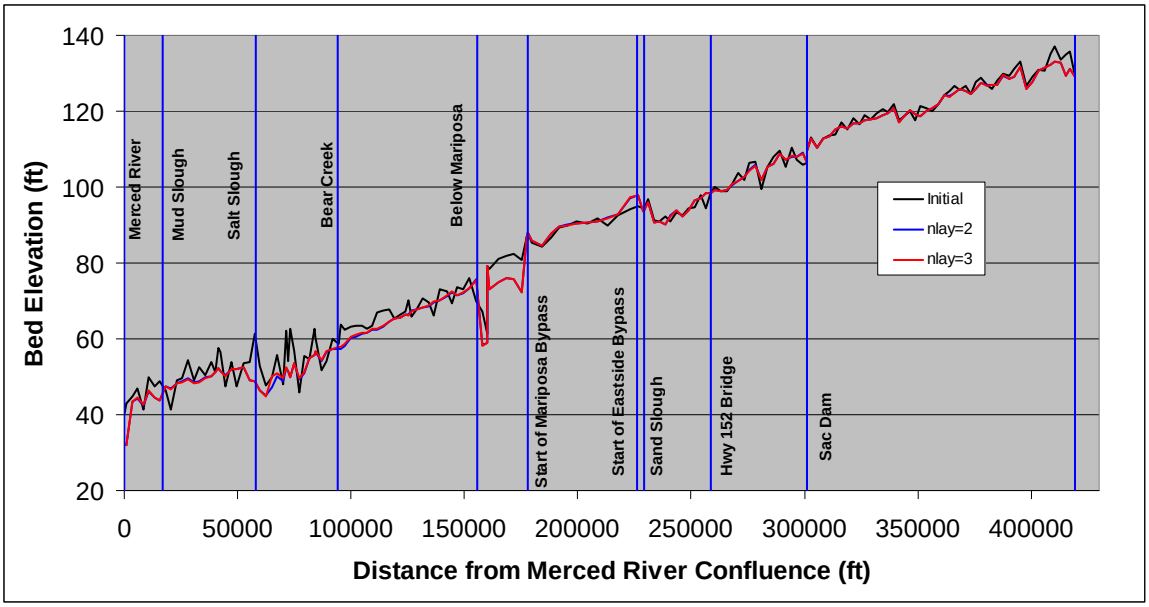

Note: Nlay represents the number of bed material layers.

Figure D-1.
Bed Profiles Simulated with Different Bed Material Layers

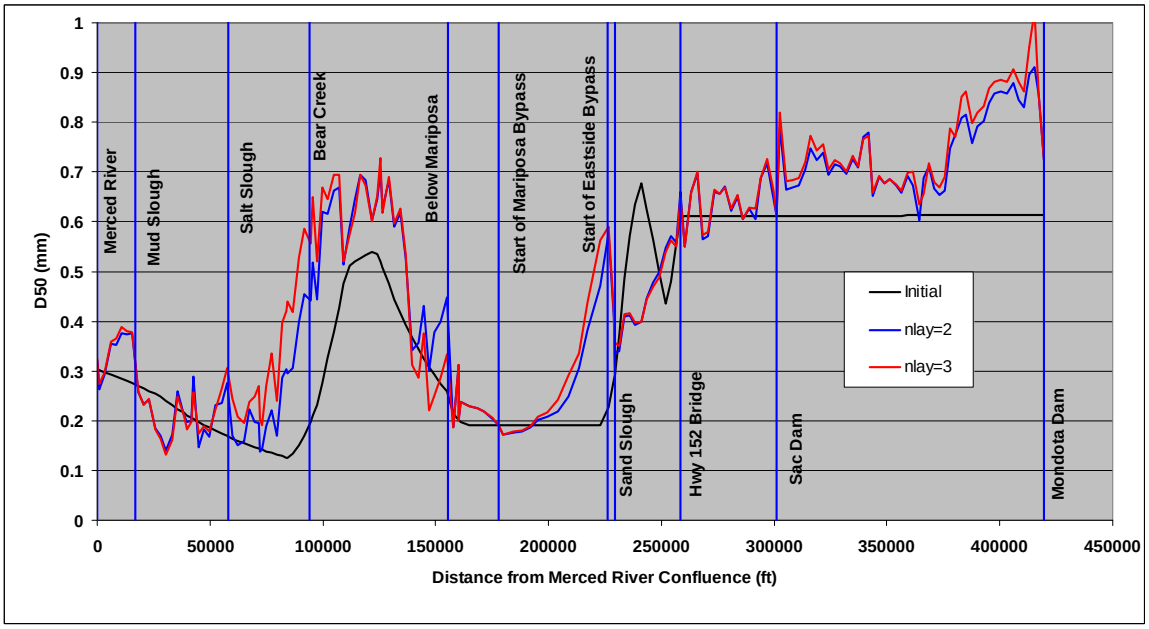

Note: Nlay represents the number of bed material layers.

Figure D-2.
Mean Sediment Size Simulated with Different Bed Material Layers

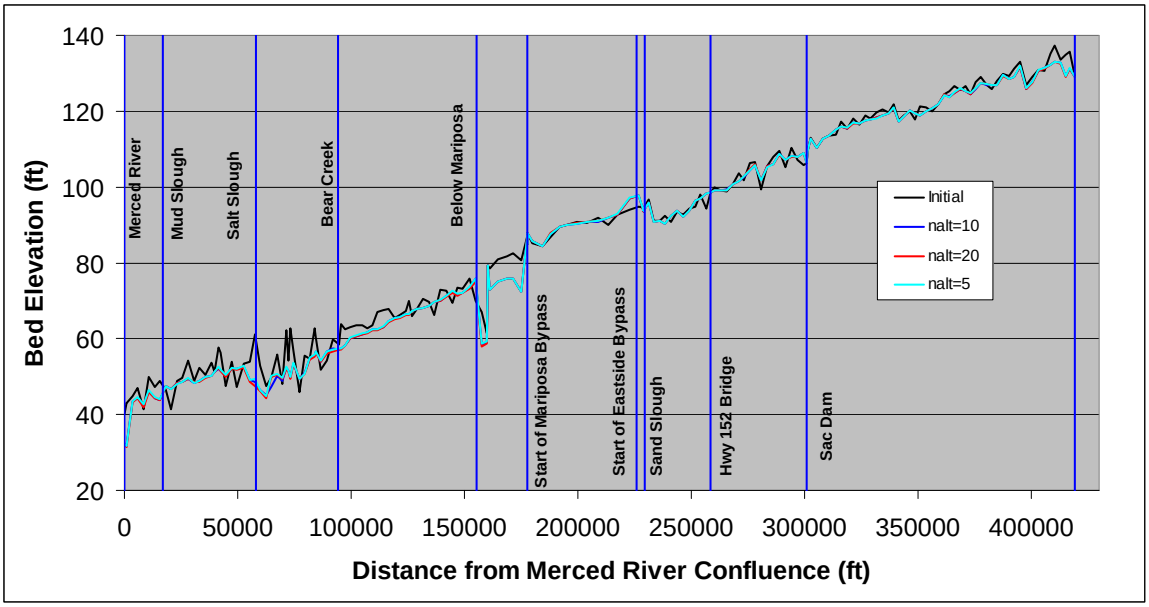

Figure D-3.
Bed Profiles Simulated with Different Active Layer Thicknesses

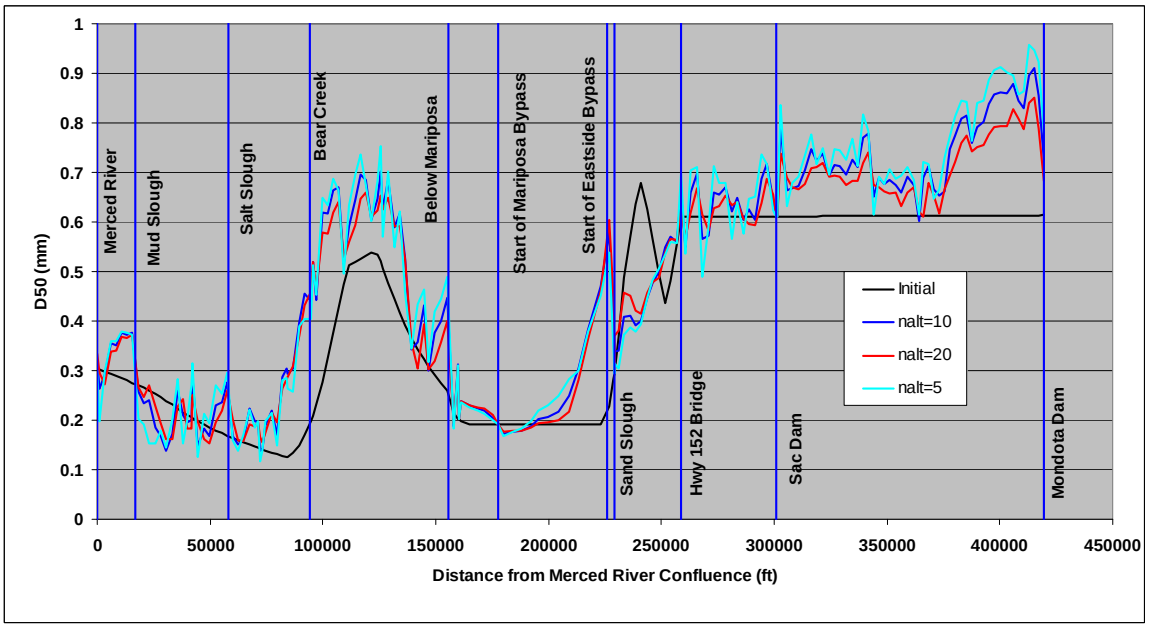

Figure D-4.
Mean Sediment Size Simulated with Different Active Layer Thicknesses

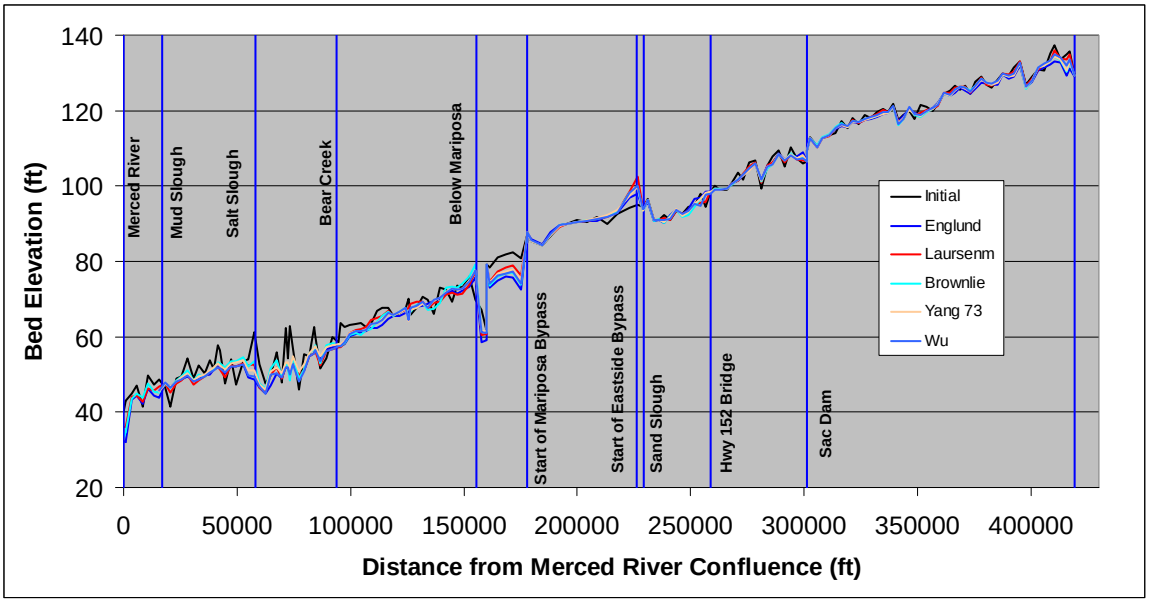

Figure D-5.
Bed Profiles Simulated with Different Sediment Transport Equations

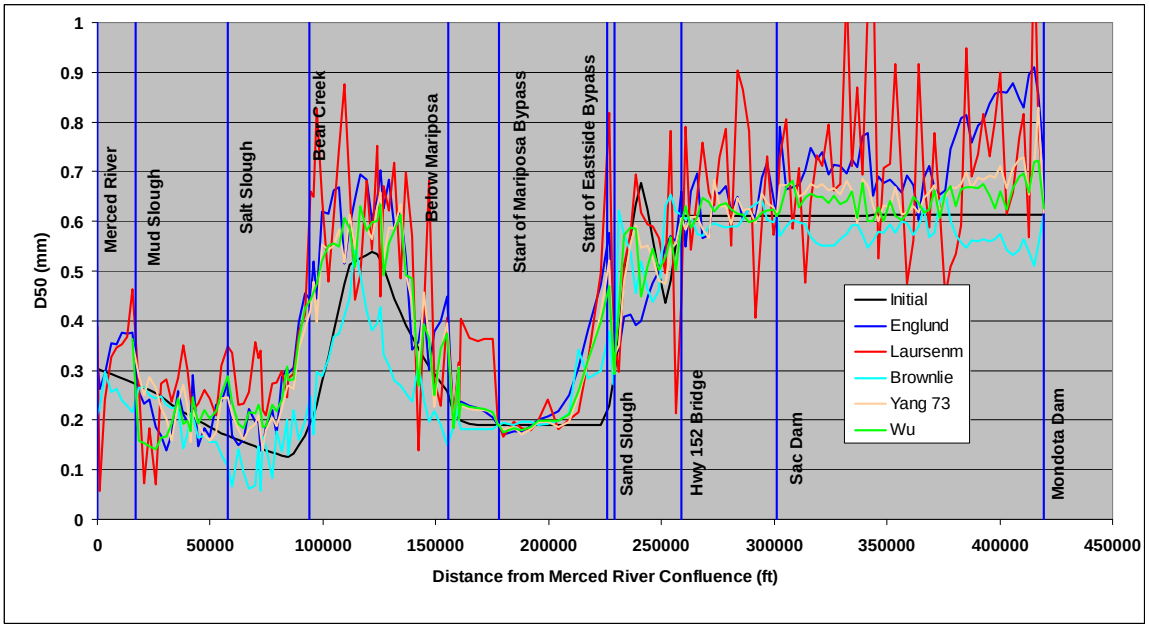

Figure D-6.
Mean Sediment Size Simulated with Different Sediment Transport Equations

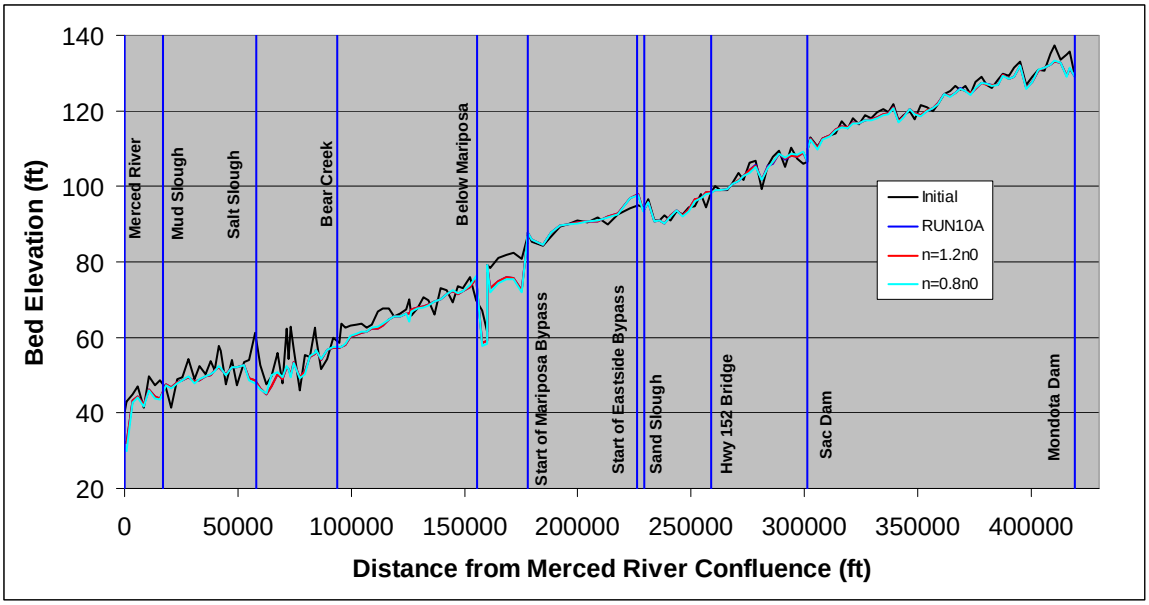

Note: n0 represents the initial Manning's roughness.

Figure D-7.
Bed Profiles Simulated with Different Manning's Roughness

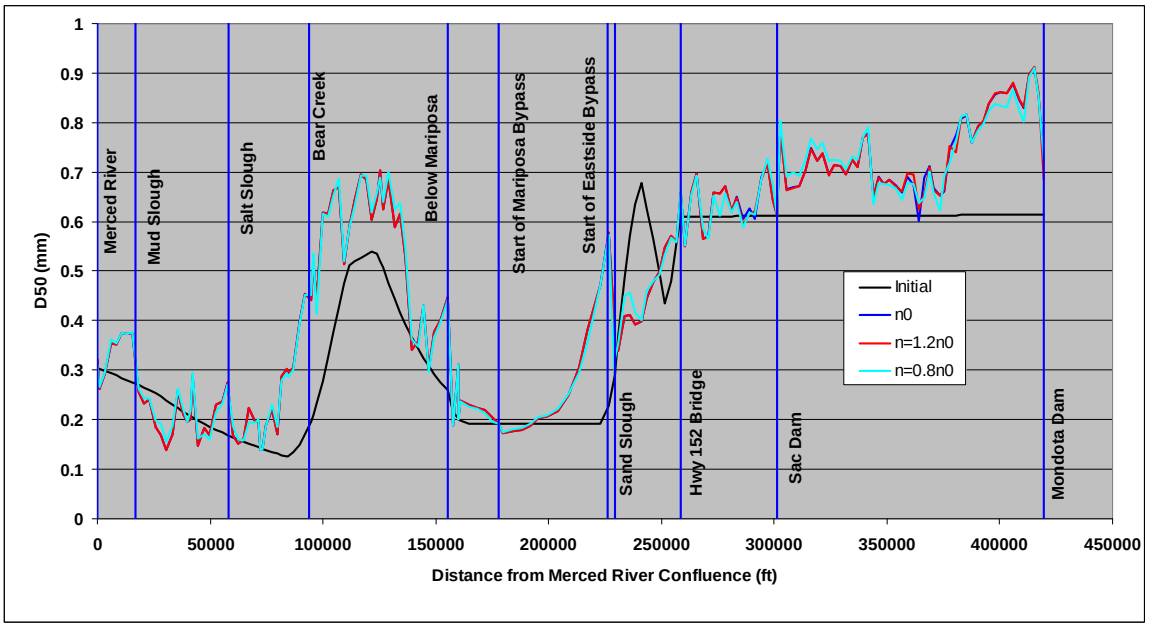

Note: n0 represents the initial Manning's roughness.

Figure D-8.
Mean Sediment Size Simulated with Different Manning's Roughness

Exhibit

Sensitivity Analysis on Incoming Sediment Loads at Mendota Dam with Baseline and Alternative Hydrology

Draft
Assessment of Sediment Transport and Channel Morphology on the San Joaquin River from Mendota Dam to Merced River Attachment

SAN JOAQUIN RIVER
RESTORATION PROGRAM

Draft
April 2011

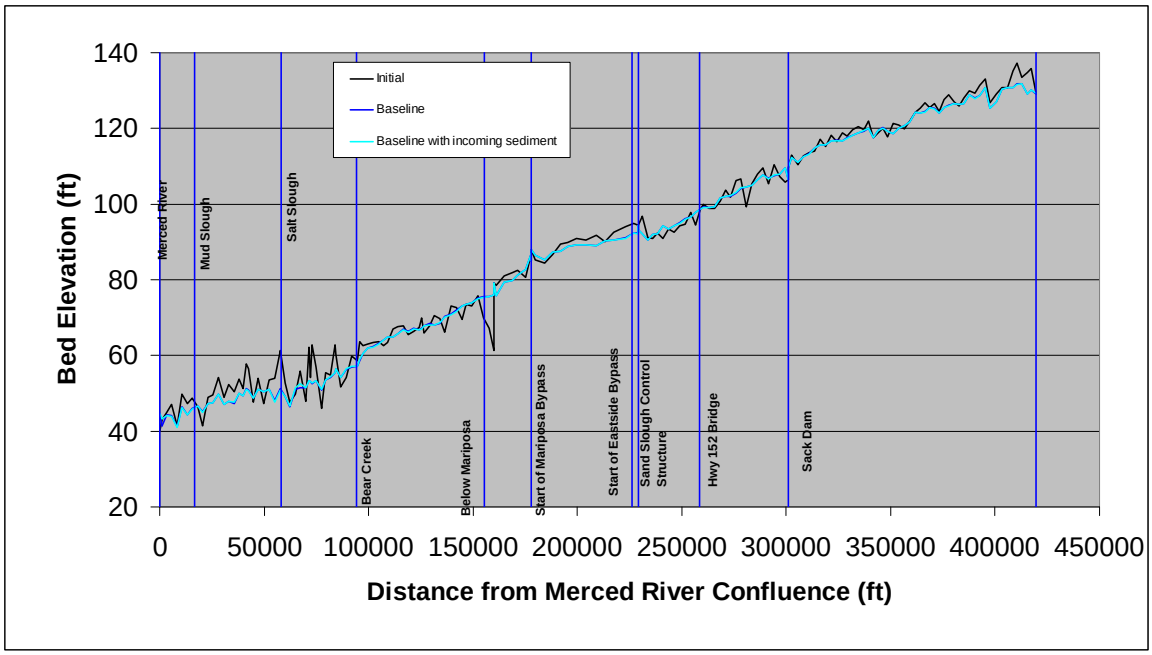

Figure E-1.
Bed Profiles Simulated with and Without Incoming Sediment Loads from Mendota Pool Using Baseline Hydrology

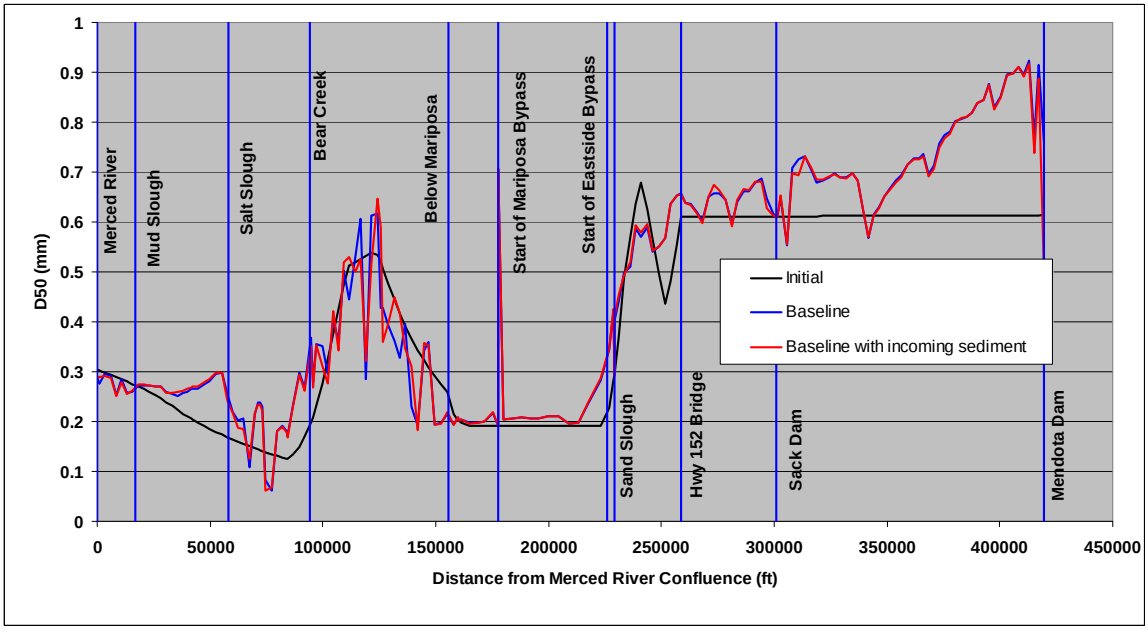

Figure E-2.
Mean Sediment Size Simulated with and Without Incoming Sediment Loads from Mendota Pool Using Baseline Hydrology

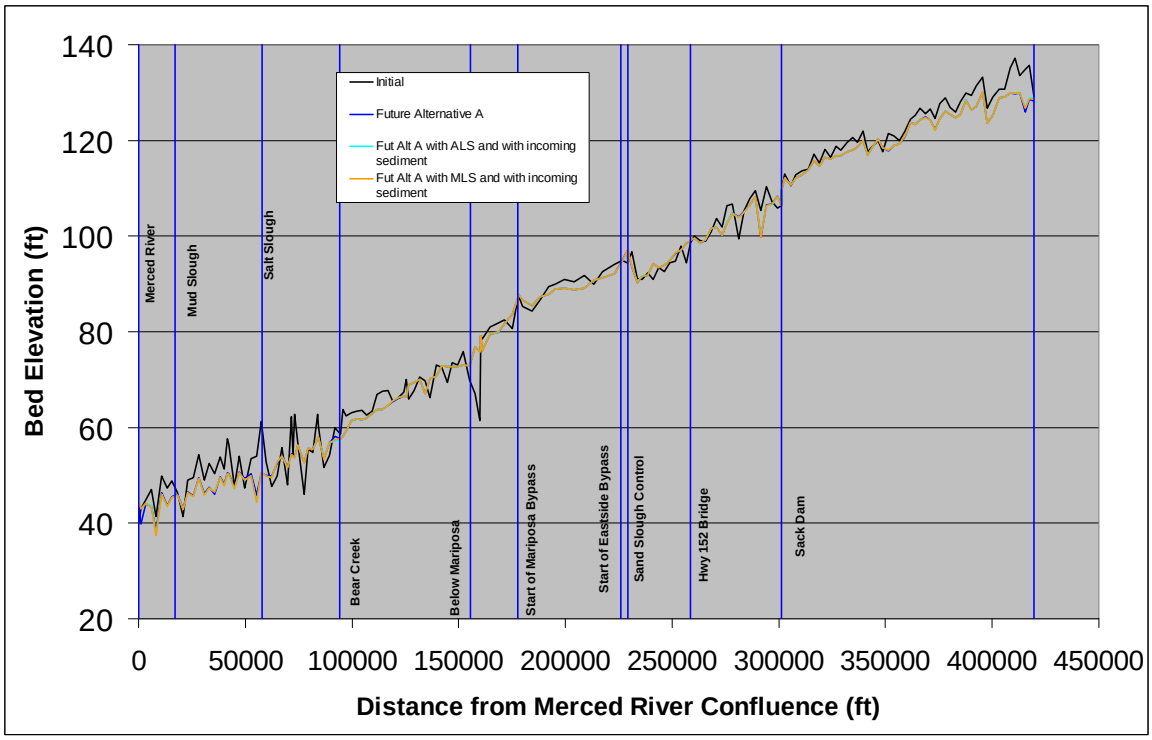

Figure E-3.
Bed Profiles Simulated with and Without Incoming Sediment Loads from Mendota Pool Using Alternative A Hydrology

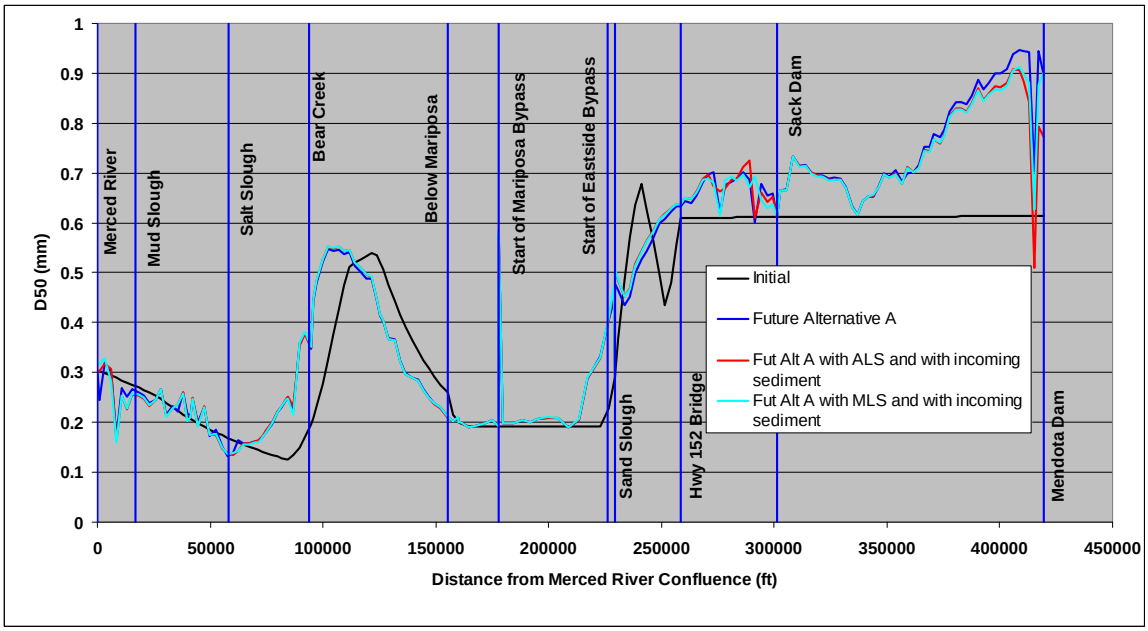

Figure E-4.
Mean Sediment Size Simulated with and Without Incoming Sediment Loads from Mendota Pool Using Alternative A Hydrology